INTELLIGENT ENERGY MANAGEMENT FOR MICROGRIDS WITH RENEWABLE ENERGY, STORAGE SYSTEMS, AND ELECTRIC VEHICLES.

Mosaddek Hossain Kamal Tushar

A thesis
in
The Department
of
Electrical And Computer Engineering

Presented in Partial Fulfillment of the Requirements
For the Degree of Doctor of Philosophy
Concordia University
Montréal, Québec, Canada

April 2017

Concordia University

Engineering and Computer Science

This is to certify that the thesis prepared

By: **Mr. Mosaddek Hossain Kamal Tushar**

Entitled: **Intelligent Energy Management for Microgrids with Renewable Energy, Storage Systems, and Electric Vehicles.**

and submitted in partial fulfillment of the requirements for the degree of

Doctor of Philosophy (Electrical And Computer Engineering)

complies with the regulations of this University and meets the accepted standards with respect to originality and quality.

Signed by the final examining commitee:

Dr. Gerard J. Gouw	Chair
Dr. Fei Richard Yu	External Examiner
Dr. Lata Narayan	External to Program
Dr. Dongyu Qiu	Examiner
Dr. John Xiupu Zhang	Examiner
Dr. Chadi Assi	Supervisor
Dr. Martin Maier	Co-supervisor

Approved _____

Chair of Department or Graduate Program Director

_____ 20 _____ _____

Amir Asif, Dean

Faculty of Engineering and Computer Science

Abstract

Intelligent Energy Management for Microgrids with Renewable Energy, Storage Systems, and Electric Vehicles.

Mosaddek Hossain Kamal Tushar, Ph.D.
Concordia University, 2017

The evolution of smart grid or smart microgrids represents a significant paradigm shift for future electrical power systems. Recent trends in microgrid systems include the integration of renewable energy sources (RES), energy storage systems (ESS), and plug-in electrical vehicles (PEV or EV). However, these integration trends bring with then new challenges for the design of intelligent control and management system. Traditional generation scheduling paradigms rely on the perfect prediction of future electricity supply and demand. They can no longer apply to a microgrid with intermittent renewable energy sources. To mitigate these problems, a massive and expensive energy storage can be deployed, which also need vast land area and sophisticated control and management. Electrical vehicles can be exploited as the alternative to the large and expensive storage. On the other hand, the use of electrical vehicles introduces new challenges due to their unpredictable presence in the microgrid. Furthermore, the utility and ancillary industries gradually adding sensors and power aware, intelligent functionality to home appliances for the efficient use of energy. Hence, the future smart microgrid stability and challenges are primarily dependent on the electricity consumption patterns of the home appliances, and EVs. Recently, demand side management (DSM) has emerged as a useful method to control or manipulate the user demand for balancing the generation and consumption. Unfortunately, most of the existing DSM systems solve the problem partially either using ESS to store RES energy or RES and ESS to charging and discharging of electrical vehicles. Hence, in this thesis, we propose a centralized energy management system which jointly optimizes the consumption scheduling of electrical vehicles and home appliances to reduce the peak-hour demand and use of energy produced from the RESs. In the proposed system, EVs store energy when generation is high or during off-peak periods, and release it when the demand is high compared to the generation. The

centralized system, however, is an offline method and unable to produce a solution for a large-scale microgrid. Further, the real-time implementation of the centralized solution requires continuous change and adjustment of the energy generation as well as load forecast in each time slot. Thereby, we develop a game theoretic mechanism design to analyze and to get an optimal solution for the above problem. In this case, the game increases the social benefit of the whole community and conversely minimizes each household's total electricity price. Our system delivers power to each customer based on their real-time needs; it does not consider pre-planned generation, therefore the energy cost, uncertainty, and instability increase in the production plant. To address these issues, we propose a two-fold decentralized real-time demand side management (RDCDSM) which in the first phase (planning phase) allows each customer to process the day ahead raw predicted demand to reduce the anticipated electricity cost by generating a flat curve for its forecasted future demand. Then, in the second stage (i.e., allocation phase), customers play another repeated game with mixed strategy to mitigate the deviation between the immediate real-time consumption and the day-ahead predicted one. To achieve this, customers exploit renewable energy and energy storage systems and decide optimal strategies for their charging/discharging, taking into account their operational constraints. RDCDSM will help the microgrid operator better deals with uncertainties in the system through better planning its day-ahead electricity generation and purchase, thus increasing the quality of power delivery to the customer. Now, it is envisioned that the presence of hundreds of microgrids (forms a microgrid network) in the energy system will gradually change the paradigms of century-old monopolized market into open, unbundled, and competitive market which accepts new supplier and admits marginal costs prices for the electricity. To adapt this new market scenario, we formulate a mathematical model to share power among microgrids in a microgrid network and minimize the overall cost of the electricity which involves nonlinear, nonconvex marginal costs for generation and T&D expenses and losses for transporting electricity from a seller microgrid to a buyer microgrid.

Acknowledgments

I would like to express my profound appreciation to many people who supported me during my Ph.D. and who helped me to complete my thesis. Their generous support made this dissertation possible.

Firstly, I would like to express my sincere gratitude to my advisor Prof. Dr. Chadi Assi for the continuous support of my Ph.D. study and related research, for his patience, motivation, and immense knowledge. His guidance helped me in all the time of research and writing of this thesis. I could not have imagined having a better advisor and mentor for my Ph.D. study. I would like to extend my honest appreciation to my co-supervisor, Dr. Martin Maier, INRS for encouraging me during the earlier stage of my Ph.D. research. I am truly indebted to them for their knowledge, thoughts, and friendship.

Besides my supervisors, I would like to thank my committee members, Dr. Lata Narayanan, Dr. Walaa Hamouda, and Dr. John Xiupu Zhang, for their Insightful comments and encouragement to widen my research from various perspectives. My sincere appreciation goes to Dr. Ivan Contreras for his insightful comments on my research work.

I would like to acknowledge Calcul Quebec and Compute Canada to facilitate an extreme supercomputing environment for academic studies. In my research, most of the computations were made on the supercomputer Briare from Universit de Montral, and Mammouth-Parallel II from Universit de Sherbrooke managed by Calcul Qubec and Compute Canada. The operation of this supercomputer is funded by the Canada Foundation for Innovation (CFI), the ministre de l'conomie, de la Science et de l'innovation du Qubec (MESI) and the Fonds de recherche du Qubec - Nature et technologies (FRQ-NT).

I gratefully acknowledge the funding sources that made my Ph.D. work possible. I was funded by the NSERC Strategic Grant and Concordia University for first three

years and the fourth year from PERSWADE, a CREATE program of NSERC, Canada as a Ph.D. Fellow.

Furthermore, I am greatly thankful to all of my colleagues in the research lab at Concordia University for providing me with the warm and friendly atmosphere.

I would like to thank my wife Upama Kabir and my daughter Anwesha Kamal for their continuous support understanding, and assistance whenever I needed them throughout my research work.

Last but not the least, I would like to thank my parents and to my brothers and sisters. I believe that without my parents, I could not be able to succeed throughout my life. I am always grateful to them for their encouragement and support.

Contents

List of Figures

List of Tables

Abbreviations

AMI	Advanced Metering Infrastructure
ANN	Artificial Neural Network
ANSI	American National Standards Institute
ARMA	Auto Regression Moving Average
BAN	Building Area Network
CEMS	Community or Central Energy Management System
COPCS	Centralized Optimal Consumption Scheduling
CVR	Conservative Voltage Regulation
CVVO	Coordinate Volt-VAR Optimization
DEMS	Distributed Energy Management System
DG	Distributed Generator
DR	Remand Response
DSM	Demand-Side Management
EMS	Energy Management System
EPRI	Electronic Power Research Institute
ESS	Energy Storage System
EV	Electric Vehicle
G2V	Grid to Vehicle
GeSi	Global E-Sustainability Initiative
GHG	Greenhouse Gas

HAN	Home Area Network
HEMS	Home Energy Management System
HMI	Human Machine Interface
HV	High Voltage
IAN	Industrial Area Network
ICE	Internal Combustion Engine
ICT	Information and Communication Technology
IEA	International Energy Agency
IEEE	Institute of Electrical and Electronics Engineers
ILP	Integer Linear Programming
IPTS	Institute for Prospective Technological Studies
ITU	International Telecommunication Union
IVVO	Integrated Volt-VAR Optimization
LCOE	Levelized Cost of Electricity
LMP	Locational Marginal Price
LRMC	Long Run Marginal Cost
LTC	Local Trading Center
LTLF	Long-Term Load Forecasting Model
LV	Low Voltage
MCP	Market Clearing Price
MEPM	Minimum Electricity Pricing Model
MESS	Microgrid Energy Storage System
MG	Microgrid
MGN	Microgrid Network
MILP	Mixed Integer Linear Programming
MIQP	Mixed Integer Quadratic Programming
MTLF	Medium-Term Load Forecasting Model

NAN	Neighborhood Area Network
NCDC	National Climate Data Center
NHTS	National Household Travel Survey
NOAA	National Oceanic and Atmospheric Administration
OECD	Organization for Economic Cooperation and Development
OECM	Optimal Energy Consumption Model
OLTC	On-Load Tap Changer
OMCP	Overall Marginal Cost Problem
OPF	Optimal Power Flow Problem
PEV	Plugin Electric Vehicle
PHEV	Plugin Hybrid Electric Vehicle
PLC	Programmable Logic Controllers
PV	Photo-Voltaic
RDCDSM	Real-time Decentralized Demand-Side Management
RES	Renewable Energy Source
RTU	Remote Telemetry Unit
SCADA	Supervisory Control And Data Acquisition
SEMS	Smart Energy Management System
SOC	State of Charge
STLF	Short-Term Load Forecasting Model
T&D	Transmission & Distribution
TOU	Time of Use
V2G	Vehicle to Grid
VAR	Volt Ampere Reactive
VVC	Volt-VAR Control
VVCDDR	Volt/VAR Control and Distributed Demand Response
VVCO	Volt-VAR CVR Optimization

Chapter 1

Introduction

1.1 Overview and Objectives

The current electrical grid is perhaps the greatest engineering achievement of the 20^{th} century and is considered to be the largest machine on the planet. However, it is increasingly outdated and overburdened, leading to costly blackouts and burnouts [59, 66, 138, 137]. Current studies show that the existing electric grid converts only one-third of fuel energy into electricity [35]. Almost 8% of the generated electricity is lost in transmission while 20% of the electric energy is generated to meet peak demands for only a short period (5%) [83]. Moreover, existing electricity networks do not contain storage units, which means that the energy generated from fossil fuels and nuclear power plants must be balanced with the energy consumed by the end users [86]. In addition, the existing electric grid suffers from domino-effect failures due to its hierarchical topology of transmission and distribution networks. In fact, nearly 90% of power disruptions occur in power distribution networks [83]. Further, the current electricity generation relies heavily on fossil fuels and causes 41% of the world greenhouse gas emissions (Figure 1.1a) [18]. Coal and peat electricity generators emit more than 70% of CO_2 of the total emission of the electricity sector (Figure 1.1b).

Conventional transportation vehicles operate on the principles of internal combustion engine (ICE) that runs on fossil fuel (i.e., gasoline, diesel). ICE emits 23% of the global CO_2 emission [18]. The above two mentioned sectors together emit two thirds of global CO_2 as shown in Figure 1.1a. Road vehicles emit 75% of the total amount of CO_2 released by the transport sector in 2008 and 2009 (Figure 1.1c).

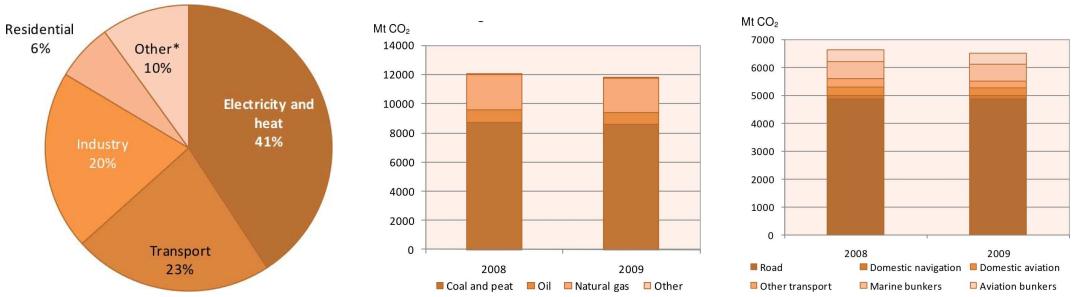

(a) World CO_2 emission by sector in 2009

(b) World CO_2 emission from electricity and heat generation

(c) World CO_2 emission from transportation in 2008-2009

Figure 1.1: World Greenhouse Gas Emission

Thus, transformation efforts are underway to make the current electrical grid *smarter*. The future smart grid could be referred to as the modernization of the current electric grid by increasing its dependency on cyberspace and renewable energy resources. The smart grid should not be the replacement of the existing grid rather it is a complement to the existing grid. Smart grid will coexist with the conventional grid and gradually add capabilities, functionalities and capacities to the existing power grid by means of an evolutionary path. This coexistence needs a topology which allows the organic growth by accommodating modern technology and full backward compatibility with the current system. Further, the organic growth and development of smart grid is anticipated to come through the plug-and-play integration of essential structures known as intelligent (or smart) microgrid [35]. Figure 1.2 compares the existing grid with the future grid.

The smart grid enables two-way flows of information and electricity in order to

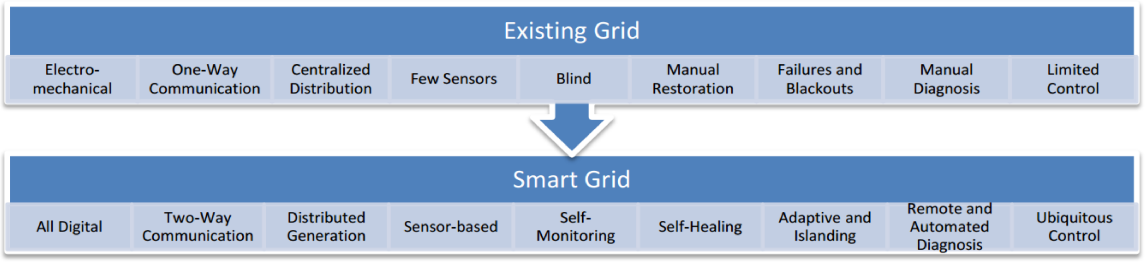

Figure 1.2: Comparing the existing grid with the Smart Grid

achieve numerous goals; it will provide consumers with diverse choices on how, when, and how much electricity they use. It is self-healing in case of disturbances, such as physical and cyber attacks and natural disasters. Moreover, smart grid's infrastructure will be able to link and utilize a wide array of energy sources including renewable energy producers and mobile energy storages. Additionally, it aims at providing better power quality and more efficient delivery of electricity. Smart microgrids, smaller versions of the smart grid, are self-sufficient clusters of distributed generators (DGs), loads, storage devices and central controller. The central controller of a microgrid is the infrastructure that coordinates all the activities of the microgrid. On of the most significant components of the central controller is an ICT-enabled energy management system (EMS), which optimally manages the usage and controls the production of energy. Microgrids encompass a wide range of environmentally friendly power generation technologies such as hydro power, wind turbine, photovoltaic, geothermal, etc. As a distributed energy generator, microgrids often generate electric power in close proximity to the customers and hence can be operated by the customers. Smart microgrids reduce greenhouse gas emission and address major shortcomings of the existing power grid such as transmission and distribution losses. They empower consumers to interact with the energy management system to adjust their energy usage and reduce their energy costs. Additionally, smart microgrids, being capable of supporting two-way energy and information flow, can estimate users demands and are able to

optimize customers power consumption [95]. Smart microgrids can be deployed in two working modes (i) grid connected microgrid, and (ii) islanded microgrid.

1.1.1 The Vision and Benefits of Smartgrid and Microgrid

The interconnection management system manages the power flow from outside the microgrid in case of shortage of power and to other microgrids or to the external power grid in case of excessive power generation. The establishment of microgrids increases the reliability of the electricity supplies by the existence of storage systems. The use of the emerging information and communication technology (ICT) is essential for the smart microgrids, i.e. intelligent power distribution networks which automatically reroute the power flow in case of unexpected line fault. During a power grid failure, smart microgrids will operate in islanded mode, which continuously supply power to the community/area intended for. Various studies (see Table 1.1)[87], assessed the global and country wide positive impact of reducing the CO_2. For example, the GeSI study [87] emphases four main ways the smart grids could reduce CO_2 emissions. The broken down contributions of the levers identified in the GeSI study (see Fig. 1.3) [87] emphasizes that the "transmission and distribution losses" and the "integration of renewable energy sources" account for most CO_2 contributions, i.e. $1,72\ Gt$ out of the total $2,03\ Gt\ CO_2$ globally. Also, a substantial reduction of $0.28\ Gt$ could be obtained by the "reduced consumption through user information". Fig. 1.4[87] summarizes the positive impact on the environment from EPRI USA studies. It shows that three major steps ("direct feedback on energy uses", "integration of renewable energy sources" and "facilitation of PHEV market") may reduce the US CO_2 emissions from $2,11\ Mt$ to $0,46\ Mt\ CO_2$. The use of efficient management and emerging technologies, such as ICT enable the smart microgrids to use Electric Vehicles (EV) batteries for power storage of the electricity generated during off-peak hours. The

Table 1.1: Impact of smart microgrids: the GeSI, EPRI and IPTS studies

	GeSI (2008)	EPRI (2008)	IPTS (2004)
Title	Smart 2020: Enabling the Low Carbon Economy in the Information Age	The Green Grid Energy Savings and Carbon Emissions Reductions Enabled by a Smart Grid	The Future Impact of ICTs on Environmental Sustainability
Time horizon	2020	2030	2020
Geographical coverage	World	US	Europe
Considered smart grid levers for the Reduction of CO_2e emissions	• Reduced transmission and distribution (T&D) losses • Integration of renewable energy sources • Reduced consumption through user information • Demand side management	• Continuous commissioning for commercial buildings • Reduced line losses • Enhanced demand response and (peak) load control • Direct feedback on energy usage • Enhanced measurement and verification capabilities • Facilitation of integration of renewable resources • Facilitation of plug-in hybrid electric vehicle (PHEV) market penetration	• Renewable energy sources
Considered impacts	• Positive impacts • Negative footprint: no consideration on the smart grid level (overall ICT level)	• Positive impacts • No consideration of negative footprints	• Positive impacts • Negative impact considered but not on the smart grid level
Rebound effects	• Only discussed in a qualitative way	• Only discussed in a qualitative way	• Quantification of the rebound effect
Methodology	• Expert interviews • Literature review: publicly available studies, academic literature • Information provided by partner companies • Case studies • Quantitative analysis (models based on the McKinsey cost curve and McKinsey emission factors)	• Calculations draw on data from single cases • Simple assumption are made to calculate impacts	• Screening and scoping • Literature analysis • Interviews • Policy-integrated scenarios • Modelling • Validation workshops • Reviews and policy recommendations (*Source*: Erdmann, 2009)
Scenario	BAU (Business as usual)	No concrete scenarios (only ranges of savings are shown which depend on different market penetration rates)	Three scenarios: • Technology • Government First • Stakeholder democracy
Plausibility	• Use of CO_2e emission data from IPCC (2007) with higher CO_2e emission prospects than prospects provided by the IEA • Possible overestimation of the positive impacts due to some assumptions • Overall, use of good data	• Possible overestimation of some effects due to some assumptions • Partially very simple assumptions and calculations	• Consideration of various effects (*e.g.* rebound effects) • Most holistic approach • Only report with validation methods
Stakeholders	• Involvement of industry stakeholders • Commissioned by GeSI (ICT industry association)	• EPRI: research institute of the power industry	• Research institutes, scientific report • Involvement of scientific and industry stakeholders *Source*: Erdmann, 2009.

Figure 1.3: Positive Environmental Impact of smart microgrids.

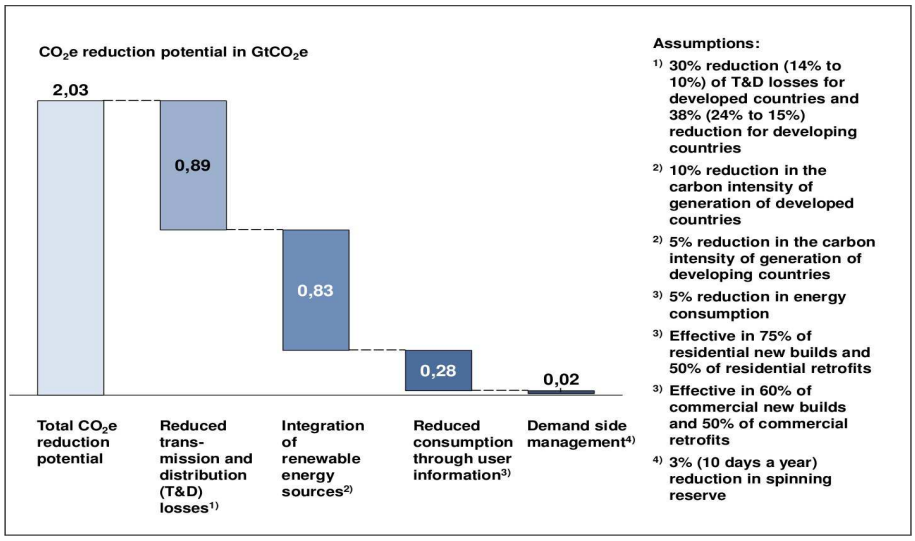

charging/discharging cycle decreases the life of the battery. It appears that if the battery degradation cost is applied, the corresponding profit alone may provide an incentive to the EVs' owner to use their battery pack for electricity storage [95]. V2G (vehicle to grid) service could be sold in an organized market as ancillary services or it could be used to avoid grid electricity surcharge. The use of wireless charging technologies allows the EVs, and eventually other household equipments to charge without delay. Currently over 40% of fossil-fuel is consumed by transportation systems and residential houses. Deployment of microgrids and EVs may substantially reduce the use of fossil-fuel near to almost negligible [87]. Charging a large population of EVs has a significant impact on the power grid [50]. The US department of transportation data indicates that, including overnight hours, a vehicle spends nearly 75% parked at home [30]. In the US, it is predicted that by 2020 25% and 2040 two thirds of light-duty vehicles ought to be EVs. Further, it is expected that current research outcomes on high power lithium-ion micro battery technology will accelerate the replacement of internal combustion cars by the EVs [97].

Figure 1.4: Positive Environmental Impact of smart microgrids according to EPRI (2008)

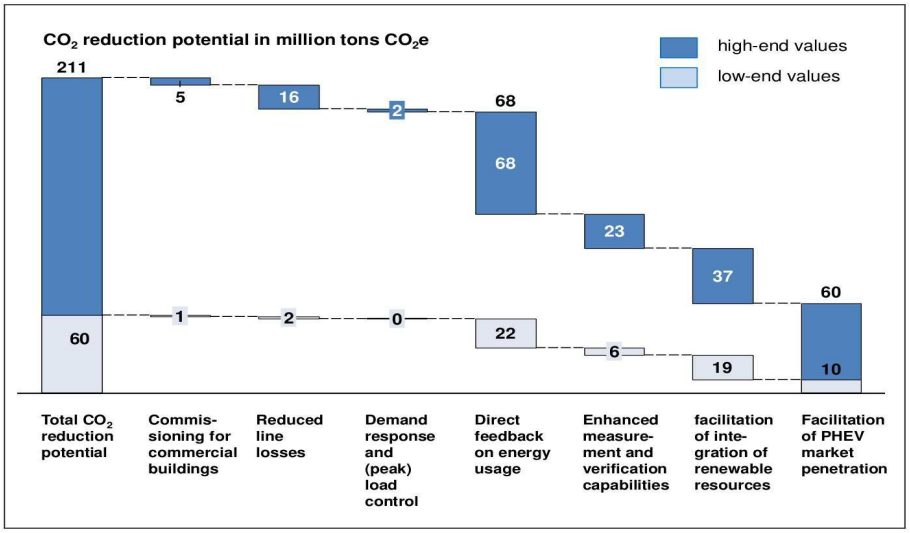

1.1.2 Technology Challenges

Given the fluctuations of power generation in microgrids as a result of unavoidable natural hazards, and also because the number of EVs charging (simultaneously) is unknown, therefore, the power sharing between neighboring microgrids must deal with the following challenges:(a) Integration of intermittent renewable energy sources. (b) V2G and G2V issues: Policy/protocol and intelligent mechanisms are needed for V2G operation to provide electric energy to the grid with the high price interval and for emergency power need. For consuming electricity, EVs need to charge in low price interval. (c) Wireless and sensor based infrastructure is needed to monitor EVs' battery charge level, charging and discharging schedule. (d) Integration of community energy storage system (ESS). (e) Communication and control required over microgrids for power generation and consumption. (f) Management System for Intelligent Power Transmission and Distribution between microgrids. (g) Transition between "grid connected" and "islanded" mode of microgrids. (h) Smart Metering (i) Frequency and voltage regulation (j) Cyber security: The smart microgrids differ from the conventional communication networks because they are able to reach every

equipment which resides in user premises, and return with energy control information to the microgrid central control system. The microgrids smartly determine the current energy requirement and decide to distribute and transfer according to the demand, possibly with valley filling algorithms. So the security of the user data and the secure transmission of control and electric energy demands are usual concerns.

1.1.3 Thesis Objectives

This research work will investigate and address fundamental and practical problems related to microgrids resource management and networking. Hence, the technical, commercial, and residential community will benefit significantly from the extensive research on microgrids. In particular, this effort will:

- Conduct a first of a kind comprehensive study on stochastic nature of the smart grid and smart microgrids utilities and renewable energy sources. This will provide critical guidelines for both, consumers and manufacturers of such utilities.
- Encourage microgrid operators to rely more on renewable energy sources rather than fossil-fuel electric generators.
- Enable EVs to be used as distributed electricity storage for microgrids, which will significantly reduce the cost, land space, and investment involved in implementing large electric storage system.
- Integrate community Energy Storage Systems (ESSs) in the grid which will play a significant role in balancing the generation planning and real-time use of electricity along with EVs.

This thesis work will focus on the main issues in power generation, distribution and communications of microgrids.

The integration of renewable energy sources and electrical vehicles (EVs) into microgrids is becoming a popular green approach. To reduce greenhouse gas emissions, several incentives are given to use renewable energy sources and EVs. By utilizing EVs as electricity storage and renewable energy sources as distributed generators, microgrids become more reliable, stable, and cost-effective. To optimize energy use, an optimal centralized scheduling method may play a significant role which jointly controls the electricity consumption of home appliances and plug-in EVs. It discharges the EVs when they have excess energy, thereby increasing the reliability and stability of microgrids and giving lower electricity prices to customers.

In a centralized scheduling, customers need to send their detailed information about the load such as load type, consumption time and duration, driving schedule of the EV, RES generation pattern, etc., which may expose a potential privacy and security breach. In addition to this, the centralized system does not give any incentives to EVs owners to participate V2G operation. Also, a centralized system does not scale well for a large sized microgrid. A distributed real-time electricity allocation scheme for microgrid based on game theoretic mechanism design may benefit both the customers and the operator to reduce the client's electricity bill and lower the generation in peak-hour. In this scheme, each of the clients is able to choose its consumption pattern, charging and discharging EVs to reduce their electricity costs and get incentives from the microgrid operator in real time. The game based mechanism design for real-time consumption will promise to (i) keep privacy of the energy consumption pattern, (ii) reduce the electricity bill of residential customers, (iii) increase the overall social benefit of the community, as well as (iv) improve the energy efficiency and reliability of the microgrid to rely on locally generated electricity.

The integration of electric vehicles (EVs), energy storage systems (ESSs) and renewable energy sources (RESs) may play a significant role in balancing the planned

generation of electricity and its real-time use. A utility operator accumulates customers day ahead predicted load and plan for the production or purchase power to serve the clients in the next day. Unfortunately, actual consumption may vary from the day ahead anticipated demand, thereby increase the instability and reduce the reliability of the power system which incurs extra cost, and in some cases load shading. The customer load varies from time to time of a day, which then needs to generate or purchase more electricity in peak hours compared to off-peak hours. A two-level real-time decentralized demand-side management may solve this problem. This system is expected to allow each customer to process the day ahead raw predicted demand to reduce the anticipated electricity cost by generating a flat curve for its forecasted future demand. Then at the time of real use, customers will mitigate the deviation between the real-time consumption and the day-ahead predicted load. To achieve this, customers exploit renewable energy and energy storage systems and decide optimal strategies for electricity consumption. It is expected that the decentralized two-level demand-side management system will help the microgrid operator better deal with uncertainties in the system through better planning its day-ahead electricity generation and purchase, thus increasing the quality of power delivery to the customer.

The smart microgrid and its demand-response characteristics are gradually changing the paradigms of the century-old electric grid and shaping the electricity market. In this new market scenario, once always energy consumers now may act as sellers due to the excess of energy generated from newly deployed renewable energy generators in the consumer premises. Hence, an optimization scheme is required for the trading of energy among the microgrids and determine overall electricity price. The marginal cost models for the power generation are nonlinear and non-convex. Moreover, the microgrid network (MGN) uses third party transmission and distribution

(T&D) system which incurred extra costs to transport electricity from seller to buyer. Therefore, the solution should be robust enough to find an optimal solution for MGN in time.

Volt-VAR optimization (VVO) is a well-studied problem, for bringing solutions to reduce the losses and demand along the transmission and distribution lines. The current VVO, however, does not acknowledge the role of elastic and inelastic loads, EVs, and RESs to reduce the reactive power losses and hence the cost of generation. Therefore, we will develop a method to solve the VVO problem by considering load shifting, EV as the storage and carrier of the energy, and use of RES. In this connection, our objective is not only to reduce the reactive load but also flatten the load curve to reduce the uncertainty in the generation and to decrease the cost. The system also considers the efficiency of the electrical equipment to enhance the lifetime of the devices.

1.2 Problem Statement and Motivation

The evolution of microgrid and the integration of renewable energy sources, electrical vehicles (EVs), and energy storage system (ESS) into microgrids is becoming a popular green approach. The overall load profile of the power grid, as well as of the microgrid, may change due to the introduction of EVs. Charging a large population of EVs has a significant impact on the power grid. In addition to this, the intermittent nature of renewable energy sources and presence of EVs introduce new challenges to the stability of the power grid. The intelligent management of the integration of EVs, ESS, and renewable energy sources, as well as of user power consumption may bring benefits to both operators and consumers.

The construction of efficient energy management systems with the objective of minimizing energy cost, balancing the energy planning and consumption, reducing the

transmission and distribution losses, sharing energy among microgrids by integration of RES, EVs, and ESS is indeed a challenging task, and some solutions already exist. Most of the existing solutions solve the problems either for integration of RESs or charging of EVs. Unlike the previous work presented in the literature (chapter 2) our thesis attempts to solves the energy management problems by utilizing RES, EVs, and ESS. The thesis investigates and formulates solutions for demand side resource management to control the power consumption, flatten the load curve, enable energy sharing among the microgrids, reduce the transmission and distribution losses of the electrical systems, thereby increasing the reliability and stability by giving lower electricity prices to customers.

1.2.1 Smart Microgrid: Optimal Joint Scheduling for EV and Home Appliances

This work investigates a microgrid that is connected to the power grid and has a fixed number of renewable energy sources (e.g., wind turbine, photovoltaic panels, etc.) for a small residential community. The microgrid consumers have home appliances and EVs. In this research, we develop a centralized joint optimal electricity consumption scheduling method for appliances and EVs with the objective to minimize the amount of imported electricity from the grid. Here, EVs are used as distributed storage to store electricity. EVs are mobile and connected to the microgrid in a random fashion. In case of shortage of power, the microgrid uses the electricity stored in EVs (with discharge capability) and in cases, when the stored electric energy is not sufficient, the microgrid gets electricity from the grid. In this model, an independent residential microgrid is considered which can be operated in islanded mode or grid connected mode. The scheduling problem is a mixed integer linear programming problem (MILP) which jointly controls electricity consumption of home appliances as

well as the charging and discharging of EVs. Our scheduling method results in the optimal use of electricity generated from renewable energy sources and minimizes the amount of imported electricity from the grid. Consequently, it reduces the electricity price for the microgrid customers. Further, the optimal scheduling method enables EVs to store electricity during peak generation hours, which may be used later during high demand. In doing so, our approach helps increase the service availability and stability of the microgrid.

1.2.2 Distributed Real-Time Electricity Allocation (DRTA) Large Residential Microgrid

The above optimal joint scheduling method is a centralized MILP based method. Therefore, it is suitable for a small residential microgrid. For a large microgrid, the centralized method may not produce optimal solutions. Also, the method needs to send user's detailed load information to the microgrid operation which may expose the privacy of the customers and yield potential security breach. Moreover, the centralized method can be implemented when the load and generation from RES for the next day is known (by prediction). Unfortunately, the load may vary at the actual time of consumption.

In this work, we address the problem described above and consider a grid-connected microgrid with a set of RESs for a large community. The microgrid has a central controller with EMS, servicing a set of homes (customers), each equipped with an AMI (Advanced Metering Infrastructure) smart meter. We assume a communication network such as NAN (neighborhood area network) which connects smart meters to each other and the central controller. We propose a new distributed real-time electricity allocation (DRTA) scheme using mechanism design to reduce the electricity bill of each microgrid customer and simultaneously increase the overall social benefit of the

community. In this mechanism design framework, the EMS acts as a controller of the game and the smart meters act like the players of the game. The smart meter plays the game to determine the energy consumption strategy of each appliance to reduce the energy bill based on the current electricity price. If the current set of strategies, lowering the electricity bill compared to the electricity bill calculated as before then each smart meter updates its electricity demand and sends it to the controller. The play will continue until there is no change in the electricity price. The game in the mechanism design is a non-cooperative repeated game. We show that the game converges to an optimal Nash equilibrium state. In this game, players signal each other to maximize the their own benefit, which simultaneously reduces the energy bill and increases fairness.

1.2.3 Real-Time Decentralized Demand-Side Management (RDCDSM)

The DRTA method modifies user consumption patterns and allocates electricity in real time, slot by slot. Hence, the power planner always needs to be aware of mitigating the variable demand of the customers. This may create an instability problem in power generation and delivery to the customers. Therefore, we consider a residential microgrid which is connected to the grid and purchases electricity from it according to its clients aggregated day-ahead predicted demand. Each client predicts its load a day-ahead and sends it to the operator. Upon receiving this information, the microgrid operator plans to purchase electricity for the next day (to satisfy its users' demands) and determine the power cost accordingly. At the time of operation, however, the actual user's demand may change, and the renewable energy generation may vary, which results in discrepancy and instability in power delivery and thus increases the cost.

To solve this problem, we develop a Real-time Decentralized system for DSM (RDCDSM) which in the first place encourages customers collectively to modify their day-ahead anticipated coarse consumption to minimize their personal electricity cost, or inversely increase their payoff to produce a fine-grain predicted demand. Customers will play a game with mixed strategy profile by sharing their day-ahead anticipated demand and continuously modify it to increase their payoff. The game terminates in a Nash equilibrium state, which results in a fine-grain price-aware predicted demand where a further change of anticipated consumption will not increase the payoff. Then, each customer sends its resultant predicted demand to the operator. Upon receiving and accumulating the forecasted demand from its clients, the operator produces the day ahead aggregate predicted demand and devise a plan to generate and purchase electricity to satisfy the customers. We define this as the prediction phase of RDCDSM. Next, in step two, known as the allocation phase, the RDCDSM system encourages customers, in real time, to adjust their consumption pattern by playing mixed strategy in another non-cooperative game to stay close to their predicted demand. Doing so will allow the microgrid to stick to its pre-determined energy generation/purchase plan and avoid the higher costs of either activating a new generator or buying electricity at an instantaneous market price. The RDCDSM will penalize (i.e., higher rate charge) each of deviated users with the proportion of the total deviation determined by the operator.

1.2.4 Microgrid Network: Energy Sharing and Optimal Electricity Pricing

It is envisioned that a microgrid network (MGN) may shortly contain hundreds or even thousands of microgrids (MG) sharing energy with each other [48]. Usually, an MG produces and consumes energy locally; in the case of shortage, it purchases

electricity from the neighboring MGs or sells whenever it has a surplus (as in DRTA, RDCDSM). In such scenarios, the MG operators may not own the transmission and distribution (T&D) system, and use the existing network which requires T&D costs besides the generation cost. For the benefit of both customers and providers, an open competitive market is desirable which accepts new suppliers and admit marginal cost prices for electricity [54, 28, 128].

Upon developing the internal energy management of the microgrid (such as DRTA, RDCDSM) an energy management scheme is required for the optimal management of energy flow amoung microgrids according to their needs. In this circumstances, we develop a novel method for optimal energy flow between microgrids and to minimize the electricity cost for the microgrid network (MGN) in a deregulated competitive electricity market. We study and find that, for a non-decreasing marginal cost, the model is nonlinear and non-convex. Hence, it does not produce an optimal solution. Therefore, we decompose the model to separate the marginal cost from the T&D cost and develop a novel method based on a divide-and-conquer strategy which is defined as MEPM (minimum electricity pricing model), to solve it optimally. First, we determine the marginal cost boundary according to the overall demand of the MGN, also known as the overall marginal cost problem (OMCP). Then, using the proposed MEPM strategy, we interactively determine the optimal electricity price by jointly optimizing the OMCP and T&D costs (allocation problem) of the system. The MEPM algorithm determines the optimal price in a polynomial time [23] for a complex bidirectional electrical network that uses ICT to control the flow of energy among the neighborhood grids or MGs. We assume that each MG internally decides its consumption using a demand response model (such as in [120]) which integrates local generation from renewable sources, dynamic loads, and storage. The total demand and the amount generated by each generator and capacity of the generator at the real

time are known to the MEPM system.

1.2.5 Volt-VAR Control through Joint Optimization of Capacitor Bank Switching, Renewable Energy, and Home Appliances

In a microgrid network (MGN) or the existing power grid, most of the energy losses in electricity transportation are due to the resistance of the energy network and reactive power which is injected by the reactive load. This causes lower operating or terminal voltage at the customer (microgrid) point which potentially increases the demand and reduces the efficiency and lifetime of the user equipment. Therefore, the generator needs to generate more power to adjust the voltage at the last mile of the electricity transmission and distribution (T&D) line which again increases losses. To adjust the voltage level at operating point and reduce the losses often power T&D system operator uses the compensation devices or mechanism to reduce the reactive power injected by the user electronic equipment. This is known as the VVO problem. Several researches have been carried out to solve the VVO problem. Unlike those, we investigated and found that integration of renewable energy, shifting consumption from one time slot to another time slot, EVs as energy storage and community (microgrid) level energy management, along with the conventional shunt capacitor compensation and CVR (conservative voltage regulation) may solve the problem optimally and reduce losses and generation cost substantially.

We formulate the problem as a non-cooperative game (VVCO/OECM) between the communities connected to the feeders. Each of the communities adjusts the consumption pattern and service drop OLTC tap to minimize its electricity cost (or maximizes payoff) according to the price signal obtained from the utility. As a result, the utility operator adjusts the capacitor banks and substation transformers tap and

recalculate the cost of electricity, known as Volt-VAR and CVR (conservative voltage regulation) optimization model. The interplay between these two schemes results in a non-cooperative game which will terminate when there is no change in electricity cost. This condition is known as the Nash equilibrium state of the non-cooperative game. The proposed system presents a fine-grain solution for the VVO problem which considers (1) micro-level DR model, (ii) energy efficiency of the equipment, (iii) rooftop solar or locally installed energy sources, and (iv) G2V and the V2G control modes of the electrical vehicles.

1.3 Thesis Contributions

The main contributions of the thesis are summarized as follows:

- We define and classify the residential appliances (in Chapters 3 and 4) according to their mode of electricity consumption. Then we present the mathematical models of the load as (i) type-I: hard load which is non-deferrable and non-interruptable consumption, (ii) type-II: soft load that is non-interruptable and deferrable consumption, (iii) type-III interruptable and deferrable soft load and finally (iV) mixed mode appliances which consume electricity like type-I, II or III in the span of its operational time slots.

- We formulate a centralized MILP mathematical model (Chapter 3) for charging and discharging of EVs, energy consumption of home appliances and integration of renewable energy sources to the microgrid to optimize electricity use throughout the day. Then we simulate the model and evaluate the performance of the developed joint scheduling method and compare the results with an existing decentralized and naive allocation method which do not consider discharging of

EVs and load shifting for a demand-side management of electricity consumption. We show that for all the cases the proposed centralized optimal joint scheduling of EV and home appliances perform better than decentralized and naive allocation methods.

- Next, we formulate a game theoretical mechanism design (DRTA) for real-time distribution of electricity to the residential customer. For the mechanism design, we define participation constraints for each residential home appliances and incentive constraints for the electric vehicle. To increase the payoff of a customer and overall social benefit, a payoff function is defined for the residential customers. We show that the formulated model converges to a Nash equilibrium state and results in an optimal solution to the problem. Then, we develop a simulation to evaluate the performance of the DRTA method and compare the results with the centralized optimal joint scheduling for EVs and home appliances, and the unregulated allocation methods. See Chapter 4 for more detail.

- To balance the day ahead of planned electricity generation and the real-time consumption, we developed a two-stage solution known as RDCDSM (see Chapter 5). In the first stage, we formulate a mixed strategy non-cooperative game with MIQP payoff function for the customer to refine their raw day ahead prediction to minimize anticipated electricity costs. Then, for the power delivery to the customer in real-time, we formulate another non-cooperative game (with mixed strategy profile) with MILP payoff function to minimize penalty thereby reduce the deviation of real-time demand from the day ahead refine or price aware predicted load. In both cases, we show that the mixed integer game converges to a Nash equilibrium state and produces optimal results.

- To solve optimal energy management and the marginal cost pricing problem of deregulated market, we develop two unique methods (see, Chapter 6). First, OMCP which determines lower and upper bound overall marginal cost for maximum and minimum T&D cost for electricity transportation accordingly. Then we devise a divide-and-conquer method to select the cost pair (overall marginal cost and T&D cost) which results in minimum electricity price. To design these solutions, we analyze the original problem and found that the original MEPM problem is nonlinear and non-convex. Therefore we decompose the problem into OMCP and allocation problem) and devise a polynomial solution for the original MEPM.

- Finally, in VVCO/OECM (see, Chapter 7), we developed a non-cooperative game to determine the terminal voltage of a community such that the efficiency of devices which are operated under this voltage will not cross a predefined acceptable range. Then, with the terminal voltage, all the communities try to adjust the VAR compensation and OLTC transformer such that power loss alone the T&D line and electricity cost is minimized. The methods work for multiple time slots interactively to find an optimal solution. Moreover, we define mathematical models for the reactive and active loads, EVs and shift them from a time slot to another slot to get the optimal results. We also prove that the proposed mathematical model ultimately converges to an optimal solution and flatten the load curve, therefore, minimizes the electricity cost.

1.4 Thesis Outline

The remainder of the thesis is organized as following. Chapter 2 presents the related work, smartgrid, microgrid, microgrid components including renewable energy

sources, EVs, ESS, and background concepts of the techniques used to develop the mathematical model and the solutions. An efficient centralized optimal joint scheduling for electrical vehicle and home appliances is presented in Chapter 3. A game theoretic mechanism design based distributed real-time electricity allocation for large residential microgrid is demonstrated in Chapter 4. Real-time demand-side management of energy by exploiting RESs, EVs and ESS to reduce the gap between planned electricity generation and real-time use of electricity is described in Chapter 5. In Chapter 6, a novel algorithm for optimal energy management and marginal cost electricity pricing for MGN is presented. Chapter 7 contains a VVCO/OECM method which demonstrates that the integration of RES, EVs and load shifting, and distributed DSM may help to reduce transmission and distribution losses in the grid. Chapter 8 concludes the thesis with future research directions.

Chapter 2

Literature Review and Preliminaries

A microgrid, a local energy network, offers integration of intermittent disseminated energy with elastic loads and energy storage which can operate autonomously to deliver electricity to customers with the cooperation of existing grid or other microgrids. In this chapter, first, we discuss the notion of microgrids, microgrid building blocks and communication networks, etc. The operation of microgrid may depend on contending interests among diverse stakeholders in electricity supply such as supply network operators, DG owners, and operators, use of electric vehicles, energy storage systems, and customers energy usage pattern. In this context, we present some solution methodologies which we apply to model most of the problems stated in Chapter 1. Finally, we will manifest contemporary and relevant research works related to our research.

2.1 Smart Grid and Smart Microgrid

The conceptual architecture of the smart grid is illustrated in Figure 2.1. The model consists of seven logical domains. Each one of the above four domains (Bulk Gen-

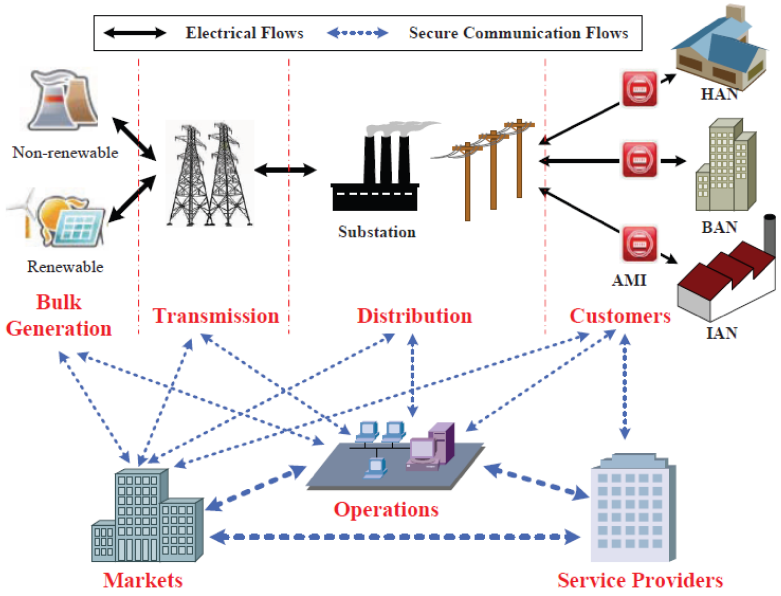

Figure 2.1: Smart Grid Conceptual Architecture

eration, Transmission, Distribution, and Customers) can generate, store, and deliver electricity in a two-way manner. The bottom three (Markets, Service Providers, and Operations) mainly manage the movement of electricity and provide relevant information and services to consumers and utilities. Three types of customers are present in this architecture: HAN (Home Area Network), BAN (Building Area Network), and IAN (Industrial Area Network). The future electric grid has a tiered architecture to supply energy to consumers. The energy starts from power generation and flows through transmission systems to distribution and eventually to consumers. The smart grid strives to utilize and coordinate various generation and production mechanisms including traditional non-renewable energy sources such as fossil fuels, and renewable energy sources such as wind, solar and hydro power. Moreover, generation plants can

be mobile or fixed depending on specific architectures. On the transmission side, a large number of substations and network operating centers manage this task. A significant number of mixed voltage power lines transmit the generated electricity from various sources to the distribution architecture. Finally, a set of complex distribution topologies delivers the electricity to regions, neighbors and premises for utilization and consumption.

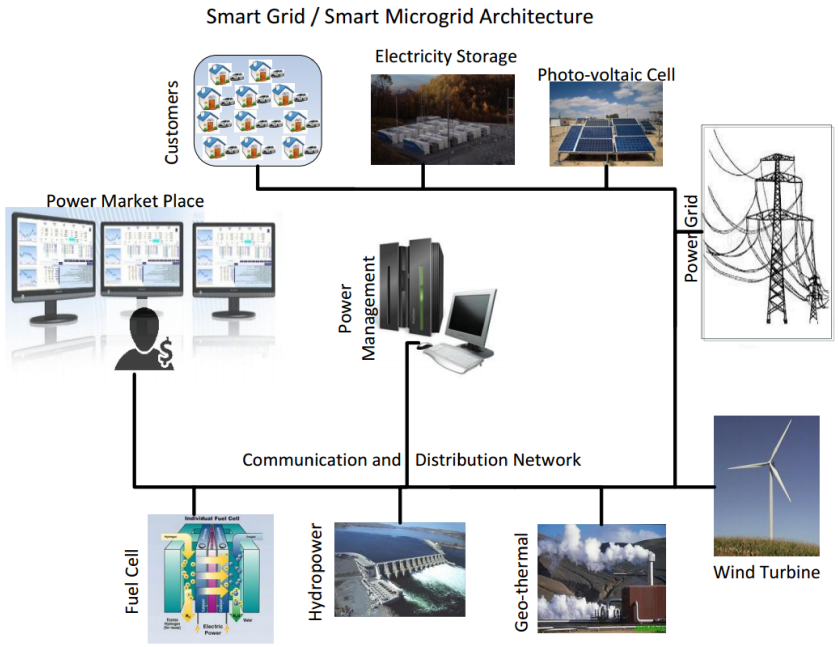

Figure 2.2: Microgrid Architecture

Figure 2.2 shows a typical grid connected microgrid and its components. Microgrids are the modern small-scale version of centralized electricity system which inherits the fundamental operational properties of the smart grid. They are designed to obtain particular local goals, such as reliability, carbon emission mitigation, diversification of energy sources, and cost reduction which is established by the community being served. Similar to the power grid, smart microgrids generate, distribute, and regulate the flow of electricity to consumers, but do so locally. Smart microgrids are the best way to integrate renewable energy sources on the community level and allow

for customer cooperation in the electricity enterprise. They form the building blocks of the ideal power system. Smart microgrids are composed of central controllers, loads (e.g., home appliances), sources of energy including wind turbines, photovoltaic systems, fuel cells, and energy storage units.

2.1.1 Smart Grid/Microgrid Components

Advanced Metering Infrastructure (AMI)

AMI [129] is dubbed as the convergence of the power grid, the communications infrastructure and the supporting information architecture. It refers to the systems that measure, collect, and analyze energy usage from advanced smart devices, including, in-home devices as well as electric vehicles charging, through various communication media, for the purpose of forwarding the data to the grid. AMI is designed to help consumers know the near real time price of electricity and thus to optimize their power usage accordingly. It as well aids the grid by obtaining valuable information about consumers power consumption in order to ensure the reliability of the electrical power system.

Supervisory Control And Data Acquisition (SCADA)

SCADA systems [33], located in the operations domain, are responsible for the real time monitoring and control of the power delivery network. Through intelligent remote control and distributed automation management, they reduce operation and maintenance costs in addition to ensuring the reliability of the power supply. There are three main elements to a SCADA system [12]; various remote telemetry units (RTUs) and programmable logic controllers (PLCs), communication systems and a Human Machine Interface (HMI). RTUs and PLCs effectively collect information from various sites and allow control actions to be performed automatically and remotely.

Communication systems bring that information from various plants or RTU sites to a central location, and occasionally returns instructions to the RTU. The HMI displays the processed information in an easily understood graphical form, archives the received data, transmits alarms and permits operator control as required.

Electricity Demand and Forecasting

Electricity demand dependent on the area such as industrial, commercial, residential, etc., but focusing on a particular environment allows a clear perception of it by sector. This will enable deployment of DR or DSM since different electricity prices could be offered based on certain guidelines set by utility companies [52]. The electricity consumption are different in different countries in different seasons and geographical position. According to 2013 world bank statistic world per person average annual electricity consumption is 4024.95 kWh, whereas USA annually consumed 12,988.256 kWh, China 3,762.08 kWh, and Canada 15,519.336 kWh [7]. Moreover, daily electricity consumption varies according to time of the day. Figure 2.3 present the daily consumption of a typical house hold customer, where energy use is high from 4:00 pm to 10 pm, moderate from 6:00 am to 3:00 pm and low from midnight to morning. The electricity use is related to daily activity and behavior of the customers.

The evolution and the concepts of the smart microgrid changes and creates new environment with diverse consideration to optimize energy uses. Inteligence deployed in building, integration of renewable energy, smart equipment, interconnected sensors to attain energy efficiency [7]. To achieve the building energy efficiency together with another model (such as prediction), the control of this equipment must be integrated within the Home Energy Management (HEMS) system. The energy efficiency can not be obtained perfectly without the load forecast. Most practical load forecast models are based on offline schemes, where predictions are conducted in advance. The

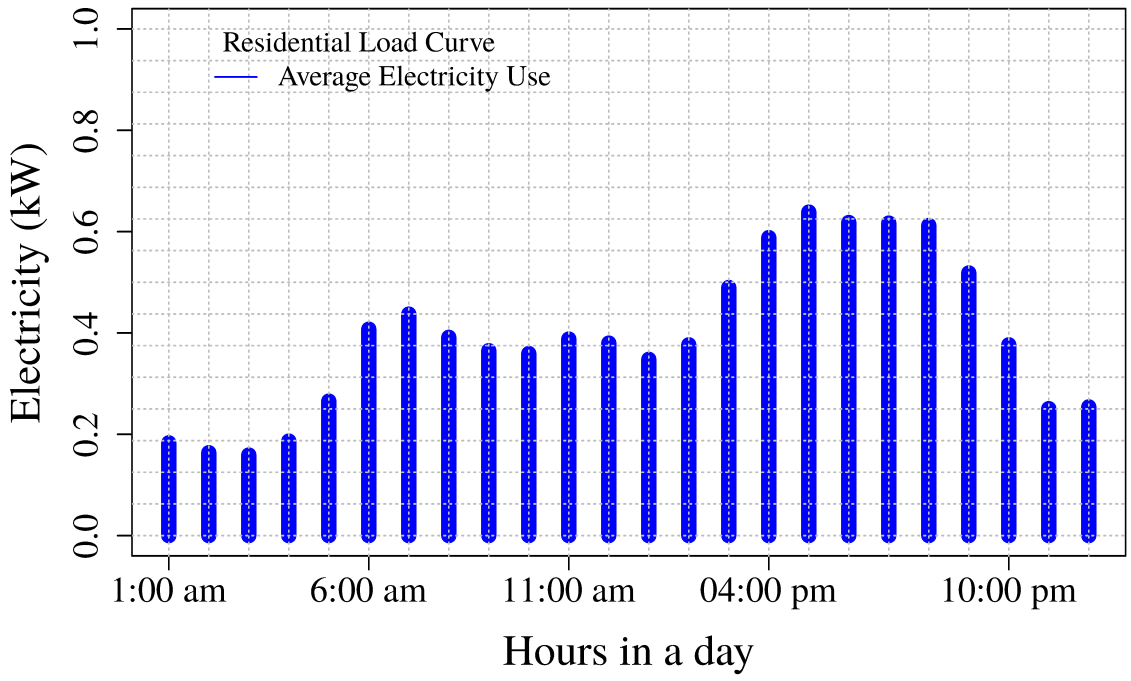

Figure 2.3: Daily average residential load

uncertainty of prediction increases with the increase of the forecast time. Demand forecast models are categorized as, (i) Very Short-Term Load Forecasting (VSTLF) that forecast loads from next seconds or minutes to several hours, (ii) Short-Term Load Forecasting (STLF): this model is used to forecast load from hours to week, and (iii) Medium-Term and Long-Term Forecast Model (MTLF and LTLF) are the forecast model which is used to forecast load from moths to year. Each of the forecast models is used for specific purpose. For more detail, please see the survey in [7].

Renewable Energy

Smart grids and smart microgrids are typically using distributed power generators. Various green power generators can be integrated to the smart microgrid such as hydroelectric, wind turbine, photovoltaic, geothermal energy, etc., as alternative energy sources. Most of the renewable energy sources are stochastic in nature [116]. Both

the availability and capacity of the renewable energy sources are dependent on the geographic position of the microgrids. Renewable energy sources such as wind turbine and solar energy need weather forecasting model for reliable generation of the targeted amount of electricity which is committed to the energy buyer market. Several stochastic models exist to predict the short-term and/or long-term power generation such as ANN, ARMA, hybrid ANN-ARAMA etc [49, 42, 55].

Electric Vehicles (EVs)

EVs and Plug-in Hybrid EVs [13] are environmentally friendly and reduce carbon emissions, in addition to being a distributed energy storage in the smart grid; that is parked EVs can supply electric power to the grid. This vehicle-to-grid concept [47] would improve the efficiency and increase the reliability of the power grid. Electrical vehicles (EVs) have been around since a century. They were very popular and were sold reasonably well till 1918 [18]. However, the use of EVs for transportation died out as the gasoline powered engine continued to improve. As environment preservation becomes an important issue around the world, EVs are poised to gain more acceptance from governments and the general public. EVs offer many benefits over traditional fuel run vehicles, such as high energy efficiency, low greenhouse gas emission, potential to use locally produced electricity (microgrid). Moreover, EVs' batteries can be used as energy storage for microgrids, since for a large amount of time (nearly 90%) they are idle [3]. The intermittent nature of the energy sources of smart microgrids requires storage to store excess power generated during off-peak hours in order to use it during peak hours. Hence, EVs may play a dual role in microgrids. They can appear as loads when charging and as energy sources when discharging. The EVs charging load on smart microgrids may vary in time as does the SOC (state of charge) of the vehicle batteries. Therefore, to charge n EVs at time t, a total electricity ($\mathcal{EV}_d(t)$) is required

from a microgrid and can be expressed as follows,

$$\mathcal{EV}_d(t) = \sum_{i=0}^{n} \{\mathcal{EV}_{i_{soc}}(t) - \mathcal{EV}_{i_{soc}}(t-1)\}, \quad n \in \mathcal{N} \tag{2.1}$$

where $\mathcal{EV}_d(t)$ equals the total energy demand of n EVs at time t, $\mathcal{EV}_{i_{soc}}(t)$ and $\mathcal{EV}_{i_{soc}}(t-1)$ represent the SOC of i-th EV at time t and $t-1$, respectively, with $1 \leq t \leq 24$ hours. $\mathcal{N}$ refers to the set of EVs in the microgrid. If the EVs are used as storage for grid electric power, then the effective electricity ($\mathcal{GE}(t)$ required at hour t is given by,

$$\mathcal{GE}(t) = \mathcal{EV}_d(t) - \sum_{j=1}^{m} \{\mathcal{EV}_{j_{soc}}(t)\}, \quad m \in \mathcal{N} \tag{2.2}$$

where $\mathcal{EV}_{j_{soc}}(t) > \mathcal{PEV}_j^{min}$, $i \neq j$, and m is the number of EVs in $V2G$ (Vehicle to Grid) operation and $m + n = |\mathcal{N}|$. $\mathcal{PEV}_j^{min}$ represents the minimum discharge (see, table 3.1) SOC of EV j, below which EV can not be discharged. If $\mathcal{EV}_{j_{soc}}(t) \leq \mathcal{PEV}_j^{min}$ then, the contribution of EV j to grid is zero.

The most significant challenges currently facing EVs are the cost and performance of their components, namely, EV batteries with \$485 to \$650 per kWh battery makes up large portion of an Electric Vehicle costs. With a usable range of $100km$, the $24kWh$ battery-powered Nissan Leaf achieves about one fifth of the compatible ICE (Internal Combustion Engine) vehicle [3]. All electric vehicle with larger battery capacity such as, $100kWh$ "Telsa Model S" offers $594km$ [81] with a greater cost which is out of range of most of the buyers [3]. These limitations seem to be holding back many potential buyers to buy EVs. Although, a survey shows that in the United States average distance traveled per person in a day is $46km$ and average trip distance is $15km$ [3]. Recently, the cost of the batteries has been steadily decreasing due to the public-private initiative in pack design optimization, cell count reduction, lower cost of cell material, economies of scale, improved manufacturing process [3].

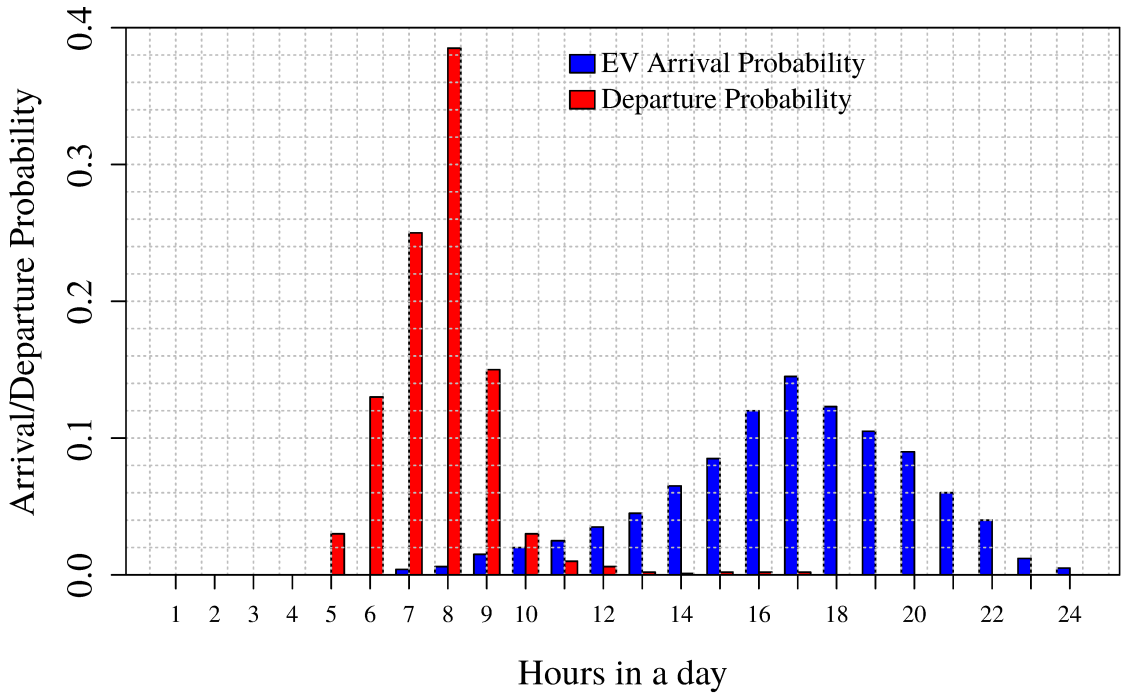

Figure 2.4: EVs arrival and departure probability

Energy Management System (EMS)

The central controller of the smart grid/microgrid is responsible for scheduling and controlling the flow of electricity from DGs (distributed generator) to the customers' home. An advanced smart meter (or aggregator) of each customer's home sends information (such as operational time slot, consumption rate, maximum and minimum capacity, etc.) of appliances to the central controller. The central controler is responsible to determine optimal (or near optimal) allocation of electricity to each home. With regard to the architecture of the energy management system, the central controller energy management system has two main approaches (i) centralized or community energy management (CEMS), and (ii) distributed electricity management system (DEMS). In CEMS architecture, the central controller accumulates all the information such as, information from the forecasting system (local load, wind, solar etc), cost function, communication network parameters from each electricity

consumer/home. The CEMS then determines the optimal (or near optimal) unit commitment for electricity allocation to achieve certain objectives. In DEMS architecture, the central controller sends all the information to all home agents in real time (or near real time). Each home agent proposes a current and future demand request to the central management system. The central management system determines the cost and sends it back to the user agent. User agent may disagree with the current cost and continue to bargain until the objective is achieved [88].

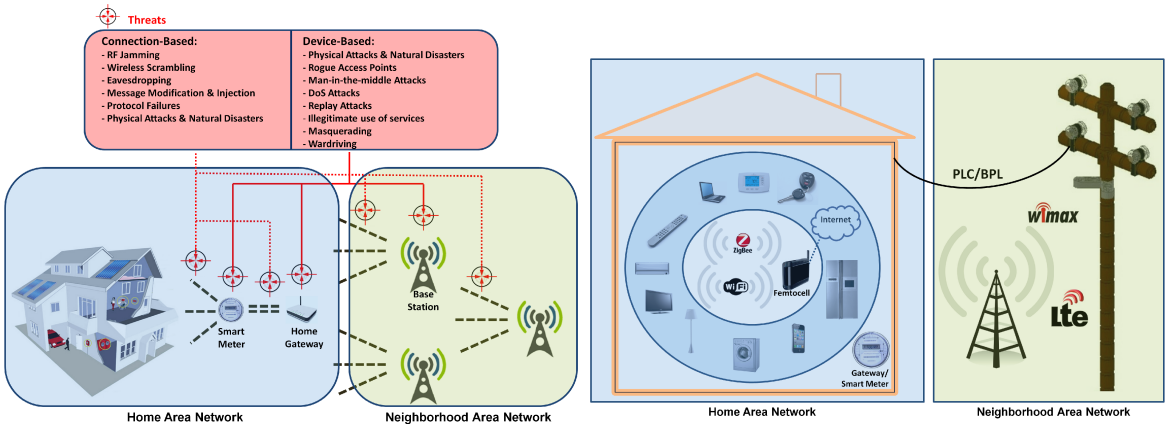

(a) Smart Grid Distribution and Corresponding threat

(b) Smart Grid Distribution network and communication mechanism

Figure 2.5: Smart Grid Communications

Communications

The operation and control of the next generation of electrical grids will depend on complex network of computers, software, and communication technologies [34]. The implementation of the smart grid will include the deployment of many new enabling technologies such as advanced sensors and metering and the integration of distributed generation resources. Such technologies and various others will require the addition and utilization of multiple communication mechanisms and infrastructures [35]. Indeed, all the goals of the smart grid could not be achieved and realized without such infrastructures that will gather and assemble data provided by smart meters, electrical

vehicles, sensors, and computer and information technology systems. Power industry gradually adopting different network technology for the partitioning of command-and-control layer of smart grid/microgrid. Fig. 2.5b [27] shows the smart grid distribution network communication mechanism. The communication networks of smart grid are classified as (i) Home Area Network (HAN) and (ii) Neighborhood Area Network (NAN).

I) Home Area Network (HAN): HANs are composed of three components, [27] (i) in-house device which provide demand side management such as energy efficiency and demand response, (ii) smart meter which collects data from the smart devices and perform specific actions according to the command sent by the grid central controller, and (iii) the gateway which connects HAN with NAN. Several network technologies are available to implement the functionality of HAN:

1. *WLAN (IEEE 802.11)*: The 802.11 is a set of standard development technology for wireless local area networks. WLAN can be a feasible solution for HAN. In case of implementation of WLAN as HAN, All smart devices (home appliances) must be equipped with WLAN adapter. All in-home smart devices communicate with WLAN enabled smart meter (home gateway) to send demand request to the smart grid/microgrid management system and receive command-response. WLAN is easy to deploy and home market penetration is high. Strengths of the WLAN are: (i) easy deployment (ii) cost is falling (iii) high home market penetration. Weaknesses are: suffer from (i) Eavesdrop, DoS attack (ii)confidentiality of sensitive information may leak.

2. *ZigBee (IEEE 802.15.4*: ZigBee is a specification for small, low power and digital radio based communication protocol and also known as low rate, wireless personal area network (LR-WPLAN). ZigBee protocols are intended for embedded applications requires for low rate and low power consumption. The ZigBee

application profile (also known as "ZigBee smart Energy") for home automation was evolved in Nov. 2007. ZigBee gateway supporting two communication stream to joining the the utility AMI central database to home appliances. Strengths of ZigBee are: (i)low power requirement (ii) low implementation cost (iii) good scalability (iv) design for home and industry use (v) relatively secure. Weaknesses are: (i) limited range, (ii) limited data rate, (iii) flooding and jamming may cause network unavailability, and (iv) single point of failure.

3. *Mobile Communication and Femtocell*: Femtocells are cellular network access point that connects home appliances (in case of HAN) to the mobile operator core network through ADSL, broadband cable Network or optical fibers network. The technology behind femtocell is UTMS, LTE and WiMAX. Femtocell is a costlier solution and signal strength varies on location of the access point (indoor, outdoor). Strengths of Femtocell are: (i) good scalability, (ii) design for home and industry use, (iii) relatively secure. Weaknesses are: (i)high cost, (ii) privacy and confidentiality, (iii) fraud and service theft, (iv) flooding attack, and (v) possible indoor health issue.

All the current HAN network protocols have their positive and negative issues in performance, coverage, cost, and security issues. For smart grid/microgrid it is challenging to choose best HAN protocol which dependent on various constraint like cost, geographic location, availability of NAN (WAN) technology etc.

II) Neighborhood Area Network (NAN): NAN (WAN) [27] technologies can be used to control and to manage smart microgrid components. There is various wide area network technology such as ADSL, cable modem, fiber to home, cellular network services, satellite services, and etc. Choice of HAN technologies will depend on various factors such as geography, population densities, availability, as well as the reliability of the technology, the cost, the security and the network infrastructure

that is already available. It is emphasized that the ADSL is highly available, but its bandwidth decreases with the increasing distance while the cable modem has high bandwidth and high availability, but inconsistent in bandwidth if the number of user increases. The fiber to the home (FTTH) is highly available in the urban area, it has high bandwidth and security, but it incurs high deployment costs. Cellular services have a high coverage area, potentially low costs, but security and policy matters. WiMax deployment does not require a huge investment as compared to the wired network, but bad weather may reduce the transmission range. The satellite service, as universally available technology, has a high cost, low effective bandwidth and low reliability during bad weather condition. BPL (Broadband over power line) can be deployed on the existing power line infrastructure specially in the rural area, but BPL deployment is high. BPL is not suited for applications as it is dependent on current on the power line and it is mostly proprietary technology. LTE is a wireless technology for fourth generation mobile network. LTE features are all IP-flat network with end-to-end quality of service operates on peak download 300Mbps and upload 75Mbps. It renders very promising choice for NAN communication network. The choice of NAN technology depends on cost, availability and geographic position of the smart grid/microgrid.

2.2 Game Theory

Game theory can be described as the subject of mathematical paradigms of conflict and interaction between intelligent, rational players or decision makers. Game theory presents general mathematical technique explaining a circumstance where two or more individuals make decisions that will affect one another actions [39, 9]. Normal form of game can be defined by the tuple (N, A, σ), where,

- N is a finite set of player,
- $A = A_1 \times A_2, \cdots, \times A_n$, where A_i is a set of finite actions of player i,
- $\sigma = (\sigma_1, \sigma_2, \cdots, \sigma_n)$, where $\sigma_i \rightarrow \mathbb{R}$ is a real-value utility (or payoff) function player i.

We will use agame model to solve the consumption scheduling or energy allocation, EV charging and discharging problem in this thesis work. In a residential microgrid, each home's HEMS acts as player which may have delivery of electricity or control consumption pattern of the equipment of the household. Each of the equipment has a set of actions for example, EVs' actions are 'charging', 'discharging' or 'remain idle', hence the action set for the EVs' are $A_{ev} = (charging_{ev}, discharging_{ev}, idle_{ev})$ and dish washer actions are: $A_d = (consume_d, idle_d)$. Now, if the player wants to charge EV and starts 'dish washer' at t, then the set of actions at t is $S_i^t = (charging_{ev}, consum_d)$ of household i. The set of actions s_i^t is the consumption strategy of player i and the player has a strategy set $s_i^t = A_{ev} \times A_d$. Therefore, player i may choose any strategy at any time t of a day such that its payoff or utility is maximized, let the payoff of player i be σ_i then we can define the payoff for player i for consumption of electricity ()say for 24 hours) to be,

$$\sigma_i = \sum_{t=1}^{24} f(s_i^t) \tag{2.3}$$

where $f(.)$ is mapping function to map consumption to cost or price. Therefore, payoff will be maximum *iff* $\sigma_i = \min \sum_{t=1}^{24} f(s_i^t)$ which means the household will pay less. If there are $\mathcal{N}$ players, then each energy household wants to maximize their individual payoff but the production cost of electricity increases with the increase of demand. Therefore the strategy of each player will affect the payoff of other player. Game theory is a very rich subject; it is used to solve the strategic problems in variety of subjects like, economics, business, computer science and logic, philosophy, biology,

political science and many others.

2.2.1 Mixed Strategy

The pure strategy of a game renders a complete description of how a player will play a game. In particular, it determines the move of a player in any circumstance he or she could handle [39, 9]. In the previous example we present the strategy of player i such as, $s_i^t = A_{ev} \times A_d$. Let the charging and discharging rate of an EV be +9.0 kWh and -9.0 kWh, and dishwasher consumption be 2.0kWh. Now, if at t the strategy $s_i^t = (+9.0, 2.0)$ is selected then the strategy s_i^t is a pure strategy. In this case the player decides to charge (9.0 kWh) the EV and dishwasher consume electricity (2.0 kWh), so the charging and consumption actions are chosen.

Now, let the actions in the strategy be selected with a probability; such as EV charging with probability p, and discharging with probability $(1-p)$ and consumption with probability q and idle with probability $(1-q)$, then the strategy s_i^t of player i is a mixed strategy.

Nash Equilibrium

Definition 2.1. (Nash Equilibrium) A (pure strategy) Nash equilibrium is a strategic form of game (N, S_i, σ_i), and the strategy profile $s^* \in S$ such that for all $i \in N$, we have

$$\sigma_i(s_i^*, s_{-i}^*) \geq \sigma_i(s_i, s_{-i}^*) \forall s_i \in S_i \tag{2.4}$$

where s_i^* is the best response (or best strategy played) of strategies (s_{-i}^*) of other players. There are many cases where a pure strategy game does not have a Nash equilibrium, i.e., the two players coin flipping game does not have a Nash equilibrium when the payoff is specified in table 2.1. Let player one strategy be on the top and player 2's strategy be on left side of the table. If the game repeated many times, then

	Head	Tail
Head	-1, 1	1 -1
Tail	1,-1	-1, 1

Table 2.1: Coin flipping game

at least one player always has options to change (best response) the current strategy to increase the payoff. [39, 9].

Definition 2.2. (Nash Equilibrium) A (mixed strategy) Nash equilibrium is a strategic form of game (N, S_i, σ_i), and the mixed strategy profile $s^* \in S$ such that for all $i \in N$ [39, 9], we have

$$\sigma_i(s_i^*, s_{-i}^*) \geq \sigma_i(s_i, s_{-i}^*) \forall s_i \in S_i \tag{2.5}$$

Here, S_i is a set of mixed strategies of any player i. Now, for the above payoff table 2.1, p and q for 'head' of player 1 and player 2 respectively. Hence, $(1-p)$ and $(1-q)$ are for choosing action 'tail' respectively. Then the game will have a Nash equilibrium.

Pareto optimality

Definition 2.3. Pareto efficiency, or Pareto optimality, is a state of allocation of resources in which it is impossible to make any one individual better off without making at least one individual worse off [39, 9]

A Pareto improvement occurs when a least one individual becomes better off without someone worse off. Pareto optimality occurs when all the household has the better price by choosing the best consumption strategy (mixed). There are no other combination of strategies which gives better results at least for one household. Nash equilibrium is not always Pareto optimal. Nash equilibrium in the other sense can be described as the local optimal solution of a problem. The bad move of a player

may stick to a point which may disable the player to increase its payoff because of the best response of other players to that move, e.g., prisoner-dilemma game. [39, 9].

2.2.2 Mechanism Design

In mechanism design, one player needs to devise a set of rules so that the other players' incentives were aligned with the first player's goals. The less-informed player works to create motives for the more informed player to take actions beneficial to the less informed. The less-informed player is called the principal (the designer) while the more-informed is referred to as the agent. The process that the principal uses to devise the correct set of incentives for the agent is known as mechanism design. One of the examples of mechanism design is auction game in which a seller wants a higher price for auction and a buyer wants a lower price; they compete to set the value of transaction neither buyer nor seller has all available information because only one party holds some information. The game theoretic mechanism design needs participation constraint and incentive constraint. Participation constraint also is known as voluntary constraints which allow with the fact that the players are not obligated to participate a mechanism but can decide whether or not to participate. The restriction creates rational places constraints for an individual on the level of expected payoff for participation. A player gets incentives in case of participation, and an incentive constraint limits the incentives to achieve the designer goal.

In our thesis (chapter 4), the operator designs the consumption game to increase the overall social benefit. Here, the operator is designer or principal of the mechanism design. Each of the households decides their energy consumption pattern to maximize the social benefit. In this mechanism design, the essential participation constraint is the strategy for charging and discharging EVs. The operator also gives incentives to EV owners those participates in V2G operation. The user decides the consumption

strategy, but the payoff and constraint are defined by the operator to achieve the maximum social benefit.

2.3 Related Work

Microgrid demand response model, use of RES, and charging of EV

Power system planners face today a pressing challenge, which requires engineering solutions to keep the system running, owing to the bulk growth of renewable energy based on variable generation technology [3]. Large scale energy storage can play a vital role in balancing supply and demand; this, however, requires vast land spaces, high installation and maintenance cost [60]. Conversely, plug-in electrical vehicles (PEV or EV) can be used as a cheap alternative to the large scale energy storage and good alternative for conventional vehicles which are considered as significant GHG emitters, producing 23% of the world GHG [1]. PEVs promise to reduce the dependency on fossil- fuel, and tap into a source of electricity that is often domestic and relatively inexpensive. In the long term, EVs are necessary to countries seeking to decarbonise the transport sector. To meet the IEA's 2DS ($2°C$ – BLUE map scenario) in 2050, transportation systems will play a major role in reducing the GHG almost by 21%. PEVs can further be used to store excess energy (known as G2V) when the production is high, and later the stored energy can be dispatched to the grid (known as V2G) when the output is low.

Evidently, the need for electricity varies throughout the day and across the seasons [2]. Current power systems are designed to meet peak demands; hence, during the off-peak period, the system remains underutilized [2]. To ensure proper functioning and quality of service, systems need to (i) estimate the load, (ii) electricity production and, (iii) a mechanism to control the electricity use. Hence, based on the electricity

and load information, smart grids or microgrids (MG) can reduce the peak demand by giving incentives to users to enable them to shift the consumption (such as EV, home appliances, etc.) away from the period of peak demand.

Several opportunities and limitations concerning the integration of EVs with the power grid and renewable energy sources were identified and used to formulate control methods for charging EVs [22]. The authors discussed two such methods: (i) a global control method for charging EVs based on global load information that is communicated utilizing load signaling, and (ii) local control methods for charging EVs based on local load conditions of the microgrid. Preliminary results show that an energy control strategy based on load information offers benefits, especially by avoiding the need for additionally generated capacity, which originates from additional peak loads. The design goal of both strategies is to charge EVs by shifting the charging from peak hours to off-peak hours to flatten the electricity demand of the grid. The authors assume that residential loads are not flexible (i.e., deferrable) to consume electricity from the grid. Further, the paper does not consider EVs for electricity storage.

A dispatch model based on a cost-benefit analysis of microgrids for selling electricity from a residential area to office buildings was presented in [76]. Simulation results show that incorporating EVs into the microgrids not only minimizes the storage and operational costs but also results in cost savings for the owners of EVs. In [76], the microgrid charges EV batteries at home at a low electricity price after office hours and dispatch the energy to office buildings at a higher rate during the day. In their work, the authors assumed that EVs do not feed power back into the grid.

The authors of [139] demonstrated a decentralized EV charging scheme using the Nash certainty equivalence principle. Their approach may be viewed as a valley filling approach. The system shifts the charging of EVs from peak hours to off-peak hours

by controlling the peak and off-peak electricity prices. The multiplayer game theory in the Nash equilibrium condition determines the peak and off-peak hour electricity price. In their work, the authors claimed that centralized control for charging a large number of EVs is computationally intractable and impractical.

Another decentralized EV charging protocol was proposed in [41]. The primary objective of this work is to shift vehicle charging from peak hours to off-peak hours by imposing a penalty on the electricity price. The proposed protocol considers different prices for different hours of the day and minimizes the peak hour load by imposing penalties on vehicles intended to be charged in peak hours.

The stochastic nature of EVs and renewable energy sources was considered for EV charging in [140] and [141]. They model the charging system using a continuous time Markov chain. Two performance metrics, called vehicle charging-blocking probability and average reward, are considered to evaluate their charging policies. They classify EVs on their different charging capacity and prioritize them accordingly [141]. The motivation of the paper is to devise an optimal charging strategy to serve the maximum number of EVs.

Most of the researchers give emphasis to use RES and microgrid technologies to charge EVs to lessen the extra burden imposed by a large number EVs to the grid. Unlike the existing research, we admit EVs as an opportunity and use as a dynamic storage which can mitigate the intermittency of RES generation by storing extra energy at high production periods and use it at peak-hour with the obligation that EV must contain target charge when departing for next drive (see Chapter 3).

Distributed strategy for real-time electricity allocation

Several researchers took initiatives to mitigate the challenges of integrating a large number of EVs, RESs and varying loads of customers. Most of the initiatives and

models are based on offline schemes and were simulated either estimating load and energy generation for a day ahead. Further, a very few of these offline algorithms consider renewable energy sources. Apart from these, a few online schemes are endeavored to mitigate the demand of microgrid customers in the microgrid scenarios which contains intermittent RESs, EVs, and loads.

In [21], the authors proposed a real time stochastic and robust optimization for a Monte-Carlo price based demand response management for residential appliances. In [56] the authors used Lyapunov optimization technique to derive an adaptive electricity scheduling algorithm by introducing the QoSE virtual queue and energy storage virtual queue to minimize the MG operation cost.

Another online-convex-optimization (OCO) programming for microgrid with single turbine-boiler generator is proposed in [82] to minimize the production cost in each time step of a microgrid. An incentive-based game-theoretic automatic energy consumption scheduling (ECS) scheme for future residential smart grid with a non-renewable energy generation is proposed in [80].

In [64] the authors proposed a hierarchical smart grid interactive architecture for grid stability and quality of service. The authors used a hidden mode Markov decision process at the controller for centralized sequential decision to maximize an accumulated reward for the microgrid and distributed auction (Vickrey auction) game to obtain optimal load profile (a solution derived by the controller) of the customers (smart homes).

The authors of [72] proposed a stochastic programming for energy planning of grid-connected microgrid, which contains renewable energy sources. The stochastic programming model is a two-stage formulation where, in the first-step, decisions are made for energy generation scheduling and adjustable load set point. In the second stage, the energy transaction as well as load adjustment decision is made based on

the load set point. The proposed stochastic programming model is a centralized management scheme, which deals with energy trading with the main grid by scheduling energy generation and load adjustment without considering the detailed characteristics of the load.

In [19] the authors presented a smart energy management system (SEMS) for optimizing the operation of the microgrid; the system consisted of a power forecasting module and an energy storage system. There, the optimal management of energy storage system across multiple time-step, considering energy price structure, stochastic generation from renewable energy sources, is evaluated and simplified to a single-object optimization problem. Finally, the authors used a matrix real-coded genetic algorithm to achieve the underlined objective of the problem.

Unlike the existing online schemes, in Chapter 4, we manifest an online distributed system which gives responsibilities and opportunities to each customer to determine their consumption profile by shifting load, utilizing EVs and RES to minimize energy costs in real-time while increase overall social benefit of the microgrid.

Power generation planning and Demand Side Management (DSM)

The rapid surge in demand for electricity is one of the most significant problems that is facing the power grid. To achieve higher reliability, robustness, and stability, the power grid is designed to serve peak demands rather than the average load. This, indeed, can result in a power generation and distribution system that is under-utilized as well as the waste of natural resources [108, 44]. Hence, utility companies are continuously adjusting the power generation of their plants to balance the total loads and their variations. Indeed, fast-responding generators such as fossil-fuel generators are costly and have a significant GHG (greenhouse gas) footprint [32]. Power system planners are also facing a pressing challenge to meet their customers surging demands

while ensuring electricity systems integrity.

To mitigate problems of uncertainties, numerous methods have been proposed to regulate users' consumption profiles. The objectives of these methods (also known as demand-side management or DSM) are to deploy the current capacity more efficiently without modifying the existing grid infrastructure [90, 69, 135, 136, 44]. The evolution of the smart grid, integration of RES, smart meters, EVs and dynamic pricing schemes have all added momentum to solve the DSM problem efficiently. Further, the widespread deployment of home energy management systems (HEMS) and communicating devices will upgrade the existing power grid structure and transform it into a more intelligent and decentralized system [17].

Recently, much research work has been done to address the DSM problem. In [69], the authors presented a heuristic-based Evolutionary Algorithm to solve the DSM based on a day-ahead load shifting technique for a microgrid which contains a large number of devices. Their results show that the proposed strategy achieves substantial savings while reducing the peak load. In [135], the authors studied the reverse power flow problem from rooftop photovoltaic (PV) elements to the substation which causes a rise in voltage when generation is larger than the aggregated load. The authors proposed a DSM system that shifts the operation of deferrable loads from peak consumption hours to high PV production periods. The simulation results showed that the proposed methods solve the voltage rise problem in an area with penetration of PVs. In [136], the authors studied a real-time based demand-side management system with advanced communication networks and proposed a game theoretic solution to smooth the peak-to-average ratio. In [79], a new approach to forecasting the residential electricity demand over 24 hours is presented; each consumer is responsible for predicting his future loads and sharing that outlook with the operator. For DSM, the authors discuss a reward which will be given to the

customers based on the accuracy of their forecasts. The authors of [17] provide a dynamic pricing scheme to motivate the customers to come up with an aggregate load profile suitable for the utility. In [105], the authors assessed the performance of exponential smoothing forecasting techniques in forecasting the energy demands of residential users. A real-time game theoretic distributed algorithm is proposed to minimize customer bills by reducing peak demand [121].RESs and EVs are used to transfer energy from one duration to another duration and schedule equipment to reduce the peak-demand and flatten the load curve [121].

In Chapter 5 we address the challenges of generation planning and DSM system and build a relation between day-ahead power planning and real-time DSM. Unlike the existing methods, our solution helps the power retailer to plan a day ahead of a cost-effective generation or purchase of electricity from the grid and deliver electricity to customers without modifying the original production plan at the time of consumption.

Enegy management and pricing in micorgrid network (MGN)

Nowadays, a regulatory body controls the vertically integrated energy supply system with an important feature that is, reliance on average-cost pricing rather than the marginal cost prices of the competitive market. Under this controlled scenario, it is nearly impossible for a new player with a small investment (e.g., a microgrid) to enter the energy market and survive [54]. For the benefit of both customers and providers, an open competitive market is desirable which accepts new suppliers and admit marginal cost prices for electricity. Several investigations have shown that the electricity market paradigm is changing with the modernization of the grid and the integration of new technology like smart grid, renewable sources, electric vehicle, and storage system [54, 28, 128].

Moreover, the evolution of smart grid, renewable energy sources (RES), and electric vehicles (EVs) are gradually changing the power flow of the network from unidirectional to bidirectional [68, 36]. It is envisioned that a microgrid network (MGN) may shortly contain hundreds or even thousands of microgrids (MG) sharing energy with each other [48]. Usually, an MG produces and consumes energy locally; in the case of shortage, it purchases electricity from the neighboring microgrids or sells whenever it has a surplus. In such scenarios, the microgrid operators may not own transmission lines, and use the existing electrical network which requires transmission costs besides the generation cost. The economic dispatch model of the MGN, therefore, is more complex than the MCP (market clearing price) and LMP (locational marginal price) model for the existing one-way energy transmission network [110].

Smart grids or microgrids add new features such as, distributed generation, storage and demand response (DR) which can improve the flexibility of demand but introduce uncertainty in the unbundled energy market. In [107], the authors studied the problem based on a game theoretical framework. They proposed an algorithm that forms MGs coalitions and minimizes the power loss and price within a coalition. In [67], the authors introduced an optimization problem that minimizes the electricity costs and peer-to-peer energy sharing losses in a distribution network consisting of MGs. They initially formulated the problem as a non-convex and later relaxed it to a second-order cone programming. For calculating the electricity price, they used TOU (time of use) price given by a central grid. In [132], the authors discussed the energy trading in a hybrid electricity market controlled by a non-profit or profit oriented local trading center (LTC) that maximizes the benefits for each consumer and seller. They formulated the trading as two optimization problems which (i) maximize the benefit of the consumer and seller with non-profit LTC and (ii) maximize the profit of the LTC by ensuring the benefits of the consumer and seller. A demand management of an

electrical network of interconnected MGs formulated as a power dispatch optimization problem is given in [38]. Here, a real time price is employed as the motivation for interaction between MGs.

To address the challenges and problems to integrate new suppliers and marginal cost pricing of electricity in an open competitive market a novel solution for sharing energy among microgrids in a microgrid network is demonstrated in Chapter 6.

Vol-VAR optimization

Currently, electric power systems use (and for many years have used) Volt-VAR (volt-ampere reactive) Optimization (VVO) to reduce the distribution losses and increase efficiency as well as to reduce the electricity peak demand [43, 71]. The primary goal of VVO is to maintain an acceptable voltage at all points of the distribution system. VVO is an advanced process which periodically responds to the operator's real-time demand using a two-way communication network and adjusts the voltage regulator and reactive compensation elements for energy delivery. Proper control of capacitor banks and voltage regulators may yield in reactive power compensation, which improves voltage regulation, power factor, and quality as well as loss reduction [74].

A few years back, the American Electric Power in Ohio took several initiatives to increase the efficiency and improve the service of the electricity delivery system. As part of the effort, a Coordinate Volt-VAR Optimization (CVVO) system is deployed to decrease the amount of energy necessary to satisfy the customers need with the quality of service [111]. One of the objectives of the CVVO is to reduce energy use and peak load by operating at the lower end of ANSI C84.1 band-A standard. Another objective is to adjust the capacitors to keep the power factor of a substation near unity [111]. In [71], the author discussed the impact of AMI smart meter,

distributed energy sources, and demand response (DR) on the Integrated Volt-VAR Optimization (IVVO). This investigation presents a significant opportunity and benefit to the IVVO and imposes additional constraint to the energy management system. In [5], the authors proposed VVCDDR (Volt/VAR Control and Distributed Demand Response), which is an integrated Volt/VAR DR control scheme to improve the reliability and efficiency of the distribution network. The authors modified the original Integrated Volt/VAR Controller (IVVC) of GridSpice to show that the IVVC with a single DR event can tighten the voltage profile and facilitate a more effective voltage conservation. A coordination scheme for DR and VVC is developed and simulated on American Electric Power distribution feeders in [115]. A different level of DR and VVC for the various types of loads show that the integration of DR and VVC in real time can reduce the demand and feeder voltage through redistribution. [84] demonstrated an Evolutionary Algorithm using the Modified Teaching-Learning-Algorithm to solve scenario based multiobjective VVC problem in a distribution network which is powered by various energy sources. In [40], the authors presented a mechanism to use the bi-directional charges and V2G function of EVs to compensate the reactive power of the distribution network. Here, the authors define a three-phase inverter topology together with DC/DC bi-directional converter which has the interface with EV battery.

In Chapter 7, we present a game prototype to address the challenges and solve the VVO problem to reduce the customer electricity cost, increase the efficiency of underline electronic devices by using RESs, EVs and shifting loads from high demand durations to low demand periods.

Chapter 3

Smart Microgrids: Optimal Joint Scheduling for Electric Vehicles and Home Appliances

In this chapter, we present an efficient centralized optimal consumption scheduling (COPCS) to solve the energy management problem of a residential microgrid by the integration of RES, optimal scheduling of charging and discharging of EVs, shifting elastic load from peak hours to off-peak hours to minimize the amount of imported electricity from the grid. We show that our COPCS system has notable performance compare to the existing DR solutions.

3.1 Motivation

In section 2.3 we present numerous aspects of synthesis of renewable energy sources, use of electric vehicles and the demand response model. Existing solutions do not consider both G2V and V2G operations of EVs, household load characteristics and intermittent nature of the RES generation to optimize residential energy use and

reduce the imported energy from external sources. The combined effect and proper scheduling of charging and discharging of EVs, shifting flexible load from one period to another period, use of renewable energy might significantly reduce the peak demand as well as demand from the external sources. Thus increase the stability, reliability, and quality of electricity service to the microgrid customers. Therefore, to obtain an optimal solution, the EVs are employed to store excess energy when generation is high compared to clients need and use the stored energy by discharging EV when demand is high. In addition to this, domestic flexible load consumptions are shifted from soaring demand duration to lower demand periods. Hence, we formulate an MILP solution for joint scheduling of home appliances and EVs charging and discharging to store and release renewable energy for balancing the need for electricity throughout the day.

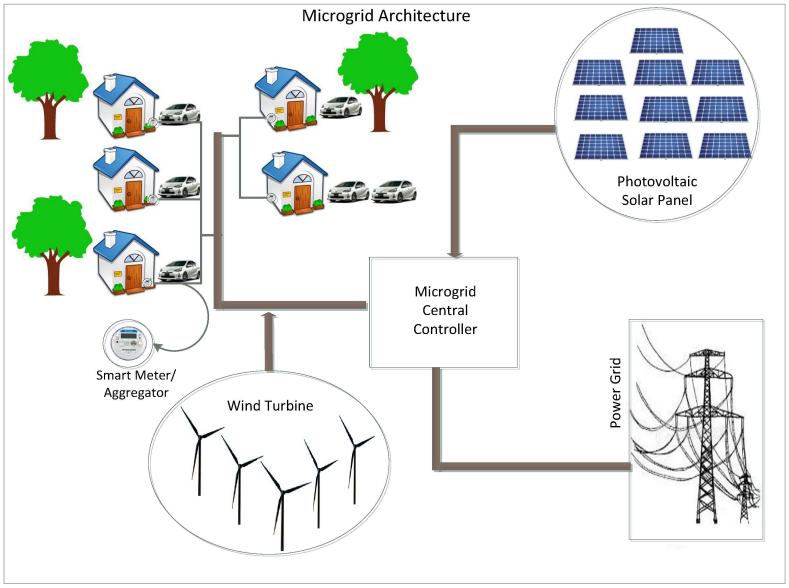

Figure 3.1: Microgrid architecture

3.2 System Model

We consider the microgrid shown in Fig. 3.1 with multiple renewable distributed generators (DGs), a central controller, a set of home appliances $\mathcal{N}$ ($|\mathcal{N}|= N$), and a set of EVs $\mathcal{M}$ ($|\mathcal{M}|= M$). For renewable energy sources, home appliances and EVs we adopt the notations of Table 3.1. The central controller of the microgrid is responsible for scheduling and controlling the flow of electricity from DGs to the customers' appliances. A smart meter or aggregator of each customer's home sends information (operational time slot, consumption rate, maximum and minimum capacity, etc.) of each appliance to the central controller. In the following subsections, we discuss each component of the system model. Finally, in Section 3.2.5 we present the objective function and constraints of the model.

3.2.1 Renewable Energy

We consider a microgrid with g renewable energy sources (wind turbine, photovoltaic cell, etc.). The total electricity generated in an hour $h \in \mathcal{H}$ is given by

$$E(h) = \sum_{g \in \mathcal{G}} \mathcal{E}_g(h). \tag{3.1}$$

Note that renewable energy sources are stochastic in nature [116]. Several stochastic models exist to predict the short-term and/or long-term power generation. In this thesis, a Markov chain state transition probability is used to predict the next 24 hours of electricity generation, as described next. Also, the proposed system model is capable to integrate any renewable, non-renewable or weather predicted energy source model. The only requirement is that the model would be able to forecast power generation in each time interval for next $\mathcal{H}$ (i.e., $\mathcal{H} = 24$) hours.

Table 3.1: Notations : Centralized Joint Scheduling of EV and Home Appliances

Symbol	Description
$\mathcal{H}$	set of time slots, ($\|\mathcal{H}\|= H$), duration of each time slots is one hour.
Energy Sources	
$\mathcal{G}$	set of Renewable Energy sources, ($\|\mathcal{G}\|= G$).
$\mathcal{E}_g(h)$	electricity (in kWh) generated from renewable energy source g at h.
$E(h)$	electricity (in kWh) generated from renewable energy sources at h.
$\mathcal{W}$	set of wind speed (in m/s^2) states, ($\|\mathcal{W}\|= W$).
$Pr(i,j)$	Markov first order transition probability from wind speed state i to j
$Pcdf(i,k)$	Markov first order cumulative transition probability from wind speed state i to k
V_l, V_r	wind speed boundary of a location, high and low respectively
Ψ	Markov transition probability matrix among solar radiation states.
$\psi_{i,j}$	Markov transition probability from solar radiation state i to j.
Ψ_I	solar radiation states (in W/m^2)
$\mathcal{Z}_i$	uniform random number over $[0,1]$.
Home appliances	
$\mathcal{C}$	set of customers.
$\mathcal{A}_c$	set of home appliances of a customer (c).
$\mathcal{N}$	set of home appliances, ($\|\mathcal{N}\|= N$).
$\mathcal{Q}$	set of type C home appliances.
$\mathcal{B}$	set of type B home appliances.
X_n^h	electricity (in kWh) consumption of appliance n in time slot (hour) h
z_n^h	indicative binary variable, for $z_n^h = 1$ equipment being used, otherwise idle
Γ_n^h	binary value, for $\Gamma_n^h = 1$ appliance n is on at h, otherwise switched off.
$\mathcal{L}_n^T$	target energy (in kWh) consumption of home appliance n
EV (Electric Vehicle)	
$\mathcal{M}$	set of EVs, ($\|\mathcal{M}\|= M$).
Y_m^h	defines charging and discharging electric energy (in kWh) of EV m in time slot (hour) h.
s_m^h	is an integer variable, where $s_m^h \in \{1, 0, -1\}$. Equivalent to 1(charging), 0(remain idle) and -1(discharging).
Λ_m^h	is a binary value, for $\Lambda_m^h = 1$ EV m is plugged-in (present) in time slot h, otherwise EV m.
$\mathcal{PEV}_m^a$	energy (in kWh) level of EV m when arrived.
$\mathcal{PEV}_m^{min}$	energy (in kWh) level lower bound for EV m.
$\mathcal{PEV}_m^{max}$	energy (in kWh) level upper bound for EV m.
$\mathcal{PEV}_m^h$	energy (in kWh) level of EV m in time slot h.
$\mathcal{PEV}_m$	net electric energy (in kWh) level consumed by EV m during a day.
$\mathcal{PEV}_m^T$	minimum or target energy (in kWh) level for EV m when departed.
$\mathcal{PEV}_T$	net electric energy (in kWh) consumed by $\mathcal{M}$ EVs during a day.

Wind turbine

Wind is a highly unstable phenomenon that cannot be fully described by any probability distribution science wind speed at every hour is correlated with the speed at previous hours. A Markov chain represents the system transition from one state to another over time. The order of the Markov chain gives the number of time steps influencing the present state of the system [113]. A first order Markov chain is used for the simulation of wind speed prediction. A second or higher-order Markov chain model can improve the wind speed prediction. Our Markov chain model for wind speed prediction uses the historical time series data for a given geographic area [98]. Suppose $\mathcal{S} = \{s_1, s_2, \cdots\}$ is the historical wind speed time series data representing the hourly wind speed in meter per second (m/s) for a long duration (3 or more years). Let $\mathcal{W}$ denote the states of wind speed for the time series wind speed data ($\mathcal{S}$). Then, the first order Markov transition probability matrix can be determined as follows:

$$Pr(i,j) = \frac{w_{i,j}}{\sum_{j=1}^{W} w_{i,j}};\ \forall i,j \in \mathcal{W}, \tag{3.2}$$

where $\sum_{j=1}^{W} Pr(i,j) = 1$ and $w_{i,j}$ is the total number of transitions from wind speed i to wind speed j for the next hour in the wind speed time series data ($\mathcal{S}$). Synthetic wind speed data can be generated by taking the cumulative probability distribution of the first order Markov state transition probability matrix of Eq. (3.2):

$$Pcdf(i,k) = \sum_{j=1}^{k} Pr(i,j);\ \forall i,k \in \mathcal{W}. \tag{3.3}$$

For generating sequences of wind speed time series data, an initial state i is selected randomly. Then a random number is chosen between 0 and 1 using a uniform random number generator. The value of the random number is compared with the values in

row i of the cumulative probability distribution of the first order or second order Markov state transition probability matrix. If the value of the random number is greater than the previous state and less than or equal to the following state, the following state is selected. Next, the speed state is converted to wind speed by using the following equation

$$V = V_l + Z_i(V_l - V_r), \tag{3.4}$$

where V_l and V_r are the wind speed boundary of the state, and Z_i is a uniformly distributed random number over $[0, 1]$. In doing so, wind speed time series of any length can be generated. The validity of this prediction model is described in more detail in [113].

From the historical (observed) or synthetic wind speed time series data, Markov first order state transition matrix can be constructed. More precisely, from the current wind speed using equations (3.3) and (3.4) the next wind speed can be predicted. Let the predicted wind speed for hour h be $V(h)$. The electricity generated from a wind turbine in hour h is then given by:

$$\mathcal{E}_g(h) = \frac{1}{2} \cdot \rho \cdot A \cdot (V(h))^3 \cdot C_p, \tag{3.5}$$

where ρ, A, and C_p represent the air density in kg/m^2, swap area of the turbine and Betz limit (maximum value of 0.59). Practical wind turbines have a cut-in and cutoff wind speed approximately from $2m/s$ to $5m/s$ and from $15m/s$ to $25m/s$, respectively. At cutoff wind speed or beyond, a wind turbine generates a constant amount of electric power at its maximum capacity, whereas below the cut-in wind speed the wind turbine does not produce any power.

Solar power

Markov models for solar radiation using historical data have been successfully used in climatology. Here, a solar radiation model with impact of cloud intensity on solar radiation is considered [85]. Solar radiation states can be expressed by the following Markov first order transition probability matrices (3.6) and (3.7).

$$\Psi = \begin{bmatrix} \psi_{0,0} & \dots & \psi_{0,k} \\ \psi_{1,0} & \dots & \psi_{1,k} \\ . & . & . \\ . & . & . \\ . & . & . \\ \psi_{k,0} & \dots & \psi_{k,k} \end{bmatrix} \tag{3.6}$$

$$\Psi_I = \begin{bmatrix} \gamma_0 & \dots & \gamma_i & .... & \gamma_k \end{bmatrix}, \tag{3.7}$$

where k is the total number of radiation states. For example, state $i = 0$ refers to the case when the sun is fully covered by clouds and solar cells do not produce any power. For $i = k$, γ_k represents the maximum intensity of solar radiation (in w/m^2). In this case (full sunlight, clear sky), solar cells produce maximum power. In (3.6) and (3.7), matrices Ψ and Ψ_I denote the transition probability matrix among solar radiation states and intensity of the solar radiation (W/m^2), respectively. Note that $\psi_{i,j}$ in matrix Ψ denotes the transition probability form solar radiation state γ_i to γ_j in Ψ_I.

Under the assumption that the cloud size is exponentially distributed with mean c_i, the solar radiation state is γ_i. Assuming that transitions among solar radiation states are sequential and circular, the transition matrix for solar radiation can be

expressed as a continuous time Markov chain [85]

$$\Psi_c = \begin{bmatrix} -\frac{S_w}{c_0} & \frac{S_w}{c_0} & & \\ & -\frac{S_w}{c_1} & \frac{S_w}{c_1} & \\ & \dots & \dots & \\ \frac{S_w}{c_k} & \dots & \dots & -\frac{S_w}{c_k} \end{bmatrix}, \tag{3.8}$$

where $\frac{S_w}{c_i}$ denotes the variation rate between solar radiations [140]. The instantaneous power of the solar panel, $\mathcal{E}_g(h)$, is directly related to the current solar radiation γ_h. Thus, the electricity generated by the photovoltaic (PV) panel can be calculated as follows [73]

$$\mathcal{E}_g(h) = \mathcal{J} \cdot \begin{cases} \frac{e_c}{K_c} \cdot (\gamma_h)^2 & 0 < \gamma_h < K_c \\ e_c \cdot \gamma_h & \gamma_h > K_c, \end{cases} \tag{3.9}$$

where the value of e_c is the corresponding efficiency which depends on the single PV cell area, ambient temperature, internal impedance, global irradiation, and other parameters at time h ($\forall h \in \mathcal{H}$). K_c is a critical radiation point in W/m^2 beyond which an increase of radiation results in a smaller increase in efficiency. $\mathcal{J}$ is the number of photovoltaic cells in the PV panel. We assume, a 0.01 m^2 PV cell with efficiency $e_c = 0.10$ (unit-less), and $K_c = 1000W/m^2$ at 25^oC.

3.2.2 Home Appliances

Let $\mathcal{C}$ be the set of customers and $\mathcal{A}_c$ be the set of home appliances (e.g., washer, dryer, refrigerator) for each customer $c \in \mathcal{C}$. Each appliance is scheduled to consume electricity or remain idle in each time interval (e.g., an hour) during the day. Residential customers may have different types of appliances namely, first, Type A (hard load), where certain appliances may have strict scheduling requirement, for example, a refrigerator should remain operational at all times, second, Type B (soft load),

where many appliances may require constant amount of electricity consumption in a continuous fashion with flexible scheduling for a limited amount of time (e.g., washing machine) and lastly, Type C (soft load), where some appliances may need a fixed amount of electricity with irregular scheduling (e.g., EV). Let X_n^h be the electricity consumption of a home appliance $n \in \mathcal{A}_c$ in time interval h. Then, the total electric energy (kWh) consumed ($\mathcal{L}_n$) by appliance n during a day is given by

$$\mathcal{L}_n = \sum_{h=1}^{H} (X_n^h \cdot \Gamma_n^h \cdot z_n^h), \quad \forall n \in |\mathcal{N}|, \tag{3.10}$$

where, $H = 24$. In case of a hard load (Type A), for each hour h, z_n^h is equal to 1 if $\Gamma_n^h = 1$. For a soft load (Type C), if an appliance consumes $\mathcal{L}_n$ unit of energy (kWh) during a day then for each hour $z_n^h \in \{0, 1\}$ if $\Gamma_n^h = 1$. In this case, when $z_n^h = 1$, appliance n consumes X_n^h units of electricity, otherwise it remains idle. Suppose that the microgrid has N home appliances, $N = |\{\mathcal{A}_1 \cup \mathcal{A}_2 \cup ... \cup \mathcal{A}_{|\mathcal{C}|}\}|$, then the total electric energy consumed by appliance (Type C) $n \in \mathcal{Q}$ ($\mathcal{Q} \subseteq \mathcal{N}$) per day must satisfy its target amount of electricity $\mathcal{L}_n^T$, which can be expressed as follows:

$$\mathcal{L}_n^T = \sum_{h=1}^{H} (X_n^h \cdot \Gamma_n^h \cdot z_n^h), \quad \forall n \in \mathcal{Q}. \tag{3.11}$$

Type B appliances consume electricity in a continuous fashion. Thus, in any time slot, if a type B equipment n is scheduled to consume electricity, it will continue to consume electricity until the total consumption is equal to the target $\mathcal{L}_n^T$ such that

$$\mathcal{L}_n^T \cdot \tau_n(k) = \sum_{h=k}^{k+r_n-1} (X_n^h \cdot \Gamma_n^h \cdot z_n^h), \quad \forall n \in \mathcal{B}, \mathcal{B} \subseteq \mathcal{N}, \tag{3.12}$$

where $r_n = \frac{\mathcal{L}_n^T}{X_n^h}$ denotes the number of time slots needed by appliance n to reach its target energy consumption $\mathcal{L}_n^T$ and $\tau_n(k)$ is a binary variable, which denotes the start

time of type B appliance n. If $\tau_n(k) = 1$, appliance n starts consuming electricity in time slot k. As type B appliances consume electricity continuously, the following constraint must be satisfied

$$\sum_{k=1}^{H} \tau_n(k) = 1 \qquad \forall n \in \mathcal{B}. \tag{3.13}$$

3.2.3 Electric Vehicle

We assume that the arrival of EVs to the microgrid follows a Poisson process with an arbitrary randomly distributed energy level. The EV stays at home (microgrid) for a random amount of time period and then departs for driving. At home, an EV charges its battery to a target energy level for the following driving schedule. EV is a special type of soft load, which can be scheduled in a flexible way i.e., charging, discharging, or remaining idle during its residence in the microgrid. If the arrival time of EV m is t_a^m and departure time is t_d^m, the energy level at arrival is $\mathcal{PEV}_m^a$ and the target energy level is $\mathcal{PEV}_m^T$. The energy consumption from the microgrid between arrival (t_a^m) and departure(t_d^m) by EV m is given by

$$\mathcal{PEV}_m = \sum_{h=t_a^m}^{t_d^m} (Y_m^h \cdot s_m^h) \tag{3.14}$$

where s_m^h denote the strategies of m (defined in 3.1). If $\Lambda_m^h = 1$ for $t_a^m \leq h \leq t_d^m$ and 0 otherwise, then the above equation (3.14) can be rewritten as

$$\mathcal{PEV}_m = \sum_{h=1}^{H} (Y_m^h \cdot \Lambda_m^h \cdot s_m^h), \tag{3.15}$$

For both safety and longevity of EVs' batteries, each EV must not discharge below

the minimum discharge level. Therefore,

$$\mathcal{PEV}_m^h \geq \mathcal{PEV}_m^{min}, \quad \forall h \in \mathcal{H}, \tag{3.16}$$

where $\mathcal{PEV}_m^h$ is defined as

$$\mathcal{PEV}_m^h = \mathcal{PEV}_m^a + \sum_{t=0}^{h} (Y_m^t \cdot \Lambda_m^t \cdot s_m^t), \ \forall h \in \mathcal{H}. \tag{3.17}$$

Note that for the proposed model when we consider only EVs without discharge capabilities, we simply ignore the state $s_m^h = -1$. In this case, s_m^h can either take 0 or 1.

Each EV may charge, discharge, or remain idle throughout the duration of its residence in the microgrid. Therefore, the net energy consumption by M EVs can be computed as

$$\mathcal{PEV}_T = \sum_{m=1}^{M} \mathcal{PEV}_m. \tag{3.18}$$

The microgrid central controller must ensure that each EV m has the target energy level when it departs for driving. Thus, the following relation must hold

$$\mathcal{PEV}_m^a + \mathcal{PEV}_m \geq \mathcal{PEV}_m^T. \tag{3.19}$$

However, an EV should not charge beyond its battery capacity and discharge below $\mathcal{PEV}_m^{min}$, as given by

$$\mathcal{PEV}_m^{min} \leq \mathcal{PEV}_m^a + \mathcal{PEV}_m \leq \mathcal{PEV}_m^{max} \tag{3.20}$$

3.2.4 Pricing Model

We define the cost function $\rho(h)$ (in hour h) as the unit price of the electricity consumption (d_i) from renewable energy sources, discharging of Evs (d_d) as well as imported power (d_e) from the external grid or microgrids, whereby

$$\rho(h) = \frac{\beta_i \cdot d_i + \beta_d \cdot d_d + \beta_e \cdot d_e}{d_i + d_d + d_e} \tag{3.21}$$

Here, β_i (e.g., $0.10\frac{\$}{kWh}$) represents a constant for local energy use and β_e (e.g., $0.15 \cdot (d_e)^{1.5}\frac{\$}{kWh}$) is a function, which increases with the increase of import from the external grid or microgrids; β_d (e.g., $0.15\frac{\$}{kWh}$) is a constant which represents the unit selling price of electricity (d_d) due to EVs battery discharge; β_d is β_i plus the compensation due to the EV's battery discharge. We assume $\beta_i < \beta_d < \beta_e$. For each hour, let the electricity price for the microgrid be $\theta(h)$. Then, we have

$$\theta(h) = \rho(h) \left(\sum_{m=1}^{M} (Y_m^h \cdot \Lambda_m^h \cdot s_m^h) + \sum_{n=1}^{N} (X_n^h \cdot \Gamma_n^h \cdot z_n^h) \right). \tag{3.22}$$

Let $\mathcal{PEV}_M^h = \sum_{m=1}^{M} (Y_m^h \cdot \Lambda_m^h \cdot s_m^h)$ and $\mathcal{L}_N^h = \sum_{n=1}^{N} (X_n^h \cdot \Gamma_n^h \cdot z_n^h)$. Therefore, the daily total electricity cost is given by

$$\theta^T = \sum_{h=1}^{H} \theta(h) = \sum_{h=1}^{H} \rho(h)(\mathcal{PEV}_M^h + \mathcal{L}_N^h) \tag{3.23}$$

The microgrid central controller adjusts the electricity unit price for the whole community by the amount of imported electricity $\delta(h)$ in each hour. The controller does not charge the price to community if the total electricity demand is equal to or lower ($\delta(h) = 0$) than that of produced. Consequently, the daily total updated electricity

price for the microgrid community is given by

$$\theta^T = \sum_{h=1}^{H} \theta(h) = \sum_{h=1}^{H} \rho(h)[(\mathcal{PEV}_M^h + \mathcal{L}_N^h) + \delta(h)]. \tag{3.24}$$

The cost of adjustment, $\delta(h)$, is as follows

$$\delta(h) = \begin{cases} 0 & \text{if } \eta(h) \leq 0 \\ \eta(h) & otherwise \end{cases}, \tag{3.25}$$

where the import electricity $\eta(h)$ is obtained as

$$\eta(h) = \mathcal{PEV}_M^h + \mathcal{L}_N^h - E(h);\ \forall h \in \mathcal{H} \tag{3.26}$$

The adjustment in Equ. (3.25) can be calculated from the following inequalities:

$$\delta(h) \leq \mathcal{PEV}_M^h + \mathcal{L}_N^h - E(h) + L(1 - \mu(h)) \tag{3.27}$$

$$\delta(h) \geq \mathcal{PEV}_M^h + \mathcal{L}_N^h - E(h) - L(1 - \mu(h)) \tag{3.28}$$

$$E(h) - \left(\mathcal{PEV}_M^h + \mathcal{L}_N^h\right) \geq \mu(h)(-L), \tag{3.29}$$

where $\forall h \in \mathcal{H}$, L is an large integer number and $\mu(h)$ is a indicating binary variable. In case of import, $\mu(h) = 1$ otherwise we set $\mu(h) = 0$.

3.2.5 Problem Formulation

To achieve best (i.e., minimum) daily price for customers, while predicting the hourly renewable energy generation $E(h)$ and fixed activation matrix for appliances (Γ_n^h) and EVs (Λ_m^h), we can write the objective function of the problem as follows:

Objective:

$$\min\left(\theta^T - \rho(h)\cdot\sum_{h=1}^{H} E(h)\right) \tag{3.30}$$

which requires to determine the values of the variables s_m^h and z_n^h. Therefore, the optimization problem Equ. (3.30) can be solved by determining the optimal schedule of the appliances and changing states of EVs during their residence in the microgrid. Formally,

$$\min(\theta^T - \rho(h)\cdot\sum_{h=1}^{H} E(h)) \tag{3.31}$$

is equivalent to

$$\min\sum_{h=1}^{H}\left[\mathcal{L}_N^h + \mathcal{PEV}_M^h - E(h) + \delta(h)\right], \tag{3.32}$$

subject to:

For type A & C

$$\sum_{h=1}^{H}(X_n^h\cdot\Gamma_n^h\cdot z_n^h) = \mathcal{L}_n^T;\ \ \forall n\in\mathcal{Q};\ z_n^h = 1\ \ for\ type\ A \tag{3.33}$$

For type B

$$\mathcal{L}_n^T\cdot\tau_n(k) = \sum_{h=k}^{k+r_n-1}(X_h^n\cdot\Gamma_n^h\cdot z_n^h);\quad \forall n\in\{\mathcal{N}-\mathcal{Q}\} \tag{3.34}$$

$$\sum_{k=1}^{H}\tau_n(k) = 1\qquad \forall n\in\{\mathcal{N}-\mathcal{Q}\} \tag{3.35}$$

For EV:

$$\mathcal{PEV}_m^{max}\ \geq\left(\mathcal{PEV}_m^a + \sum_{h=1}^{H}(Y_m^h\cdot\Lambda_m^h\cdot s_m^h)\right)\geq\mathcal{PEV}_m^T,\ \forall m\in\mathcal{M} \tag{3.36}$$

$$\left(\mathcal{PEV}_m^a + \sum_{h=1}^{H}(Y_m^h\cdot\Lambda_m^h\cdot s_m^h)\right)\ \geq\mathcal{PEV}_m^{min},\ \forall m\in\mathcal{M}, \tag{3.37}$$

and Eqs. (3.27)-(3.29).

The formulated mathematical model contains continuous (s_m^h and z_n^h) and discrete ($\delta(h)$) decision variables, and hence forms an MILP (Mixed Integer Linear Programming) model). By solving the above MILP problem, we can obtain the optimal schedule for different working states of home appliances and EVs, respectively. The minimization of imported electricity model Equ. (3.32) shifts soft loads to consume electricity from low power generation time slots to high power generation time slots. EVs charge their batteries in high power generation time slots and discharge, when the amount of power generated by the microgrid is low. The formulated MILP problem for joint scheduling of home appliances and EVs is solved using the IBM CPLEX MILP solver.

3.3 Naive Scheduling Scheme

In our naive scheduling scheme, the microgrid central controller schedules home appliances and EVs for electricity consumption without prior knowledge of the amount of generated electricity and operational time slots of the home appliances and EVs. Thus, as soon as a home appliance and/or an EV is ready, the central controller of the microgrid schedules the appliance and/or EV to consume electricity regardless of the amount of electricity generated by the microgrid. Therefore, the amount of imported electricity from the external grid or microgrids in an hour can be expressed as:

$$\eta(h) = \sum_{n \in \mathcal{N}} X_n^h + \sum_{m \in \mathcal{M}} Y_m^h - E(h), \tag{3.38}$$

where $\forall h \in \mathcal{H}$ and

$$\begin{cases} \mathcal{PEV}_m^{max} \geq \mathcal{PEV}_m^a + \sum\limits_{h=1}^{H} Y_m^h \geq \mathcal{PEV}_m^T & \text{if } m \in \mathcal{M} \\ \sum\limits_{h=1}^{H} X_n^h = \mathcal{L}_n^T & \text{if } n \in \mathcal{N} \end{cases}. \tag{3.39}$$

The total amount of imported electrical energy is given by

$$\eta^T = \sum_{h=1}^{H} [\eta(h)], \tag{3.40}$$

where,

$$\eta(h) = \begin{cases} 0, & \text{if } \eta(h) > 0 \\ \eta(h) & \text{otherwise.} \end{cases} \tag{3.41}$$

3.4 Decentralized EV charging control using non-cooperative game

A Decentralized EV charging control strategy allows each EV to determine its own charging pattern. The decentralized model is composed of a utility responsible for collecting all optimal charging strategies proposed by all EVs and broadcasting the aggregated EV demand along with predicted base demand. The problem is formulated as a non-cooperative game where each EV is a player and utility of the microgrid is the controller of the game. Each EV reacts with an optimal charging strategy for minimizing its own electricity costs by receiving the base and aggregated EV demand. The game continues until there are no changes in the charging strategy or total energy costs of any of the EVs. The game is a non-cooperative selfish game because each EV decides its "happiness" (charging scheme) by knowing all other EVs' charging strategies [139] [70]. For an individual EV m, we adopt the notation in Table 3.1. Here, base load is calculated by summing up the amount of the electricity requested by each individual home. Each appliance is scheduled to consume electricity as soon as an appliance is ready. Therefore, the base load ($\mathcal{L}_b^h$) in each hour h is given by:

$$\mathcal{L}_b^h = \sum_{n \in \mathcal{N}} X_n^h, \ \forall h \in \mathcal{H}. \tag{3.42}$$

For each time slot h between arrival (t_a^m) and departure (t_d^m), EV m's charging control can be defined as follows:

$$\mathcal{PEV}_m^{h+1} = \mathcal{PEV}_m^h + (Y_m^h \cdot s_m^h),\ h \in \{t_a^m, t_a^m + 1, ..., t_d^m\}, \quad \forall h \in \mathcal{H}, \tag{3.43}$$

with an initial energy level of $\mathcal{PEV}_m^a$. Each EV m must be charged to a target energy level at the time of departure (t_m^d). Moreover, the energy level of EV m must not violate the upper and lower bound while residing in the microgrid. Therefore, the following conditions must hold:

$$\mathcal{PEV}_m^T \leq \mathcal{PEV}_m^a + \sum_{h=t_a^m}^{t_d^m} (Y_m^h \cdot s_m^h), \tag{3.44}$$

and

$$\mathcal{PEV}_m^{min} \leq \mathcal{PEV}_m^T \leq \mathcal{PEV}_m^{max}, \tag{3.45}$$

where s_m^h represents the charge control strategy at time slot h and Y_m^h denotes the maximum charging and discharging rate of EV m. Value s_m^h can be chosen from any finite number of integer values between $\{-1, 1\}$ that represent the strategies of EV m. To compare with the proposed optimal charging strategy, the same strategies (1:charging, 0:remain idle and -1:discharging) are chosen. Therefore, we can define the set of feasible charging strategies for a predefined target as

$$\mathcal{U}^m = \{u^m = (s_m^h); \forall m \in \mathcal{M}, satisfy\ (3.44)\ \&\ (3.45)\}. \tag{3.46}$$

Let

$$u = \{u^m; 1 \leq m \leq M\} \tag{3.47}$$

be the set of charging strategies of EVs and

$$u^{-n} = \{u^m; n \neq m\} \tag{3.48}$$

the set of charging strategies for EVs without EV m. Each EV minimizes its own operating cost by determining a charging strategy with respect to the charging strategy adopted by other EVs. More specifically, the cost function of EV m can be expressed as follows:

$$J^m(u) = \sum_{h=t_a^m}^{t_d^m} \{\rho(h) \cdot s_m^h \cdot Y_m^h + \sigma(s_m^h \cdot Y_m^h - avg(u_h))^2\}, \tag{3.49}$$

where the tracking cost σ is a non negative constant and

$$avg(u_h) = \frac{1}{M} \sum_{m \in \mathcal{M}} Y_m^h \cdot s_m^h. \tag{3.50}$$

The price is given by

$$\rho(h) = \rho(\mathcal{L}_b^h + M \cdot avg(u_h)). \tag{3.51}$$

Here, ρ is defined as

$$\rho = (\beta_i \cdot d_{res}) + (\beta_d \cdot d_{discharge}) + (\beta_e^{initial} \cdot (d_{import})^{\epsilon}), \tag{3.52}$$

where $d_{res},\ d_{discharge},\ d_{import}$ represent the amount of electricity used by the microgrid customers from renewable energy sources, discharged EV battery, and imported electricity from the grid, respectively. The parameter values of the price function used for simulation a set to $\beta_i = 0.10\frac{\$}{kWh}$, $\beta_d = 0.15\frac{\$}{kWh}$ and $\beta_e = 0.15r^{1.5}\frac{\$}{kWh}$. Here, r is the amount of electricity imported from the grid. Here, β_i, β_d are constant and β_e is convex [70], therefore, ρ is a convex function. Optimal charging strategy for an EV is obtained via negotiation between electricity cost and cost incurred deviating from

the strategy. The decentralized charge control strategy thus forms a non-cooperative dynamic game. Each EV resides at home shares base load information and also tracks the average charging strategy of the whole EV population. A set of charging controls u is at Nash-equilibrium if, for all EVs m, $u^m \in \mathcal{U}^m$ is the charging strategy that minimizes the operation cost (3.49) with respect to U^{-m} [139] [70]. The negotiation of charging strategies for a day can be determined by the following procedure [139] [70]:

(S1) The utility broadcasts the predicted base load $\mathcal{L}_b^h; \forall h \in \mathcal{H}$ to all EV agents.

(S2) Each EV agent proposes a charging control strategy to minimizes its operating cost (3.49) with respect to the common aggregated EV demand broadcast by the utility.

(S3) The utility collects all proposed charging control strategies ($S2$), and updates the aggregated EV demand. The EVs' aggregated demand is broadcast to all EVs.

(S4) Repeat step ($S2$) and ($S3$) until the proposed optimal charging strategy of each EV no longer changes.

Higher values of tracking cost σ put more emphasis on minimizing the deviation from the average strategy, and on the other hand lower values put more emphasis on the electricity price. The authors of these algorithms chose $\sigma = 0.007$, which converge the homogeneous system to the Nash-equilibrium by smoothing the valley filling curve [139] [70]. For heterogeneous system the game converges to ϵ-Nash equilibrium. For each EV agent the minimization of equation (3.49) with the constraints from equation (3.44) to (3.45) and base load $\mathcal{L}_b^h$, becomes the mixed integer quadratic problem(MIQP). We solve the problem by using the IBM CPLEX MIQP solver.

3.5 Simulation

3.5.1 Simulation Setup

In this section, we evaluate our proposed algorithms (EVs with and without discharge capabilities) and compare the results with our optimal results with those obtained from naive scheduling and decentralized EV charging control schemes. In our proposed model, we consider a wind turbine with radius $10m$, air density 1.28 kg/m^2, cut-in wind speed $2m/s$, cut-off wind speed $25m/s$, $C_p = 0.59$) and photovoltaic energy sources with maximum radiation: $1000W/m^2$, photovoltaic panel area $50m^2$, and with a maximum production capacity of $1.5MWh$ (from equ. (5)) and $0.5MWh$ (from equ. (9)), respectively. The amount of electricity from the renewable energy sources is predicted for each hour of a day by using the renewable energy models described in Section 3.2. To generate synthetic time series we took observed wind speed time series during one day from the NCDC (National Climate Data Center) of NOAA (National Oceanic and Atmospheric Administration, USA). We assume a small community with 200 residential subscribers for the simulation. In the simulation, we select 1400 appliances randomly distributed over these 200 household customers. Note that each customer owns 6 to 8 appliances. Such appliances include hard and soft loads. Hard loads with daily and hourly consumption include: a 4.0 kWh (2.0kWh per hour) electric oven, a 0.8 kWh (0.8 kWh per hour) microwave, five (0.1 kWh per hour each) 2.0 kWh light bulb, a 0.36 kWh (0.12 kWh per hour) flat screen TV, a 3.6 kWh (0.150 kWh per hour) refrigerator, a 6 kWh (1.0 kWh per hour) heating system, and a 0.25 kWh (0.05 kWh per hour) laptop. Soft loads (Type B) with daily and hourly consumption include: a 1.6 kWh (0.8 kWh per hour) washing machine, a 2.4 kWh (1.2 kWh per hour) dishwasher, a 6 kWh (2.0 kWh per hour) dryer, and a 0.027 kWh (0.009 kWh per hour) battery charger. For the simulation, we vary the number of

EVs from 10 to 600, where each EV applies 3 kWh per hour charging and discharging rate with 24 kWh capacity and 3 kWh (13.5%) minimum discharge energy level. The arrival and departure of each EV in a time slot follows a Poisson process, and the initial $\mathcal{PEV}_m^a$ ($\mathcal{PEV}_m^a \geq \mathcal{PEV}_m^{min}$) and target energy level ($\mathcal{PEV}_m^T$ is in between 70% to 100% of $\mathcal{PEV}_m^{max}$) are selected randomly, with the restriction that the time span of each EV is sufficient to charge its battery to the target energy level. We have also considered certain real life EVs pattern where most of the EVs are unavailable during morning to afternoon. In this case we took the EVs arrival and departure pattern extracted from the investigation of NHTS [25].

3.5.2 Numerical Results

To evaluate the performance of the proposed system we developed the simulation program using C++ and IBM CPLEX. We execute the simulation with 40 iterations and compare the obtained results with decentralized and naive methods by considering both V2G and G2V modes of EV.

Fig. 3.2 depicts the amount of imported electricity vs. number of EVs for optimal (EV with and without discharge capabilities) and naive scheduling. The amount of imported electricity is always high in naive scheduling in comparison to the optimal scheduling schemes. The reason of this improvement in optimal scheduling schemes over naive scheduling is that optimal scheduling is able to predict future loads and power generation whereas the naive approach schedules appliances and EVs without any prior knowledge. We also observe that the optimal scheduling with EVs having discharge capabilities performs substantially better than EVs without discharge capabilities. Note that both schemes can predict future loads and the amount of generated electricity but the storage and discharge capabilities EVs leads to a significantly improve performance.

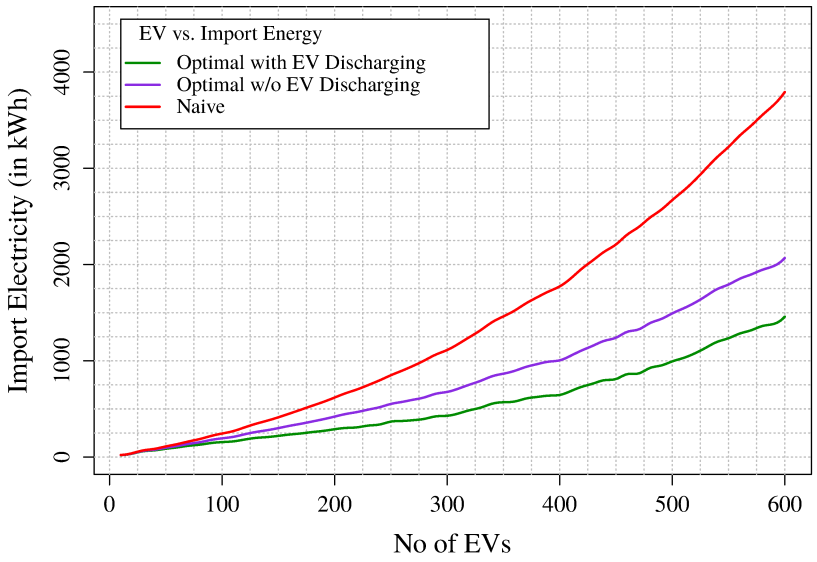

Figure 3.2: Amount of electric energy imported from the external grid/microgrid

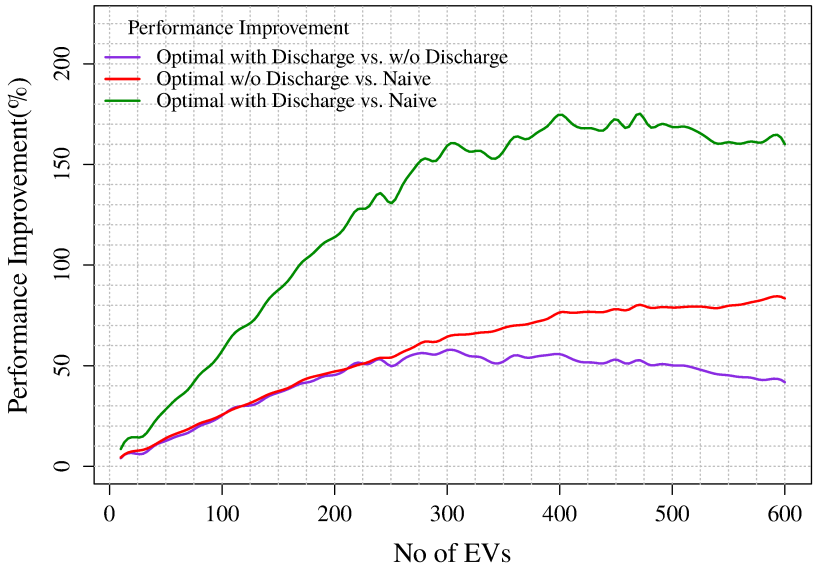

Figure 3.3: Performance Improvement

Fig. 3.3 shows the performance improvement of the proposed optimal scheduling compared to naive scheduling solution. In the case of optimal (EV with discharge) vs. naive scheduling, the performance of the optimal solution is much better and the performance gain increases as the number of EVs increases. Specifically for 10 EVs the performance improvement is nearly 8.5%, while for 400 EVs the performance

improvement is 175.37%. As the number of EVs increases, the storage capability of the system increases as well and the optimal scheduling (EV with discharge) shows a clearly superior performance over the naive approach. The optimal (with discharge) scheduling also outperforms optimal scheduling (w/o discharge), as shown in Fig. 3.3. Optimal (w/o discharge) scheduling performs better than the naive scheduling scheme. In this case, for 10 and 590 EVs the performance improvement is 4.30% and 84.34%, respectively. Fig. 3.3 also shows that after reaching a certain number of EVs (470) the performance improvement(optimal scheduling with EVs discharge) decreases as the number of EVs increases. This is because the overall load of the microgrid increases and a small amount of electricity is available to store.

Next, we compare the hourly imported electricity during a day for optimal and naive scheduling schemes. In most cases, both optimal scheduling models require less imported electricity than the naive scheduling. However, in some cases (e.g., hour 24 in Fig. 3.4) the imported electricity using the naive scheme is less than that of optimal scheduling (without EV discharge capability). This is due to the fact that the optimal scheduling algorithm intelligently shifts the soft load in order to consume electricity during high power generation hours. In contrast, naive scheduling schedules a load in a time slot if it is ready at that time and still has not yet achieved its target consumption. As a result, the total amount of imported electricity is much higher compared to the optimal scheduling schemes.

Fig. 3.5, depicts the imported electricity with respect to hourly load and hourly renewable (here, solar cell) energy generation during a day. Fig. 3.5 illustrated how the optimal scheduling with or without EV discharge capabilities shifts some loads from low power generation regions to high power generation regions in order to minimize the amount of imported electricity. Furthermore, Fig. 3.5 depicts that the

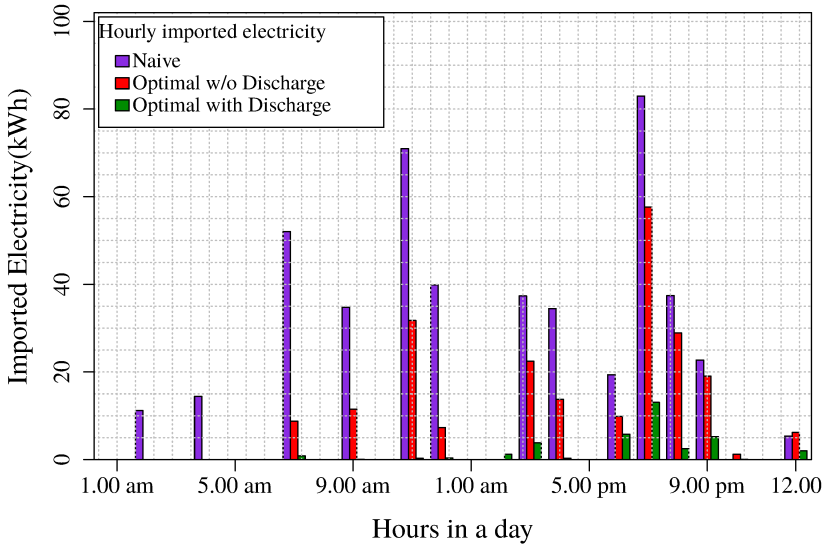

Figure 3.4: The hourly amount of electricity imported during a day

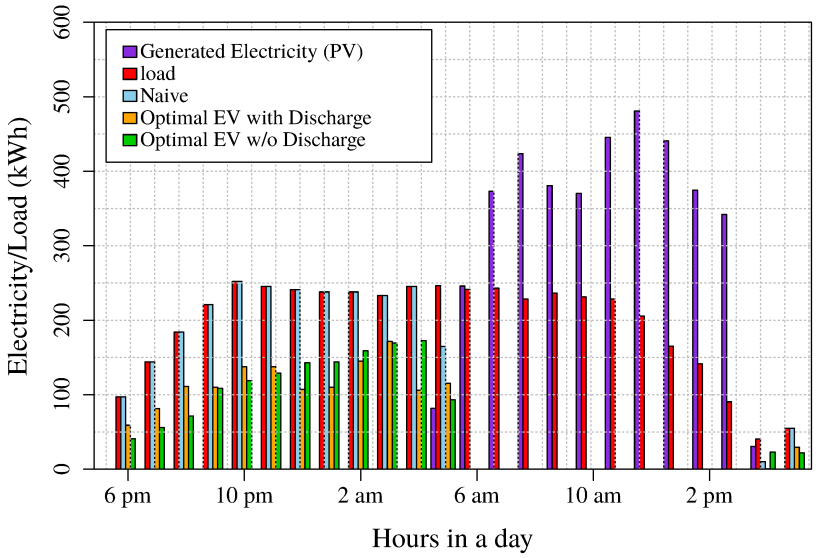

Figure 3.5: Hourly electricity imported with Naive, EVs with and EVs w/o discharge Scheduling (generation-vs-demand), using only photovoltaic energy source.

naive scheme does not shift any load from peak hours to off-peak hours, this is because naive scheme does not have any prior knowledge about the amount of future power generation and future loads. In this case, naive scheduling imports the same amount of electricity as demanded to fulfil the actual demand of an hour (i.e., in

Fig. 3.5: from 8pm to 6am). In all other cases, the amount of imported electricity in the naive algorithm is the difference between the amount of electricity demanded and the amount of electricity generated in each hour (i.e., daytime). Now, if we compare the imported electricity between the optimally scheduling EVs with discharge capability and optimal scheduling without EVs discharge capability, in most cases, the optimal scheduling with EV discharge capability imports less electricity than optimally scheduling EV without discharge capability. In few cases (i.e., 7:00 and 19:00 in Figs. 3.5), however, this not true because the optimal solution with EV discharge capability schedules appliances such that the imported electricity is minimized. Fig.

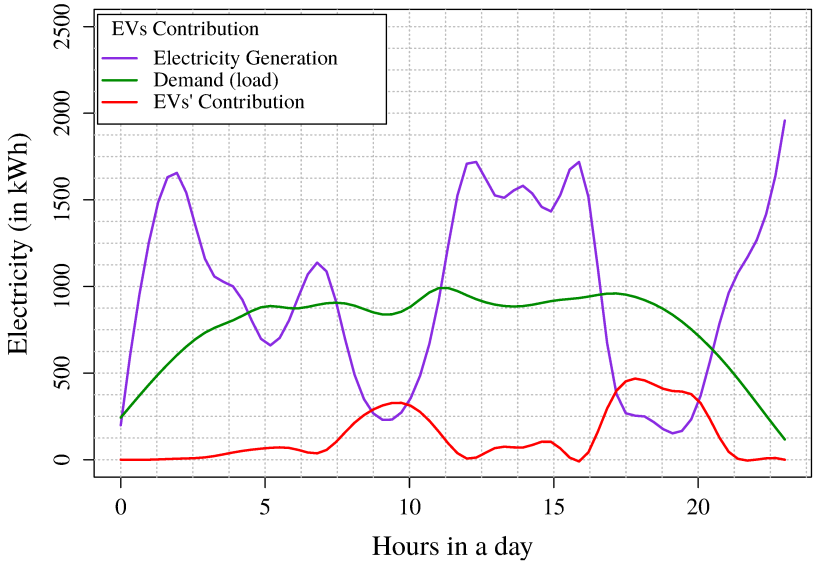

Figure 3.6: EVs' contribution (stored electricity) to microgrid.

3.6 shows the EVs contribution (amount of discharged electricity) to the microgrid in each hour during a day with respect to hourly load and hourly electricity generation. We observed that optimal scheduling with EV discharge capability discharges EVs batteries if the demand in an hour is higher than the amount of electricity generated in that hour. In most cases, the number of EVs discharging their batteries increases while the amount of load increases. In Fig. 3.6, the time period from 12 to 16 hours shows that some EVs discharge their batteries while the amount of actual load is

lower than the amount of electricity generation. The optimal scheduling shifts some of the loads from the low power generation hours (with higher load) to high power generation hours with lower load (shown in Fig. 3.7) to minimize the amount of imported electricity. Fig. 3.7 shows the amount of generated electricity, actual load,

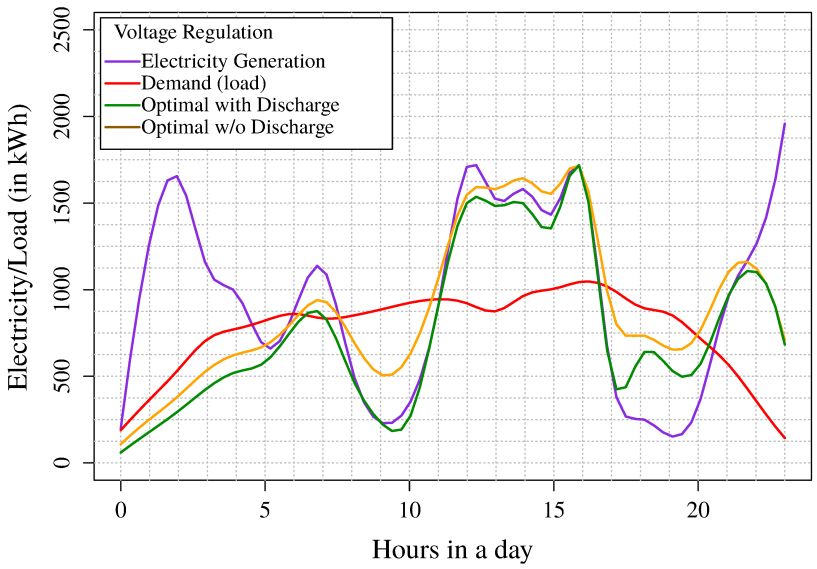

Figure 3.7: Optimal load Scheduling for EVs with and w/o discharge capability.

and effective load (distributed by both optimal scheduling) in each hour of a day. Both optimal scheduling (EVs with or w/o discharge capability) schedule loads with respect to the amount of electricity generated from the renewable energy sources in an hour. The resultant load regulation shifts loads from high periods to low periods in order to follow the renewable energy generation curve. In our solution, the results presented in Figs. 3.6 and 3.7 clearly show that the optimal scheduling with EV discharge capability shifts both load and the already generated electricity from one time slot to another time slot and thereby minimizes the amount of imported electricity. On the other hand, optimally scheduling EV without discharge capability, only shifts loads from one time slot to another time slot. As a result, both optimal scheduling strategies minimize the amount of imported electricity by effectively scheduling home appliances and EVs to consume less power. In case of optimal scheduling without EV

discharge capability, the amount of imported electricity is higher than the amount of imported electricity achieved by the optimal scheduling scheme with EV discharge capability as we observed from Fig. 3.7 from 17 to 22 hours. During these hours, the optimal scheduling with EV discharge capability, EVs discharge to mitigate the extra load, as shown in Fig. 3.6. Thus, the optimal scheduling with EV discharge capability outperforms the optimal scheduling without EV discharge capability.

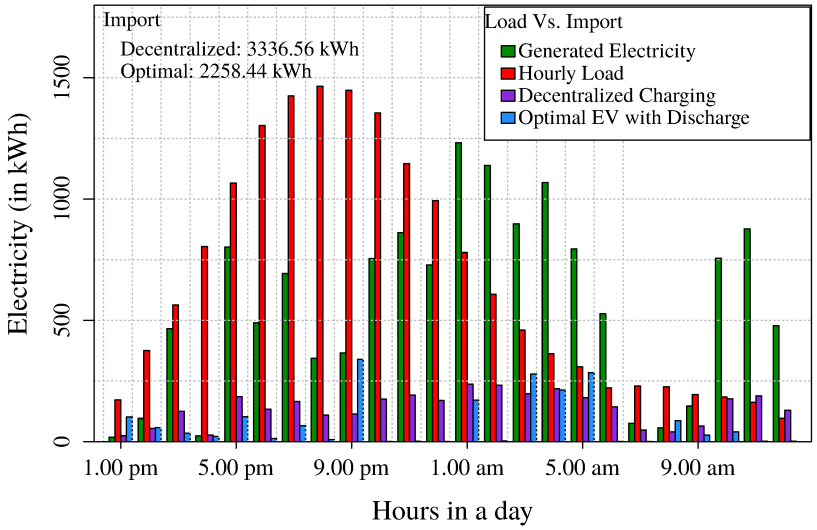

Figure 3.8: Hourly load vs. import electricity of decentralized charging and optimal EV with discharge. Electricity from renewable sources.

Next we compare our proposed optimal (EV with discharging) strategy with the decentralized Ev charging control strategy of Section 3.4. We consider both renewable and non-renewable energy sources. In our comparison, for every cases, the decentralized EV charging control strategy imports more energy than the optimal EV with discharging policy. Figs. 3.8 and 3.9 show the amount of hourly imported electricity of the decentralized EV charging control strategy and the proposed optimal with EV discharging during a day. In most cases, the amount of electricity imported by the optimal EV with discharge is less than that of the decentralized EV charging control scheme. In some cases such as, hour 21, 03, 05, 08 in Fig. 3.8 and 20, 22, 24, 01-06

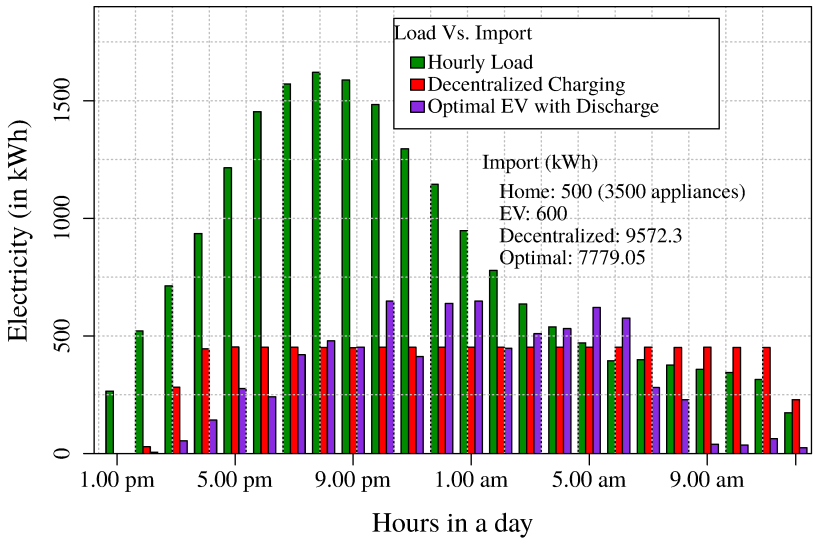

Figure 3.9: Hourly load vs. import electricity of decentralized charging and optimal EV with discharging. Power Generator: non-renewable.

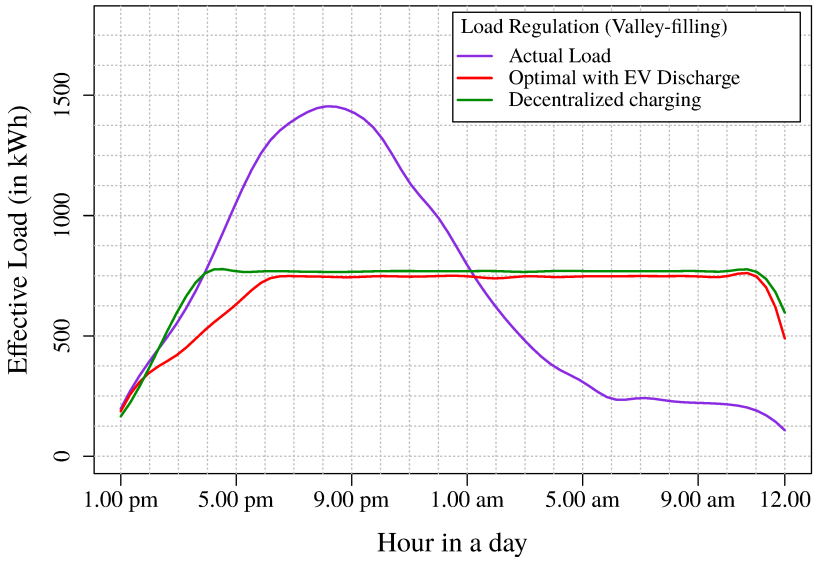

Figure 3.10: Load regulated (valley-filling) by decentralized and optimal EV with discharging schemes. Power generator: non-renewable (750kW).

in Fig. 3.9, the decentralized algorithm import less electricity than the optimal EV discharge, but the total import are higher in decentralized EV charging scheme. This is because the objective of the decentralized EV charging control scheme is to valley filling by shifting load from low generation periods to high generation periods. On

the other hand, optimal with EV discharge scheduling scheme minimizes the total import in a day by jointly determining the optimal scheduling of EVs and home appliances to consume electricity. Therefore, our proposed optimal EV with discharging imports less electricity compared to the decentralized EV charging control algorithm in a day. This is also true because the decentralized algorithm only (i) regulates EV load while the proposed algorithm regulates all soft load including EVs and (ii) for non-homogeneous systems the decentralized EV charging control method produces ϵ-Nash equilibrium. Fig. 3.10 shows the comparison of the hourly requested load, load regulated by the decentralized EV charging control and the proposed optimal EV with discharging. Both optimal and decentralized schemes schedule loads with respect to the amount of electricity generated from the non-renewable energy sources in each hour. The resultant load regulation shifts loads from peak hours to off-peak hours in order to follow the energy generation curve. Both algorithms fill the valley by shifting load from peak hours to off-peak hours. In Figs. 3.8, 3.9, and 3.10, our simulations started at 1:00pm and ended next day at 1:00pm. Here, the load is shifted from the evening high demand period to the midnight low demand period. Next, Figs. 3.11 and 3.12 show the comparison between the decentralized EV charging scheme and our proposed optimal EV with discharging scheme. In both cases, our proposed scheduling strategy imports less energy than the decentralized EV charging strategy. Fig. 3.11 shows the comparison between the amount of electric energy imported by the decentralized EV charging control strategy and our proposed optimal EV with discharging policy, while using a non-renewable energy source with a capacity of 300kW in each hour. Also, Fig. 3.12 represents the comparison of both schemes with respect to the amount of imported energy. For both cases, we vary the number of EVs to determine the effect of EV population on the imported energy. The amount of imported electric energy reduces for the increasing number of EVs (Fig. 3.12). This

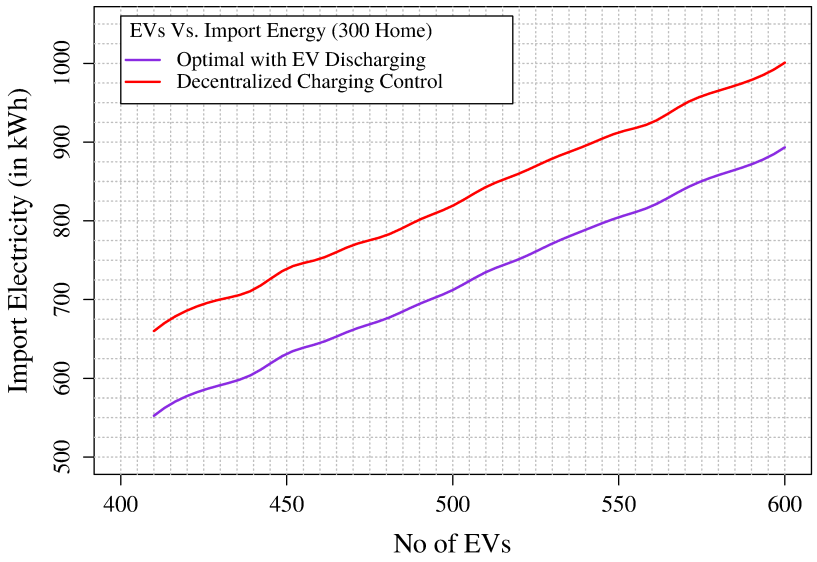

Figure 3.11: Decentralized EV charging control vs. optimal EV with discharging: effect on the energy import by varying the number of EV. Power generator: non-renewable

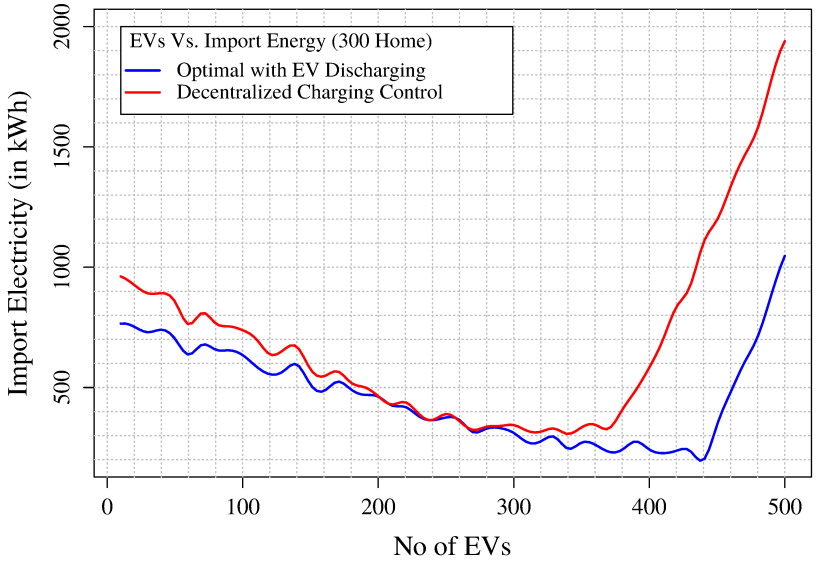

Figure 3.12: Decentralized EV charging control vs. optimal EV with discharging: effect on the energy import by varying the number of EV. Power generator: renewable

is due to valley filling characteristics of both of the algorithms. Further, increasing the number of EVs increases the amount of imported energy. This is because after a certain number of EVs, the total effective demand increases for both algorithms

(Figs. 3.11 and 3.12). The rate of increment of imported energy for optimal EV with discharging is less compared to the decentralized EV charging control. This is because the optimal schedule with EV discharging jointly schedules home appliances and EVs optimally, while the decentralized EV charging control only schedules EVs for charging and discharging.

3.6 Conclusions

In this chapter, we presented a centralized joint scheduling of EVs and home appliances for a grid connected residential microgrid with an aspiration to rely on renewable energy sources. The simulation results showed that the proposed centralized (COPCS) model reduce the amount of imported energy from the external grid. Also, we observed from the simulation results that the proposed optimal scheduling method flatten the load curve throughout the day by using the advanced features of EVs and home appliances. The proposed scheme is suitable for small to moderate sized microgrids. For large microgrid, the may require a long time to produce the solution.

Chapter 4

Distributed Real-Time Electricity Allocation Mechanism For Large Residential Microgrid

In the previous chapter, we devised a solution for the centralized joint scheduling of EVs and home appliances to minimize and balance the electric load of a microgrid throughout the day. The model is profoundly dependent on the day-ahead load forecast and predicted energy generated from RES. In this chapter, we manifest a distributed real-time electricity allocation model to meet the immediate demand of a microgrid customers. The model relies on the real consumption and generation of a time slot and predicted consumption and generation for rest of the day.

4.1 Motivation

The centralized model COPCS presented in the previous chapter can produce a solution for small and moderate sized microgrid. The COPCS model does not scale well for a microgrid with a large number of customers. Also, the COPCS is an offline

solution and heavily dependent on the day-ahead prediction of load, EVs arrival, and departure, renewable energy generation, etc., which may differ at the time of real consumption. Moreover, the COPCS is a centralized model thereby all detail specification of appliances, and EVs usage pattern should be sent to the central controller or EMS which may violate the privacy of the microgrid customers and pron to possible security risks. To address those problems, we investigated (see section 2.3) and developed an online distributed solution to schedule load based on the real-time use of electricity at time slot and predicted load as well as energy generation for the rest of the day. We use mechanism design to emphasize the user choice for scheduling their consumption and EVs' charging and discharging operations. Under the mechanism design, customers play a mixed strategy in a non-cooperative repeated game to adjust their equipment use, RES energy consumption, storage decision, and charging and discharging of EVs to decrease the personal energy cost which results the increase of the overall social benefit for the microgrid community.

4.2 System Model

In our mechanism design, the grid connected residential microgrid (MG) contains a set of renewable energy sources ($\mathcal{W}$), a set of homes connected each to a smart meter; each home has a set of appliances including EVs, and a central controller with EMS. Let $\mathcal{N}$ denote the set of residential users and $\mathcal{A}_n$ be the set of appliances of residential home $n \in \mathcal{N}$. The net electricity generation is $\mathcal{E}(t)$ at time slot t, where $t \in \mathcal{T}$ and $\mathcal{T} \triangleq \{t_s, t_s + \Delta t, ..., t_e\}$; t_s and t_e are current real time slot and end of schedule time horizon respectively. For energy sources, home appliances, load, electricity price, etc., we adopt the notations of Table 4.1.

Table 4.1: Mathematical Notations for DRTA

Notation	Description
$\mathcal{W}$	set of renewable energy sources
$\mathcal{N}$	set of residential homes
$\mathcal{A}_n$	set of appliances of home n
n	index of a residential home, $n \in \mathcal{N}$
$\mathcal{E}(t)$	net electricity (in kWh) generation from renewable at t
$\mathcal{T}$	set of time slots
Δt	interval between two consecutive time slots
$f_{ren}(t, w)$	electricity (in kWh) generated from source w at t
$\mathcal{F}_{load}$	load forecast model
$t_i,\ t_d$	start and end operational time slots of an appliance
$\mathcal{T}_{n,a}$	set of operational time slots of appliance a of home n
$\mathcal{D}(t)$	total load (in kWh) of the microgrid at time slot t
$\mathcal{D}_{-n}(t)$	total electric load (in kWh) of home n at time slot t
t_e	end time slot of simulation time
t_s	start time slot of simulation
$\rho_t(.)$	cost function to calculate electricity price at t
$d_r(t)$	electricity (in kWh) consumed form renewable at t
$d_d(t)$	electricity (in kWh) consumed from EV discharge at t
$d_e(t)$	electricity (in kWh) consumed from grid at t
β_r	unit electricity price for consumption form renewable
β_e	unit electricity price for consumption form grid
β_d	unit electricity price for consumption form EV or storage
$l^t_{n,a}$	consumption/discharge strategy at t of appliance a of n
$\mathcal{L}_{n,a}$	target electricity consumption (in kWh) of a of n
$X^I_{n,a}$	electricity consumption (in kWh) of type-I appliance
$X^{II}_{n,a}$	electricity consumption (in kWh) of type-II appliance
$\mathcal{A}^I_n$, $\mathcal{A}^{II}_n$, $\mathcal{A}^{III}_n$	set of type-I, II & III appliances of n
$\tau^k_{n,a}$	binary; consumption : continuous (1) or no (0) at k
$c^t_{n,a}$	charging of EV a of n at time t
$d^t_{n,a}$	discharging of EV a of n at time t
$\Phi^c_{n,a}$, $\Phi^d_{n,a}$	charging and discharging efficiency of EV a
$\mathcal{L}^{init}_{n,a}$	EVs' energy at arrival
$\mathcal{L}^{max}_{n,a}$, $\mathcal{L}^{min}_{n,a}$	EVs' maximum and minimum energy level
$\Omega_{n,a}$	set of feasible strategies
$\sigma_{n,a}$	feasible strategy
p^t_n	total electricity price of residential customer n at t
p^t_{-n}	total electricity price of all customers except n at t
$\mathcal{D}_n(t)$	total demand of the community except customer n
$\theta(t)$	Excess energy at time slot t
$\zeta(t)$	shortage of energy at time slot t
M	is a very big number
$\gamma(t)$	binary variable to determine shortage or excess of energy at t

4.2.1 Renewable Energy

Renewable energy sources (RES) are random in nature [116]. RES, such as wind and solar energy, need weather forecasting model for reliable generation of the targeted amount of electricity which is committed to the energy buyer market. Several stochastic models exist to predict the short-term, medium term and/or long-term energy generation such as ANN (Artificial Neural Network), ARMA (Auto Regression Moving Average), etc., [49, 42, 55]. Short term prediction is more accurate than medium term and long term prediction [31]. Roughly, a day ahead predicted wind/solar energy varies from 15% to 24% in MAPE (Mean Absolute Percentage Error [63]) from the actual generation [49, 42, 55]. Hence, for residential microgrid, in every real time slot (t_s), the prediction of the electricity generated in the next few time slots ($\{t_s + \Delta t, \cdots, t_e\}$) is updated. Let the predicted amount of electricity be $\mathcal{E}(t)$ and the amount of predicted electricity generated from $w \in \mathcal{W}$ be $f_{ren}(t, w)$ at time t, then,

$$\mathcal{E}(t) = \sum_{w \in \mathcal{W}} f_{ren}(t, w), \quad \forall t \in \{\mathcal{T} \setminus t_s\} \tag{4.1}$$

where $f_{ren}(t, w)$ can use any of the prediction models mentioned above.

4.2.2 Load Forecast

Over the last few decades, several researchers attempted to predict the anticipated load of the power grid to estimate the production capacity. Among all the load forecast models, ARMA, ARIMA, ANN are the most famous and popular [130]. The predicted load varies from the actual real-time load. The variation increases with the increase of forecast time. STLF (short term load forecast) is more accurate than MTLF (midterm load forecast) or LTLF (long-term load forecast) load prediction. Several investigations show that STLF varies from 0% to 3% whereas LTLF varies

up to 19.3% [63, 134]. In the proposed system, we suppose each smart meter is equipped with a load prediction model $\mathcal{F}_{load}$[1] and estimates the start (t_i) and end (t_d) of operation time slots of the appliance if the appliance does not propose. Therefore, the start and end instances of operation ($t_i,\ t_d$) for appliance a of customer n can be estimated by the forecast method $\mathcal{F}_{load}$, where $\{t_i, t_d\} \Leftarrow \mathcal{F}_{load}(a, n)$. Accordingly, the set of operational time slots of appliance a of n can be defined as $\mathcal{T}_{n,a} \triangleq \{t_i, (t_i + \Delta t), \cdots, (t_d - \Delta t), t_d\}$, and $\mathcal{T} \triangleq \bigcup_{a \in \mathcal{A}_n, n \in \mathcal{N}} \mathcal{T}_{n,a}$. Now, the total load of the microgrid $\mathcal{D}(t)$ at any time slot t can be calculated as:

$$\mathcal{D}(t) = \sum_{n \in \mathcal{N}} \mathcal{D}_n(t); \quad D_n(t) = \sum_{a \in \mathcal{A}_n} l^t_{n,a} \ \ \forall t \in \mathcal{T}, \tag{4.2}$$

where $l^t_{n,a}$ is the amount of electricity consumed by appliance a of home n in the time slot t.

4.2.3 Electricity Price

We define the cost function $\rho_t(\mathcal{D}(t))$ at time slot t as the cost of the energy consumption from (i) RES ($d_r(t)$), (ii) discharging of EVs ($d_d(t)$) as well as (iii) imported amount of electricity ($d_e(t)$) from the outside grid or neighboring microgrids; hence:

$$\rho_t(\mathcal{D}(t)) = \beta_r \cdot d_r(t) + \beta_d \cdot d_d(t) + \beta_e(d_e(t)), \tag{4.3}$$

and $\mathcal{D}(t) = d_r(t) + d_d(t) + d_e(t)$. Here, β_r (e.g., $0.067\frac{\$}{kWh}$ TOU (Time of Use) off-peak price [119]) represents a constant for local energy use and $\beta_e(.)$ (e.g., mid-peak 10.4 cents/kWh, $0.104 \cdot (d_e)^{1.2}\frac{\$}{kWh}$) is a function, which increases with the increase of import from the outside grid or microgrids; β_d (e.g., with 1.3 cents compensation, $0.08\frac{\$}{kWh}$) is a constant which represents the unit selling price of electricity ($d_d(t)$) due

[1] $\mathcal{F}_{load}$ can follow any of the forecast models such as ARMA, ARIMA, ANN, etc.

to EVs battery discharge. We assume $\beta_r < \beta_d < \beta_e$ and $\beta_r, \beta_d, \beta_e \geq 0$. Let the net electricity generation from the renewable (local generator) sources be $\mathcal{E}(t),\ \forall t \in \mathcal{T}$ and demand is $\mathcal{D}(t)$ then equation (4.3) can be evaluated by determining the value of $d_e(t)$, $d_r(t)$ and $d_d(t)$, $\forall t \in \mathcal{T}$.

$$d_d(t) = \sum_{n \in \mathcal{N}} \sum_{a \in \mathcal{A}_n} d^t_{n,a} \tag{4.4}$$

$$d_r(t) = \begin{cases} \mathcal{D}(t) & \text{if } \mathcal{D}(t) \leq \mathcal{E}(t) \\ \mathcal{E}(t) & \text{otherwise} \end{cases} \tag{4.5}$$

$$d_e(t) = \begin{cases} 0 & \text{if } (\mathcal{D}(t) - d_d(t)) \leq \mathcal{E}(t) \\ \mathcal{D}(t) - d_d(t) - \mathcal{E}(t) & \text{otherwise} \end{cases} \tag{4.6}$$

4.2.4 Residential Load

Each residential customer n has a set of appliances $\mathcal{A}_n$. Let us assume that each appliance $a \in \mathcal{A}_n$ consumes electricity at any time slot between $X^{low}_{n,a}$ and $X^{high}_{n,a}$. Suppose, the consumption at time slot t is $l^t_{n,a}$ then the value of $l^t_{n,a}$ is determined by the proposed strategy as $X^{low}_{n,a} \leq l^t_{n,a} \leq X^{high}_{n,a}$. The consumption rate can either be continuous or take discrete values between $X^{low}_{n,a}$ and $X^{high}_{n,a}$. In our proposed scheme, the set of consumption rates is also interpreted as the action set of the appliance. The operation window $\mathcal{T}_{n,a}$ of each appliance (a) of a residential home is either defined by the user or the appliance (smart) or predicted by the smart metering system. In the Section 3.2.2 we have discussed basic types of home appliances, here we classify and explain the home appliance more precisely.

Load Classification: We classify the appliances based on the mode of operation as (i) Type I : hard load, (ii) Type II : soft load with non-interruptable and deferrable consumption, (iii) Type III : soft load with interruptible and deferrable consumption,

and (iv) Type-IV: mixed mode appliance, the consumption pattern is the combination more than one load type. Now, suppose the target electricity consumption of an appliance a of n is $\mathcal{L}_{n,a}$, then each appliance must meet the following participation constraints [39].

Type I: Hard load

Certain appliances may have strict scheduling requirement; for example, a TV, refrigerator, etc., should remain operational between the period of operations. For each type I appliance, the total electricity consumption is,

$$\sum_{t \in \mathcal{T}_{n,a}} l_{n,a}^{t} = \mathcal{L}_{n,a}, \ \forall a \in A_n^I \tag{4.7}$$

where $l_{n,a}^{t} = X_{n,a}^{I}$ and $(X_{n,a}^{I} = X^{low} n, a = X_{n,a}^{high})$ is the non-zero constant consumption for any time slot t. The consumption strategy, $l_{n,a}^{t} = 0$, iff $t \notin \mathcal{T}_{n,a}$; otherwise, $l_{n,a}^{t} = X_{n,a}^{I}$.

Type II: Soft load

Many appliances (such as dishwasher, washing machine etc) may require constant amount of electricity consumption in a continuous fashion with flexible scheduling for a limited number of time slots (e.g., washing machine, dishwasher, dryer, etc.). Once the consumption starts, the appliance continues to consume electricity until the target consumption is achieved. Let the consumption or action profile of type-II appliance $(a \in \mathcal{A}_n^{II})$ be $l_{n,a}^{t} \in \{0, X_{n,a}^{II}\}$ at any time $t \in \mathcal{T}_{n,a}$. Here, $X_{n,a}^{II} = X_{n,a}^{low} = X_{n,a}^{high}$. The total consumption of such appliance must satisfy the following:

$$\sum_{t \in \mathcal{T}_{n,a}} l_{n,a}^{t} \geq \mathcal{L}_{n,a}, \quad \forall a \in \mathcal{A}_n^{II}, \forall n \in \mathcal{N} \tag{4.8}$$

Also, the continuous consumption of type-II appliance should follow the following relations,

$$\sum_{t=k}^{k+r_{n,a}-1} l_{n,a}^{t} \geq \left(\mathcal{L}_{n,a} \cdot \tau_{n,a}^{k}\right), \quad \forall k \in \mathcal{T}_{n,a}, \tag{4.9}$$

and,

$$\sum_{k \in \mathcal{T}_{n,a}} \tau_{n,a}^{k} = 1, \quad \tau_{n,a}^{k} \in \{0,1\}, \tag{4.10}$$

where $r_{n,a}$ is the required time slots ($r_{n,a} = \frac{\mathcal{L}_{n,a}}{X_{n,a}^{II}}$) to achieve the target consumption. The consumption strategy $l_{n,a}^{t} = 0$ for no consumption at $t \notin \mathcal{T}_{n,a}$; for all other cases the consumption strategy is determined in a way that the total electricity price for home n is minimized.

Type III: Soft load

Some appliances are flexible to consume electricity in irregular fashion (e.g., EVs). The US NHTS study shows that the arrival and departure of EVs vary over time [109]. For example, the number of EVs is higher in the evening because EV owners come back home after work and leave at morning. Now, let the EVs' charging and discharging strategy be $l_{n,a}^{t} \in \{-X_{n,a}^{low}, \cdots, 0, \cdots, X_{n,a}^{high}\}$, where $-X_{n,a}^{low}$ denotes extreme discharge rate and $X_{n,a}^{high}$ denotes the maximum charging rate. Now, let the amount of charging and discharging of an EV at time t be $c_{n,a}^{t}$ and $d_{n,a}^{t}$ respectively, then:

$$0 \leq c_{n,a}^{t} \leq (X_{n,a}^{high} \cdot \alpha_{n,a}^{t}) \tag{4.11}$$

$$0 \leq d_{n,a}^{t} \leq (X_{n,a}^{low} \cdot (1 - \alpha_{n,a}^{t})), \tag{4.12}$$

$$d_{n,a}^{t} \leq (X_{n,a}^{low} \cdot \Phi_{n,a}^{d});\ c_{n,a}^{t} \leq (X_{n,a}^{high} \cdot \Phi_{n,a}^{c}), \tag{4.13}$$

and

$$l_{n,a}^{t} = c_{n,a}^{t} - d_{n,a}^{t}. \tag{4.14}$$

Where, α is a binary variable and $\alpha^t_{n,a} = 1$ indicates EV a charging its battery at time t, otherwise discharging, and $\Phi^c_{n,a}$, $\Phi^d_{n,a}$ denote the charging and discharging efficiency of EV a. We assume that the EV's battery must be charged to a target energy level before leaving the microgrid for the next driving schedule. Hence, for EVs, the following constraint must hold,

$$\mathcal{L}^{init}_{n,a} + \sum_{t \in \mathcal{T}_{n,a}} l^t_{n,a} \geq \mathcal{L}_{n,a}, \ \forall a \in \mathcal{A}^{III}_n \tag{4.15}$$

Note that EV's battery has a minimum discharging and a maximum charging capacity. For both safety and longevity, this should always be maintained. Thus, for any time slot $t \in \mathcal{T}_{n,a}$, EVs' battery must not discharge beyond the minimum discharge level $\mathcal{L}^{min}_{n,a}$, and charge over the battery capacity $\mathcal{L}^{max}_{n,a}$. Thus, the following equation must be satisfied,

$$\mathcal{L}^{max}_{n,a} \geq \mathcal{L}^{init}_{n,a} + \sum_{t=t_i}^{t_k} l^t_{n,a} \geq \mathcal{L}^{min}_{n,a}, \quad \forall t_k \in \mathcal{T}_{n,a}, \tag{4.16}$$

All other (non-EV) appliances of Type-III must satisfy equations (5.9) to (5.11) and (4.16) (eg., Backup Battery Bank).

Incentive to the EV owners: EV owners are encouraged to participate in V2G operation when the demand is high, and production is low. In other words, EVs should discharge their stored energy when the total demand exceeds the total electricity generation in a time slot.

Type IV (Mixed Mode Appliance)

Some appliances (e.g., heat water tank, water reservoir, ice reservoir for cooling system, etc.,) perform a mix of operations similar to type I and Type II appliances. When the water or ice level is less than the minimum threshold, the appliance needs

to start immediately and continues its operation until the level is above the minimum threshold. The controller of these appliances should constantly monitor, and take actions to start the appliance to keep the water or ice level above the minimum threshold. Suppose, at a time t_i a water motor is switched on to keep the water tank filled with water above the minimum level. Now, if the water level in the tank is lower than the minimum threshold, then the motor will be started immediately and maintain its operation up to t_k to raise the water level (to a safety level) above the minimum level. Next, the water motor will be started sometime later between t_{k+1} and t_l to keep the water in the safety level. The controller of the water motor estimates that after t_l the water level will be lower than the minimum threshold. Hence, the appliance is operated like Type II appliance.

Uncertain Behavior of appliances: Now, suppose the duration of operation changes from $\mathcal{T}_{n,a}$ to $\mathcal{T}'_{n,a}$ for appliance a of home n. The changes may occur due to a prediction error or an unpredictable behavior of the appliance. The system will automatically adjust the changes in the subsequent time slot. For example, an EV owner may want to leave earlier due to inevitable circumstances. Therefore, a new finish time and target (energy level) for the EV is assigned. Depending on the changes in operational time slots, a new target energy level, and current energy consumption, the appliances will be operated as type-I, type-II or type-III.

4.2.5 Social welfare and game formulation

Suppose, the unit price of electricity at time slot t is $\eta_t = \frac{\rho_t(\mathcal{D}(t))}{\mathcal{D}(t)}$, where η_t is constant to every home during each optimization step, and η_t changes (recalculated) before each optimization step begins. Let $\Omega_{n,a}$ be the set of all feasible consumption strategies and $\sigma_{n,a}$ ($\sigma_{n,a} \in \Omega_{n,a}$) be any feasible consumption strategy of appliance a at home n. Here, we define $\sigma_{n,a} \triangleq \{l^t_{n,a} | t \in \mathcal{T}_{n,a}\}$. Then, the electricity price (in \$) of home n

at time slot t is:

$$p_n^t = \sum_{a \in \mathcal{A}_n} (\eta_t \cdot l_{n,a}^t), \quad \forall t \in \mathcal{T}, l_{n,a}^t \in \sigma_{n,a} \tag{4.17}$$

Hence, the optimal electricity price (in \$) of home n at time t is,

$$p_n^{*t} = \sum_{a \in \mathcal{A}_n} (\eta_t \cdot l_{n,a}^t), \quad \forall t \in \mathcal{T}, l_{n,a}^t \in \sigma_{n,a}^* \tag{4.18}$$

where $\sigma_{n,a}^* \in \Omega_{n,a}$ is the optimal strategy of appliance a of home n. Therefore, $p_n^t \geq p_n^{*t}$. Before optimization, if the total electricity price of the residential home n at time slot t is $P_n^{init}(t)$, then the utility function $u(\mathcal{D}_n(t), \eta_t)$ for residential home n can be defined as, $u_n(D_n(t), \eta_t) = (P_n^{init}(t) - p_n^t)$. For the optimal strategy of each appliance, the utility/payoff at any time period is $u^*(D_n(t), \eta_t) \geq u(D_n(t), \eta_t)$, and the benefit for the residential customer can be defined as,

$$\sum_{t \in \mathcal{T}} u^*(D_n(t), \eta_t) = \sum_{t \in \mathcal{T}} \left(P_n^{init}(t) - p_n^{*t} \right), \tag{4.19}$$

where, the electricity cost p_n^t of home n is determined by playing the dominant strategy[2] [114] $l_{n,a}^t$ of each appliance a at any $t \in \mathcal{T}$. Home n will get the maximum benefit by determining the optimal strategy $l_{n,a}^t$ of each appliance $a \in \mathcal{A}_n$ minimizes the total electricity cost. Next, the highest social benefit of the microgrid can be achieved by summing up the individual benefits (optimal) of all residential homes:

$$\sum_{n \in \mathcal{N}} \sum_{t \in \mathcal{T}} (P_n^{init}(t) - p_n^{*t}) \tag{4.20}$$

We assume that players are rational, and they play the game to increase its benefit (or payoff) which ultimately increases the overall social benefit (sum of all customers personal benefits). Therefore, a home customer will change its current strategy of its

[2]The formal definition of dominant strategy is given in section 4.4.

appliances *iff* there is an increase in its payoff (eq. (4.20)). Hence, the objective of each home n can be expressed as,

$$\max(\sum_{n\in\mathcal{N}}\sum_{t\in\mathcal{T}} P_n^{init}(t) - (\sum_{t\in\mathcal{T}} p_n^t + \sum_{t\in\mathcal{T}} p_{-n}^t)), \tag{4.21}$$

where p_{-n}^t is the total electricity cost of all homes without n. Therefore, in each time slot, customer n independently maximizes its own benefit and updates its charging (or consumption), discharging strategy $l_{n,a}^t, \forall a \in \mathcal{A}_n$. Next, the microgrid operator wants to maximize (minimize the unused energy) the use of local energy and minimize the amount of imported energy from the outer grid. The amount of excess or shortage of energy for a microgrid can be expressed as,

$$d_{es}(t) = \mathcal{E}(t) - \{\mathcal{D}_n(t) + \mathcal{D}_{-n}(t)\} \tag{4.22}$$

where $\mathcal{D}_n(t) = \frac{p_n^t}{\eta_t}$ and $\mathcal{D}_{-n}(t) = \frac{p_{-n}^t}{\eta_t}$. At each time slot, either $d_{es}(t)$ is positive (excess energy $\theta(t)$) or negative (shortage of energy $\zeta(t)$). If $d_{es} = 0$, there is nothing to do and $\theta(t)$ and $\zeta(t)$ can be expressed as,

$$\theta(t) \leq d_{es} + \{(1-\gamma(t)) \cdot M\}, \tag{4.23}$$

$$\theta(t) \geq d_{es} - \{(1-\gamma(t)) \cdot M\}, \tag{4.24}$$

$$\{\gamma(t) \cdot M - d_{es}(t)\} \geq 0, \quad \theta(t) \geq 0, \quad \zeta(t) \geq 0, \tag{4.25}$$

$$\zeta(t) \leq -d_{es} + \{\gamma(t) \cdot M\}, \ \zeta(t) \geq -d_{es} - \{\gamma(t) \cdot M\} \tag{4.26}$$

where $\gamma(t) = 1$ indicates the excess of energy and otherwise, a shortage of electricity. The above equations (4.23) to (4.26) are the logical constraints; these constraints always produce positive value or zero for the objective function in (4.27). Accordingly,

this will force a customer to either consume energy or restrain from consumption (or discharge) for certain time slots. Now, the objective function in eq. (4.21) ($n \in \mathcal{N}$) is modified as follows,

$$Z = \max \left[\sum_{n \in \mathcal{N}} \sum_{t \in \mathcal{T}} P_n^{init}(t) - \sum_{t \in \mathcal{T}} \eta_t \cdot \{\theta(t) + \zeta(t)\} \right] \tag{4.27}$$

The above objective function eq. (4.27) is the social benefit of the community when observed from the community point of view and in that case consumption strategies of all players are determined to get an optimal social benefit. On the other hand, to an individual player, it is the payoff function where all other players consumption is known, and the player will play its strategy for the use of electricity to increase personal benefit or payoff. Note that the electricity bill is dependent on the total demand for a particular time. Hence a player cannot decrease its electricity bill ignoring the demand of other players. The consumption strategy of one player will affects the electricity price for the whole community. A player cannot increase its payoff by harming payoffs of other players. Therefore, the simultaneous and repeated play of the game will improve the overall social benefit of the microgrid community.

4.3 Game Theoretic Mechanism Design

Game Controller: The central controller calculates the unit price η_t of electricity for each time slot and sends it to each home (smart meter). The central controller executes the following steps in each time slot (t_s),

(S1) Receive initial load information from all ($n \in \mathcal{N}$) customers and calculate initial total load $\mathcal{D}(t)$, $\forall t \in \mathcal{T}$.

(S2) Forecast electricity generation $\mathcal{E}(t)$, $\forall t \in \{\mathcal{T} \setminus t_s\}$

(S3) Calculate electricity price η_t, $\forall t \in \mathcal{T}$, total Initial price P^{init}, and $D_{-n}(t)$, $n \in \mathcal{N}$, $t \in \mathcal{T}$.

(S4) Send η_t, $\mathcal{D}_{-n}(t)$,$\forall t \in \mathcal{T}$ and P^{init} to home n upon receiving a request from home n.

(S5) Receive the proposed load $\mathcal{D}_n(t)$ from home n and update the total load $\mathcal{D}(t)$, and unit price η_t, $\forall t \in \mathcal{T}$.

(S6) Compare the calculated price in (S5) with the electricity price calculated before. If there is no change in price, go to (S7). Otherwise, repeat (S4) to (S6).

(S7) Allocate electricity for time slot t_s and update $t_s \leftarrow (t_s+1)$ and $t_e \leftarrow (t_e+1)$ in $\mathcal{T}$ and go to (S1).

Players: In each real time slot, with a finite number of iterations, residential homes n (eq. (4.27)) play the non-cooperative repeated game to maximize its own benefit. Here, the formulated non-cooperative repeated game calculates payoff for the current time slots without considering payoffs calculated in the previous (past) time slots. Each player (home) will change the strategy ($l^t_{n,a}$) of its appliances if the total cost of electricity is less (or get more benefit) than before. The game converges to optimal scheduling when there is no change in either the benefit or electricity price. Each player will continue (repeatedly) to play the game in a time slot t_s until the its own benefit (for current and future slots) does increase. In each play, a home customer tries to maximize its benefit using the objective (or utility) function expressed in equation (4.27) and with the constraints in equations (4.7) to (4.16), (4.22) to (4.26)

(S1) Each player (independently) will select an optimal strategy for each of its appliances to achieve the objective of eq. (4.27).

(S2) Determine new hourly load profile $\mathcal{D}_n(t)$ and calculate the electricity price and payoff (or benefit).

(S3) Compare the benefit with that from the previous iteration; if no improvement in benefit, the customer will keep the previous strategy, otherwise a new strategy is adopted and the calculated hourly load $\mathcal{D}_n(t)$ is sent to the central controller with a request for the updated $\mathcal{D}_{-n}(t)$ and η_t for the next iteration.

The game will end whenever there is no improvement in each player's personal benefit which results from the maximum social benefit of the community. In other words, the game ends at a Nash equilibrium when the players are unwilling to change their current strategies if there is no improvement in its benefit. The overall social benefit for the community will increase for any improvement of a player's personal payoff. Further, the operator can terminate the game anytime by broadcasting an hourly unit price more than once, which facilitates for the microgrid management system to set the time bound for the electricity allocation process.

4.4 Analysis of the game

Definition 4.1 (Dominant Strategy)**.** A strategy is dominant, if a player is always better off choosing it instead of choosing all other strategies, regardless of the strategy chosen by all other players. To be more precise, a strategy is strictly dominant if the payoff for choosing this strategy is always strictly higher than the payoff of any other strategy. A strategy is a weak dominant strategy if payoff for choosing this strategy is as high as the payoff for choosing some other strategies.

Definition 4.2 (Dominant Strategy of MG)**.** Let, $S_n \triangleq \{l^t_{n,a} | \forall a \in \mathcal{A}_n, \forall t \in \mathcal{T}\}$ be the set of strategies played by a player n. S_n is dominant if it increases the overall

social benefit defined in eq. (4.27) and no other strategy can achieve a higher benefit. If S_n is dominant, we say S_n satisfies (4.27).

At each iteration, player n determines the strategies of its appliances which minimize the electricity price and increase the overall social benefit. The strategy S_n is the best response to the current strategies (S_{-n}) of all the players. The strategies (S_{-n}) of other players are fixed at the time of optimization. Hence, S_n is a dominant strategy of all appliances of customer n.

Note: If there exists one (or more) strategy $S_n^{'}$ which results in the same social benefit as S_n, then the strategy S_n is referred to as a weak dominant strategy.

Lemma 4.4.1 (Nash Equilibrium)**.** *The $\mathcal{N}$ player game with a set of strategies $\{S_n | n \in \mathcal{N}\}$ and with objective function* (4.27) *converges to a Nash equilibrium.*

Proof Nash equilibrium: η_t is constant when there is no import and discharge of energy, otherwise η_t increases with the increase of discharge and/or import energy (Section 4.2.3).

- case 1 (constant η_t) : The game will terminate immediately with the current strategy, therefore current strategy of the game is the dominant strategy and forms a Nash equilibrium. In this case $\zeta(t)$ of eq. (4.27) becomes zero $\forall t \in \mathcal{T}$, and $\theta(t)$ is minimized by charging the EVs beyond their target up to the maximum capacity, otherwise $\theta(t)$ does not have any effect to change the current strategy of the players.

- case 2 (η_t is an increasing function for any $t \in \mathcal{T}$): Each player n deviates from the current strategy (to a new strategy $S_n^{'}$), as a best response to the other players current strategies (S_{-n}) to minimize $\sum_{t \in \mathcal{T}} \eta_t \cdot \{\theta(t) + \zeta(t)\}$ and to increase its own benefit (eq. (4.27)). Let t_i and t_j be two time slots in the simulation time horizon $\mathcal{T}$, where $\theta(t_i), \zeta(t_j) > 0$ and $\theta(t_j), \zeta(t_i) = 0$. Therefore, by definition

(Section 4.2.3) $\eta_{t_i} < \eta_{t_j}$. Let, the payoff (or overall social benefit) be Z . Now, player n changes its strategy from S_n to $S_n^{'}$, and let, the new benefit be $Z^{'}$. Then the changes in the benefit of the player became,

$$(Z^{'} - Z) = \eta_{t_i}^{'} \cdot \theta^{'}(t_i) - \eta_{t_i} \cdot \theta(t_i) + \eta_{t_j}^{'} \cdot \zeta^{'}(t_j) - \eta_{t_j} \cdot \zeta(t_j) \quad (4.28)$$

where $\theta(t_i), \theta^{'}(t_i)$ are the old and new excess energy, and η_{t_i} and $\eta_{t_i}^{'}$ are the unit prices at t_i. Similarly, ζ_{t_j}, η_{t_j} and $\zeta_{t_j}^{'}, \eta_{t_j}^{'}$ represent the old and new shortage of energy and unit prices at t_j. Now, according to equation (4.27), the change of strategy minimizes $\theta(t_i)$ and $\zeta(t_j)$. Which definitely forces player n to consume (and/or charge EVs) energy at t_i and seize consumption of those appliances and/or discharge EVs at t_j. We know, $\beta_r < \beta_d < \beta_e$ (Section 4.2.3). Therefore, $\eta_{t_i} = \eta_{t_i}^{'}$ and $\eta_{t_j} > \eta_{t_j}^{'}$ while $\theta_{t_i}^{'} \geq 0$ and $\zeta_{t_j}^{'} \geq 0$. Hence, the overall benefit will increase. The player n will change its strategy. Conversely, the players will not change its current strategy if the change causes $\eta_{t_j} \leq \eta_{t_j}^{'}$. The game terminates where the change of strategy will not improve the benefit of the player. Therefore, the game always converges to a Nash equilibrium. Further, at the Nash equilibrium state, the benefit calculated by each user is the social benefit of the microgrid community because the payoff function of each player has included the benefits for all other customers.

Lemma 4.4.2 (Optimal Solution)**.** *The Nash equilibrium state of $\mathcal{N}$ player microgrid game (in section 4.3) is an optimal solution of the problem.*

Proof Let Z be the optimal solution of the problem which produces Nash equilibrium of the game. For the proof, let us assume that there are at least two slots t_i and t_j of player n, where increasing of consumption at t_i and decreasing of consumption at t_j produce an optimal solution $Z^{'}$ (i.e., increases social benefit from Z). Therefore,

$$Z^{'} - Z \ > 0 \implies [\eta_{t_i} \cdot \theta(t_i) - \eta_{t_i}^{'} \cdot \theta^{'}(t_i) + \eta_{t_j} \cdot \zeta(t_j) - \eta_{t_j}^{'} \cdot \zeta^{'}(t_j)] > 0 \quad (4.29)$$

But, if such strategy exists for player n, then the player n must play the strategy because by definition the strategy for $Z^{'}$ is the dominant strategy (eq. (4.27)). Either, no such strategy exists (impossible) or the strategy produces the same results as Z, otherwise, it is a contradiction.

4.5 Simulation and numerical results

4.5.1 Simulation setup

In this section, we evaluate our proposed real time energy allocation algorithm and compare the results with those obtained from COPCS [120] based on the observed load and the observed energy generation. In our proposed model, we consider wind turbines, each with a maximum radius of $3.5m$, air density 1.28 kg/m^2, cut-in wind speed $2m/s$, cut-off wind speed $25m/s$, $C_p = 0.59$ with a maximum hourly production capacity of $200kWh$. We also consider photovoltaic energy sources with a maximum radiation $1000W/m^2$, panel area $5m^2$, and with $50kWh$ production capacity. The amount of electricity from the RES is predicted for each hour of a day by using the renewable energy models described in [120]. We consider microgrid communities sized from 100 to 1.0×10^6 homes for the simulation. For each microgrid community, we choose the number of RES such that the generated energy can fulfill at least 50% of the demand. Next, in each time step the energy from the renewable sources for next 24 hours (starting from noon (0h) to next day before noon (23h)) is amended (with random values) based on the multinational model forecast error growth chart [31]. The load amendments includes variation of switch on and/or switch off time, amount of target energy consumption, addition of new appliances, and elimination from existing appliances of homes.

In the simulation, we choose 10 to 15 appliances at random for each home. Such

appliances include hard (type I) loads (7 to 10), soft (type II & III) and mixed (type IV) loads (3 to 5). Hard loads with daily and hourly consumption include electric ovens, microwave oven, light bulbs, flat screen TV, refrigerators, heating system, and laptops. Soft loads include washing machines, dishwashers, dryers, and battery charger. For detailed specification, see [120]. In the simulation, we choose 0 to 2 EVs randomly for each home. Each EV applies 2.0 to 6.0 kW (0.5 kW interval) per hour charging and discharging rate with 24 kWh capacity, and randomly selected 3.0 to 7.5 kWh minimum discharge energy level. We assume the charging and discharging efficiency of each EV to be 0.85 (85%) and 0.95 (95%) respectively. The arrival and departure of each EV (66% of all EVs) in a time slot follows a Poisson distribution and the initial $\mathcal{L}_{n,a}^{init}$ ($\mathcal{L}_{n,a}^{init} \geq \mathcal{L}_{n,a}^{min}$) and target energy level ($\mathcal{L}_{n,a}^{T}$ is in between 70% to 100% of $\mathcal{L}_{n,a}^{max}$) are selected randomly, with the restriction that the time span of each EV is sufficient to charge its battery to the target energy level. We have also considered certain real life EVs pattern where most of the EVs (34%) are unavailable during the morning to afternoon. In this case, we took the EVs arrival and departure pattern extracted from the investigation of NHTS [109]. In addition, we also admit mixed mode appliances such as hot water tank (capacity 60 gallons, energy consumption 1.2kW, minimum water level 60% of the capacity, minimum and maximum water temperature 49°C and 60°C), ice bank cooling system (capacity: 2000kg, initial freezing time: 8 hours with 2kW, minimum ice temperature: -5°C to -3°C, consumption rate (in operation): 1.2kW), etc. In case of electricity price we admit the charging rate from Hydro ONE (see, http://www.hydroone.com/TOU), add incentive ($CAD\$0.02$) for EV discharge and CAD0.0012(d_e)^{1.2}$ for each 1kWh energy imported from the grid.

We use C++ MPI, IBM CPLEX concert technology to develop the simulation programs. The dominant (best response) strategy of each play (iteration) of a player

is determined by the IBM CPLEX MILP optimizer. The simulation is executed several times with various setups to get more accurate results. The simulations were executed on HP cirrus cluster which composed of composed of 100 computing nodes with AMD Opteron processors x86, 64 bit, 4 to 8 cores in our university.

4.5.2 Numerical results

To evaluate the performance of the DRTA algorithm, we execute both allocation schemes on variable sized residential microgrid which comprises, $100 \cdots 1000$ homes. At each time slot, the microgrid EMS estimates the electricity generation (a day ahead) for the future slots and correct the errors of previous prediction. We consider current time slot t_s in real time; hence the energy generation at t_s gives the actual amount of electricity. At this slot, all homes correct their appliances predicted operational time slots and amount of electricity consumption. All homes are playing the game independently to increase the overall social benefit in a rational way. The microgrid EMS allocates energy to the appliances for the slot (t_s) as soon as the game converges, forward to the next time slot, and repeat the whole procedure again and again. At the end of the simulation of the 24 time slots, the centralized optimal algorithms (COPCS) is executed using the observed load and amount of energy generated. Next, we run the simulation for 2K, 5K, 50K, 100K, 200K, 500K, and 1M homes and evaluate the performance of the proposed DRTA algorithm.

Fig. 4.1 shows the hourly amount of imported electricity of the day for COPCS, DRTA and a naive (UREG) system for the microgrid with 500 homes. The UREG is a consumption scheduling scheme that allocates electricity to the appliances as soon as it receives a consumption request [120]. The figure shows that the total amount of electricity imported by UREG is always higher than the amount of electricity imported by DRTA and COPCS. Next, we found that the distribution of the hourly

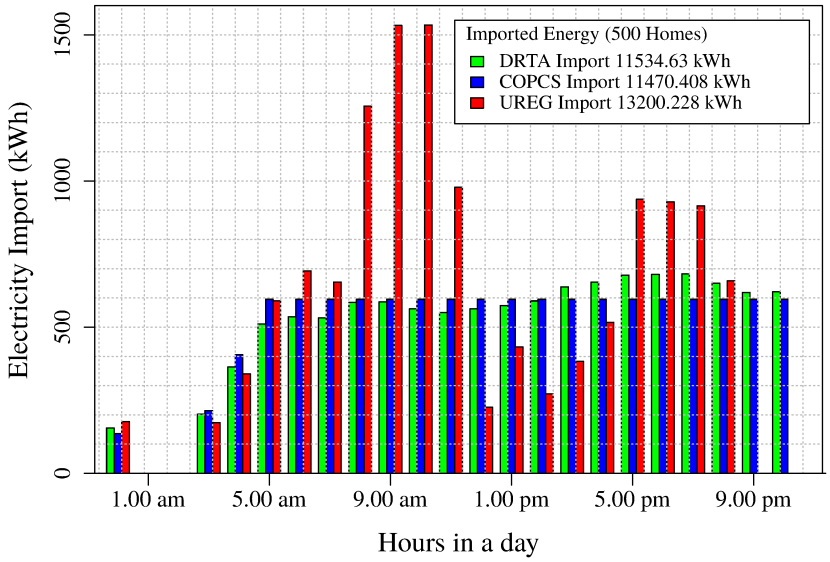

Figure 4.1: Comparison between COPCS and DRTA on hourly amount of imported electricity

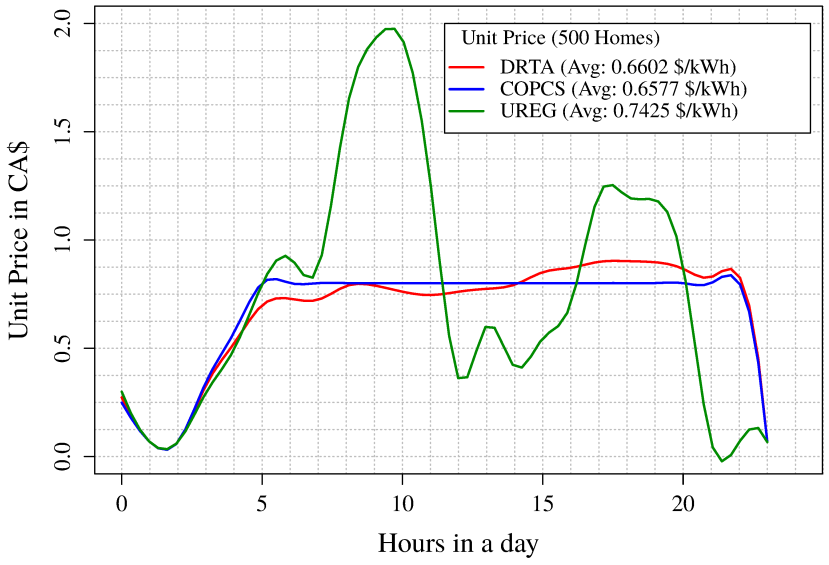

Figure 4.2: Comparison between COPCS and DTRA on hourly electricity price.

amount of electricity imported in the UREG system is irregular, which in effect increases the electricity production overhead and price as shown in Fig. 4.2. However, the distribution of imported electricity in COPCS and DRTA is almost regular. The reason of this improvement in COPCS and DRTA schemes over UREG system is that, both schemes are able to predict future loads and electricity generation whereas the UREG schedules appliances and EVs without any prior knowledge. We also observe that COPCS imports smaller amount of electricity than DRTA (Fig. 4.1), and that the hourly distribution of the amount of imported energy is more linear than DRTA, but for both cases the deviation is very small as shown in Fig. 4.2. The proposed DRTA scheme optimizes the electricity allocation and schedules appliances with the knowledge of the current energy production and future estimation of energy and load; however, the COPCS scheme schedules appliances based on observed energy and load. In reality, however, the COPCS scheme based on the observed load and energy generation is not practical and is used as a benchmark for evaluating the efficiency of DRTA. Further, DRTA outperforms the COPCS scheme based on a day ahead load and energy prediction (Fig. 4.3). Note that both COPCS (based on prediction) and DRTA predict future load and electricity generation but the real time adjustment of load and energy prediction of DRTA significantly improves performance and energy efficiency over COPCS.

One of the main goals of IEA 2DS is to build energy efficient equipment and/or to improve the energy efficiency of the existing system. Fig. 4.4 demonstrates the improvement of energy efficiency of the microgrid, as well as the appliances connected to it. The DRTA allocates energy in a way that all the appliances can use the microgrid energy efficiently. This helps the energy sector to build a sustainable energy system. Fig. 4.4 clearly shows that DRTA and COPCS schemes perform better and are more energy efficient than UREG. This is because DRTA and COPCS regulate

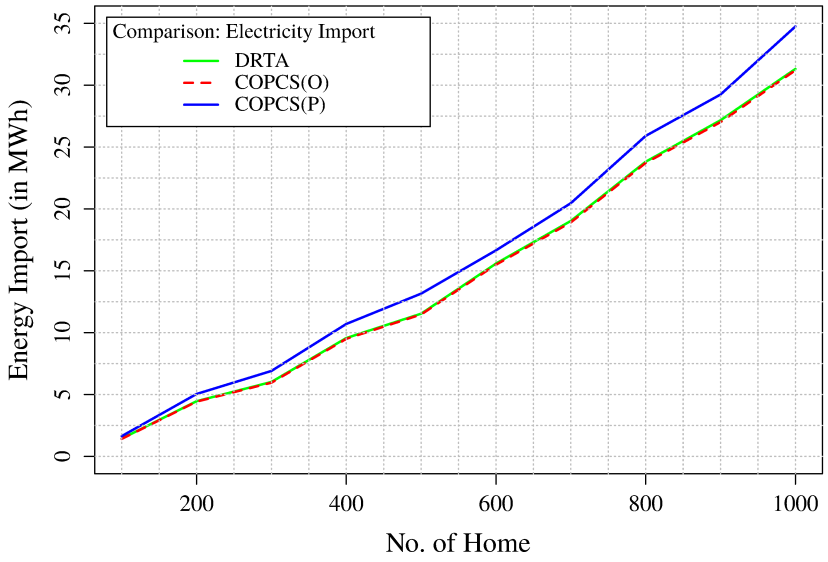

Figure 4.3: Amount of electricity imported: COPCS based on prediction (COPCS(P)) vs. COPCS based on observed load and energy (COPCS(O)), and DRTA

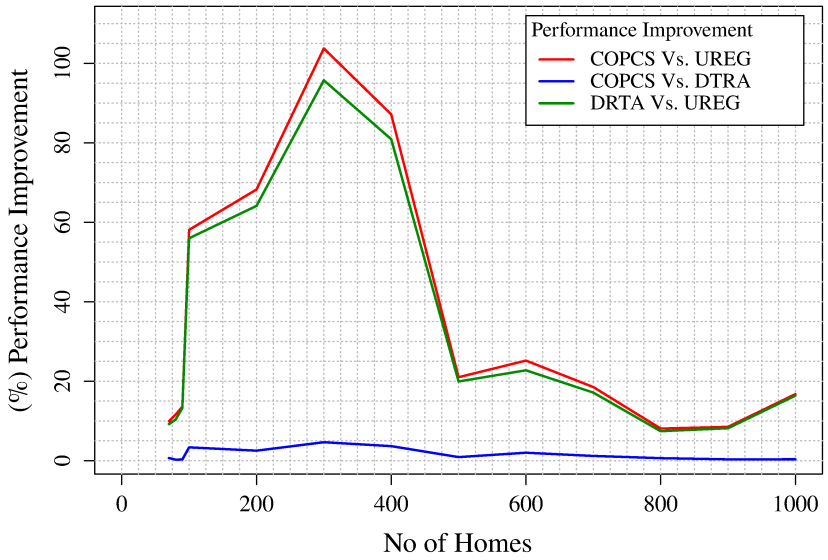

Figure 4.4: Microgrid performance (energy efficiency) improvement: COPCS vs. DRTA

both load and energy, and shift load from low energy production duration to high energy generation duration and also, use the dynamic storage (EVs) to shift excess energy from off-peak duration to peak demand duration. In some cases, COPCS is a little more efficient (0 to 3%) than DRTA. This is because COPCS is a centralized optimal allocation scheme which simulates the system based on the observed load and energy production. On the other hand, DRTA is a real time distributed energy allocation scheme that allocates energy, and adjusts errors in prediction at every step.

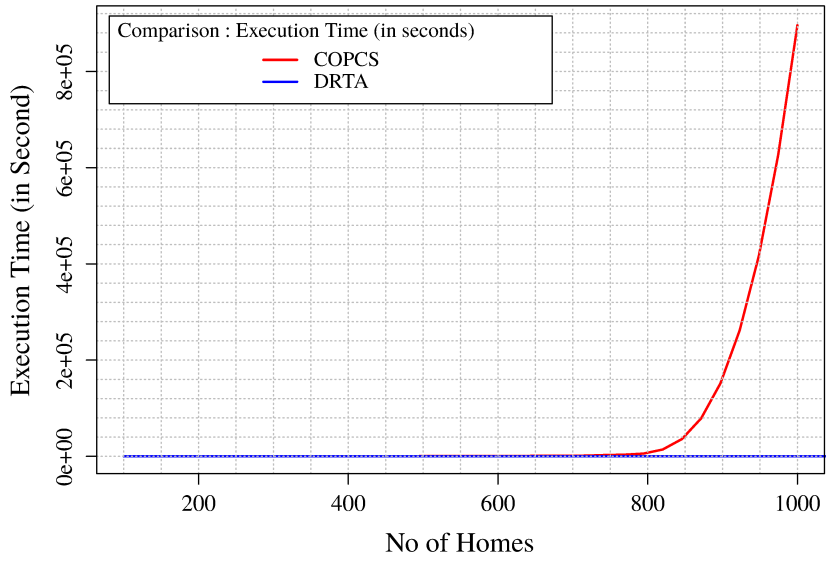

Figure 4.5: Execution time with respect to number of homes : COPCS Vs. DRTA.

Fig. 7.5 depicts the comparison of computation time of both COPCS and DRTA schemes. We have simulated both scheme on HP cirrus cluster (composed of 100 computing nodes with AMD Opteron processors x86, 64 bit, 4 to 8 cores) and recorded the execution time for both schemes, in Fig. 7.5; both COPCS and DRTA ran quite similar when the number of homes is less than 900. For 900 homes and above, COPCS becomes very slow in searching for the optimal solution. Hence, for a large community, COPCS becomes unscalable and impractical because the execution time of COPCS grows exponentially with the increase of the number of homes as shown in Fig.7.5.

On the other hand, the execution time is nearly constant for DRTA. In the DRTA scheme, all homes independently optimize their energy use and the execution time for the optimization dependent on the number of iterations required to reach an optimal solution.

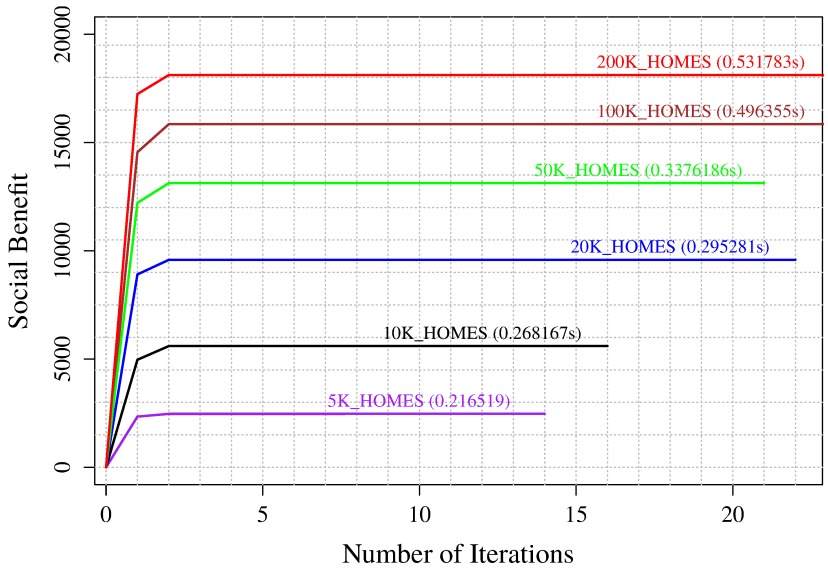

Figure 4.6: Game converging to optimal.

Fig. 4.6 presents the number of iterations needed at each time slot to reach a stable state, where no player wants to change its strategy. Before reaching the stable state, all players change their strategies repeatedly to increase their own payoffs and the overall social benefit. We assume that players are rational; therefore, a player changes its strategy if there is no decrease in overall social benefit. No decrease in social benefit means the players will change their strategies such that they will not harm the benefit of the community. In Fig. 4.6 we have found that only a small number of iterations is needed to reach a stable state.

Fig. 4.7 shows the observed load and energy vs. regulated load of COPCS and DRTA schemes. Both schemes try to fit the load with the observed energy curve by shifting the load from one time slot to another time slot, and/or carrying electricity energy from on duration to another duration. This unique characteristic of both

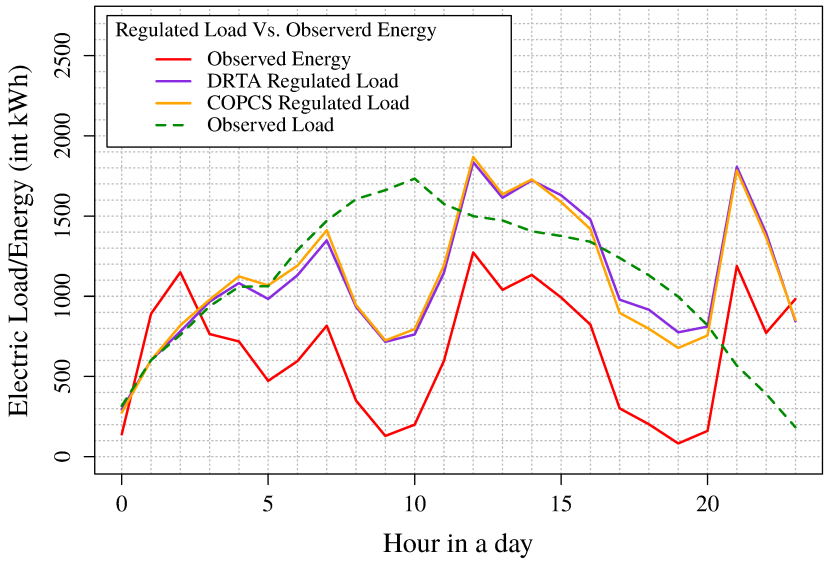

Figure 4.7: Load regulation centralized optimal Vs. real time allocation.

schemes results (Fig. 4.1) in a minimum import as well as optimal electricity (Fig. 4.2) unit price to the customer.

Similar to the valley filling scheme [41], the DRTA scheme (Fig. 4.8) achieves a smooth load, fill the valley of load curve by the shifting load from the peak of the curve to the valley. The DRTA scheme minimizes both import and excess energy, and emphasizes more on minimization where import and/or excess energy is more compared to other time slots, because a higher import or excess energy results in less social benefit. As a result, the DRTA forces homes to change their consumption strategies from the time slot where the import is high to those time slots where the microgrid needs less import or having excess energy. Conversely, DRTA forces homes to store energy or to consume in those time slots when the microgrid has excess energy. Therefore, the load curves become more linear (smoother) in case of non-renewable energy, and load curve follows the curvature of the energy profile.

Figs. 4.9 and 4.10 show the performance of DRTA scheme with high density of hard load (type-I) and low density of soft load (type II, III and IV) where the ratio of energy to load is high (1.14 & 1.38). We have executed the DRTA scheme for

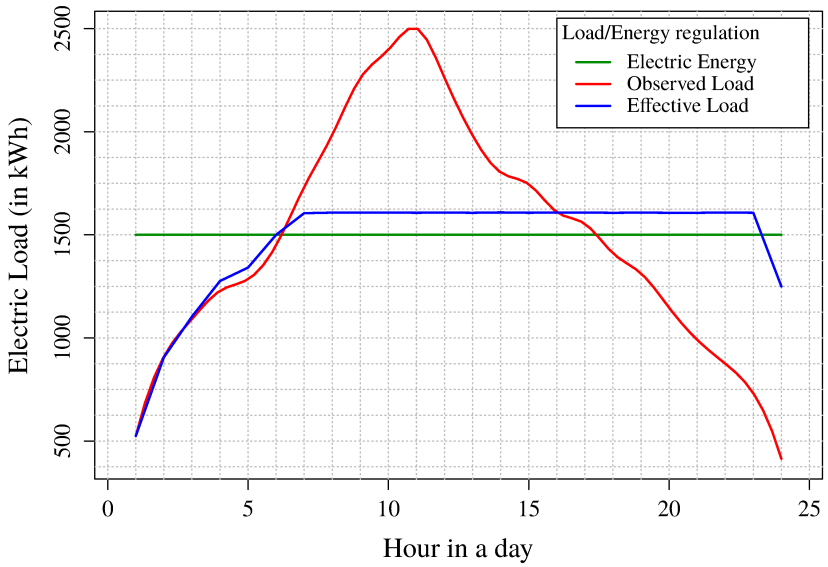

Figure 4.8: Valley filling (using non-renewable energy): Load shifting/regulation in DRTA scheme.

2000 homes; (i) with twenty type-I, zero to one EVs (type-III) and seven type II, type-III (other than EV) type-IV appliances for each home; and (ii) with twenty type-I, three type II, type-III (other than EV) type-IV for each home and one EV for each three homes. The results show that a higher energy to load ration increases the percentage of both cost and energy savings compared to results presented in table 4.2 for 2000 homes. It is true that if the production of energy increases compared to the load, the scheduling (consumption and/or discharge of the energy) of soft loads (including EVs) appliances become more flexible, therefore, both cost and energy savings increase. Alternatively, the percentage of energy and cost savings decrease when the number of soft loads decreases as shown in Fig. 4.10. Clearly, in this case, the DRTA scheme has a lower number of appliances and/or storage to change (i.e., less flexibility) its original scheduling for consume and discharge of energy. The result will be similar to the UREG scheme if there are no soft loads and zero energy storage capacity of the microgrid.

Table 4.2 shows the contribution of DRTA scheme to improve the energy efficiency

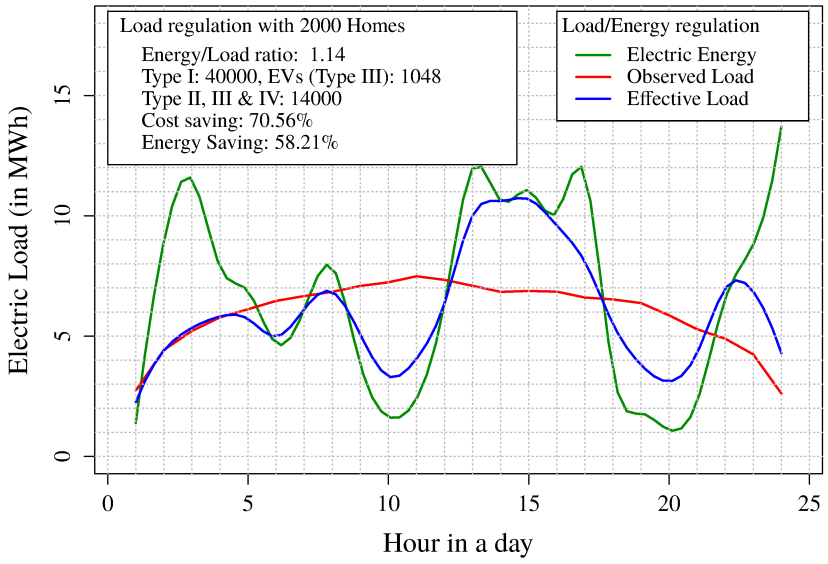

Figure 4.9: Load shifting/regulation in DRTA scheme with high energy to load ratio.

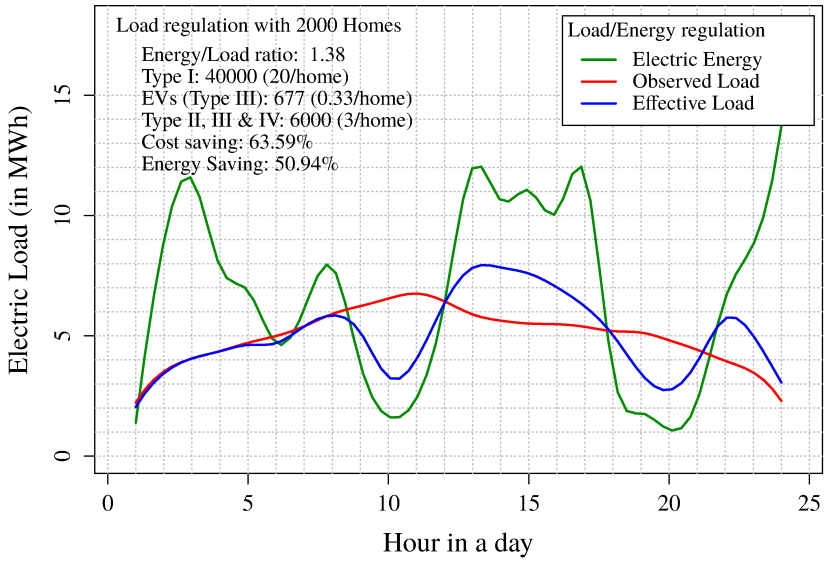

Figure 4.10: Load shifting/regulation in DRTA scheme with high energy to load ratio with lower density of EVs (Type-III), Type-II, Type-III (other than EV), and Type-IV appliances.

Table 4.2: Energy efficiency : increase Microgrid efficiency (%).

Home	E/L	Saving (%)	Home	E/L	Saving(%)
1.0×10^3	0.57	29.43%	5.0×10^4	0.79	46.27%
2.0×10^3	0.81	39.23%	1.0×10^5	0.94	67.18%
5.0×10^3	0.80	44.39%	2.0×10^5	0.98	81.08%
1.0×10^4	0.99	70.56%	5.0×10^5	0.96	76.32%
2.0×10^4	0.97	72.45%	1.0×10^6	0.93	72.74%

Table 4.3: Fairness Index: UREG Vs. DRTA.

No. Home	Fairness Index		No. Home	Fairness Index	
	UREG	DRTA		UREG	DRTA
1.0×10^3	0.96	0.99	5.0×10^4	0.87	0.97
2.0×10^3	0.95	0.99	1.0×10^5	0.85	0.97
5.0×10^3	0.93	0.98	2.0×10^5	0.86	0.98
1.0×10^4	0.91	0.98	5.0×10^5	0.87	0.97
2.0×10^4	0.89	0.99	1.0×10^6	0.82	0.97

and energy cost savings of the microgrid/smart grid. We are unable to present the percentage of electricity cost saving for COPCS due to the extremely long running time and large memory requirement to solve the model. From table 4.2, it is evident that DRTA increases the % electricity cost saving for the microgrid community as the energy to load ratio (column 2 & 4) increases. Indeed, DRTA flatten the load curve to minimize the distance between hourly load and energy which results in minimum imports and decrease the hourly electricity charges for the customers. Also, the higher energy to load ratio in a randomized system usually increases the deviation (positive and negative) between hourly load and energy profiles.

Finally, we show that the DRTA scheme not only increases the social benefit but also increases the fairness of electricity billing for the customers. Table 4.3 demonstrated the fairness index of the proposed DRTA and UREG schemes. To calculate the fairness index, we use the Jain's fairness index described in [61]. Here, for a given

vector $y_n \in \mathbb{R}_+^{|\mathcal{N}|}$, let $J : \mathbb{R}_+^{|\mathcal{N}|} \to \mathbb{R}_+$ be the fairness index given by,

$$J(y) = \frac{(\sum_{n\in\mathcal{N}} y_n)^2}{|\mathcal{N}|\cdot(\sum_{n\in\mathcal{N}} {y_n}^2)}, \tag{4.30}$$

where y_n represents the average electricity unit price for home n that is calculated as, $y_n = \frac{\sum_{t\in\mathcal{T}} p_n^t}{\sum_{a\in\mathcal{A}_n}\sum_{t\in\mathcal{T}_{n,a}} l_{n,a}^t}$. In table 4.3, the DRTA scheme constantly shows a very high fairness in electricity billing for the customers. This is because the DRTA scheme decreases the electricity price to a near-optimal value by lowering the amount of import energy and increase the use of local energy.

4.6 Conclusion

We developed a real-time distributed model for energy allocation method to minimize the electricity cost and increase the overall social benefit of the microgrid customers. The DRTA scheme reduces the time to obtain a solution for large residential microgrid and transfers responsibility on the consumer to make the decision of their RES energy use, schedule their appliances and EV for power consumption. We simulated the DRTA model and compared the results with the centralized COPCS scheme which was illustrated in Chapter 3. The DRTA model offers better electricity price for the microgrid customers because it considered immediate demand and decided the allocation of power instantly. The design may help the microgrid customers to reduce their electricity costs but does not support microgrid operator enough for a day ahead of planned generation or purchase of electricity from the grid.

Chapter 5

Demand-Side Management by Regulating Charging and Discharging of the EV, ESS, and Utilizing Renewable Energy

In Chapter 4 we described an online electricity allocation model, DRTA to allocate power to the microgrid customers according to the immediate need by adjusting the consumption scheduling for the current time slot, and future anticipated demands. The DRTA scheme exhibits outstanding performance and results in continuous modification of the electricity usage pattern in each time slots which may increase the instability in the generation plant. To minimize the uncertainty in the production plant, we develop a real-time decentralized demand-side management (RDCDSM) system to help the energy producer or microgrid operator to sketch a price-ware consumption profile for the next day and deliver electricity to the customer according to day-ahead plan.

5.1 Motivation

The DRTA method in the previous chapter allocates electricity based on current demand and adjust the consumption schedule for the rest of the day. The DRTA scheme is a game based mechanism design which gives preference to the user choice to determine the current allocation and future consumption profile such that the social benefit of the whole community is increased conversely reduce the electricity cost. The DRTA method may introduce instability in power generation and price because, in each time slot, the DRTA system may change the consumption amount for current and rest of the time slots. Therefore production plant may face an uncertain demand which may differ from the original estimation in the previous time slot. In some cases, this may force the utility to start or shut down a generator instantly or increase or decrease the amount of generation due to changes in consumption pattern. Generators need a certain amount of time to lowering or raising the production; therefore immediate changes in use may increase the electricity generation costs or cannot be honored at all.

To solve this problem and balancing between electricity prediction and consumption, we review some related work in section 2.3 and proposed RDCDSM scheme which initially encourages customers to estimates their loads, renewable generation and processes the predicted load by sharing energy and storage capacities among the users to obtain a flat load curve for the operator. Thus, results in lower electricity price. Then, at the time of consumption customers are again encouraged to minimize the variation from the estimated price-ware predicted load by sharing and depreciate the differences by using energy stored in the storage in case of shortage or saving the excess energy.

5.2 System Model

We consider a grid connected residential microgrid (shown in Fig. 7.1) which comprises a set of residential customers $\mathcal{N}$. Each of the customers may be equipped with a RES source with an ESS and an EV (with V2G capabilities). We assume each home is connected to a HEMS (Home Energy Management System, such as a smart meter) which connects it to the microgrid operator as well as with other consumers. Each day, the HEMS of each user forecasts the load, energy generation from RES,

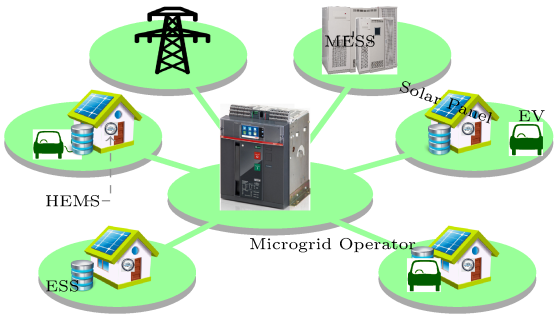

Figure 5.1: Residential Smart Microgrid.

and (if applicable) the EV target energy and its driving schedule, thus determining a probable consumption profile for the next 24 hours. The predicted demand of a customer n is calculated as,

$$p_n^t = l_{n,p}^t + \alpha_{n,p}^t + \theta_{n,p}^t + \alpha_{\mathcal{N}}^t - w_{n,p}^t, \quad \forall t \tag{5.1}$$

where $p_n^t,\ \alpha_{n,p}^t,\ \alpha_{\mathcal{N}}^t,\ \theta_{n,p}^t \in \mathbb{R}$ define the probable consumption profile, customer ESS, centralized ESS, and EV's charging/discharging energy level of customer n. The predicted load and the amount of energy used from RES are $l_{n,p}^t$ and $w_{n,p}^t$ respectively and $l_{n,p}^t, w_{n,p}^t \in \mathbb{R}^+$. Each customer optimizes its predicted load profile and communicates its fine-grain predicted demand (p_n^t) for next 24 hours with the microgrid operator. The microgrid operator is responsible for planning and controlling the flow of electricity among users in the network. Let $\mathcal{G}(t)$ be the amount of electricity purchased from the power main grid at time t to support the fine-grain projected demands of $\mathcal{N}$ at

t. At consumption time, each customer compares its real demand with the proposed predicted demand p_n^t. Any discrepancy/deviation triggers the customers to play an allocation game between them to minimize the gap between the predicted and actual demands. For all t, our proposed system allocates electricity from the microgrid to every home based on the home's actual consumption.

To develop a mathematical model for real-time demand-side management, we analyze and investigate the prediction of residential loads, energy generation from RESs, ESS features, as well as the EVs' driving schedules and distances. For simplicity purposes, we illustrate the consumption pattern of each of the components of the residential home. We present the mathematical model of each of the elements before formulating the RDCDSM problem.

5.2.1 Residential Load ($l_{n,p}^t$)

Most practical load forecast models are based on offline schemes, where predictions are conducted in advance. The uncertainty of prediction increases with the increase of the forecast time [121]. The STLF is thus more accurate than MTLF (midterm load forecast) or LTLF (long-term load forecast) [121]. Currently, several STLF techniques exist, but aside from their varieties, these methods mainly depend on historical demands, weather forecasts, and other variables to estimate the aggregated demand of all consumers [57]. However, the efficiency of any forecasting algorithm depends not only on the accuracy and time horizon of the forecast but also on its capability to reduce the complexity, cost, and memory needed for predicting the demand of customers [57, 105]. In the proposed system, we suppose that each residence is connected to a HEMS. These HEMSs are enabled to assist consumers in forecasting their demand based on an average household demand [6], refine and send the data over a data network to other customers and the operator [57]. Moreover, the HEMSs

provide a real-time two-way interaction with the microgrid operator and other clients. A consumer first sends its predictions for the next 24 hours at the start of the day. Next, at each time slot, a consumer determines its consumption strategy for its actual demand in the current time slot, and modify its forecast demand for the rest of the day. This forecasting approach reduces the complexity of real-time electricity demand by shifting the forecast burden from the operator to the customers, enhances the accuracy of the predictions. Now, let the predicted household load of n be $l^t_{n,p}$ and the predicted load of the microgrid be δ^t_p at t then,

$$\delta^t_p = \sum_{n \in \mathcal{N}} l^t_{n,p}, \ \forall t \tag{5.2}$$

5.2.2 Renewable Energy ($\omega^t_{n,p}$)

It is assumed that RESs are available for some residences. RESs such as Solar PV and wind turbines generate electricity in a random manner [117]. However, the RES provides a great promise for significantly improving the efficiency of distribution, and residential renewable energy generation is becoming more popular as the installation cost is decreasing and electricity prices are rising [65, 117]. Hence, several stochastic models have been developed to forecast the energy generation over time, and thereby, to enhance RESs exploitation and penetration in smart grids. In our proposed system, the customer decides whether to store the energy generated by the RES or to supply it to other clients, according to the power demands in every real-time slot (t_s). Let $\omega^t_{n,p}$ be the predicted amount of electricity used from RES where the predicted generation is denoted by $\Omega^t_{n,p}$ and entire predicted generation at t be ω^t_p. Then,

$$\omega^t_{n,p} \leq \Omega^t_{n,p} \tag{5.3}$$

$$\omega^t_p = \sum_{n \in \mathcal{N}} \omega^t_{n,p}, \ \forall t \tag{5.4}$$

5.2.3 Energy Storage System - ESS ($\alpha^t_{n,p}$)

The introduction of new types of batteries with higher storage capacities has encouraged ESS to emerge as a way to improve the power management in smart grid [127, 37]. ESSs play a vital role in matching the generation with demand which leads to an increase in the efficiency and reliability of the system against uncertainties. In general, every home with a RES has an ESS installed to store the excess energy which is used later when the demand is high. Now, let the charging and discharging strategies of an ESS b of n at time t be $\alpha^t_{n,b} \in \{-X^{low}_{n,b}, \cdots, 0, \cdots, X^{high}_{n,b}\}$, where $-X^{low}_{n,b}$ denotes extreme discharge rate and $X^{high}_{n,b}$ denotes the maximum charging rate of a given ESS b. Let the amount of charging and discharging of ESS of n at time t be $c^t_{n,b}$ and $d^t_{n,b}$, then $\forall t$ we have:

$$0 \leq c^t_{n,b} \leq (X^{high}_{n,b} \cdot \eta^t_{n,b}) \tag{5.5}$$

$$0 \leq d^t_{n,b} \leq (X^{low}_{n,b} \cdot (1 - \eta^t_{n,b})) \tag{5.6}$$

where, $\eta^t_{n,b}$ is a binary variable; $\eta^t_{n,b} = 1$ indicates that ESS b is charging at time t, otherwise it is discharging. Let $\Phi^c_{n,b}$, $\Phi^d_{n,b}$ be the charging and discharging efficiency of b then,

$$\alpha^t_{n,b} = \frac{c^t_{n,b}}{\Phi^c_{n,b}} - d^t_{n,b} \cdot \Phi^d_{n,b}. \tag{5.7}$$

Note that ESS's has a maximum capacity and minimum discharge level. For both safety and longevity, this should always be maintained. Thus, for any time slot t, ESS b must not discharge below its minimum discharge level $\mathcal{C}^{min}_{n,b}$, and charge over the capacity $\mathcal{C}^{max}_{n,b}$. Thus,

$$\mathcal{C}^{max}_{n,b} \geq \mathcal{C}^{init}_{n,b} + \sum_{t=t_s}^{T} (c^t_{n,b} - d^t_{n,b}) \geq \mathcal{C}^{min}_{n,b} \tag{5.8}$$

where, $\mathcal{C}_{n,b}^{init}$ is the initial energy stored in the ESS at the start of the day. Now, let the probable strategy of battery b at time t be $\alpha_{n,p}^{t}$, then $\alpha_{n,p}^{t} = \alpha_{n,b}^{t}$. We assume that each residential customer has an ESS which is connected to the RES.

5.2.4 Electric Vehicle ($\theta_{n,p}^{t}$)

Large-scale energy storage requires vast land spaces, high installation, operation, and maintenance costs [121, 77]. Conversely, compared with oversized storage devices, plug-in EVs can be used as a cheap way to store and transport the surplus of energy. EVs may appear as loads during charging periods, meanwhile they may also be used as storage to store the surplus of energy or discharge stored energy to balance the demand and generation in the smart grid[77]. Hence, EV may charge, discharge, or remain idle throughout the day. According to [92] we assume the EVs arrive home in the evening an arbitrary initial energy level. An EV stays connected to the home for a random amount of time and then leaves home in the morning for the next driving. When connected to the microgrid, the energy stored in a given EV must attain a certain target level required for the following driving schedule. Let the arrival and departure time of a given EV e of consumer n be $t_{n,e}^{a}$ and $t_{n,e}^{d}$ respectively. Also, let, $\mathcal{T}_{n,e}$ be the set of time slots during which an EV e of n is connected to the grid, where $\mathcal{T}_{n,e} \triangleq \{t_{n,e}^{a}, t_{e}^{a} + \Delta t, t_{e}^{a} + 2 * \Delta t, ..., t_{n,e}^{d}\}$. Now, suppose the charging and discharging rate of the EV be $\theta_{n,e}^{t} \in \{-Y_{n,e}^{low}, \cdots, 0, \cdots, Y_{n,e}^{high}\}$; where $-Y_{n,e}^{low}$ denotes extreme discharge rate and $Y_{n,e}^{high}$ denotes the maximum charging rate. For EVs, similar to the ESSs, equations (5.5) to (5.8) must be satisfied only for timeslots $t \in \mathcal{T}_{n,e}$. Let the amount of charging and discharging of an EV e of consumer n at time t be $r_{n,e}^{t}$ and $v_{n,e}^{t}$ accordingly, then:

$$0 \leq r_{n,e}^{t} \leq (Y_{n,e}^{high} \cdot \zeta_{n,e}^{t}) \tag{5.9}$$

$$0 \leq v_{n,e}^{t} \leq (Y_{n,e}^{low,e} \cdot (1 - \zeta_{n,e}^{t})) \tag{5.10}$$

$$\theta_{n,e}^{t} = \frac{r_{n,e}^{t}}{\Phi_{n,e}^{r}} - v_{n,e}^{t} \cdot \Phi_{n,e}^{v}. \tag{5.11}$$

Where, $\zeta_{n,e}^{t}$ is a binary variable and $\zeta_{n,e}^{t} = 1$ indicates EV charging at time t, otherwise discharging, and $\Phi_{n,e}^{r}$, $\Phi_{n,e}^{v}$ denote the charging and discharging efficiency of EV. Similar to ESS (eq. (5.8)), for any time slot t, EVs' strategy must satisfy,

$$\mathcal{R}_{n,e}^{max} \geq \mathcal{R}_{n,e}^{init} + \sum_{t=t_{n,e}^{a}}^{t_{n,e}^{d}} (r_{n,e}^{t} - v_{n,e}^{t}) \geq \mathcal{R}_{n,e}^{min}, \quad \forall t \in \mathcal{T}_{n,e}, \ \forall e \in \mathcal{V} \tag{5.12}$$

where, $\mathcal{R}_{n,e}^{init}$, $\mathcal{R}_{n,e}^{max}$ and $\mathcal{R}_{n,e}^{min}$ are the initial, minimum discharge and maximum capacity of the EV. Moreover, before leaving the home for the next driving schedule, the energy stored in a given EV must attain a certain target level $\mathcal{L}_{n,e}$ (in KWh). Then, for an EVs the following equation must hold,

$$\mathcal{R}_{n,e}^{init} + \sum_{t \in \mathcal{T}_{n,e}} (r_{n,e}^{t} - v_{n,e}^{t}) \geq \mathcal{L}_{n,e} \tag{5.13}$$

In general, an EV consumes $0.13 - 0.20$ kWh/km [92] and the average daily trip length of 90% of EVs is between 20 to $60km$ [131, 94, 104]. Most customers also use their vehicles from 6 : 00 am to 10 : 00 am to drive to work and return home after work from 4 : 00 pm to 8 : 00 pm. Let $\tau_{n,e}$ be the trip length of an EV and the amount of energy stored in an EV (before the trip) be $\mathcal{L}_{n,e}$; then, the initial energy stored in an EV (when arrived at home) can be calculated as,

$$\mathcal{R}_{n,e}^{init} = \mathcal{L}_{n,e} - \tau_{n,e} * \rho_{n,e} \tag{5.14}$$

where $\rho_{n,e}$ is an amount (kWh) of electricity consumed by the EV to drive $1km$. Now Let us assume that a customer has an EV. Then the probable EV consumption profile

$\theta^t_{n,p}$ at t can be assigned as $\theta^t_{n,p} = \theta^t_{n,e}$

5.2.5 Problem Formulation

As discussed earlier, we assume the microgrid operator plans its energy production and/or purchase a day ahead, based on the aggregate demand it received from its users. However, the actual user's consumption and need for energy during the day may vary from its predicted demand. The frequent changes of the demand force the microgrid to produce a variable amount of power which may not be possible, or expensive, on a short notice. Moreover, the start or shut down of a generator to match the user variable demands involve substantial cost and time. Thus, our system will help the microgrid operator as well as the users to close the gap between the real time and instantaneous actual and predicted aggregate demands. The integration of ESS, EVs, and an intelligent energy management system may help in mitigating the problem and thereby reduce the electricity costs and instability in the power generation. We address these issues and design an intelligent solution (RDCDSM) to reduce the electricity costs by flattening the predicted demand at the start of a day. The system delivers electricity to the customers according to their actual demands, such that the deviation between nominated and anticipated amounts is minimized. The RDCDSM has two consecutive phases: (i) prediction or planning phase and (ii) allocation phase.

Prediction phase

At the start of each day, each home predicts its load, renewable energy generation, EV arrival and departure times and target energy. Next, all customers individually optimize their anticipated consumption pattern to reduce the electricity cost, and then sends the resultant predicted load to the operator. To devise a fine-grain predicted

consumption profile, each customer plays a mixed strategy with others to determine the consumption strategy which is expressed by the variables, $\alpha^t_{n,p},\ \epsilon^t_{n,p},\ \theta^t_{n,p},\ \omega^t_{n,p}$ $\forall t \in T$, where $\epsilon^t_{n,p}$ is the charging or discharging strategy of the MESS (microgrid ESS). Let γ^t_n be the feasible strategy of n such that $\gamma^t_n = \{\alpha^t_{n,p},\ \epsilon^t_{n,p},\ \theta^t_{n,p},\ \omega^t_{n,p}\}$. Now, let γ^t_{-n} be the strategy of all other customers which results in a consumption p^t_{-n} at t given by,

$$p^t_{-n} = \sum_{m \in \mathcal{N} \setminus n} (l^t_{m,p} + \alpha^t_{m,p} + \epsilon^t_{m,p} + \theta^t_{m,p} - \omega^t_{m,p}),\ \forall t \in T \tag{5.15}$$

and consumption p^t_n of customer n is calculated as,

$$p^t_n = (l^t_{n,p} + \alpha^t_{n,p} + \epsilon^t_{n,p} + \theta^t_{n,p} - \omega^t_{n,p}),\ \forall t \in T \tag{5.16}$$

where $(p^t_n + p^t_{-n}) \geq 0,\ \forall t$. Let γ^t_{-n} or p^t_{-n} be known to customer n which is the current load of all other customers due to their current consumption strategies. Each time a customer sends its load profile to other clients when the change of its previous strategy is profitable. Upon receiving the load profiles from other clients, customer n determines its next strategy $\gamma^t_n\ \forall t$ to increase the payoff which is given by,

$$\sigma_n(\gamma^t_n, \gamma^t_{-n}) = Z - \min \left[\sum_{t \in T} (aP^2_t + bP_t + c) \right] \tag{5.17}$$

where Z is a positive constant, a, b, c are positive coefficients and $a >= b$. $aP^2_t + bP_t + c$ is a quadratic cost function for electricity. The variable P_t is the total amount of electricity which will be consumed at t and it is defined as,

$$P_t = p^t_n + p^t_{-n},\ \forall t \in T \tag{5.18}$$

$P_t \geq 0$, thus the cost function $aP_t^2 + bP_t + c$ is convex and the strategies in γ_n^t are all continuous and therefore the game will converge to a Nash equilibrium state and gives an optimal solution. At a Nash equilibrium state, let the strategy of any customer n be γ_n^{t*}, then for any other strategies γ_n^t, $\sigma_n(\gamma_n^{t*}, \gamma_{-n}^{t*}) \geq \sigma_n(\gamma_n^t, \gamma_{-n}^{t*})$. Once done, then all customers send their fine-grain predicted demand $p_n^{*t},\ \forall t$ (for the strategy γ_n^{t*}) to the microgrid operator. Upon receiving the predicted demand, the operator sets a plan to produce or purchase electricity from the grid. Hence, the day-ahead predicted load ($P_{\mathcal{N}}^t,\ \forall t$) determined by the microgrid operator is,

$$P_{\mathcal{N}}^t = \sum_{n \in \mathcal{N}} p_n^t,\ \forall t \in T \tag{5.19}$$

Allocation Phase

Unfortunately, the uncertainties in household demands, RES generation, EVs arrival and departure times and target energy may vary at the time of consumption from the predicted one. In that case, each customer needs to adjust its use of electricity to reduce the gap between the actual and the predicted demand. Otherwise, the microgrid will respond by purchasing the extra energy needed (to satisfy the demands) and hence charges an extra cost (or penalty) proportional to the deviation between the actual and predicted demand of electricity. Let us assume that the current time slot is t_s. Then the optimal consumption determined in the prediction phase from t_s to $|T|$ may not be optimal in the current scenario. Hence, each customer plays mixed strategy of a new non-cooperative game, at t_s, with the current (real time) need and the modified (adjusted) predicted demand for rest of the day. Therefore, the objective of the play is to reduce the penalty for the deviation of present and anticipated future needs from that of the submitted consumption pattern. Let Q be a fixed amount of additional cost (penalty) charged for one unit of electricity due to

the deviation from the original consumption profile. Then, the payoff for customer (n) can be calculated as,

$$\bar{\sigma}_n(\gamma_n^{t_s}, \gamma_{-n}^{t_s}) = Z - \min \sum_{t=t_s}^{T} Q|P_{\mathcal{N}}^t - \bar{p}_n^t - \bar{p}_{-n}^t| \tag{5.20}$$

where $\bar{p}_n^t$ is the current (t_s) and future demands based on the current and projected household demands $\bar{l}_{n,p}^t$, EVs' consumption (charging and discharging) $\bar{\theta}_n^t$ with respect to new arrival and/or departure times and target energy, ESS consumption $\bar{\alpha}_n^t$, current and modified predicted generation of RES $\bar{w}_n^t$, and new charging and discharging strategies of the MESS $P_{\mathcal{N}}^t$. The absolute part of the payoff (eq. (5.20)) can be simplified as,

$$\bar{\sigma}_n(\gamma_n^{t_s}, \gamma_{-n}^{t_s}) = Z - \min \sum_{t=t_s}^{T} Q y^t, \tag{5.21}$$

such that,

$$y^t \geq (P_{\mathcal{N}}^t - \bar{p}_n^t - \bar{p}_{-n}^t) \tag{5.22}$$

$$y^t \geq (\bar{p}_n^t + \bar{p}_{-n}^t - P_{\mathcal{N}}^t) \tag{5.23}$$

Where $\bar{p}_n^t$ for the strategy $\gamma_n^{t_s}(\bar{\theta}_n^t, \bar{\alpha}_n^t, \bar{\epsilon}_n^t, \bar{w}_n^t)$ at time t_s can be determined as,

$$\bar{p}_n^t = \bar{l}_n^t + \bar{\alpha}_n^t + \bar{\epsilon}_n^t - \bar{w}_n^t, \ \forall t \tag{5.24}$$

where $t_s \leq t \leq |T|$, and $\bar{p}_{-n}^t$ is,

$$\bar{p}_{-n}^t = \bar{l}_{-n}^t + \bar{\alpha}_{-n}^t + \bar{\epsilon}_{-n}^t - \bar{w}_{-n}^t, \ \forall t \tag{5.25}$$

Similar to the game in the earlier Section 5.2.5, the allocation game also terminates at a Nash equilibrium state where no consumer is willing to change its strategy which results in reducing the payoff.

Centralized Allocation Model with Naive Prediction

The centralized allocation model can easily be realized by modifying the parameter p_n^t of eq. (5.18) and the terms $l_{m,p}^t,\ \alpha_{m,p}^t,\ \epsilon_{m,p}^t,\ \theta_{m,p}^t,\ \omega_{m,p}^t$ of eq. (5.15) to variables. Hence, the solution of the model with the objective function defined by eq. (5.17) results in the optimal predicted consumption profile of the microgrid. All customers transfer their predicted load profile, RES generation, EV and ESS parameters (for a day) to the microgrid operator. For each time slot, the allocation of the electricity for each home can be determined, by the operator, by solving (5.21) with the related constraints where $\bar{p}_{-n}^t$ and the terms in eq. (5.25) are considered as variables. Hence, the objective function for the centralized model is,

$$\min \sum_{t=t_s}^{|T|} |\tilde{P}_{\mathcal{N}}^t - \sum_{n \in \mathcal{N}} \tilde{p}_n^t|,\ \forall t_s \in T \tag{5.26}$$

where $\tilde{P}_{\mathcal{N}}^t$ is the predicted load, which is determined by the microgrid at the beginning of the day by accumulating raw predicted load sent by the customers (naive prediction). Here, $\tilde{P}_{\mathcal{N}}^t = \sum_{n \in \mathcal{N}} (l_{n,p}^t + \theta_{n,p}^t - \omega_{n,p}^t)$ such that $\tilde{P}_{\mathcal{N}}^t \geq 0$, which keeps a balance between energy production and consumption. $\theta_{n,p}^t$ designates the charging of EV; here, as soon as an EV arrives, it starts charging at full charging capacity until a target ($\mathcal{L}_{n,e}$) is achieved. $\tilde{p}_n^t$ is the load which presents the current (i.e., in time slot t_s) and modified future demand of customer n.

5.3 Numerical Evaluation

5.3.1 Simulation Setup

We consider grid connected microgrids with 100, 200, 300, $\cdots$, 1000 homes connected with each other through an electrical and a data network. Each customer has an

energy management system (HEMS) which is responsible for forecasting the load, RES generation, EV arrival and departure times and target energy level, and for sending (and receiving) information about energy, load, and other control information to other HEMSs. Each HEMS runs the energy optimization (RDCDSM) model to optimize the energy usage of the owner. A data network carries load and control information from one HEMS to other HEMSs as well as to the operator. The HEMS forecasts the household load for a day based on the average residential load hourly load which given in [6, 121]. A typical household in U.S./Canada consumes 11,000 kWh to 12,000 kWh whereas in China a customer uses 1,349 kWh per year. For our simulations, we assume that each household consumes around 4 to 20kWh per day. We consider RESs with capacities between 0.5 and 1 kW, and the long term RES generation during a day and forecast is presented in [120]. Both EV and ESS (such as Tesla, Nissan, Toshiba, Toyota, and etc) configurations are assumed as shown in Table 5.1. The arrival and departure times, and consumption (kWh/Km) while

Table 5.1: EV and Storage (ESS) configuration

Type	**Capacity** (kWh)	**Min Capacity** (kWh)	**Max Charging** (kW)	**Max Discharging** (kW)
ESS	6.4, 6.3, 10.0	0.32,0.32, 0.5	2.0, 2.0, 2.5	2.0, 2.0, 2.5
Centralized ESS	2500	500	740	740
EV	90, 85, 70, 60, 24	9, 8.5, 7.0, 6.0, 2.4	9, 9, 9, 8, 3	6, 6, 6, 5, 2.5

driving are assumed as discussed in Section 5.2.4. For electricity price, we assume the values of coefficients a, b, and c to be 0.0001, 0.0001, and 0.05 respectively. We also assume the penalty (Q) for each kWh is 0.01 \$. We use Cplex and Java to develop the simulation program and execute the simulation on a desktop computer running Linux OS with 8 GB RAM, Intel Core i7 processor.

5.3.2 Numerical Results

Fig. 5.2 presents the predicted (naive) load, actual load, and hourly electricity delivery by the centralized method to all 1000 customers throughout the days of a week. In

all the cases, centralized allocation system modifies the actual load by exploiting the RESs, ESSs, MESS, and EVs to match with the naively predicted demand. Therefore, the differences between the predicted demand and allocated (modified actual) electricity are minimized (see the gray and black curve in Fig 5.2). The average difference between predicted and actual load was $0.1164591 MW/h$ (total 19.56513 MWh) without using the centralized method whereas in the case of the centralized method the difference was $0.04791264 MW/h$ (total 8.049323MWh). This reduction is possible because of the centralized method utilizes RES, ESSs, MESS and rescheduling charging and discharging of EVs to carry electricity from a duration to another, and modify the actual demand to match with the predicted load. Unfortunately, the centralized allocation with naive-predicted method does not reduce the electricity cost and variation of demand/delivery throughout the day (see Fig. 5.5) which will be presented later.

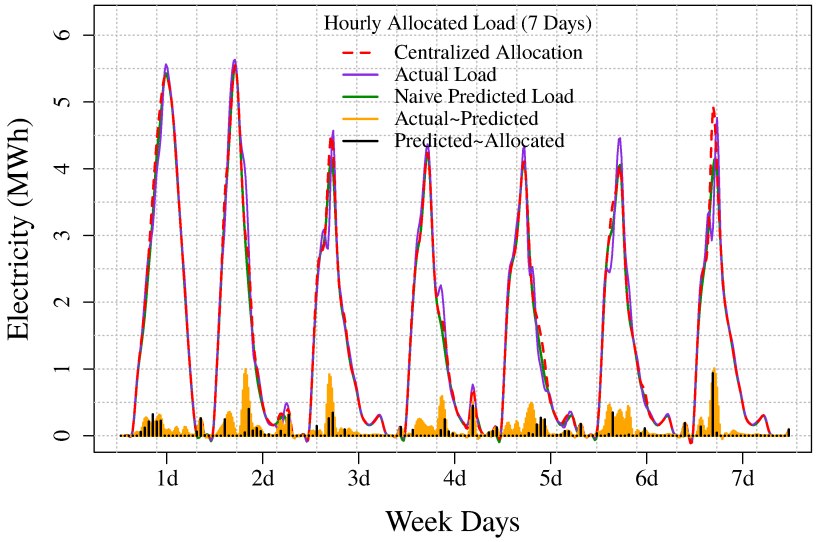

Figure 5.2: Electricity allocated by the centralized with naive prediction.

Fig. 5.3 shows the day ahead of RDCDSM prediction and on-line real-time allocation or delivery of electricity to all 1000 customers for seven consecutive days. At the beginning of the week, we assume that the EVs stored energy is minimum therefore

the load at day 1 is higher than any other days of the week. Our RDCDSM flattens the demand for a day ahead prediction and follow the same pattern and modify the actual need (see Fig. 5.2) to deliver energy to the customers. This happens because RDCDSM employs ESS, MESS, and EVs to transfer excess RES energy from one-time slot to another time slot and reschedule EVs consumption to minimize the cost of electricity in the planning or prediction phase and thereby reduces the gap between modified predicted demand and delivery of power in the allocation round. Hence, increases the reliability, stability and quality of electricity service with reduced cost to the customer.

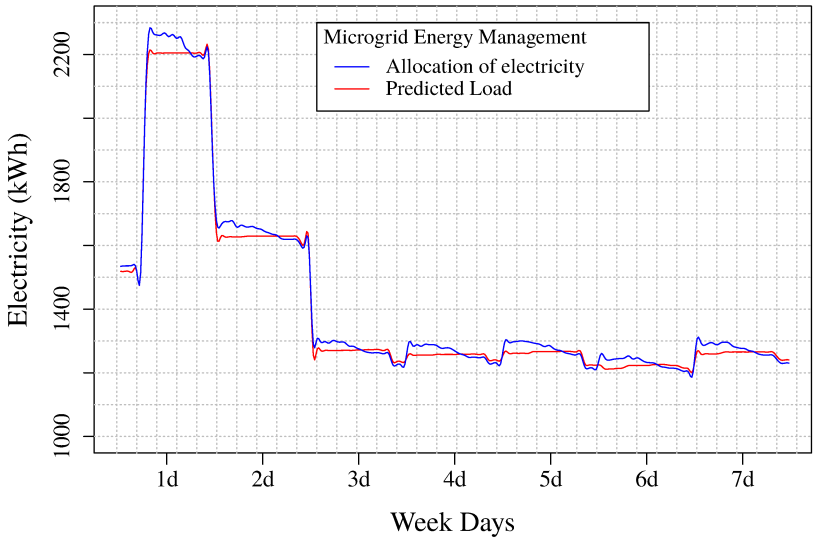

Figure 5.3: RDCDSM : prediction and allocation of electricity

Fig. 5.4 (day 2 of Figs. 5.2 and 5.3) illustrate the results clearly for a day where both the RDCDSM and centralized allocation try to match the distribution to the predicted demand. The delivery of power for the centralized methods varies whereas RDCDSM results in a flat load curve. This is because in case of the centralized method we use anticipated load as the customers predicted demand without any further refinement, whereas RDCDSM refines projected demand and then both approaches utilize ESSs, EVs, RES and MESS to modify the actual based on predicted demand and

provide power to the client. Further, the centralized took days and weeks, sometimes months to produce a result for a large microgrid whereas RDCDSM needs less than a minute. Moreover, centralized method suffer from potential privacy issue because it requires customers detail consumption pattern and load character for the optimization and allocation of electricity. Whereas, RDCDSM only needs total projected need or actual request for rest of the customers.

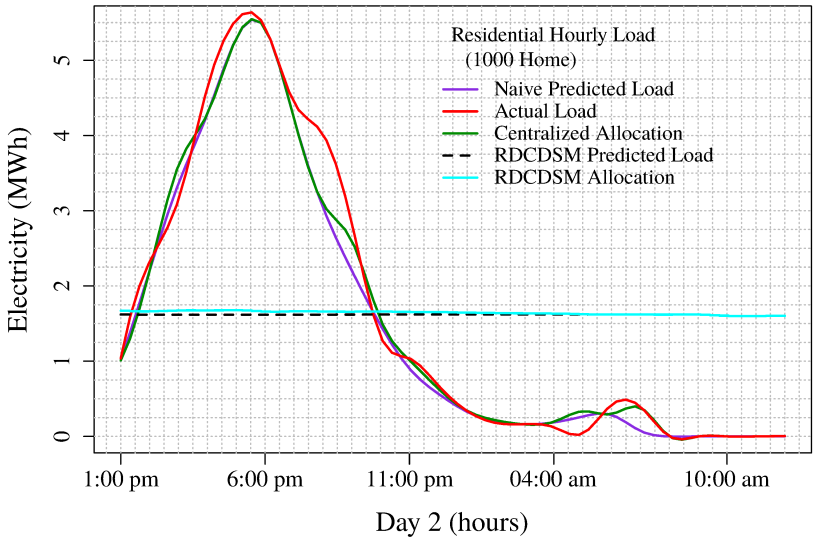

Figure 5.4: RDCDSM and centralized predicted, allocation with actual load.

Fig. 5.5 compares the total cost of electricity in a days of a week determined by the proposed RDCDSM and centralized allocation with naive prediction method. In all the cases, electricity cost is lower in RDCDSM than the electricity cost determined by the centralized distribution with naive prediction method. This is because electricity cost increases with the increase of demand. Moreover, customers of the centralized method are not abide by their prediction method as it is in RDCDSM system thereby produces peaks and valleys in the demand curve. Whereas, RDCDSM utilities MESS, ESS, EVs to carry energy from low load duration to peak load period and shifts load from peak hours to off-peak hours. Further RDCDSM method increases the performance of the electrical system by flattening the demand throughout the hours of

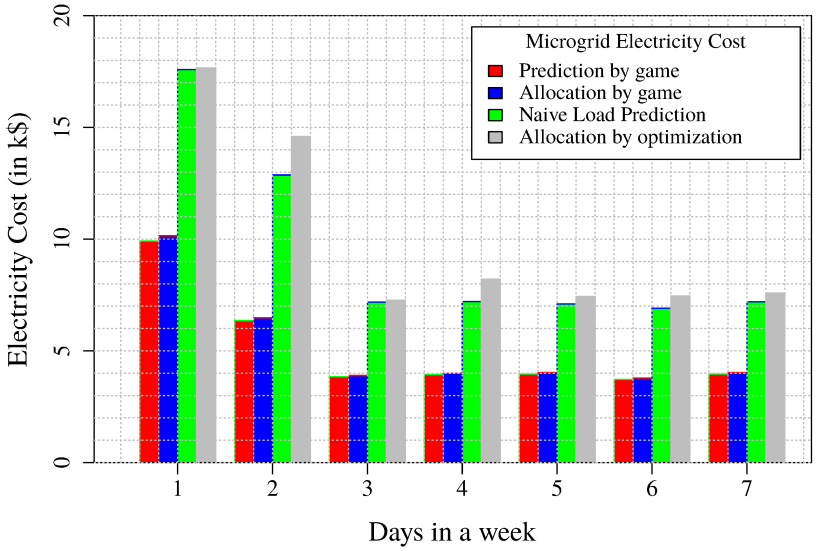

Figure 5.5: Electricity cost for centralized and game model.

the day. The performance improvement of the RDCDSM compared to the centralized method is depicted in Fig. 5.6 for various size of the microgrid. In all the cases, proposed system perform better. In Fig. 5.6, it is found that the performance of RDCDSM increases when the load is high and decreases when the load is low. This is because, system become more flexible in high load condition, thereby RDCDSM redistribute loads and power more smoothly.

Figs. 5.7 and 5.8 demonstrate the charging and discharging strategies of EVs and ESSs (including MESS) in RDCDSM. Integration of RES is an important objective of the modern power grid. Unfortunately, the RES is intermittent in nature because the amount of energy generated from RES is dependent on the weather condition. One of the solutions to integrate RES to the grid is likely by utilizing ESSs and EVs, but ESSs and EVs have limited capacity. Hence an intelligent system like RDCDSM enables to store and use renewable energy by exploiting ESSs and EVs optimally. The red and blue lines in Figs. 5.7 and 5.8 demonstrate charging and discharging pattern of the ESSs and EVs. When we observe Figs. 5.7, and 5.8, we will find that the charging of ESSs and some of the EVs are scheduled when the generation from

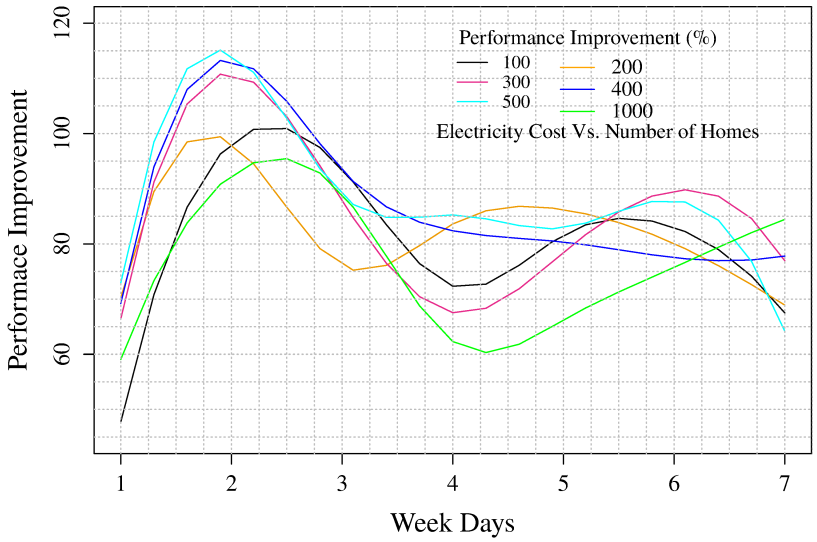

Figure 5.6: RDCDSM Vs. centralized: performance improvement.

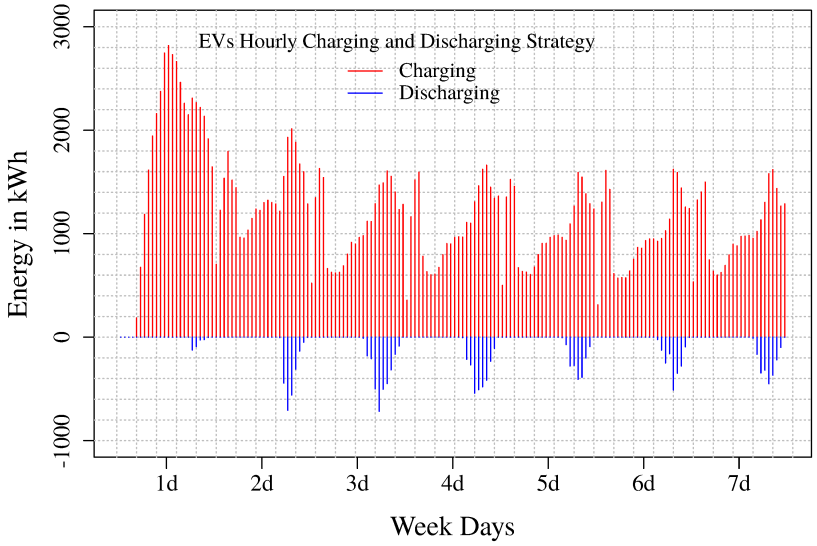

Figure 5.7: RDCDSM: EVs charging and discharging strategy.

RES is high (daytime) and discharging when load is high (evening) or no generation. This is an important feature of RDCDSM system which balances the microgrid load between time slots and eases the integration of RES with the existing grid.

Finally, Fig. 5.9 represents the penalty imposed by the microgrid to the those customers for requesting more or less quantity of electricity compared to the proposed

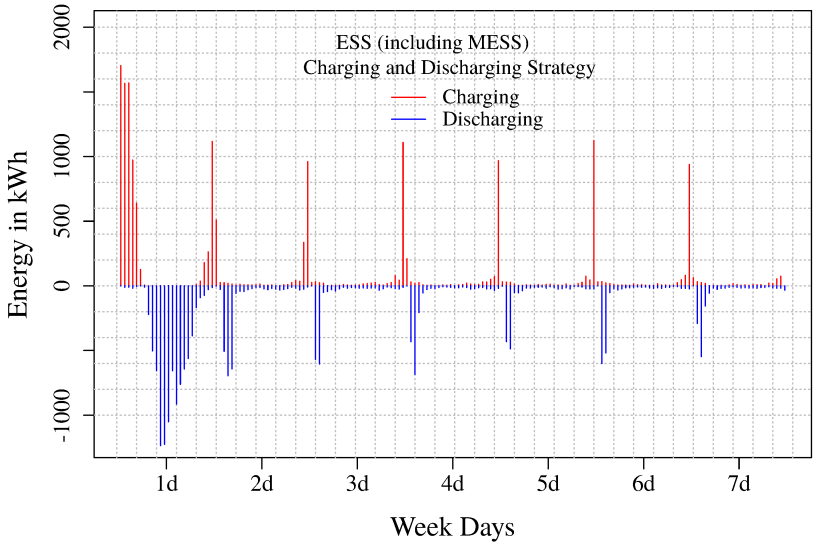

Figure 5.8: RDCDSM: ESSs charging and discharging Strategy.

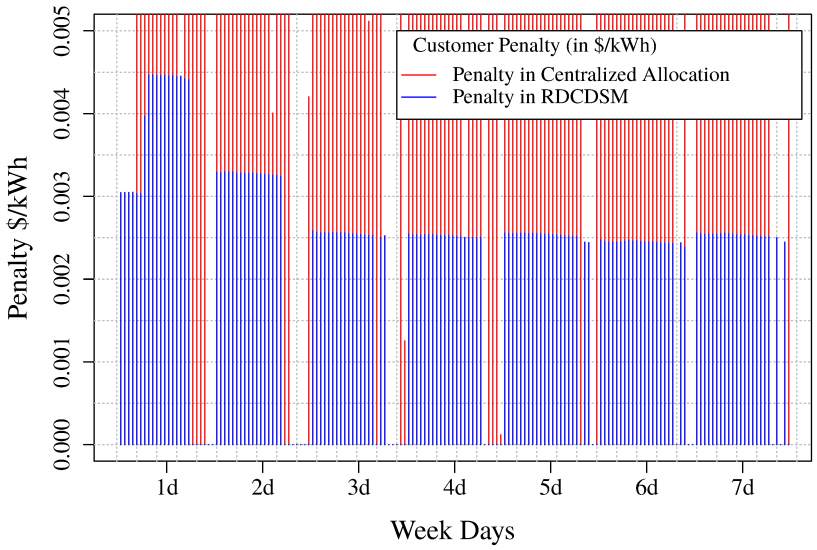

Figure 5.9: Penalty imposed to customers.

day ahead predicted demand. The penalty is little in RDCDSM compared to the penalty imposed by the operator of centralized allocation scheme. This is because the load was not properly balanced among the time slots in the naive prediction thereby a part of the renewable energy may remain uncounted due to no place to store or use. Moreover, a situation may arise at the time of allocation (centralized

distribution system) that due to capacity and other constraints the ESSs and EVs may not collectively supply energy to a time slots where demand is very high. On the other hand, RDCDSM system uses ESSs and EVs optimally such that RES energy can be used properly. It is also found that the penalty is higher in high load duration compare to the light load period. This is evident because the actual demand changes more in high load compare to the low or moderate amount of load duration.

5.4 Conclusion

We formulated two separate non-cooperative games with mixed strategy profiles to generate the price-ware estimation of electricity use for the next day and deliver power in real-time according to the price-ware predicted load. Moreover, we developed a simulation program to evaluate the validity and performance of the RDCDSM method. In theory, we showed that the proposed RDCDSM scheme converge to an optimal Nash equilibrium state and produce optimal results. We believe that the RDCDSM system will help the energy planner to plan for electricity generation and reduce the power production costs while providing the quality of electricity service to the customers.

Chapter 6

A Novel Algorithm for Optimal Electricity Pricing in a Smart Microgrid Network

In this chapter, we investigate and present a new algorithm for energy management and pricing of electricity in a microgrid network (MGN). The primary goal of this methodology is to control the flow of energy among the microgrids to minimize transmission (T&D) and generation costs of electricity for MG customers.

6.1 Motivation

It is anticipated that shortly the energy network may contain hundreds and thousands of microgrids (which are using DSM, such as DRTA, RDCDSM, etc.) may need to share electricity and storage to meet their demands as a whole. The MGN network creates new market scenarios where once always consumer may act as a supplier. It is nearly impossible for these new providers to enter the existing regulatory market which is controlled by a governing body. For the benefit of both supplier and

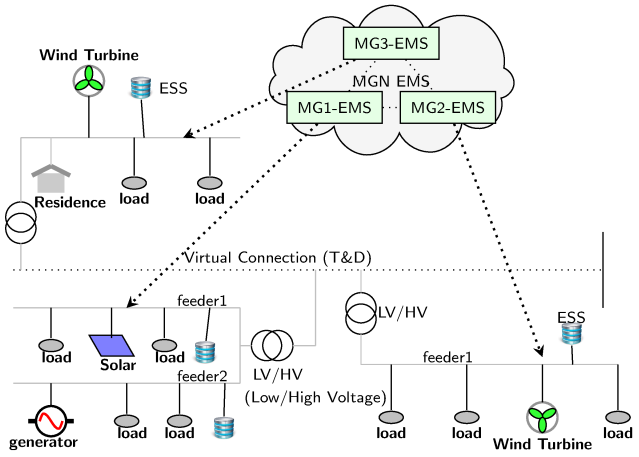

Figure 6.1: Smart Microgrid Network (MGN)

consumer, an open competitive market is desirable which accepts new providers and ensure marginal cost price for the electricity. Moreover, the microgrid may not own any transmission and distribution network to transfer energy from seller microgrid to a buyer microgrid, therefore, rely on the third party owned T&D networks. Hence, the microgrid needs to pay transmission costs and costs for various losses such as reactive, and resistive losses. Some work has been done to partially resolve the challenges of MGN which we have discussed in section 2.3. Unlike the existing work, to address the challenges of the new market scenarios we develop a new algorithm MEPM, which minimize the electricity cost (T&D and generation costs) for the customers of the MGN. The combined marginal cost (for more than one generator) of the generation is nonlinear, and a nonconvex therefore the optimal solution is difficult to achieve. To obtain an optimal solution, we split the problem into two subproblems and solve it optimally.

6.2 System model

We consider a MGN (Fig. 6.1), consisting of a set of N smart microgrids $\mathcal{N}$, connected with each other by means of transmission lines. Let the set of transmission lines

(feeders) be L which are connected with each other using a bidirectional LV/HV interfaces (transformers) as shown in Fig 6.1. The set of feeders represents the virtual connections between MGs, therefore creating our MGN. Let a set of all pairs (seller, buyer) of MGs be K_i ($K_i \subset \mathcal{N} \times \mathcal{N}$), each connected through a feeder l_i ($l_i \in L$). A feeder l_i has a capacity limit Γ_i. The flow of energy among them is controlled by mutual decisions of the management system. At any instance of time, let $\mathcal{M}$ and $\mathcal{B}$ be the set of sellers and buyers, where $\mathcal{M} \cap \mathcal{B} = \emptyset$ and $\mathcal{M} \cup \mathcal{B} \subseteq \mathcal{N}$. Each MG has a set of DGs $\mathcal{W}_n$ ($n \in \mathcal{N}$), primarily to fulfill the local demand. A MG sells energy in case of surplus or buys energy, when the demand is more than its production. Let $c_{m,b}$ be the cost of transporting one unit (1 kWh) of electricity from seller m ($m \in \mathcal{M}$) to buyer b ($b \in \mathcal{B}$), and $E_{n,w}$ ($n \in \mathcal{N}, w \in \mathcal{W}_n$) be the pre-authorized amount of electricity generation of energy source w with capacity $E^C_{n,w}$ of smart microgrid n. Here, $E_{n,w} \leq E^C_{n,w}$, and the pre-authorized generation ($E_{n,w}$) of DG w of n is controlled by the energy management system (EMS). The EMS decides the price (μ), to satisfy the MGN electricity demand $\tilde{D}_{\mathcal{B}}$ (total amount of electricity buyers want to buy), from the prices (monotonic non decreasing) proposed by each of the seller MGs. Then, the buyer b ($b \in \mathcal{B}$) contacts the sellers ($\mathcal{M}$) to buy electricity from them to compensate for its shortage.

6.2.1 System Assumption

We employ ANSI C84.1 standard voltage rating for the MGN. Similar to several Volt-VAR optimization research, we assume that the MGN system uses a lower voltage (from range A of C84.1) as the service voltage to minimize the losses. Each of the MGs has a linear vector that comprises the cost of electricity transportation from the sellers to the buyers, and the capacity of the transmission lines. To minimize the thermal losses, we assume the maximum capability of the transmission line is predefined,

Table 6.1: MEPM mathematical notation

Notation	Description
$\mathcal{N}$	Set of Microgrids
L	set of transmission lines
K_i	set of microgrids connected by transmission line l_i
Γ_i	capacity of the feeder l_i
$\mathcal{B}$, $\mathcal{M}$	Set of Buyers and Sellers
b, m	buyer and Seller
n	a microgrid
$\mathcal{W}_n$	Set of DGs in a Microgrid n
$E_{n,w}$	amount electricity needed from DG w of n
$E^C_{n,w}$	generation capacity of DG w of n
$\tilde{D}_{\mathcal{B}}$	buyers excess demand or shortage
w	generator of a microgrid
$\mu_{m,w}(E_{m,w})$	marginal cost function for w of m
$c_{m,b}$	Electricity Transmission Cost from m to b in $\$/kWh$
$\mu(E)$	combined or overall marginal cost function
E	Total Generation of $\mathcal{M}$
$R^{l_i}_{m,b},\ X^{l_i}_{m,b}$	resistance and reactance of l_i from m to b
$I_{m,b}$	amount of current flow from seller m to buyer b
$\pi_{m,b}$	capacitance of capacitor bank added to the input of b
$x_{m,b}$	amount of electricity transported from m to b without loss
V_b	voltage at buyer MG (b) (predefined)
$x^d_{m,b}$	electricity transmission loss from m to b
V_m	voltage at seller MG m (predefined)
$\tilde{x}_{m,b}$	Actual amount of electricity transferred from m to b with losses
$\tilde{D}_b$	excess demand or shortage of b
$\tilde{E}_m$	Excess or surplus of m
Γ_i	transmission capacity of the line l_i connecting K_i
μ^l	lower bound overall marginal cost
μ^u	upper bound overall marginal cost
$\mu^o,\ \hat{P}^q_{\mathcal{B}}$	pair of optimal marginal and T&D costs
$\hat{P}^l_{\mathcal{B}},\ \hat{P}^u_{\mathcal{B}}$	lower and upper bound T&D costs
D_m	demand of seller m

whether they use a shared or dedicated transportation system. Also, transmission cost $c_{m,b}$ is payable to the owner of the transmission and distribution network which is imposed by the transmission and distribution operator in a competitive electricity market. The transmission is equipped with VAR compensation component at the receiving point to raise the power factor to unity (or near unity). We also assume that i) bi-directional electricity flow, ii) coupling between microgrids, and iii) integration of renewable energy sources to the grid should comply with the standard found in [24, 8, 89] and IEEE1547A, IEEE1547.4 standard. The energy generated from the renewable sources in predicted using the model described in [120].

6.2.2 Marginal Cost & Cost Function

It is widely accepted that the cost functions are cubic in nature (approximated) but in reality the only and most important feature of the cost curve is to be monotonic non-decreasing [45]. The cost of a product (such as electricity) is dependent on various factors such as, quantity, investment, labor, fuel (such as gas, oil, wind, solar radiation etc), market demand, establishments, etc. Therefore, it is nearly difficult to express the cost by a regular curve (function) [45, 46, 51, 102]. The truth is that a unit cost (marginal cost) or total cost never decreases with the increase of the amount of production. The amount of production is determined by the total demand of a market for an instance of time. Let $E_{m,w}$ be the amount of electricity generated by a generator w of a seller microgrid m; then the total cost of producing $E_{m,w}$ is [45, 102]:

$$C(E_{m,w}) = v(\alpha, E_{m,w}) + cE_{m,w} + d, \tag{6.1}$$

where $\alpha, c, d \in \mathbb{R}_+$, and c & d are the minimum cost (fixed) for producing one unit of electricity and producing nothing respectively, which is dependent on capital or initial

investment. $v(.)$ is the variable cost which is a non-decreasing monotonic function. The parameter α is dependent on the running cost of the system which includes labor, fuel, maintenance and various other costs. For a sufficient long running system, the short running fixed cost (c) becomes a variable because investment in facilities, equipment, and basic organization cannot be significantly reduced in a short period [75, 112]. Each time, a utility company determines the marginal cost of the product and uses it to determine the selling price of the product. For the survival of the utility company, the selling price must be higher than the marginal cost of the product.

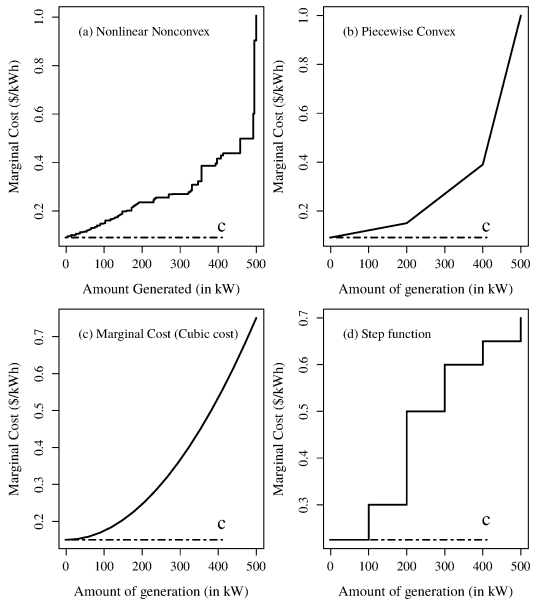

Figure 6.2: Electricity marginal cost curve for (a) nonlinear noncovex, (b) piecewise convex, (c) cubic, and (d) step cost functions.

Definition 6.1 (Marginal Cost)**.** The marginal cost function $\mu_{m,w}(E_{m,w})$ of generator w of operator m, represents the price of electricity for producing one more unit [45, 93]. For any cost function in eq. (6.1), it is defined as,

$$\mu_{m,w}(E_{m,w}) = \frac{\partial C(E_{m,w})}{\partial E_{m,w}} \tag{6.2}$$

The marginal cost is a non-decreasing monotonic function, and it can be determined by the first order derivative of the total cost function. Hence, the marginal cost function can be expressed by a linear, quadratic, step, piecewise convex or nonlinear non-convex cost-function (see fig. 6.2). For simplicity, most researchers assume the marginal cost or cost function to be convex or approximate it near to a convex function [45, 93, 53, 125, 133]. In reality, however, this is not accurate; the marginal cost can not be expressed by a regular function such as linear, nonlinear, convex. Indeed, it is a function which is irregular in nature and non-decreasing with the increase of the production quantity. Also, the marginal cost function of a company having more than one generator is more complex and certainly nonlinear non-convex, even if the individual cost function is linear [93, 46]. The operation and maintenance cost of the non-renewable energy sources increase with the amount of production. Therefore, the marginal cost described in the Appendices (from 6.2.2 to 6.2.2) are suitable for the non-renewable energy sources. Whereas the operation and maintenance cost of the renewable energy sources barely increases with the amount of the electricity generation. The LRMC (long run marginal cost) also known an LCOE (Levelized cost of electricity) is used to determine the energy cost of the renewable energy sources (see section 6.2.2).

Quadratic Marginal Cost function

It is widely accepted that the total cost functions are cubic in nature [45] and according to eq. (6.1) the cubic cost function for electricity is defined as [45]:

$$C(E_{m,w}) = \alpha E_{m,w}^3 - \beta E_{m,w}^2 + cE_{m,w} + d \tag{6.3}$$

where $\alpha, \beta, c, d \in \mathbb{R}_+$ and therefore, the marginal cost function for cubic cost is quadratic (def. 6.1, see Fig. 6.2) [45],

$$\mu_{m,w}(E_{m,w}) = \frac{\partial C(E_{m,w})}{\partial E_{m,w}} = 3\alpha E_{m,w}^2 - 2\beta E_{m,w} + c \tag{6.4}$$

Fig. 6.2(c) shows the quadratic marginal cost curve. For the monotonic non-decreasing quadratic cost function, we assume $\alpha \geq \beta$ in eqs. (6.3) and (6.4). Here, c is the long term minimum cost for one unit of electricity production. Eq. (6.4) determines the marginal cost for the amount of generation from generator w of m. Now, let the marginal cost $\mu_{m,w}(E_{m,w})$ for $E_{m,w}$ be given as μ, such that $\mu_{m,w}(E_{m,w}) = \mu$. Then, by solving (6.4), a utility company can determine the maximum amount of electricity which needs to generate from a certain generator when the marginal cost is given, thus

$$E_{m,w} = \frac{2\beta + \sqrt{4\beta^2 - 12\alpha(c-\mu)}}{6\alpha};\ E_{m,w} \leq E_{m,w}^C \tag{6.5}$$

otherwise,

$$E_{m,w} = E_{m,w}^C \tag{6.6}$$

Here the generation is only possible when $\mu \geq c$.

Linear Marginal Cost function

Similarly, marginal cost for a quadratic cost function is linear i.e.

$$\mu_{m,w}(E_{m,w}) = \alpha E_{m,w} + c, \tag{6.7}$$

where α and c are constants. For the linear marginal cost, when the marginal cost (i.e., $\mu_{m,w} = \mu$) for the generation is known, then the amount of generation is determined

as,

$$E_{m,w} = \frac{\mu - c}{\alpha};\ \text{where}\ E_{m,w} \leq E^{C}_{m,w} \tag{6.8}$$

otherwise, eq. (6.6), and the generation is possible when $\mu \geq c$.

Piecewise Marginal Cost function

Sometimes a marginal cost function is expressed as a piecewise convex function to accommodate the peak hour and off-peak hour electricity price (see Fig. 6.2(b)). The function is a monotonic increasing function and has a set of convex functions. Therefore,

$$\mu_{m,w}(E_{m,w}) = \max(f_1(E^1_{m,w}), f_2(E^2_{m,w}), \cdots f_k(E^k_{m,w})), \tag{6.9}$$

and $E_{m,w} = \sum_{j=1\cdots k} E^j_{m,w}$, where $f_1(.), f_2(.), ..., f_k()$ are the convex functions to calculate the costs for various specific range (amount) of production. For the piecewise convex marginal cost function, we assume that the convex functions are sorted (or indexed) according to the lower cost μ^i_l with the amount of generation $E^i_{m,w}$. The appropriate function f_i is selected such that $\mu^i_l \leq \mu \leq \mu^{i+1}_l$ (where μ: $\mu_{mw} = \mu$ is the given cost), and the amount of generation is given by,

$$E_{m,w} = E^i_{m,w} + \arg f_i(\mu - \mu^i_l);\ \text{where}\ E_{m,w} \leq E^C_{m,w}, \tag{6.10}$$

otherwise, eq. (6.6).

Nonlinear Non-Convex Marginal Cost function

Sometimes, the rate of a product increases or remain the same for increasing the generation of one more unit of electricity. In this case, the marginal cost function is

a nonlinear and non-convex function such as (see Figs 6.2(a) and 6.2(d)),

$$\mu_{m,w}(E_{m,w}) = \alpha_{nl} E_{m,w} + c \tag{6.11}$$

where α_{nl} and $E_{m,w}$ both are variables and $\mu_{m,w}(E_{m,w}+1) \geq \mu_{m,w}(E_{m,w})$. The amount of electricity $E_{m,w}$ needed from generator w of m for a given cost μ ($\mu_{m,w} = \mu$) can be calculated as,

$$\begin{aligned} E_{m,w} &= \frac{\mu - c}{\alpha_{nl}};\ \text{where } E_{m,w} \leq E^C_{m,w} \\ E_{m,w} &= E^C_{m,w};\ \ \text{otherwise} \end{aligned} \tag{6.12}$$

Eq. (6.12) is similar to eq. (6.8) but here, the denominator α_{nl} is a variable which varies according to the amount of generation. Therefore, the cost of electricity can be calculated instantly by maintaining a sorted (according to the cost $\mu_{m,w}$) linear list containing distinct generation costs and the corresponding maximum amount of generation. Therefore, for a given cost μ ($\mu_{m,w} = \mu$), the amount of electricity $E_{m,w}$ can be determined from the linear list. Let the sorted linear list be $\{\mu_1 \rightarrow E^1_{m,w}, \cdots, \mu_i \rightarrow E^i_{m,w}, \cdots\}$, where μ_i is the unique marginal cost and $E^i_{m,w}$ is the corresponding maximum amount of electricity generated from the generator w of m. Now, suppose the given cost is μ, then the amount of electricity is $E^j_{m,w}$, if $\mu_{j-1} < \mu \leq \mu_j$.

Levelized Cost of Electricity (LCOE)

Levelized Cost of Energy (LCOE) is the most transparent metric used to measure the electricity generation cost for renewable. LCOE is used for renewable energy since the renewable energy does not need fuel, maintenance cost is very low, government incentive for customers and producers, and the technological innovation has reduced manufacturing cost 100 times [14, 96]. The important and most influential cost for the RES is land cost, and long term investment costs. Also, in a competitive market

when grid parity is considered, then the long term average cost or LCOE is used to calculate the cost of the renewable energy. The most important aspect for renewables cost calculation is that the variable expense is negligible. The LCOE is a measure of the marginal cost (MC) of electricity over a long duration and sometimes is referred to as Long Run Marginal Cost (LRMC) [14, 96]. LCOE cost is calculated in $\$/kWh$ considering total cost and energy generated over the life time of the energy generating system [14]. LCOE is sensitive to the input assumption. Let the life time of a RES be Yr, in year y, the initial investment/cost of the system be I_y, operation and maintenance cost be O_y, interest expenditure be F_y, discount rate be r, energy production E_y, and degradation rate be dg, then the LCOE for a renewable energy source w of m can be written as [14, 16],

$$LCOE_{m,w} = \frac{\sum_{y=0}^{Yr} \frac{(I_y+O_y+F_y)}{(1+r)^y}}{\sum_{y=0}^{Yr} \frac{E_y(1-dg)^y}{(1+r)^y}} \tag{6.13}$$

where $LCOE_{m,w}$ is the electricity cost or rate (in $\$/kWh$) of a renewable sources w in a seller microgrid m. The renewable energy cost therefore be a no decreasing constant value for a instance of time and can be written as,

$$\mu_{m,w}(E_{m,w}) = LCOE_{m,w},\ \forall E_{m,w} \tag{6.14}$$

Given a marginal cost μ, the amount of generation used is,

$$\begin{aligned} E_{m,w} &= E^C_{m,w};\ \text{where } \mu \geq LCOE_{m,w} \\ E_{m,w} &= 0;\ \text{otherwise} \end{aligned} \tag{6.15}$$

As mentioned, for the survival of a company, the selling price should not be less than the marginal cost. The marginal cost is a monotonic non-decreasing function

[93]. Now, let E be the total amount of electricity generated by the MGN system, then the total cost of the electricity to fulfil excess demand $\tilde{D}_{\mathcal{B}}$ is,

$$\mu(E) \cdot \tilde{D}_{\mathcal{B}} \tag{6.16}$$

where $\mu(E)$ is the overall marginal cost of the MGN system, $\mu(E) \geq \mu_{m,w}(E_{m,w})$, and $E = \sum_{m \in \mathcal{M}} \sum_{w \in \mathcal{W}_m} E_{m,w}$. We use the marginal cost functions from Appendices 6.2.2 to 6.2.2 to calculate the cost of nonrenewable energy sources and LCOE (Appendix 6.2.2) for renewable energy sources. The model is applicable for any of the other marginal cost functions by replacing the marginal cost functions illustrated above with the appropriate non-decreasing marginal cost function.

6.2.3 Electricity Transportation

In our MGN system, we assume that all the microgrids are connected with each other using electricity transmission and distribution lines. Most of the energy losses in electricity transportation are due to the resistance of the energy network and reactive power which is injected by the reactive load. The T&D (transmission and distribution) losses for a transmission and distribution line is $I^2_{m,b}(R^{l_i}_{m,b} + jX^{l_i}_{m,b})$, where $R^{l_i}_{m,b}$ is the resistance, $X^{l_i}_{m,b}$ is the reactance of the transmission line from m to b, and j is the complex variable dependent on the phase of the voltage V_m (voltage at seller m) and current $I_{m,b}$ (amount of current a seller m sends to b). The values of $R^{l_i}_{m,b}$ and $X^{l_i}_{m,b}$ are dependent on the physical characteristics of the transmission line. $X^{l_i}_{m,b}$ (in ohm) is the reactance of the transmission line which can be expressed as,

$$X^{l_i}_{m,b} = \omega L^{l_i}_{m,b} => 2\pi f L^{l_i}_{m,b} \tag{6.17}$$

where $L^{l_i}_{m,b}$ is the inductance (in henries) of the transmission line l_i from m to b, f is the frequency in Hz. Therefore, the power factor of the transmission line is $\cos\theta = \frac{R^{l_i}_{m,b}}{\sqrt{(R^{l_i}_{m,b})^2+(X^{l_i}_{m,b})^2}}$. Here, θ is the angle between apparent power and active power. Now, to reduce the losses, let the power factor of the transmission be $cos\phi$ (near to unity and $\theta >> \phi$); that is θ is reduced to ϕ. To do so, a reactive compensation equipment (such as, a shunt capacitor bank) is added at the input of the buyer microgrid (b). Let the capacitance of the capacitor bank be $\pi_{m,b}$ and the amount of energy transferred (without loss) from m to b be $x_{m,b}$ then, (according to [91]),

$$\pi_{m,b} = \frac{(x_{m,b} + x^d_{m,b})\cos\theta(\tan\theta - \tan\phi)}{2\pi f V_b^2}, \tag{6.18}$$

where V_b is the voltage at buyer microgrid and $x^d_{m,b}$ is the total loss (resistive and reactive) of electricity while transmitted from m to b. In general the value of the receiving voltage (V_b) should be within $\pm 5\%$ ($V_m \pm 5\%$) of voltage (V_m) at m [91]. Here, we assume V_b is chosen a value between V_m and $(V_m - 1\%)$. Therefore, the energy loss $x^d_{mb,}$ due to transportation of electricity from a seller m to a buyer b is,

$$x^d_{m,b} = I^2_{m,b}(R^{l_i}_{m,b}\cos\phi + X^{l_i}_{m,b}\sin\phi), \tag{6.19}$$

and the total amount of electricity needed to be transported by a seller m to a buyer b is,

$$\tilde{x}_{m,b} = x_{m,b} + x^d_{m,b} \tag{6.20}$$

Then, the total transportation cost of MGN is,

$$TC = \sum_{b\in\mathcal{B}, m\in\mathcal{M}} (c_{m,b} \cdot \tilde{x}_{m,b}) \tag{6.21}$$

A buyer may choose another seller to decrease the buying amount if the transmission (or transportation) loss is lower than the current seller. Let $\tilde{D}_b$ be the shortage of electricity of buyer b, then $\sum_{m \in \mathcal{M}} x_{m,b} = \tilde{D}_b$

Definition 6.2. [Allocation Problem] The optimal matching of sellers and buyers which will minimize the overall energy costs to the customers can be formulated as,

$$\min TC = \min \sum_{b \in \mathcal{B}, m \in \mathcal{M}} (c_{m,b} \cdot \tilde{x}_{m,b}) \tag{6.22}$$

Transformer thermal limit

Both ends of the transmission line are connected to a delivery (at m) and a receiving (at b) transformer. The amount of current flow through these transformers generate heat which is typically resolved by coolant (such as oil). Hence, a transformer has an upper limit of energy handling capacity to sustain and extend its life time. Beyond this limit, the transformer temperature increases and may burn out or shorten the life of a transformer. Therefore, a transformer must not handle electricity beyond a rated power. The hot-spot temperature of the transformer can be computed for any load by using the following standard relations which are given in [15],

$$\omega_{HS} = \omega_{TO} + \Delta\omega_{HR} \left(\frac{I_{m,b}}{I^R_{m,b}} \right)^{2e} \tag{6.23}$$

where ω_{HS}, ω_{TO}, and $\Delta\omega_{HR}$ are hot-spot temperature, top-oil temperature, and rated hot-spot temperature rise above top-oil respectively. $I_{m,b}$, $I^R_{m,b}$, and e are load current, rated current and winding exponent accordingly. Now, if the voltage at the input of the transformer is V_b then, the rated power of the transformer is:

$$P_{m,b} = I^R_{m,b} V_b \tag{6.24}$$

where $P_{m,b}$ is the rated power of the transformer and therefore it limits the input energy of the transformer as,

$$x_{m,b} \leq P^r_{m,b}, \text{ for receiving transformer} \tag{6.25}$$

and

$$\tilde{x}_{m,b} \leq P^d_{m,b}, \text{ for delivering transformer} \tag{6.26}$$

where $P^r_{m,b}$ and $P^d_{m,b}$ are the receiving and delivering rated power of transformers at m and b.

6.3 Electricity Pricing Model

It is clear that the electricity price a buyer has to pay is dependent on both the overall marginal cost and the transportation cost of electricity. For simplicity, we assume that the profit of the seller for selling electricity is included within the marginal costs. Therefore, the price (paid by the buyer) of electricity can thus be expressed as:

$$\mu(E) \cdot \tilde{D}_{\mathcal{B}} + \sum_{b \in \mathcal{B}} \sum_{m \in \mathcal{M}} (c_{m,b} \cdot \tilde{x}_{m,b}) \tag{6.27}$$

Here, the overall marginal cost ($\mu(E)$) depends on the marginal costs of the sellers. Hence, there are ample scopes to determine the optimal electricity price by jointly considering overall marginal cost and transmission losses, in an optimization model, and subsequently solve it optimally. Therefore, a model needs to be developed which will concurrently minimize the overall electricity price (6.27).

6.3.1 Minimum Electricity Pricing Model (MEPM)

Eq. (6.27) illustrates the total payment of electricity of the MGN buyers. Therefore, the minimum total payment for electricity can be determined by solving the following model,

$$\min \left(\mu(E) \cdot \tilde{D}_{\mathcal{B}} + \sum_{b \in \mathcal{B}} \sum_{m \in \mathcal{M}} (c_{m,b} \cdot \tilde{x}_{m,b}) \right) \tag{6.28}$$

Subject to,

$$\sum_{m \in \mathcal{M}} x_{m,b} \ = \tilde{D}_b, \ \forall b \in \mathcal{B} \tag{6.29}$$

$$\sum_{l_i \,:(m,b) \in K_i} \tilde{x}_{m,b} \ \leq \Gamma_i, \forall l_i \in L \tag{6.30}$$

$$\tilde{x}_{m,b} \ = x_{m,b} + x^d_{m,b}; \ x^d_{m,b} \leq x_{m,b}, \ \forall m, \forall b \tag{6.31}$$

$$x^d_{m,b} = I^2_{m,b}(R^{l_i}_{m,b} \cos\phi + X^{l_i}_{m,b} \sin\phi) \ \ \forall m, \forall b \tag{6.32}$$

$$I_{m,b} \ = \frac{\tilde{x}_{m,b}}{V_m}, \ \forall m \in \mathcal{M}, \forall b \in \mathcal{B} \tag{6.33}$$

$$\pi_{m,b} \ = \frac{\tilde{x}_{m,b} \cos\theta(\tan\theta - \tan\phi)}{2\pi f V_b^2}, \ \forall m, \forall b \tag{6.34}$$

$$V_m = V_b + I_{m,b}(R^{l_i}_{m,b} \cos\phi + X^{l_i}_{m,b} \sin\phi) \tag{6.35}$$

$$x_{m,b} \ \leq P^r_{m,b}, \ and \ \tilde{x}_{m,b} \leq P^d_{m,b}, \ \forall m, \forall b; \tag{6.36}$$

$$\sum_{b \in \mathcal{B}} \tilde{x}_{m,b} \ \leq \tilde{E}_m, \ \forall m \in \mathcal{M} \tag{6.37}$$

$$\tilde{E}_m = \sum_{w \in \mathcal{W}_m} E_{m,w} - D_m, \ \forall m \in \mathcal{M} \tag{6.38}$$

$$\sum_{m \in \mathcal{M}} \tilde{E}_m \geq \tilde{D}_{\mathcal{B}}, \ \text{where } \tilde{D}_{\mathcal{B}} = \sum_{b \in \mathcal{B}} \tilde{D}_b \tag{6.39}$$

$$\mu(E) \ \geq \mu_{m,w}(E_{m,w}),\ \forall m \in \mathcal{M},\ \forall w \in \mathcal{W}_m \tag{6.40}$$

$$E \geq \sum_{m \in \mathcal{M}} \sum_{w \in \mathcal{W}_m} E_{m,w} \geq D_{\mathcal{B}} \tag{6.41}$$

where variable $\tilde{E}_m$ is the excess generation of electricity by seller m, and $D_{\mathcal{B}},\ D_m$ represent the total actual demand of the MGN buyers and the seller demand respectively. Γ_i $(l_i : (m, b) \in K_i)$ is the transmission capacity of the line (l_i) which connects a pair of MGs in K_i. The solution to the above optimization model (from eqs. (6.28) to (7.11)) will yield the joint optimal overall marginal cost and transportation cost for the MGN. Eq. (6.29) states that the electricity transmitted from sellers $(\mathcal{M})$ must be equal to the total shortage (or excess demand: $\mathcal{D}_b$) of the buyer microgrid (b). The constraint in eq. (6.30) limits the total flows of electricity from m to b through a transmission or distribution line which should not surpass the capacity of the line. Second part of eq. (6.31) ensures that the amount of electricity transported from m is zero when $x_{m,b}$ is zero. A number of current flows through l_i from m to b is calculated in eq. (6.33). Constraint (6.36) ensures that the delivering and receiving electricity should be less than the power rating ($P^d_{m,b}$ and $P^r_{m,b}$) of the transformers attached. The selling amount of the power should satisfy the amount of electricity buyers $(\mathcal{B})$ wants to buy from a seller m which is outlined in eq. (6.37). Eq. (6.38) asserts that the total excess amount of generation is equivalent to the sum of excess electricity generated by all sellers. The MGN total excess production must satisfy the shortage of electricity which is manifested in eq. (6.39). Finally, the overall marginal cost of the electricity for the MGN is determined by eq. (6.40).

Here, if all the marginal cost functions $\mu_{m,w}(E_{m,w})$ are convex, then the MEPM problem remains a nonlinear and non-convex problem due to the overall marginal cost which is the superimposition [103] of all the marginal costs. Therefore, the above MEPM problem is a difficult (NP-Hard) problem, and no polynomial solution exists [124]. Moreover, in practice, the marginal cost function does not need to be

convex; rather, the more accurate property of the marginal cost function is monotonic non-decreasing [45]. The monotonic non-decreasing function will increase or remain the same by increasing the production of electricity. To obtain a polynomial time solution of the MEPM problem, we decompose into two subproblems, the overall marginal cost problem (OMCP) and an optimal electricity allocation. These two sub-problems are both used as modules in our solution methodology of MEPM to determine the optimal solution to our original problem. OMCP is used to determine a feasible interval for the optimal marginal cost, with a lower bound (μ^l) and an upper bound (μ^u). Now, the problem reduces to a search for the optimal marginal cost that yields optimal overall price of electricity ($\mu^c + \hat{P}^c_{\mathcal{B}}$). The MEPM performs a search for the optimal marginal cost and at each iteration (after solving an allocation problem) it removes a segment of the feasible interval that is of no use (i.e., a marginal cost in a segment removed by the method will always result in higher overall price). Our solution methodology follows a divide and conquer approach since such method is deterministic (it will always converge and return the optimal result) and enjoys low complexity. In the following sections, we describe the decomposition and polynomial time solution of MEPM.

6.4 Decomposition of MEPM

The MEPM clearly is a combination of two inter-related optimization problems, (i) minimum overall marginal cost problem (OMCP) by setting the value of $c_{m,b} = 0$ and $E_{m,w} = E^C_{m,w}$, and (ii) minimum transportation cost problem (allocation problem) by setting the value of $\mu(E) = 0$ in the objective function (Def. 6.2). The overall marginal cost has lower and upper bound values. The MEPM is infeasible below the lower bound overall marginal costs. Beyond the upper bound value, the system will always produce the same cost for transportation but the overall marginal cost will

increase.

Definition 6.3. [Lower Bound Overall Marginal Cost, μ^l] The lower bound overall marginal cost, $\mu^l \equiv \mu(E)$ is the combined marginal cost that is calculated while $(\forall w \in \mathcal{W}_m,\ \forall m \in \mathcal{M})$, $E_{m,w}$ and $c_{m,b}$ of MEPM are set to $E^C_{m,w}$ and 0 respectively. In other words, the overall marginal cost below μ^l must be infeasible for the MGN, i.e., $E < \tilde{D}_{\mathcal{B}}$, where $E_{m,w} \leq E^C_{m,w}$.

Definition 6.4. [Upper Bound MGN Overall Marginal Cost, μ^u] The upper bound overall marginal cost, $\mu^u \equiv \mu(E)$ is the combined marginal cost that is calculated after the optimization of the transportation costs. The optimization of transportation costs is carried out with an initial setting of MEPM, where $\mu(E) = 0$ and $E_{m,w} = E^C_{m,w}$, $(\forall w \in \mathcal{W}_m,\ \forall m \in \mathcal{M})$.

The overall marginal cost beyond μ^u does not have any effect on the transportation cost (TC) because any value of $E_{m,w}$ between the value determined by the optimization of transportation cost and $E^C_{m,w}$ will yield the same transportation cost TC and the MGN system is infeasible for $E_{m,w} > E^C_{m,w}$.

Lemma 6.4.1. *The decrease of the overall marginal cost $\mu(E)$ from upper bound μ^u to lower bound μ^l will monotonically increase the value of the minimum transportation cost (TC).*

Proof Consider two marginal costs $\mu(E)$ and $\mu(E')$ of the MGN, where $\mu(E) \geq \mu(E')$ and $E, E' \geq \tilde{D}_{\mathcal{B}}$. In this case, $E > E'$, and $E' = \sum_{m\in\mathcal{M}} \sum_{w\in\mathcal{W}} (E_{m,w} - \Delta E_{m,w})$, where $\Delta E_{m,w} \geq 0$ and $E = \sum_{m\in\mathcal{M}} \sum_{w\in\mathcal{W}} E_{m,w}$. Here, $(E_{m,w} - \Delta E_{m,w})$ indicates the amount of production of some generators which will decrease due to decrease of the marginal cost from $\mu(E)$ to $\mu(E')$. Now, suppose for a generator m, $\sum_{b\in\mathcal{B}} \tilde{x}_{m,b} \geq \tilde{E}_m$. If $\sum_{b\in\mathcal{B}} \tilde{x}_{m,b} = \tilde{E}_m$ then the transportation cost remains the same but if $\sum_{b\in\mathcal{B}} \tilde{x}_{m,b} > \tilde{E}_m$, then, we have to find one or more lower cost generators which have surplus electricity to fulfill the need

of buyer b. Suppose, all these new sellers are S, then $c_{m,b} \leq c_{m',b},\ \forall m' \in S\ \&\ m \neq m'$. Therefore, $\sum_{m\in\mathcal{M}}\sum_{b\in\mathcal{B}}(\tilde{x}_{m',b}\cdot c_{m',b}) \geq \sum_{m\in\mathcal{M}}\sum_{b\in\mathcal{B}}(\tilde{x}_{m,b}\cdot c_{m,b})$. Similarly, if we decrease the overall marginal cost, then the transportation costs will increase gradually or remain unchanged. The system will choose the same set of generators, and the amount of electricity generation of the selected generators remain the same if $E = E'$. Therefore, the overall marginal costs in both cases remain the same, i.e., $\mu(E) = \mu(E')$.

From the lemma 6.4.1, we find that each overall marginal cost, μ^i ($\mu^l \leq \mu^i \leq \mu^u$) has a minimum transportation cost (TC^j) or minimum average transportation cost $\hat{P}^j_{\mathcal{B}}$, where, $\hat{P}^j_{\mathcal{B}} = \frac{TC^j}{\tilde{D}_{\mathcal{B}}}$. Let the optimal solution of the MEPM problem be $\mu^o \times \tilde{D}_{\mathcal{B}} + \hat{P}^q_{\mathcal{B}} \times \tilde{D}_{\mathcal{B}}$, then, $\mu^o \times \tilde{D}_{\mathcal{B}} + \hat{P}^q_{\mathcal{B}} \times \tilde{D}_{\mathcal{B}} \leq \mu^i \times \tilde{D}_{\mathcal{B}} + \hat{P}^j_{\mathcal{B}} \times \tilde{D}_{\mathcal{B}},\ \forall \mu^i \in \{\mu^l, \mu^u\} \setminus \mu^o$ and $\forall \hat{P}^j_{\mathcal{B}} \in \{\hat{P}^u_{\mathcal{B}}, \hat{P}^l_{\mathcal{B}}\} \setminus \hat{P}^q_{\mathcal{B}}$, and $\hat{P}^q_{\mathcal{B}}$ is the minimum average transportation cost due to marginal cost set to a value, μ^o.

6.4.1 Algorithmic Solution for MEPM

The MEPM algorithm chooses a value for μ^i between μ^u and μ^l, and determines the minimum transportation cost ($\hat{P}^j_{\mathcal{B}}$). The optimal solution is the lowest value of the summation of μ^i and $\hat{P}^j_{\mathcal{B}}$. An efficient polynomial solution (divide-and-conquer) of the MEPM problem is presented in Fig. 6.3. In Fig. 6.3, steps (III) to (XIV) are repeated while all the partitions are deleted and the MEPM scheme terminates with minimum (optimal) per kWh price $\mu^c + P^c_{\mathcal{B}}$ of the MGN network. In short, the MEPM method divides the marginal cost space (Fig. 6.3, step (IV)) into two partitions, then determines the average transmission cost (Fig. 6.3, step (VI)). Then, the MEPM discards one or both partitions when the minimum possible cost of the partition(s) is greater than $\mu^c + P^c_{\mathcal{B}}$ (Fig. 6.3, steps (VIII) and (XII)). Otherwise, it updates the $\mu^c + P^c_{\mathcal{B}}$ (Fig. 6.3, steps (IX) and (XIII)) and repeat the same divide-and-conquer method. The MEPM solution contains two sub-problems, hence the solution of the

MEPM is derived by combining the solution of OMCP (Fig. 6.3, step (I)) and the allocation problem (Fig. 6.3, step (VI)) interactively.

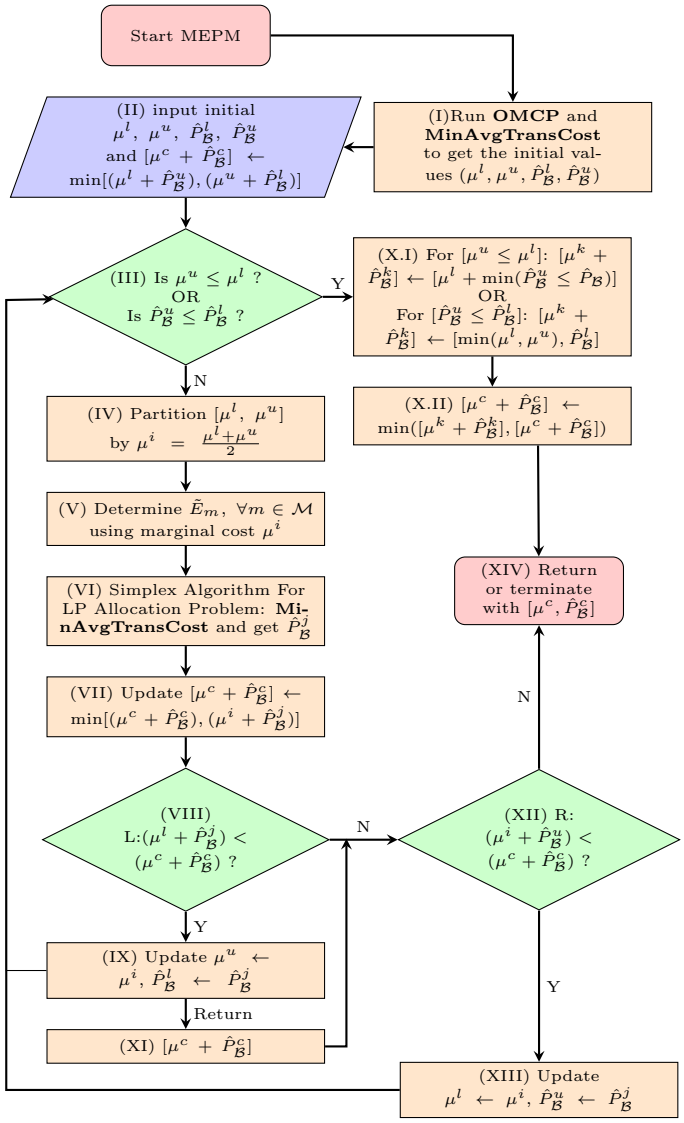

Figure 6.3: Schematic diagram of MEPM Algorithm; L: left partition; R: right partition

Algorithm for OMCP

One of the objectives of our MEPM algorithm is to determine the overall marginal cost and $\tilde{E}_m,\ \forall m \in \mathcal{M}$, by solving the OMCP which is described in Section 6.4.

Suppose, both $\mu(E)$ and $\tilde{E}_m$ are unknown and the excess demand $\tilde{D}_{\mathcal{B}}$, $E^C_{m,w}$ are known. The mathematical model for OMCP can be realized by replacing $\tilde{x}_{m,b} = 0$ in eq. (6.28) (objective) and eqs. (6.38) – (7.11) as constraints of the objective. The solution of the OMCP model will determine the overall marginal cost $\mu(E)$ by achieving the minimum total cost of the excess demand $\tilde{D}_{\mathcal{B}}$ for any configuration of the MGN. Then, $\mu(E)$ and $\tilde{E}_m$ can be determined by the following steps which are also shown in Fig. 6.4.

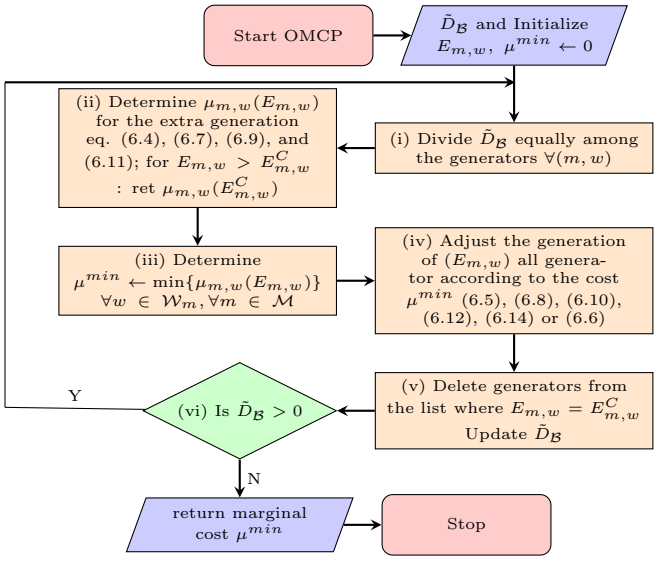

Figure 6.4: Schematic diagram of OMCP Algorithm

Step 1: Divide the excess demand $\tilde{D}_{\mathcal{B}}$ among the generators ($\forall w \in \mathcal{W}_m$) of all sellers ($\forall m \in \mathcal{M}$), and determine the marginal costs $\mu_{m,w}(E_{m,w})$ (see, eq. (6.4), (6.7), (6.9), (6.11), and (6.14)). Take the $\mu^{min} = min\{\mu_{m,w}(E_{m,w})|w \in \mathcal{W}_m, m \in \mathcal{M}\}$.

Step 2: Adjust $E_{m,w}$ with a calculated (step 1) marginal cost μ^{min} using eqs'.(6.5), (6.8), (6.10), (6.12), (6.15) or (6.6).

Step 3: modify $\tilde{D}_{\mathcal{B}}$ with the new amount of generation, such as, $\tilde{D}_{\mathcal{B}} = (\tilde{D}_{\mathcal{B}} - \sum_{m \in \mathcal{M}} \tilde{E}_m)$ and discard $w \in \mathcal{W}_m$, $E_{m,w} \geq E^C_{m,w}$. Repeat Step 1 to Step 3 while $\tilde{D}_{\mathcal{B}} > 0$.

Step 4: $\tilde{E}_m = \sum_{w \in \mathcal{W}_m} (E_{m,w} - D_m),\ \forall m \in \mathcal{M}$ and $\mu^l = \mu^{min}$.

Step 1 (above) and (ii) in Fig. 6.4, return the marginal costs of a generator to produce the excess amount of electricity. However, since a generator cannot produce more electricity than its capacity, the OMCP (ii in Fig 6.4) will then return a marginal cost of a generator with only its maximum generation capacity if the requested excess amount of generation exceeds the capacity ($E^C_{m,w}$).

Second, let $E_{m,w}$ be known, then the overall marginal cost is $\mu^i = \max\{\mu_{m,w}(E_{m,w}) | w \in \mathcal{W}_m,\ m \in \mathcal{M}\}$, and $\mu_{m,w}(E_{m,w})$ is determined by Step 2. This is the case when the allocation of electricity ($\tilde{x}_{m,b}$) is determined by solving the allocation problem before solving the OMCP. With maximum capacity of the DGs, the solution results into the upper bound overall marginal cost μ^u ($\mu^u = \mu^i$).

Third, when the value of μ^i is known, then the suggested generation of the DGs is determined at Step 2 or (iv) in Fig. 6.4. This calculation is repeatedly used in the MEPM algorithm to determine $\tilde{E}_m$ (in Fig. 6.3, V).

Lemma 6.4.2 (Optimal Overall Marginal Cost)**.** *The solution of OMCP (Fig. 6.4) determines the optimal overall marginal costs for any configuration of MGN.*

Proof Let the overall marginal cost determined by the solution of OMCP presented in Fig. 6.4 be $\mu^{'}(E)$, where $E = D_{\mathcal{B}}$ (total demand of the MGN). Now, let the optimal overall marginal cost for the MGN configuration be $\mu^*(E)$. If $\mu^{'}(E) \leq \mu^*(E)$, then $\mu^{'}(E)$ is the optimal overall marginal cost. Now, suppose, the OMCP shown in Fig. 6.4 is unable to produce an optimal solution of the overall marginal cost for a configuration of MGN, i.e., $\mu^{'}(E) > \mu^*(E)$. If this is true, then there are at least two generators (in the proposed solution), which generate different amount of electricity

compared to the optimal solution (shown below):

$$
\begin{aligned}
&\text{Optimal Solution Generation Set (G*)}\\
&G^* = \{E_{1,1}, \cdots, E_{m,w}, \cdots, E_{m',w'} \cdots\}\\
&\text{and}\\
&\mu^*(E) = \max(\mu_{1,1}(E_{1,1}) \cdots, \mu_{m,w}(E_{m,w}), \cdots,\\
&\mu_{m',w'}(E_{m',w'}), \cdots)\\
&\text{where}\\
&E = \sum_{m \in \mathcal{M}} (\sum_{w \in \mathcal{W}_m} E_{m,w} - D_m) = \tilde{D}_{\mathcal{B}}
\end{aligned}
\tag{6.42}
$$

$$
\begin{aligned}
&\text{MEPM Generation Set } (G')\\
&G' = \{E_{1,1}, \cdots, E'_{m,w}, \cdots, E'_{m',w'} \cdots\}
\end{aligned}
\tag{6.43}
$$

$$
\begin{aligned}
&\text{and}\\
&\mu'(E) = \max(\mu_{1,1}(E'_{1,1}) \cdots, \mu_{m,w}(E'_{m,w}), \cdots,\\
&\mu_{m',w'}(E'_{m',w'}), \cdots)
\end{aligned}
\tag{6.44}
$$

$$
\begin{aligned}
&\text{where}\\
&E = \sum_{m \in \mathcal{M}} (\sum_{w \in \mathcal{W}_m} E'_{m,w} - D_m) = \tilde{D}_{\mathcal{B}}
\end{aligned}
\tag{6.45}
$$

Let the index of the two generators be (m, w) (generator w of microgrid m), and (m', w') (generator w' of microgrid m'). Now, suppose the amount of generation of both generators determined by optimal solution be $E_{m,w}$ and $E_{m',w'}$ (eq. (6.42)) and OMCP be $E'_{m,w}$ and $E'_{m',w'}$ (eq. (6.43)). Let us also assume (without loss of generality) that (m, w) is a low-cost generator and (m', w') is a high-cost generator. Now, the claim $(\mu'(E) > \mu^*(E))$ is true if and only if $E'_{m,w} < E_{m,w}$ and $E'_{m',w'} > E_{m',w'}$, therefore, the costs which are calculated in the optimal solution $(\mu^*(E))$ are less than the costs determined by the OMCP solution $(\mu'(E))$. This leads us to a fact that the low-cost generator (m, w) must produce more or equal (at least) amount of electricity (with a greater overall marginal cost $\mu'(E)$) in OMCP than the amount

of electricity produced by the same generator in the optimal solution (see, step (iv) in Fig. 6.4)[1]. This is always true because the marginal cost is non-decreasing (see Section 6.2.2). Therefore, the total amount of excess electricity produced by the generators in OMCP must be greater than the total demand of the buyers or $E > \tilde{D}_{\mathcal{B}}$ which is a contradiction according to the steps (i) and (vi) of the OMCP solution presented in Fig. 6.4. In general, let E' be the electricity produced by the OMCP, then we claim that $E' = E = \tilde{D}_{\mathcal{B}}$, but

$$\begin{array}{l} \text{if } \mu'(E') \ > \mu^*(E) \text{ then} \\ E' \ > E, \end{array} \tag{6.46}$$

because, some or all generators in OMCP will produce more electricity (without violating the capacity constraint) than the amount determined by the optimal solution. This is a direct violation of steps (i) and (vi) of the OMCP solution (see Fig. 6.4). The steps (i) and (vi) of the OMCP solution controls the amount of total excess production to the total demand of the buyers. The solution is valid, if only if both or all (in general) generators produce the same amount of electricity which is determined by the optimal solution. Thus, the OMCP method always determines the optimal overall marginal cost of any configuration of the MGN system.

Solving the Allocation Problem (MinAvgTransCost)

Step (VI) of Fig. 6.3 is the solution for the allocation problem (defined by Def. 6.2) by setting the value of $\mu(E) = 0$ of the MEPM objective function in eq. (6.28) and taking (6.29) to (6.39) as the constraints. We use the Simplex method to solve this problem. The inputs to the allocation problem are $\tilde{E}_m, \ \forall m \in \mathcal{M}$ which are determined by the algorithm for OMCP and the output is the minimum transportation cost $\hat{P}^j_{\mathcal{B}}$. The value of $\hat{P}^j_{\mathcal{B}}$ is the lower bound value ($\hat{P}^l_{\mathcal{B}}$) for electricity transportation, when

[1]At a higher marginal cost, a generator will produce more electricity compared to the amount electricity generated due to lower marginal cost.

$\tilde{E}_m = (\sum_{w \in \mathcal{W}_m} E^C_{m,w} - D_m)$, and upper bound value ($\hat{P}^u_{\mathcal{B}}$) when $\tilde{E}_m$ is the output of OMCP for μ^l. The mathematical model of the allocation problem is a LP problem with continuous variables $\tilde{x}_{m,b}$ ($\forall m \in \mathcal{M},\ \forall w \in \mathcal{W}_m$). Hence, the problem can be solved (using the Simplex algorithm) in a polynomial time and takes at least $\mathcal{O}(|\mathcal{B}|\times|\mathcal{M}|)$ comparisons.

Once the minimum transportation cost ($\hat{P}^j_{\mathcal{B}}$) is determined (for μ^i), then, we update $[\mu^c, \hat{P}^c_{\mathcal{B}}] \leftarrow \min([\mu^c, \hat{P}^c_{\mathcal{B}}], [\mu^i, \hat{P}^j_{\mathcal{B}}])$ (see, steps (VII) and (XII) of Fig. 6.3), and compare the possible minimum payment $\mu^i + \hat{P}^l_{\mathcal{B}}$ and $\mu^l + \hat{P}^j_{\mathcal{B}}$ of right ($[\mu^i, \mu^u]$) and left ($[\mu^l, \mu^i]$) partitions with the current minimum payment ($\mu^c + \hat{P}^c_{\mathcal{B}}$) (see, Alg. 6.1 from lines 11 to 17). If any or both of the partitions' possible minimum costs are lower than ($\mu^c + \hat{P}^c_{\mathcal{B}}$), then Alg. 6.1 (or the steps (III) to (XIV) of Fig. 6.3) is repeated with one (left or right) or both partitions, otherwise ($\mu^c + \hat{P}^c_{\mathcal{B}}$) is the minimum payment. The details of the MEPM algorithm are presented in Alg. 6.1. Initially, the algorithm (from lines 5 to 7) compares the upper and lower bound values of both overall marginal costs and transportation costs. Alg. 6.1 will terminate, if the upper and lower values of the overall marginal costs or transportation costs are found similar, otherwise, the algorithm continues as discussed above.

6.4.2 Analysis of the MEPM algorithm

Lemma 6.4.3 (Minimum Payment)**.** *Algorithm 6.1 determines the optimal price for electricity.*

Proof Alg. 6.1 divides the overall marginal cost space $[\mu^l, \mu^u]$ into two, $[\mu^l, \mu^i]$ and $[\mu^i, \mu^u]$, then, it determines the minimum transportation cost, $\hat{P}^j_{\mathcal{B}}$ for overall marginal cost μ^i. The solution of the allocation problem (QLP problem) always gives the optimal value $\hat{P}^j_{\mathcal{B}}$ for an overall marginal cost μ^i. Alg. 6.1 discards one partition ($[\mu^l, \mu^i]$ or $[\mu^i, \mu^u]$) or both when the minimum possible cost of each partition is

Algorithm 6.1 Algorithm for MEPM.

1: **procedure** MinMGNCost($\mu^l, \mu^u, \hat{P}^l_{\mathcal{B}}, \hat{P}^u_{\mathcal{B}}, \mu^c, P^c_{\mathcal{B}}$)
▷ $\mu^c, \hat{P}^c_{\mathcal{B}}$ are the global variables, function min() returns the value pair, sum of which is minimum
2: Initialize: $[\mu^c, \hat{P}^c_{\mathcal{B}}] \leftarrow \min([\mu^l, \hat{P}^u_{\mathcal{B}}], [\mu^u, \hat{P}^l_{\mathcal{B}}])$
3: $0 < \epsilon << 1$ ▷ ϵ is a very small value
4: Begin
5: **if** $\left|\mu^u - \mu^l\right| \leq \epsilon$ **then return** $\left[\mu^u, \min(\hat{P}^l_{\mathcal{B}}, \hat{P}^u_{\mathcal{B}})\right]$
6: **else if** $\left|\hat{P}^u_{\mathcal{B}} - \hat{P}^l_{\mathcal{B}}\right| \leq \epsilon$ **then return** $\left[\hat{P}^u_{\mathcal{B}}, \min(\mu^l, \mu^u)\right]$
7: **end if**
8: $\mu^i \leftarrow \frac{\mu^l + \mu^u}{2}$
9: $\hat{P}^j_{\mathcal{B}} \leftarrow$ MinAvgTransCost($\mathcal{B}, \mathcal{M}$) ▷ Simplex method for solving the allocation problem.
10: $[\mu^c, \hat{P}^c_{\mathcal{B}}] \leftarrow \min([\mu^c, \hat{P}^c_{\mathcal{B}}], [\mu^i, \hat{P}^j_{\mathcal{B}}])$
11: **if** $(\mu^l + \hat{P}^j_{\mathcal{B}}) < (\mu^c + \hat{P}^c_{\mathcal{B}})$ **then** ▷ left partition
12: $[\mu^k, \hat{P}^k_{\mathcal{B}}] \leftarrow$ MinMGNCost($\mu^l, \mu^i, \hat{P}^j_{\mathcal{B}}, \hat{P}^u_{\mathcal{B}}, \mu^c, \hat{P}^c_{\mathcal{B}}$)
13: $[\mu^c, \hat{P}^c_{\mathcal{B}}] \leftarrow \min([\mu^c, \hat{P}^c_{\mathcal{B}}], [\mu^k, \hat{P}^k_{\mathcal{B}}])$
14: **end if**
15: **if** $(\mu^i + \hat{P}^l_{\mathcal{B}}) < (\mu^c + \hat{P}^c_{\mathcal{B}})$ **then** ▷ right partition
16: $[\mu^k, \hat{P}^k_{\mathcal{B}}] \leftarrow$MinMGNCost($\mu^i, \mu^u, \hat{P}^l_{\mathcal{B}}, \hat{P}^j_{\mathcal{B}}, \mu^c, \hat{P}^c_{\mathcal{B}}$)
17: $[\mu^c, \hat{P}^c_{\mathcal{B}}] \leftarrow \min([\mu^c, \hat{P}^c_{\mathcal{B}}], [\mu^k, \hat{P}^k_{\mathcal{B}}])$
18: **end if**
19: **return** $[\mu^c, \hat{P}^c_{\mathcal{B}}]$
20: End
21: **end procedure**

greater than the current global minimum cost $(\mu^c + \hat{P}^c_{\mathcal{B}})$. Suppose, partition $[\mu^i, \mu^u]$ is discarded. We claim that there is an overall marginal cost μ^k, $(i \leq k \leq u)$ and transportation cost $\hat{P}^q_{\mathcal{B}}$ $(j \geq q \geq l)$ which produce minimum payment $((\mu^k + \hat{P}^k_{\mathcal{B}}) \times D_{\mathcal{B}})$ of MGN. The claim indicates that $(\mu^k + \hat{P}^k_{\mathcal{B}}) < (\mu^c + \hat{P}^c_{\mathcal{B}})$, but it is not possible because $\mu^i \leq \mu^k \leq \mu^u$ and $\hat{P}^j_{\mathcal{B}} \geq \hat{P}^k_{\mathcal{B}} \geq \hat{P}^l_{\mathcal{B}}$, thus $(\mu^k + \hat{P}^k_{\mathcal{B}}) \geq (\mu^i + \hat{P}^l_{\mathcal{B}})$ and Alg. 6.1 discards a partition (lines 11 and 15), *iff* $(\mu^i + \hat{P}^l_{\mathcal{B}}) > (\mu^c + \hat{P}^c_{\mathcal{B}})$, hence the claim is false. Further, if the values for any pair (overall marginal costs or transportation cost) are the same ($\mu^l = \mu^u$ or $\hat{P}^l_{\mathcal{B}} = \hat{P}^u_{\mathcal{B}}$), then Alg. 6.1 returns the minimum cost by taking the minimum of inequal cost pair (overall marginal cost or transportation cost) and value of equal cost pair. Thus, Alg. 6.1 solves the MEPM problem correctly. The complexity of the MEPM algorithm is given in Appendix 6.4.2.

Complexity of Algorithm Alg. 6.1

In general the complexity to the quadratic linear programming (QLP) problem can be solved in polynomial time using interior point method [11]. Our allocation problem

takes polynomial time to solve, let the complexity be $\mathcal{O}(Q)$ (a polynomial function). For the divide and conquer, let there be η discrete marginal costs between μ^l and μ^u which produce η distinct values between $\hat{P}^u_{\mathcal{B}}$ and $\hat{P}^l_{\mathcal{B}}$. Let the largest buyer wants to buy 2^ρ unit (in MWh or kWh) of electricity, then it is meaningless (or negligible) if the total payment (in dollar or any currency unit) contains more than two digits after the decimal point. Therefore, the set contains less than $(\mu^u - \mu^l) \times 2^\rho$ values. Therefore, the precision value for decimal number of Alg.1 is selected as $\epsilon = 2^{-\rho}$. To determine the complexity of the MEPM, let $\eta = (\mu^u - \mu^l) \times 2^\rho$ or $\eta = 2^{log_2(\mu^u - \mu^l)+\rho}$. Then, for the best case, the algorithm takes $\mathcal{O}(Q)$, that is in the first iteration the MEPM deletes both partitions. Now, let $k = log_2(\mu^u - \mu^l) + \rho$,thereby $\eta = 2^k$. In the worst case the MEPM method expands the search for the minimum electricity price to the depth k of the binary tree of the MEPM search space. Each level the MEPM compares 2×2^l, where l is a level of the search space. Therefore the worst case complexity of the MEPM is $\mathcal{O}(Q \times 2^k) \equiv \mathcal{O}(Q \times \eta)$. For the average case, the algorithm may terminate at any level l of the tree. Therefore, the average number of comparisons of the search space 2^k with depth k is

$$\begin{aligned}
\frac{1}{2^k}\sum_{i=1}^{k}\sum_{j=1}^{i} 2^j &= \frac{1}{2^k}\{2(k) + 4(k-1) + \cdots + 2^k\} \\
&< \frac{1}{2^k}(2k + 4k + \cdots + 2^k k) \\
&< \frac{k}{2^k}(1 + 2^1 + 2^2 + 2^3 + \cdots + 2^k) \\
&= \frac{k(2^{k+1} - 1)}{(2-1)2^k} < \frac{k(2^{k+1})}{2^k} = 2k.
\end{aligned} \tag{6.47}$$

Hence in general, the average case complexity of the proposed MEPM is $\mathcal{O}(Q \times \log_2 \eta)$ or $\mathcal{O}\left((\mu^u - \mu^l) \times 2^\rho Q\right)$.

6.4.3 The role of ESS to handle the uncertainty in electricity generation and load

In case of intrinsic uncertainty of electricity load and generation, we use electricity storage system to store or supply electricity. The storage system will not be used as the regular electricity source or storage. It is included to resolve the instantaneous variation of load and generation after the decision is made by the MEPM method. The price of the electricity to supply is the price decided by the MEPM system for the MGN. The storage system is an intrinsic part of the demand-response algorithm of a microgrid which we assume to be the internal energy management system of a microgrid (whether a buyer or a seller).

Further, in the microgrid level, ESS can play a vital role to reduce the uncertainty in the power generation and load prediction which leads to an increase in the efficiency and reliability of the system. At the time of actual consumption, ESS can be used to store extra energy or release energy to compensate the shortage compare to the amount of energy planned for trading. Studies showed that demand and power generation varies between 0 to at most 10% from one hour before the prediction. Hence, the uncertainty of the power system maybe mitigated by storing at least 10% of the energy which maybe required for next hour and 10% excess storage capacity to store presumably excess of energy. Let the minimum and maximum capacity to reduce the uncertainty of the ESS be Ess_n^l (i.e., 60% of ESS capacity) and Ess_n^h (i.e., 80% of ESS capacity) then the amount of energy needed to be stored or released to meet the uncertainty is x_n^s, thus $Ess_n^l \leq Ess_b^c + x_n^s \leq Ess_n^h$, where Ess_b^c is the current amount of energy stored in the ESS, x_n^s can be a zero, positive or negative value which is accumulated with the demand. In the time of actual purchase, buyers and sellers charge or discharge energy from the ESS if there is excess energy (demand is reduced or surplus RES generation) or shortage of energy (or increase demand), thereby the

mitigation is trivial.

6.5 First Come First Serve (FCFS) Allocation

In FCFS method, the EMS first decides the marginal cost according to the buyers' demand and a series of bid prices placed by the sellers. Then, it assigns the amount of electricity to be transported from a seller microgrid to a buyer according to the minimum transportation costs and not exceeding the capacity of the connected transmission line. The FCFS scheme first determines the overall marginal costs for total excess demand of the buyers (line 6), then, assigns each of the buyers (b) to the available sellers to buy $\tilde{x}_{m,b}$ amount of electricity from seller m (from lines 10 to 30). First, in line 9 the transmission costs are sorted in ascending order according to the buyer. Next, we select a buyer-seller pair and allocate electricity to fulfill the demand of buyer b with the restriction that the capacity of connected transmission line l_i is not exceeded. Otherwise, we select next seller-buyer pair and continue the allocation of electricity from a seller to a buyer accordingly. In every successful allocation, we modify the demand of the buyer with the allocation amount. We assume that the transmission lines have sufficient capacity for the allocation of electricity and at the end, demands of all the buyers are fulfilled.

6.6 Simulation

6.6.1 Simulation Setup

We consider an MGN system which contains a set of MGs, each with a number of energy sources (DGs) randomly chosen from a set of renewable and non-renewable energy sources; such as, (i) renewable: we choose the random (given LCOE range

Algorithm 6.2 First Come First Serve (FCFS) Allocation

procedure FCFS($\mathcal{B}, \mathcal{M}$)
  $\mathcal{D}_{\mathcal{B}} \leftarrow 0; t\_cost \leftarrow 0$
  for $\forall b \in \mathcal{B}$ **do**
    $\mathcal{D}_{\mathcal{B}} \leftarrow (\mathcal{D}_{\mathcal{B}} + \tilde{D}_b)$
  end for
  Determine μ^{opt} for $\mathcal{D}_{\mathcal{B}}$ by Alg. OMCP of Sec. 6.4.1 (step1 to step4)
  $C_{m,b} \leftarrow \{c_{m,b} | \forall b \in \mathcal{B}, \forall m \in \mathcal{M}\}$
  Randmize($C_{m,b}$)
  sort values in $C_{m,b}$ of each b in ascending order
  for $c_{m,b} \in C_{mb}$ **do**
    if $\tilde{D}_b > 0$ **then**
      if $\tilde{D}_b \leq (\tilde{E}_m)$ & $\tilde{D}_b > 0$ & $(\Gamma_i - \tilde{D}_b) \geq 0$ **then**
        $x_{m,b} \leftarrow \tilde{D}_b$, $\tilde{D}_b \leftarrow 0; \tilde{E}_m \leftarrow (\tilde{E}_m - \tilde{D}_b)$
        calculate $x^t_{m,b}$ and $\pi_{m,b}$ (eqs. (6.33),(7.7), (6.32))
        $\tilde{x}_{m,b} \leftarrow (x_{m,b} + x^d_{m,b})$
        $t\_cost \leftarrow (\tilde{x}_{m,b} \times c_{m,b})$
      else if $\tilde{E}_m \leq \Gamma_i$ **then**
        $\tilde{D}_b \leftarrow (\tilde{D}_b - \tilde{E}_m); x_{m,b} \leftarrow \tilde{E}_m; \tilde{E}_m \leftarrow 0$
        calculate $x^t_{m,b}$ and $\pi_{m,b}$ (eqs. (6.33),(7.7), (6.32))
        $\tilde{x}_{m,b} \leftarrow (x_{m,b} + x^d_{m,b})$
        $t\_cost \leftarrow (\tilde{x}_{m,b}) \times c_{m,b}$
      else
        $d \leftarrow \Gamma_i$
        $\tilde{D}_b \leftarrow (\tilde{D}_b - d); x_{m,b} \leftarrow d; \tilde{E}_m \leftarrow (\tilde{E}_m - d)$
        calculate $x^t_{m,b}$ and $\pi_{m,b}$ (eqs. (6.33),(7.7), (6.32))
        $\tilde{x}_{m,b} \leftarrow (x_{m,b} + x^d_{m,b})$
        $t\_cost \leftarrow (\tilde{x}_{m,b}) \times c_{m,b}$; $\Gamma_i \leftarrow 0$
      end if
    end if
  end for
return $(\mu^{opt} + t\_cost)$
end procedure

in brace) price of the electricity for offshore wind turbine (\$0.15 to \$0.218/kWh), onshore wind (\$0.05 to \$0.116/kWh), solar energy (\$0.05 to \$0.15/kWh), hydropower (\$0.030 to \$0.059/kWh). The amount of electricity from the RESs is predicted for each hour of a day by using the renewable energy models described in our previous work in [120], (ii) non-renewable: gas turbine generator (\$0.144/kWh) with given unit production costs (\$) in [96]. We choose one to five generators at random to power each of the MGs. For non-renewable sources, in the cubic cost function α, and β are given random values from $0.2\times10^{-6} \sim 0.8\times10^{-6}$, and $0.05\times10^{-6} \sim 0.2\times10^{-6}$, respectively. We generate a set of convex functions to simulate the piecewise convex marginal cost and choose α between $0.2 \times 10^{-6} \sim 0.8 \times 10^{-6}$ for the linear marginal cost function. Also, nonlinear non-convex costs are generated with the random values chosen for α with the variation of $E_{m,w}$. For all the cases, we choose a random value between \$0.002 to \$0.008 for c. The capacity of each generator is chosen randomly from $300kW$ to $1MW$, and demand for each MG is also chosen at random between $200kWh$ to $2400kWh$. We have chosen ANSI/IEEE standard network transformer with $300kVA$ to $2500kVA$ power range, primary voltage up to 34.5 KV and secondary voltage is up to 600V [26]. Once the capacity of the generators is fixed, a forecasting algorithm [120] based on the historical meteorological data is executed to estimate the amount of electricity generated from the RESs. For the simulation, we place the capacitor banks with a maximum of 600 MVAR and the impedance of the transmission/distribution lines (with 11/33KV base voltage) are considered which is given in [29]. An energy transportation network is set up among the smart microgrids, each of which costs $c_{m,b}$ (\$0.05/$kWh \sim$ \$0.1/kWh) to transport one unit of electricity. We implemented the algorithms for MEPM in C++ programming language used IBM CPLEX concert technology to resolve the allocation problem.

6.6.2 Numerical results

We execute MEPM, FCFS algorithms on variable sized MGN, which comprise, 50, 100 , $\cdots$, 1950, 2000 smart microgrids. We execute the algorithms more than fifty times for each MGN configuration for the targeted time slot and take the average of the outputs to compare. To get the results we have executed the simulation several (50) times for each configuration (with random demand and new predicted generation of the RESs) and we present the results in the following graphs.

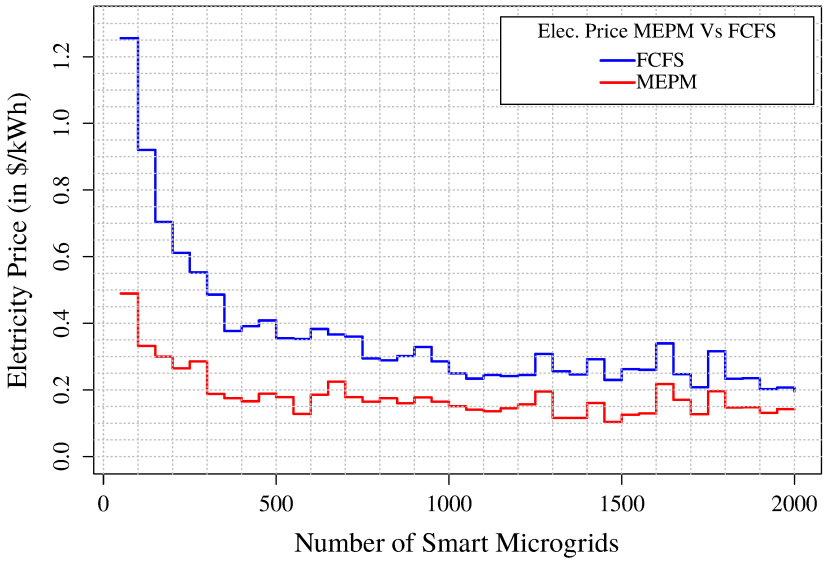

Figure 6.5: Overall Electricity price in \$/kWh for FCFS, and MEPM.

Fig. 6.5 shows the amount of money (in $\$/kWh$) to spend for purchasing one unit of electricity in MEPM, and FCFS schemes. Clearly, the electricity unit price is higher under FCFS in comparison to MEPM. Indeed, MEPM minimizes the overall electricity price for any configuration of the MGN compared to the price determined by the FCFS scheme. To put this into perspective, in 2013, the Quebec annual demand was $173.3TWh$ [58], therefore a reduction of $\$0.01/kWh$ will save 1.73 billion dollars [2]. Hence the use of an efficient method (MEPM) to determine the electricity

[2]This monetary saving is indeed not due to only lowering the electricity price, but rather directly related to lowering the cost of generation, ultimately equally benefiting the supplier and buyer.

price may play a very important economical role. Fig. 6.5 also shows that the MEPM algorithm reduces the electricity price more when the number of microgrids is less. This is because, the MGN has a fewer number of suppliers (sellers), which left fewer options for the FCFS algorithm to choose electricity transportation costs for the lower bound marginal costs. In addition, for all the schemes, the electricity cost reduces while the number of smart microgrids increases in the MGN. Clearly, this increases the problem space and present more opportunities for buyers to choose potential sellers to minimize both the price and the transportation cost. In the FCFS scheme, a buyer chooses sellers to minimize its personal electricity price, which results in a lack of coordination among the buyers to lower the cost. On the other hand, the MEPM scheme chooses sellers with the objective to minimize electricity price of the whole MGN community. Moreover, Fig. 6.5 together with Fig. 7.7 clearly represent the performance (in respect to the electricity price and saving) of the MEPM compared to FCFS.

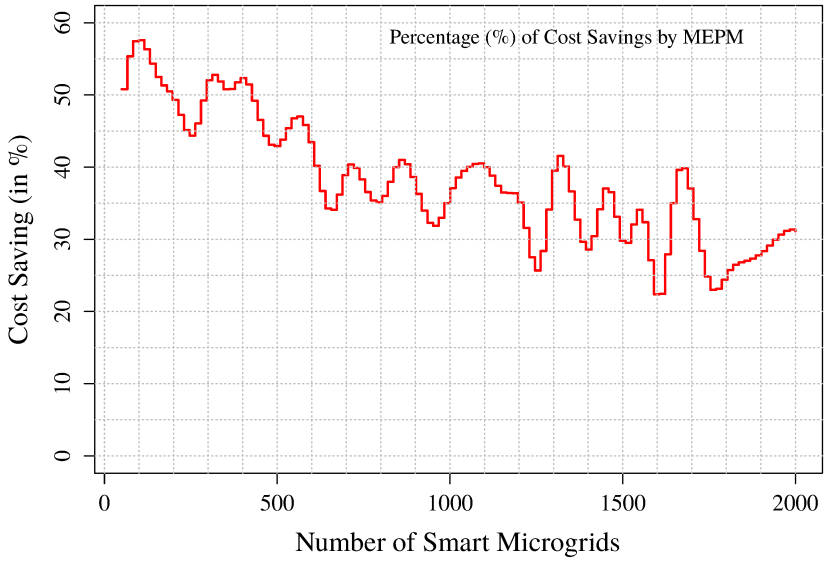

Figure 6.6: Percentage of cost saving of MEPM compared to FCFS

Fig. 7.7 presents the percentage of electricity price reduction of MEPM with respect to FCFS for various instances. We run both FCFS and MEPM algorithms more

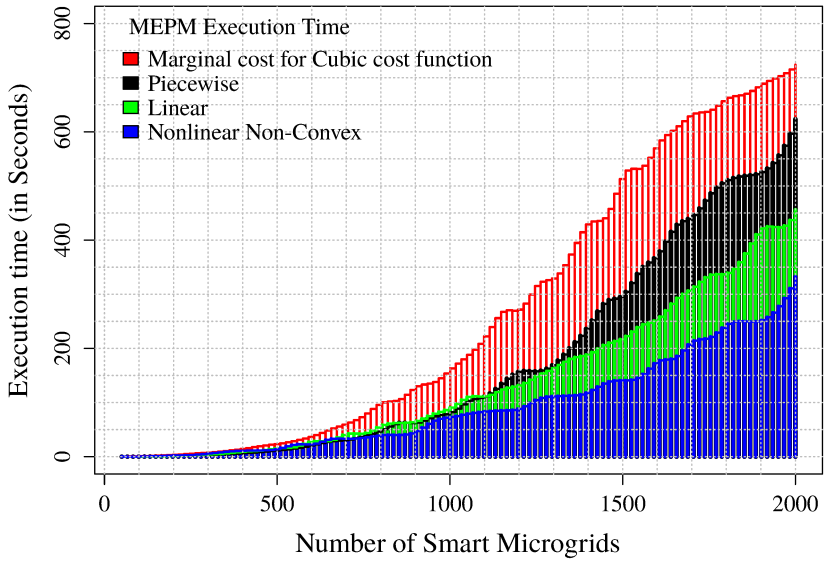

Figure 6.7: Performance of the MEPM algorithm

than 50 times on MGN with various configurations, which contain $50, 100, \cdots, 2000$ smart microgrids. For each iteration, the simulation selects the number of generators, production capacity, and demand of each MGN independently, such that the set of sellers and buyers are changed dynamically. We took the average of the resultant costs of the same sized MGNs and calculate the percentage of average price savings by the MEPM with respect to the FCFS scheme. We found that the percentage of savings (i.e., better spending) is higher for smaller sized MGN and decreases with the increase of the size of the MGN for both MEPM. The percentage of saving decreases because, in the large sized MGN, the buyers have more opportunities to choose potential sellers to buy electricity compared to a small sized MGN. Hence, the percentage of cost saving of a large MGN system is less than the percentage of saving in a smaller MGN.

Figs. 6.7 and 6.8 show the average runtime of MEPM algorithms for various MGN configurations and marginal costs. We develop a sequential divide and conquer method in C++ to implement and evaluate the performance of MEPM. We execute the program several times on a computer system containing Intel Core i7, 2.67GHz

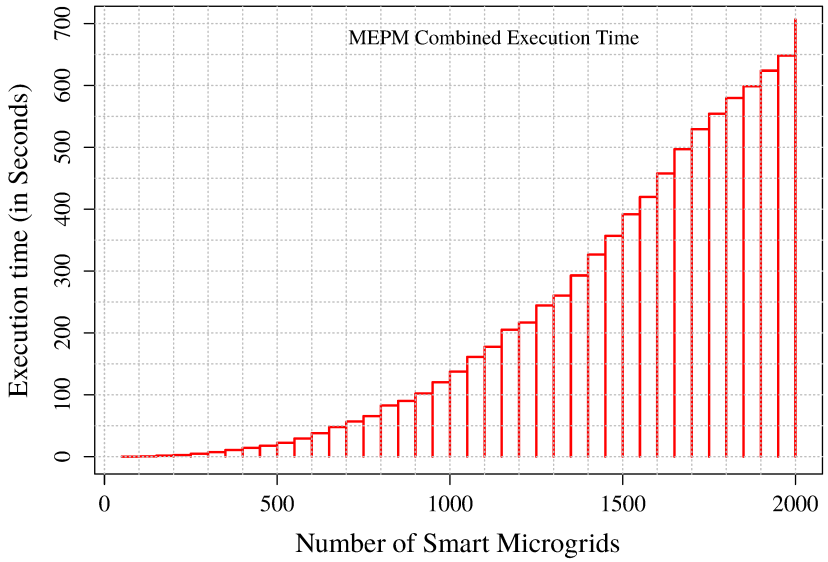

Figure 6.8: Combined Execution Time of the MEPM algorithm

clock speed with 6GB RAM. The results presented in Fig. 6.7 show that the MEPM algorithm indeed is a polynomial time algorithm irrespective of the marginal cost functions. Also, MEPM run times are dependent on the size of the MGN; thus the runtime increases near linear (polynomial) while the number of participants (MGs) increases. We have considered a large enough electricity market with 2000 MGs. Fig. 6.7 represent the overall run time of the algorithm that includes the duration needed to determine the upper and lower bound of the combined marginal cost. The calculation of lower bound marginal cost takes at most three (3 Secs for 2000 microgrids) seconds which is used only once for the whole process. On the other hand, the calculation of upper bound marginal costs takes few milliseconds ($<$ 10 milliseconds) which is used at each iteration of the MEPM algorithm. Fig. 6.8 depicts the average time required to determine the electricity cost for various configurations of the MGN system. Moreover, Fig. 6.7 to 6.8 represent an important evidence that our MEPM algorithm can determine the optimal electricity price of an electricity system without approximation (unlike existing solution) of the marginal costs. To further reduce the overall execution time, a parallel/distributed algorithm can be designed

to reduce the run time of the MEPM algorithms. The parallel implementation of the algorithms is simple: each partition of the overall marginal cost space is assigned to a separate thread of the processor and runs the MEPM algorithm. Each process sends $([\mu^c, \hat{P}^c_{\mathcal{B}}])$ to all other processes when it determines a new lower cost. Each process will discard a partition if the minimum possible cost of the partition is more than the current minimum costs.

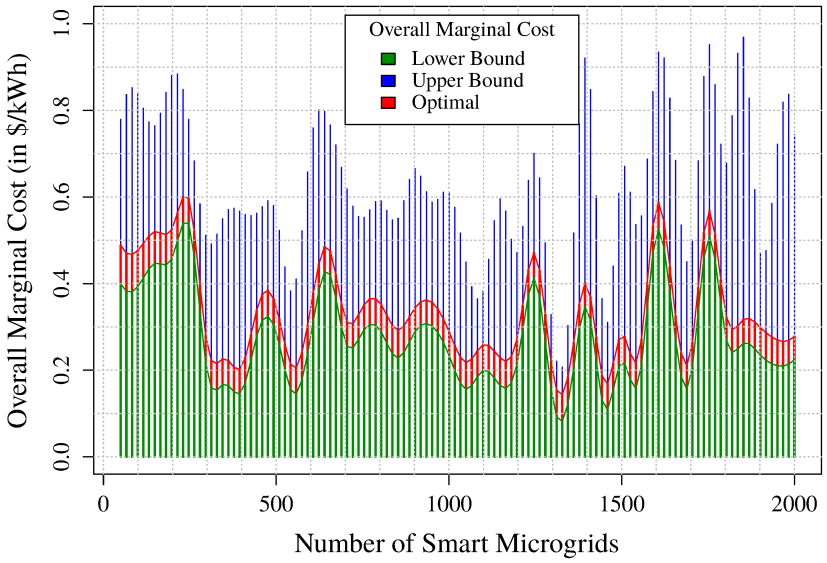

Figure 6.9: Optimal Vs. lower and upper bound overall marginal costs.

Fig. 6.9 compares the optimal overall marginal costs determined by the proposed MEPM scheme and the lower and upper bounds marginal cost of the MGN system with various configurations. The upper and lower bounds of the overall marginal costs are determined by the OMCP solution which is the feasible region for the MEPM. The lower bound marginal cost is determined by assuming the transmission cost is the same (or zero) for all the transmission lines of the MGN, which results in the lowest overall marginal cost. On the other hand, the upper bound of the overall marginal cost is determined by allocating energy from sellers to buyers with the best possible transmission lines and then the overall marginal cost is calculated. The optimal overall marginal cost deviated from the lower bound marginal cost due to

the trade-off between the transmission and overall marginal costs which results in optimal electricity price for the MGN (shown in Fig 6.5). In most cases, the pattern of the two results (optimal and lower bound overall marginal costs) are similar, but there are cases (such as a lower number of MGs) where the deviation is higher. This is because, the higher generation capacity (compared to the excess demand), and availability of more alternate sellers for buyers, will result in a better overall marginal cost for the proposed scheme. The case of tight demand-generation ratio (near to unity) will result in higher deviation between the lower and optimal overall marginal costs. However, for all the cases, the lower bound overall marginal cost is always lower (or equal) to the optimal overall marginal costs. The difference between lower bound and the optimal overall marginal cost is not the same for all cases; for example, for 50 and 100 MGs the difference is 0.089 and 0.083. Whereas the differences between the overall marginal costs for 600 and 650 MGs are 0.065 and 0.055, and for 1350 and 1400 are 0.060 and 0.053, etc.

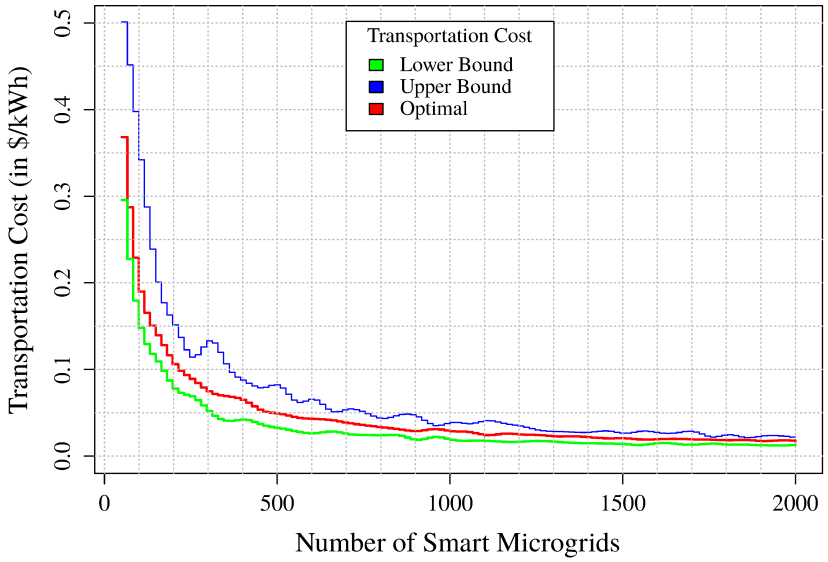

Figure 6.10: Optimal Vs. lower and upper bound transportation cost.

Fig. 6.10 represents the relation between optimal, lower and upper bound transportation costs for the various MGN configuration. The optimal transportation cost

is always greater or equal to the lower bound transportation cost. The deviation is large when the number of microgrids in the MGN system is low and small when the population size of the MGN system is high. This is because, for a large MGN, the buyers have more alternate sellers than the small size MGN. Therefore, the increment of number of alternate sellers may result in better transportation cost. This is true if the excess generation of the sellers is high compared to the excess demand of the buyers.

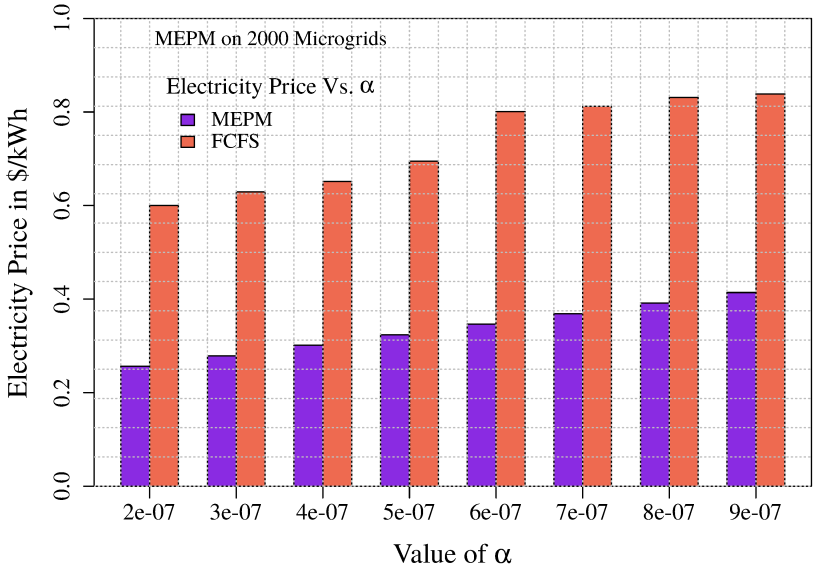

Figure 6.11: MEPM Vs. FCFS with respect to value of cost function coefficient α for 2000 MGs.

Fig. 6.11 compares the electricity prices for FCFS and MEPM with respect to the different values of α (cost function coefficient) for a MGN with 2000 microgrids. It is found that the electricity price for both FCFS and MEPM increases with the increase of α. The increase is evident because α is a positive coefficient of the marginal cost functions, and the value of the marginal costs of the energy generated by non-renewable sources increases with α. Thus, the change in electricity price determined by MEPM is linear with the linear increase of α. The price calculated by FCFS exhibits a near linear behaviour on the value of α. This is because every buyer tries

to buy electricity from the available sellers with lower transmission costs. Therefore, the selection of buyer is dependent on the random order of customers request in real time; thus, in the following run, the list of sellers for a buyer may change. In all cases, the electricity price is higher in FCFS system compared to the MEPM system which is reasonable because MEPM always results in optimal electricity price. Note that, the change of α in unit electricity price seems to be insignificant, however the variation in electricity price due to the variation of α becomes vital when a buyer buys a bulk amount of electricity from the sellers.

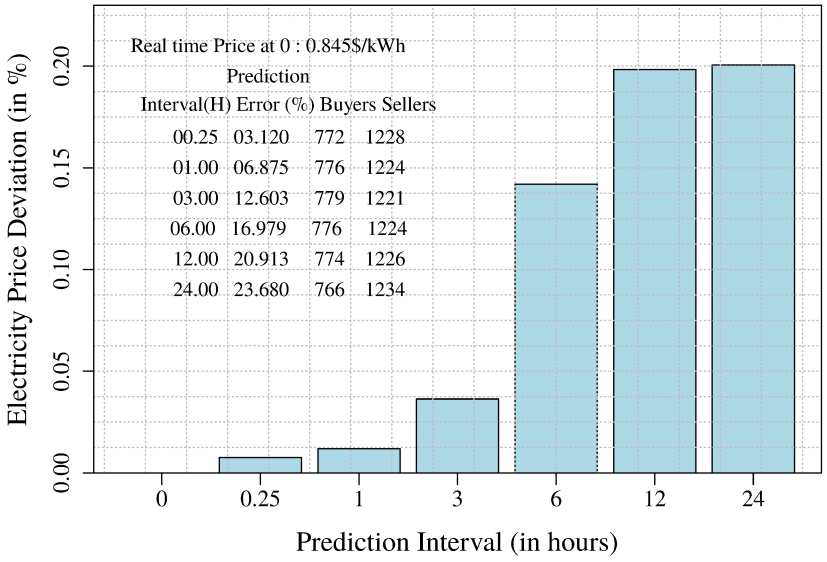

Figure 6.12: MEPM : electricity price deviation Vs prediction interval.

Fig. 6.12 shows the deviation (%) of the predicted from real electricity price. The prediction errors (maximum range in %) used in this experiment are listed in Fig. 6.12. We estimate the amount of generation from the renewable sources for 0.25, 1, 3, 6, 12, and 24 hours and determine the actual value of production by adjusting the errors (see Fig. 6.12). Then, we ran the MEPM on the predicted and real amount of generation for 0.25, 1, 3, 6, 12, and 24 hours to determine the optimal electricity prices for both. We found that the deviation increases (positive or negative) with the expansion of the prediction duration. Compared to the prediction error, the

price deviation is negligible for the 0.25 and 1 hours which is 0.008 and 0.0129 % respectively. The low (0.008% to 0.21%) error in the predicted price is due to the deviation of the generation amount for each DG. The prediction error also changes the number of buyers and sellers which was determined by the MEPM dynamically and depicted in Fig. 6.12. However, the MEPM method determines the electricity price for a given amount of production from each generator at any time, whether it is real or predicted. Hence, a good prediction function makes MEPM more reliable to estimate the electricity price for the next few hours.

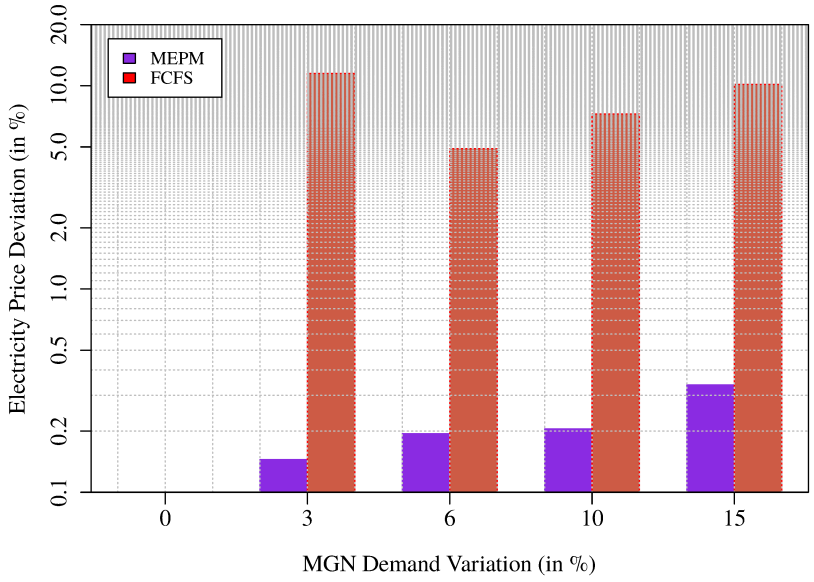

Figure 6.13: MEPM : electricity price deviation Vs demand variation.

Fig. 6.13 illustrates the percentage of deviation (absolute value) of electricity prices (in logarithmic y-scale) determined by FCFS and MEPM for the variation of the demand. In the case of MEPM, the deviation in electricity price increases when increasing the variation (positive or negative) of the demand. Whereas, in the case of FCFS, the price variation is irregular because FCFS does not optimize the electricity price of the MGN, and preferably attempt to minimize the electricity price of each microgrid. Thus, the overall price of the system is not decreased, and the pattern of the deviation is irregular. For all the cases, the difference of electricity price in

MEPM is always lower than the variation in FCFS electricity price. Also, it is found that the change of electricity price in MEPM system is insignificant (less than 0.5%). Therefore, the MEPM system is more stable in predicting the electricity price for any configuration of the MGN.

6.7 Conclusion

We developed an energy management system and marginal cost-based electricity pricing scheme for the MGN. We showed that our proposed MEPM scheme determines optimal energy flow among the microgrids with a minimum electricity price for the MGN customers. We simulated the MEPM algorithm and compared the results with an FCFS system to evaluate the performance of MEPM. We found that the MEPM always performed better compared to the FCFS system.

Chapter 7

Volt-VAR Control through Joint Optimization of Capacitor Bank Switching, Renewable Energy, and Home Appliances

In the previous chapter 6 we have presented a scheme for MGN system to determine the optimal electricity price by reducing T&D and generation costs of the electricity. In fact, the T&D losses are assumed to be compensated by the use of compensation devices (such as capacitor bank) along the transmission and distribution network. Several types of research have been performed (see section 2.3) to reduce T&D losses which are known as VVO (Volt-VAR optimization). In this chapter, we provide a solution for VVO where compensation is jointly done by shifting flexible loads consumption from peak demand duration to off-peak demand period and integrating renewable energy sources into the grid.

7.1 Motivation

It is evident from the discussion in section 2.3 that VVO works by adjusting the feeders and substation components in response to the operator's demand to reduce losses. Further, the addition of renewable energy sources and electric vehicles (EVs), and home appliances with flexible consumption featured the power grid with a new load dimension. Such load dynamism has become an attractive feature, triggering activities to reduce peak load and adjust the demand, according to the generation. Moreover, studies show that many electrical devices operate more efficiently at reduced voltage [71]. However, beyond a certain minimum operating voltage, the efficiency of the device drops. Unfortunately, all the solutions (see, section 2.3) for VVO/VVC select the lower voltage from ANSI C84.1 standard without considering the performance of the appliances. With the recent technology advancement, a cost-effective fine-grain solution for the VVO could be achieved while maintaining maximum efficiency of the devices. Moreover, such solution will provide a quality electricity service without reducing the lifespan of the equipment but with reduced generation and cost. To address these challenges, we develop a new VVCO/OECM scheme to decrease the electricity costs, adjust OLTC TAP and capacitor bank for Volt-VAR compensation while rendering a lower terminal voltage to maintain efficient operations of electrical and electronic devices in the customer premises.

7.2 System Model

We consider a distribution network which is shown in Fig. 7.1, having n feeders : $f_1, f_2, \cdots, f_n$. Each of the feeders, i.e., f_i $(1 \leq i \leq n)$ supplies electricity to a set of neighborhood[1] microgrids $r_{i,j}$ $(\{r_{i,j}|1 \leq j \leq m_i\})$,$\forall i$ and m_i is the number

[1] A neighborhood is also considered to be a microgrid.

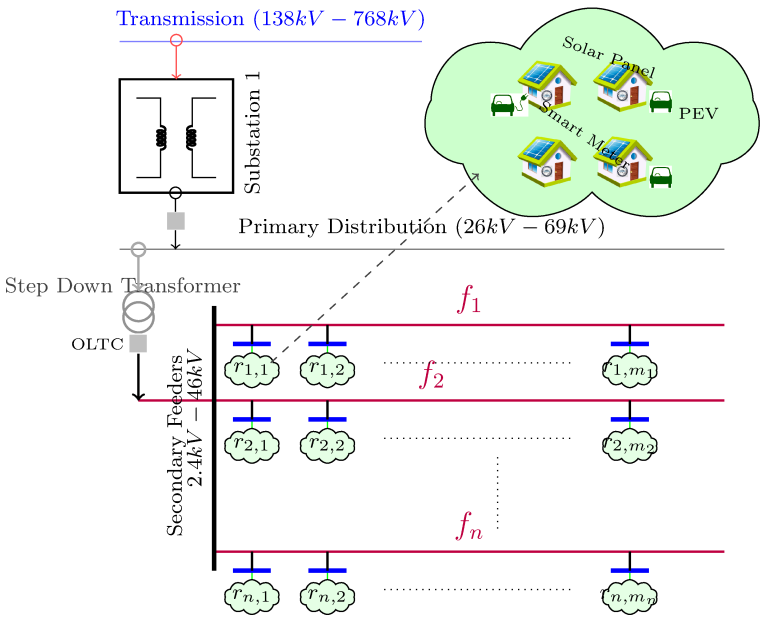

Figure 7.1: Electricity Transmission and Distribution System

of communities attached to a feeder f_i (see Fig. 7.1). A service-drop transformer connects the neighborhood to the feeder. Each of these transformers serves $120/240V$ with a maximum apparent power rating from $10KVA$ to $200KVA$. Customers are assumed to have roof-top solar panels to serve a fraction of the electricity needed by the neighborhood.

Each of the customers deploys a HEMS, which sends the current and projected load, energy, and least operating terminal voltage to the CEMS. Also, the HEMS is capable of identifying appliances and controlling the consumption of the equipment with the control information received from the CEMS. On the other hand, the CEMS (one for each $r_{i,j}$) takes the terminal voltage of the community, adjusts the voltage regulator (or OLTC) and sends the demand to the substation energy management system (EMS). Let t and τ be the time (hour) and total hours of a day, where $t \in \tau$. The EMS at the substation regulates the generation, fixes the OLTC transformer TAP, adjusts the capacitor bank switches and calculates the electricity cost $\mu(E_g^t)$ (total generation at t is E_g^t) and reduces the distribution losses. Next, the EMS sends

the electricity cost $\mu(E_g^t)$ to the CEMS. Upon obtaining the electricity cost, each of the community improves the consumption pattern and transfer the control to the HEMS.

We assume that HEMS connects the appliances of a customer through an HAN (home area network), and a NAN (neighborhood area networks) connects the HEMS to the CEMS. Also, CEMSs are connected to the substation EMS using a WAN (wide area network) to transfer control and measurements between them. Besides, all other components of the grid (PMU, PDC, etc.) are dedicated to monitoring and reporting measurements for the stability and the fault-free operation of the electrical network according to the decision made by the EMS. Based on the mentioned system architecture, our proposed system is composed of two major energy management schemes: (i) VVCO and (ii) OECM which are shown in Fig. 7.3 which interact to achieve the minimum energy generation cost and billing of the customer while satisfying the demand.

7.3 Volt-VAR and CVR Optimization Model (VVCO)

The primary objective of our proposed VVCO system is to minimize the electricity generation cost by adjusting the capacitor bank switches and OLTC transformer TAP (at the substation) to serve the customers demand at time t. The objective can be accomplished by minimizing losses along the distribution feeders.

7.3.1 Distribution Losses and Volt-VAR

Let the capacitor banks and PMUs (Phasor Measurement Unit) be placed on the distribution feeders (i.e., f_i) to compensate for the reactive power losses and obtain the measurements (voltage, current, and phase). Let, $\kappa_{i,j}$ be the set of communities

for which a capacitor bank j is installed, where $R_{i,j}$ and $X_{L_{i,j}}$ are the resistance and inductance of the feeder f_i at location j (see Fig. 7.2). Further, assume that the phase between voltage and current at j is $\theta^t_{i,j}$. Let $I^t_{i,j}$ be the amount of current flowing through the feeder to serve the demand of the communities $\kappa_{i,j}$ during time slot t. Then, for the communities load, the voltage drop $V^t_{d_{i,j}}$ (magnitude) on the feeder f_i at j can be calculated using the phasor diagram in Fig 7.2 (above) as,

$$V^t_{d_{i,j}} = I^t_{i,j} R_{i,j} \cos\theta^t_{i,j} + I^t_{i,j} X_{L_{i,j}} \sin\theta^t_{i,j} \tag{7.1}$$

Now, assume a shunt capacitor is added to compensate for the inductive loss; hence the voltage drop $V^t_{d_{i,j}}$ is modified and equation (7.1) becomes,

$$\begin{aligned} V^t_{d_{i,j}} = I^t_{i,j} R_{i,j} \cos\theta^t_{i,j} + I^t_{i,j} X_{L_{i,j}} \sin\theta^t_{i,j} \\ - I^t_{c_{i,j}} X^t_{c_{i,j}} \sin\theta^t_{i,j}, \end{aligned} \tag{7.2}$$

where $X^t_{c_{i,j}}$ is the impedance of the capacitor bank at j on the feeder f_i. The value of $X^t_{c_{i,j}}$ can be adjusted to minimize the loss, more specifically the loss is reduced when,

$$I^t_{i,j} X_{L_{i,j}} \sin\theta^t_{i,j} - I^t_{c_{i,j}} X^t_{c_{i,j}} \sin\theta^t_{i,j} = \eta. \tag{7.3}$$

where η is a very small positive number near to zero. Next, we assume the PMUs at communities $\kappa_{i,j}$ send the phasor measurement data such as, voltage ($V^t_{i,j}$), current ($I^t_{i,j}$), and phase (θ). If a PMU is not available for some or most of the communities, then data from RTU and SCADA (Supervisory control and data acquisition) can be used to calculate the phase. Note that, the received data from PMUs or RTUs may have errors which must go through a filtering and screening process to increase the accuracy of the measurements to an acceptable level [78]. We assume the power system has such capabilities.

Now, by applying the measurements, we can easily evaluate the terms of the above equation (7.2) in real time. The power balance equation for the communities $\kappa_{i,j}$ of

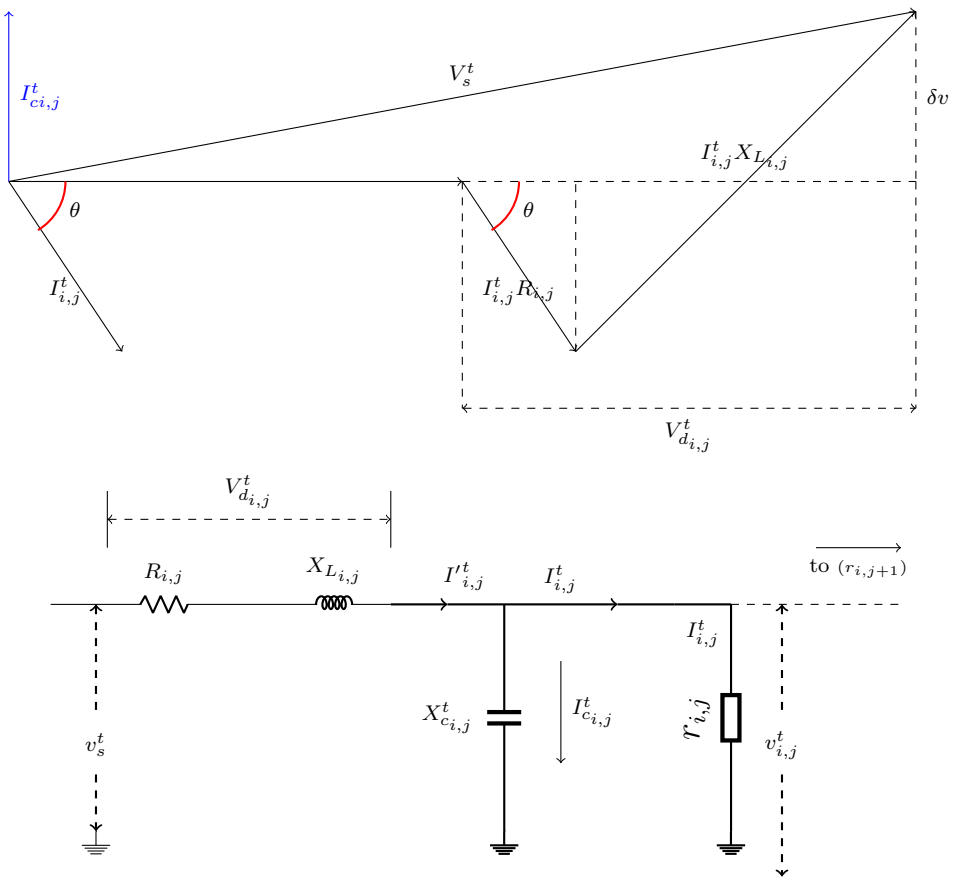

Figure 7.2: Distribution Feeder and Phasor Diagram

feeder f_i is,

$$P^t_{i,j} = \sqrt{(P^t_{R_{i,j}})^2 + (P^t_{X_{L_{i,j}}})^2} \tag{7.4}$$

where, $P^t_{i,j}$, $P^t_{R_{i,j}}$, $P^t_{X_{L_{i,j}}}$ are the apparent, real, and reactive power of the feeder at time t for communities $\kappa_{i,j}$. Let $P^t_{X_{C_{i,j}}}$ be the energy supplied by the capacitor to compensate the reactive power at $\kappa_{i,j}$ then,

$$P^t_{X_{L_{i,j}}} = P^t_{X_{C_{i,j}}} \tag{7.5}$$

from eqs. (7.3) and (7.5), it is evident that the reactive power of the feeder will only be compensated when the capacitive power is equal to the induction (reactive) power, then,

$$X^t_{L_{i,j}} = X^t_{C_{i,j}} \tag{7.6}$$

Assume the capacitor bank contains a series of identical capacitors which can be switched on/off electronically (e.g., using thyristors). Assume the capacitor bank has l capacitors and s^t switching state, where, $s^t = 0$ means all capacitors are switched off at t, and $s^t = k$ $(1 \leq k \leq l)$ indicates that k of l capacitors are switched on. Now, let the capacitance of each capacitor in the bank at (i, j) be $c_{i,j}$, and then at t,

$$X^t_{C_{i,j}} = \frac{s^t}{2\pi f c_{i,j}}, \tag{7.7}$$

where the value of variable s^t is defined as, $0 \leq s^t \leq l$, f is the frequency of the line (50 or $60Hz$) and $c_{i,j}$ is the capacitance of each identical capacitor of the bank.

To ensure the quality electricity service, besides capacitor bank switching, the substation EMS must ensure that the voltage of the furthest service-drop of a feeder is greater than or equal to the minimum primary voltage of the community (r_{i,m_i}). Assume the OLTC of the distribution feeder (f_i) has ψ_i taps, indicated as $TAP_1, TAP_2, \cdots, TAP_{\psi_i}$. Each TAP_i represent the ratio of primary and secondary windings of the distribution transformer. Now, let the primary (at the substation) voltage be V^t_p and the secondary feeder input voltage for feeder f_i at t be V^t_s. To ensure uninterrupted services and quality of power, the following must be satisfied,

$$V^t_s = V^t_{i,m_i} + \sum_{j=1}^{m_i} V^t_{d_{i,j}}, \forall i, \tag{7.8}$$

$$V^t_s \geq V^t_p \times TAP_k,\ 1 \leq k \leq \psi_i \tag{7.9}$$

where V^t_{i,m_i} is the terminal voltage of the last customer on feeder f_i. Now, the energy loss on the distribution system at t is (using eq. (7.2)),

$$E^t_{loss} = \sum_{i=1}^{n} \sum_{j=1}^{m_i} \sum_{k=1}^{j} V^t_{d_{i,j}} I^t_{i,j}, \tag{7.10}$$

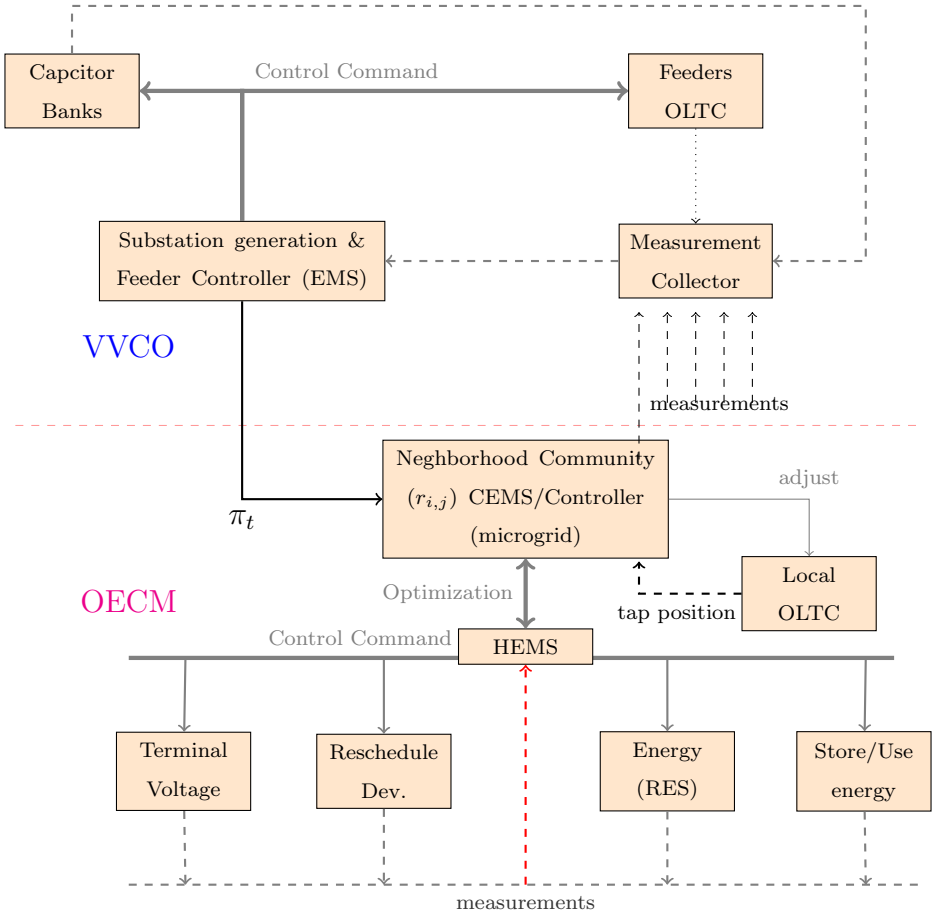

Figure 7.3: VVCO and OECM interactions, Volt-VAR and energy management.

Next, let the terminal (primary) voltage of each of the communities at j of feeder f_i be $V_{i,j}^t$, then the total amount of electricity which needs to be supplied/generated at t is,

$$E_g^t = \sum_{i=1}^{n} \sum_{j=1}^{m_i} I_{i,j}^t V_{i,j}^t + E_{loss}^t, \forall t \tag{7.11}$$

7.3.2 Electricity Cost

Let $\mu(E_g^t)$ be the cost function of the electricity generation at t. We assume that $\mu(E_g^t)$ is increasing and strictly convex. Therefore, if $E_g^t > \tilde{E}_g^t$ then $\mu(E_g^t) > \mu(\tilde{E}_g^t)$

[45] and the cost function is a quadratic function as [80],

$$\mu(E_g^t) = a(E_g^t)^2 + bE_g^t + c \tag{7.12}$$

where $a > 0$ and $b, c \geq 0$ and E_g^t is the amount of electricity generated by the energy source or generator. The electricity cost is solely dependent on the total demand of the customers and various losses throughout the distribution system.

7.3.3 VVCO Mathematical Model

The mathematical model is depicted as follows:

$$\text{Objective:} \quad \min \sum_{t=1}^{\tau} \mu(E_g^t) \tag{7.13}$$

subject to, Eq. (7.2), (7.3), (7.7), (7.8), (7.9), (7.11), and (7.12)

After solving the above VVCO model, the utility determines the amount of energy to be generated (E_g^t) and the cost $\mu(E_g^t)$. Note that this was decided according to the input obtained from the CEMS (such as $I_{i,j}^t$), a shown in Fig. 7.3. The rate of the electricity $\pi_t, \forall t$ ($\pi_t = \frac{\mu(E_g^t)}{E_g^t}$) is now sent back to the CEMS, so that each community can solve an optimal energy consumption model (OECM) to reschedule local loads, decide the charging/discharging state of EVs as well as the use of renewable energy. The objective here is to redistribute the load, using the current price and send back to the utility for a new decision from the VVCO model.

7.4 Optimal Energy Consumption Model (OECM)

In our proposed model, each community is assumed to be connected to the distribution feeder through a step-down transformer, known as a service drop transformer. The

transformer has two hot legs (Hot L1 and L2) output voltage (+120V, -120V) with opposite phase and a center tap known as neutral. The multi-wire (L1, L2 and neutral) branch circuit supplies 120/240V for the residential appliances. The hot leg L1/L2 and neutral are used to supply 120V and for the 240V appliances are connected to L1 and L2. Some appliances (like EV, electric motor, etc.) are connected to 240V circuit to get better performance. Devices such as, light bulb, television, microwave oven, dishwasher, dryer, etc. are connected to the 120V circuit. We assume a voltage regulator connected to 120V circuit to adjust the voltage level (ANSI C84.1 standard between 108 to 120V) according to the requirement determined by the CEMS.

7.4.1 Customer Load

A customer may have elastic appliances (such as an EV, heat water tank, heating/air conditioning system, washing machine, dishwasher, etc.,) and inelastic appliances (such as light bulbs, electric oven, electric iron, etc.) [121, 120]. Contemporary technology advances are emerging as one of the growing trends for home appliances. Evolution of such new devices and IEEE 802.15.4, ZigBee, are enabling the HEMS with easy access to appliances information and consumption control. Moreover, numerous studies have been done and are ongoing to recognize the non-intelligent home appliances consumption patterns [20, 4, 62, 106]. Once the operating appliances are detected, the HEMS can pull the efficiency voltage specification from the local database. Next, the HEMS sends the measurement (such as minimum terminal voltage, consumption duration, admittance, etc.) to the CEMS. The CEMS adjusts the consumption pattern, and the terminal voltage according to the energy cost received from the substation EMS. Moreover, to reduce the consumption from the grid, the CEMS may schedule V2G on EV, and energy use from renewable. Then, the CEMS sends the demand (current, voltage) to the substation EMS to improve the energy

cost.

Let w ($w \in r_{i,j}$) be a customer, A_w be set appliances of customer w, and a ($a \in A_w$) be an appliance. Now, for simplicity an elastic and inelastic load of a customer can be represented by a tuple as follows,

$$L_{w,a} = (V, E_{w,a}, v^l_{w,a}, T_{w,a}) \tag{7.14}$$

where V is a voltage set (within ANSI C84.1 utilization voltage range) with interval of 1 volt, $E_{w,a}$ is a set of power (ZIP power) consumed by a load (appliance) a of customer w for an operation voltage of V, $v^l_{w,a}$ is the minimum operating voltage, below this voltage the efficiency is low [122, 71], which may cause a shorter lifespan of the appliances. We assume that $v^l_{w,a}$ is a value between the standard voltage range of ANSI C84.1. $T_{w,a}$ is the acceptable period of operation such that an appliance a of customer w may consume electricity exactly for one slot[2] in $T_{w,a}$ ($|T_{w,a}|> 0$. When $|T_{w,a}|= 1$, then the load is an inelastic load, otherwise it is an elastic load. Let $P^k_{w,a}$ and $Q^k_{w,a}$ be the active and reactive power of a load a of w at operating voltage V_k (where $V_k \in V$). Then for the constant current, power and impedance, the ZIP model [118, 10] for the active and reactive power of the load can be expressed as,

$$P^k_{w,a} = P_0 \left[Z_p(\frac{V_k}{V_0})^2 + I_p\frac{V_k}{V_0} + P_p \right], \ \forall V_k \in V, \tag{7.15}$$

and

$$Q^k_{w,a} = Q_0 \left[Z_q(\frac{V_k}{V_0})^2 + I_q\frac{V_k}{V_0} + P_q \right], \ \forall V_k \in V, \tag{7.16}$$

where P_0 and Q_0 are the active and reactive power consumed at nominal voltage V_0. Z_p,I_p and P_p are the ZIP coefficients for active power and Z_q,I_q and P_q are the ZIP coefficients for reactive power [10]. Therefore the magnitude of the consumed energy

[2]Multiple slots operation of the appliance can easily be extended from this model.

by load a of w is,

$$E^k_{w,a} = [(P^k_{w,a})^2 + (Q^k_{w,a})^2]^{\frac{1}{2}} \tag{7.17}$$

For each voltage $V^k \in V$, the corresponding power consumption of each a of w can be determined. Thus, a set $E_{w,a}$ is determined and $E^k_{w,a} \in E_{w,a}$ corresponds to the operating voltage V^k.

Now, let the terminal voltage of community $r_{i,j}$ at t be $V^t_{i,j}$; then,

$$V^t_{i,j} = \sum_{k=1}^{h} V^k \alpha^{k,t}_{w,a},\ \forall t, \forall w, \forall a \tag{7.18}$$

where $h = |V|$ and $\alpha^{k,t}_{w,a}$ is a binary variable which determines the status of the load a of w at t. $\alpha^{k,t}_{w,a} = 1$ indicates that the load is consuming energy at t, otherwise it remains idle. For energy efficiency and long life operation of the equipment, the following constraint should be satisfied,

$$V^t_{i,j} \geq v^l_{w,a} \alpha^{k,t}_{w,a},\ \forall w, \forall a \tag{7.19}$$

and the energy consumption of the load a of w at t is

$$E^t_{w,a} = \sum_{k=1}^{h} E^k_{w,a} \alpha^{k,t}_{w,a}, \forall t \tag{7.20}$$

The VVCO system must ensure that each of the elastic loads must be scheduled to consume electricity for one slot within the duration ($T_{w,a}$) specified in the tuple (eq. (7.14)). Therefore,

$$\sum_{k=1}^{h} \sum_{t \in T_{w,a}} \alpha^{k,t}_{w,a} = 1 \tag{7.21}$$

Therefore, the total electricity consumption of the community $r_{i,j}$ at t can be expressed as,

$$E^t_{i,j} = \sum_{w \in r_{i,j}} \sum_{a \in A_w} E^t_{w,a} \tag{7.22}$$

7.4.2 Electric Vehicle (EV)

Assume each customer has one or a set of electric vehicles EV_w which participate in both V2G and G2V operation. Let the target charging (energy) of the electric vehicle be $E_{w,e}$, and initial energy stored in the EV be $E^i_{w,e}$, where $e \in EV_w$, the constant charging rate be $C_{w,e}$ and maximum discharging rate be $D^{max}_{w,e}$. Also, let the set of slots of the EV at home be $T_{w,e}$, and discharging rate at t be $d^t_{w,e}$ then,

$$\text{G2V Mode} \ : \ c^t_{w,e} = \alpha^t_{w,e} C_{w,e} \phi_c \tag{7.23}$$

$$\text{V2G Mode} \ : \ (1 - \alpha^t_{w,e}) D_{w,e} \leq d^t_{w,e} \phi_d \leq 0 \tag{7.24}$$

$$E_{w,e} \ \leq E^i_{w,e} + \sum_{t \in T_{w,e}} E^t_{w,e} \leq E^{max}_{w,e} \tag{7.25}$$

$$E^t_{w,e} \ = c^t_{w,e} + d^t_{w,e} \tag{7.26}$$

$$E^{min}_{w,e} \ \leq E^i_{w,e} + \sum_{t=t_s}^{t_i} E^t_{w,e} \leq E^{max}_{w,e}; \forall t_i \in T_{w,e} \tag{7.27}$$

where ϕ_c and ϕ_d are the charging and discharging efficiency of an EV. $E^{min}_{w,e}$ and $E^{max}_{w,e}$ are the discharging and charging limit of the EV, and t_s is the starting slot in set $T_{w,e}$. Term $\alpha^t_{w,e}$ in equations. (7.23) and (7.24) is a binary variable which indicates that EV e of w charging its battery when ($\alpha^t_{w,e} = 1$) and otherwise discharging at t. Now, for the community $r_{i,j}$, EV load at t can be expressed as,

$$E^t_{i,j,e} = \sum_{w \in r_{i,j}} \sum_{e \in EV_w} E^t_{w,e} \tag{7.28}$$

7.4.3 Residential Energy Sources

Assume that some customers may have roof-top solar panel or micro wind turbine to meet the partial demand. Let $E^t_{w,s}$ be the electricity produced by the renewable source of customer w at t and the maximum capacity be RES_w. Then,

$$0 \leq E^t_{w,s} \leq RES_w, \tag{7.29}$$

and for the community, the total renewable energy at t is,

$$E^t_{i,j,s} = \sum_{w \in r_{i,j}} E^t_{w,s} \tag{7.30}$$

7.4.4 OECM Mathematical Model

To minimize the energy price for a duration T, each of the communities must solve the following model,

$$\begin{aligned} &\text{Objective: } \min \sum_{t \in T} \pi_t (E^t_{i,j} + E^t_{i,j,e} - E^t_{i,j,s}) \\ &\text{Subject To: eqs. from (7.17) to (7.30)} \end{aligned} \tag{7.31}$$

where π_t is the unit cost of the electricity at t which is received from the EMS of the substation. We assume that each community always consumes a certain amount of electricity from the grid. Therefore, $E^t_{i,j} + E^t_{i,j,e} - E^t_{i,j,s} > 0$.

7.5 Non-cooperative Game: Iteraction between VVCO and OECM

The problem presented in Fig. 7.4 can be modelled using a non-cooperative game with mixed strategy. Let the payoff of each community (player) be $\beta(\sigma_{i,j}, [\pi_t | \forall t])$ and $\sigma_{i,j}$ be a set of actions (consumption or discharging) for each of the elastic (including EV)

and inelastic load of the community $r_{i,j}$ in response to the electricity price $\pi_t; \forall t \in T$. The payoff of the community is the negative of the cost of total electricity drawn from the distribution feeder f_i. Thus (from eq. (7.31)),

$$\beta(\sigma_{i,j}, [\pi_t | \forall t]) = \max \sum_{t \in T} \pi_t (E^t_{i,j,s} - E^t_{i,j} - E^t_{i,j,e}) \tag{7.32}$$

Unfortunately, the payoff in Eq. (7.32) does not guarantee an optimal solution in a Nash equilibrium state of the system. At each iteration, upon receiving the cost due to the strategy determined in the previous state, the game forces the community to reschedule the consumption to those time slots which have lower electricity costs. Thus, in the successive iteration, the cost of slots which have lower cost in the previous iteration will increase, and the expenses of the other slots will decrease. Therefore, the payoff of each community may not increase. In fact, the payoff of a player is dependent on the strategies played by other communities, which are unknown. To design a good payoff function which always results from higher payoff in the following games, let us consider the ideal scenario where the average load of each client is nearly the same, and the loads are uniformly distributed throughout the hours of a day. In this typical scenario, the average cost can be expressed as,

$$\bar{\pi} = \mu(\bar{E^t_g}), \text{ where, } \bar{E^t_g} = \frac{\sum_{t=1}^{T} E^t_g}{T}, \tag{7.33}$$

Lemma 7.5.1. *Any deviation from the average cost will decrease the payoff of the players of the game VVCO/OECM.*

Proof Let the average consumption in each time slot t be $\bar{E}_g$. Therefore, the cost of

electricity at each time slot t is,

$$\bar{\pi} = a(\bar{E}_g)^2 + b\bar{E}_g + c \tag{7.34}$$

then, the total cost for the whole time span is,

$$\pi_T = \bar{\pi}T = (a(\bar{E}_g)^2 + b\bar{E}_g + c) \cdot T \tag{7.35}$$

Now, let a player shift its consumption (smallest possible) from time slot t to $t^{'}$, thus the utility need to decrease generation ΔE_g at t and increase ΔE_g (where $\Delta E_g > 0$) at $t^{'}$, then the total electricity $\pi_T^{'}$ is,

$$\begin{aligned} \pi_T^{'} &= (a(\bar{E}_g)^2 + b\bar{E}_g + c) \cdot (T-2) + a(\bar{E}_g + \Delta E_g)^2 \\ &\quad + b(\bar{E}_g + \Delta E_g) + c) + a(\bar{E}_g - \Delta E_g)^2 \\ &\quad + b(\bar{E}_g - \Delta E_g) + c) \\ &= (a(\bar{E}_g)^2 + b\bar{E}_g + c) \cdot T + 2a(\Delta E_g)^2 \\ &> \pi_T \end{aligned} \tag{7.36}$$

Therefore, the payoff defined in eq. (7.32) will decrease for the player deviated from the average costs. A higher deviation further will reduce the payoff of the committed players. Thus, the optimal solution of the OECM game can only be obtained by setting the consumption strategies such that the overall consumption in each slot t has a minimum deviation from the average consumption. Hence, each player can maximize its payoff by playing a strategy which minimizes the deviation of the resultant costs from the average costs.

Therefore, the target of each community is to achieve an electricity cost near the cost expressed in the above Eq. (7.33). This will result in minimum changes in OLTC transformer TAP and capacitance of the capacitor bank, flatten the generation curve, and increases the life of the distribution system components. In practice, however, the

load may not be uniformly distributed or might not be achieved by rescheduling the variable loads and the discharging of EVs. Without loss of generality, we assume that the total consumption of the system is the same. Therefore, for optimal scheduling of load,

$$\sum_{t=1}^{T} \pi_t^* E_g^t \geq \sum_{t=1}^{T} \bar{\pi} \bar{E}_g^t \tag{7.37}$$

where π_t^* is the optimal electricity costs at any t, and the cost π_t^* has the minimum average distance from $\bar{\pi}$. Therefore, we redefine the payoff function as,

$$\beta(\sigma_{i,j}, [\pi_t | \forall t]) = \max\{\bar{\pi} \bar{\mathscr{L}}_{i,j} T - \sum_{t=1}^{T} S_{i,j}^t\} \tag{7.38}$$

Subject to:

$$S_{i,j}^t \geq \bar{\pi} \bar{\mathscr{L}}_{i,j} - \pi_t \mathscr{L}_{i,j}^t, \tag{7.39}$$

$$S_{i,j}^t \ \geq \pi_t \mathscr{L}_{i,j}^t - \bar{\pi} \bar{\mathscr{L}}_{i,j};\ S_{i,j}^t \geq 0, \tag{7.40}$$

Eqs. (7.17) to (7.30) where $\mathscr{L}_{i,j}^t = E_{i,j}^t + E_{i,j,e}^t - E_{i,j,s}^t$, and constant $\bar{\mathscr{L}}_{i,j} = \frac{\sum_{t=1}^{T} \mathscr{L}_{i,j}^t}{T}$ is the average load. Let the optimal payoff of the community be $\beta^*(\sigma_{i,j}^*, [\pi_t | \forall t])$ then,

$$\beta^*(\sigma_{i,j}^*, [\pi_t | \forall t]) = \max\{\bar{\pi} \bar{\mathscr{L}}_{i,j} T - \sum_{t=1}^{T} S_{i,j}^{t*}\} \tag{7.41}$$

This is possible when each player plays its best strategy, and all other strategies will result in less payoff for some or all of the communities. This is known as Nash equilibrium of the mixed strategy game. The game is a non-cooperative multi-player mixed strategy game because the player may draw the non-discrete amount of electricity from the feeders, and discharge continuous (non-discrete) amount of electricity from the EVs and consume energy from RES. Other than these, the elastic loads have discrete strategies. In each iteration, the communities play the best strategy to minimize (OECM) its consumption cost and send the demand to the EMS, which runs

the VVCO scheme and returns the electricity unit costs to the community OECM scheme. The interaction will continue until the game ends in a Nash equilibrium state. The community CEMS will act as the player of the game while the substation serves as the controller of the game.

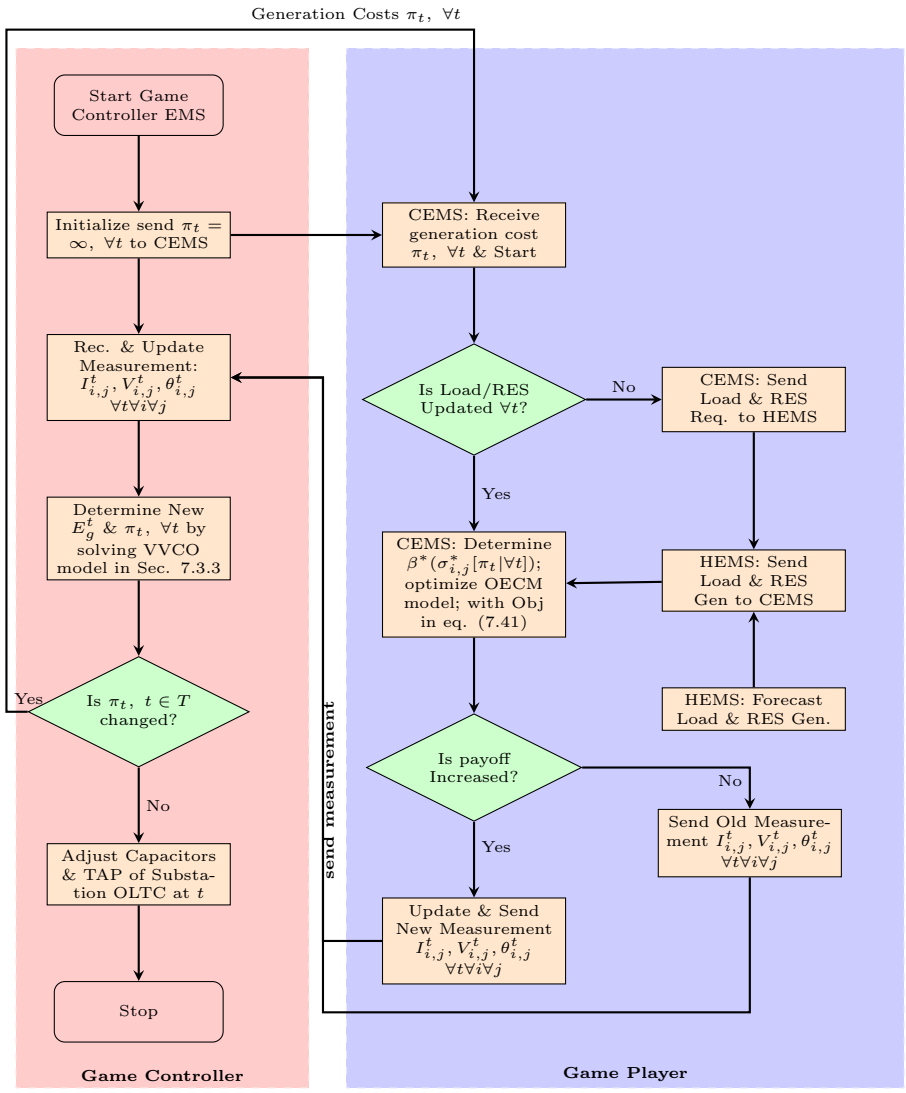

Figure 7.4: Volt-VAR optimization : VVCO/OECM Game.

Players: Each CEMS is the player of the game. In each slot, with a finite number of iterations, community $r_{i,j}$ plays the game (eq. (7.38)) to maximize its payoff. The player will change its strategy σ to maximize the payoff for electricity cost (π_t) received

from EMS. The player will continue its play until the payoff reaches its maximum. Let $\pi_t^{'}, \ \forall t \in T$ be the one-time cost of the electricity. Then steps (OECM) of the play are shown in Fig. 7.4.

Game Controller: The substation EMS will act as the controller of the game. Upon receiving the demand from the communities, the EMS calculates the electricity costs $\pi_t, \ \forall t \in T$ using eq. (7.13) for the amount of electricity E_g^t (eq. (7.11)) and send it to the CEMS. The interactions of EMS (VVCO) with the CEMS (OECM) are shown in Fig. 7.4. Once the game reached to a Nash equilibrium state, then the substation controller will send the switching command to all the capacitor bank and set the OLTC tap of the feeder at the substation. Each of the communities also adjusts voltage regulator or OLTC according to the terminal voltage selected by the optimization process.

7.5.1 Uncertainty of the community load

Load variation and uncertainty of load is common in the existing electrical network as well as for the VVO system [100, 101, 126]. The VVO system is designed to minimize the impact of the uncertainity of the load. The introduction of EV, customer load, and the uncertainty of customer's behaviors will affect the VVO. Most of the solutions consider and try to minimize the forecast errors [100, 101, 126] which is also applicable to our proposed system. Moreover, we find that the correct response to the uncertainty of load is to mitigate and adjust the load locally (community) and minimize the effect on the electrical network in real time. The proposed VVCO/OECM is a decentralized method and the response time of the system is low (less than 15 Seconds) hence the community load and corresponding capacitor bank can be adjusted more accurately just before the consumption. Moreover, to reduce the uncertainty the VVCO/OECM can be run in each operational (just before the time of actual

consumption) time slot without any modification. Further, shorter time slot (such as 1 to 5 minutes) will decrease the uncertainty near to zero. A local storage (community grade) system may be used to mitigate the change (instantaneous) of load due to unpredictable behavior of the user. The charging and discharging of the local storage system are similar to that of EV without the constraint which is presented by equation (7.25). In this case, the storage system may consume extra energy or discharge stored energy for the instantaneous change in community load.

7.6 Numerical Evalution

7.6.1 Simulation Setup

We consider a distribution system with several feeders, each of which connects 50 to 100 communities by inexpensive OLTC transformers. Also, an OLTC transformer connects the distribution line to the substation. Each community has 20 to 25 residential homes with or without the renewable sources, one or more EVs, 5 to 15 inelastic, and elastic loads. The consumption corresponds to terminal voltages ranging from 108 to 127 (with skip 1 volt) volts and are calculated using the ZIP model (eq. (7.17)) for each elastic and inelastic load. To calculate the load, we use the values of ZIP coefficients given in [10]. The renewable sources have the maximum capacity to produce 3 to 10 kW electricity. Here, we use ARMA prediction method to predict the amount of generation from the renewable sources for the next 24 hours. In our simulation, the residential load was chosen between 10 to 20 kWh for a day [123]. We assume that each home has a level 2 charger to charge the EV. The battery capacity of EV is chosen randomly from 18, 24, 60, 70, and 85kWh with charging and discharging efficiency 80%-95%. For the simulation, we place the capacitor banks with a maximum of 600 MVAR for 10, 20, 30, 40, or 50 communities and the impedances of

the distribution lines (with 33KV base voltage) are considered which is given in [29]. We implement the VVCO/OECM model in OpenMPI C++ and IBM CPLEX where each process represents a community and act as the CEMS, and one of the processes serve as the substation EMS. Each time a process determine its optimal consumption strategy (OECM) and send the measurements to the EMS, then the EMS calculates the electricity cost and sends it to the CEMS. The CEMS accepts the current strategy if the cost of electricity consumption is less than the previous cost or increases the payoff (Eq. (7.38)).

7.6.2 Numerical Results

We run the simulation for various configuration of the distribution system which contains 10, 15, ..., or 60 distribution feeders or lines (see Fig. 7.5). We repeat the simulation 50 times for each distribution system configuration.

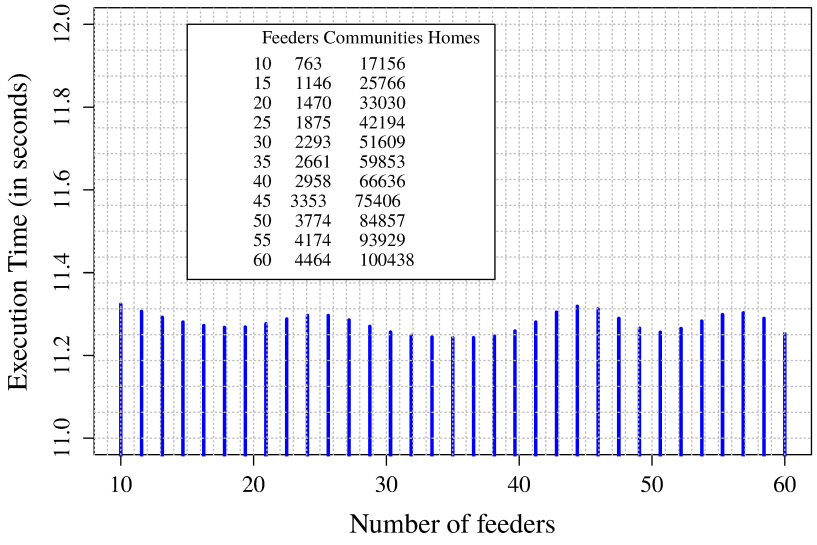

Figure 7.5: Execution time for VVCO-OECM converge to optimal results.

The VVCO/OECM model is a decentralized solution with a controller (substation EMS) which will act as an IESO (Independent Electricity System Operator) to

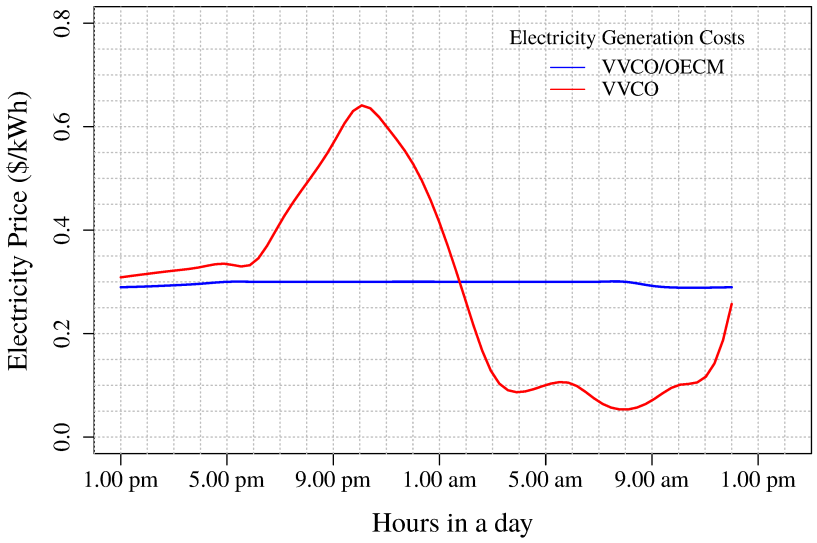

Figure 7.6: Compare electricity generation costs determined by VVCO and VVCO/OECM

determine and control the generation and costs according to the demand. Fig. 7.5 shows the total time to obtain the optimal results (peak load shaving, capacitor bank setting, OLTC transformer TAP setting, and evaluating optimal costs) for a distribution system. Each of the solution process OECM: (i) chooses the optimal consumption strategy (ii) send the message to the controller process (VVCO) and (iii) receive the electricity cost. The interaction finally ends by determining the optimal power generation costs and peak demand shaving with a few iterations (5 to 10). The system took a few seconds (10 to 15) to converge to an optimal solution irrespective of the size of the network. This is because CEMS independently play the VVCO/OECM game to achieve the maximum payoff regardless of the solution determined by other processes (CEMSs). The main burden of the system is the calculation of the costs and reactive compensation due to the change of consumption pattern. Fortunately, the process took a constant time and can process the measurements sent by the several CEMSs.

Fig. 7.6 shows the electricity generation costs ($/kWh) determined by the VVCO

and the proposed VVCO/OECM. We ran the simulation for all the configuration listed in Fig. 7.5. In all the cases, we found that the proposed system flattened the demand curve as well as the electricity generation cost of the distribution system. Here, we only present electricity costs obtained for the distribution system with 50 feeders. It is also found that the proposed VVCO/OECM results in almost same power generation cost throughout the hours of a day. On the other hand, the conventional Volt-VAR optimization system does not flatten the load, and therefore the production varies between the hours of a day. One of the primary goals of the proposed system is to flatten the load curve along with the VVO to minimize the variation of the amount generation which is also a prime target for the utility companies. The VVCO/OECM flatten the load curve by optimally shifting the elastic load, determining the optimal EV charging and discharging strategy, and using (consume or store) renewable energy. Therefore, the burden in the peak hours is distributed to the off-peak hours.

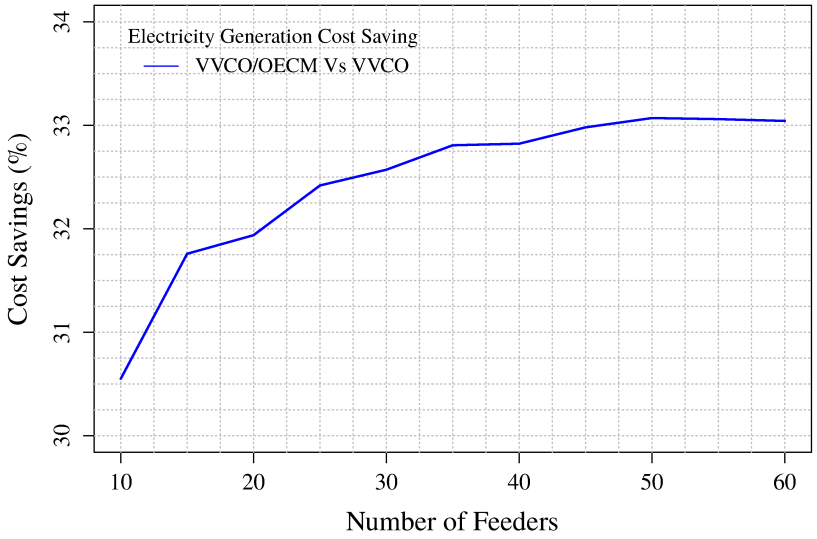

Figure 7.7: Generation cost saving by the proposed VVCO/OECM model.

Fig. 7.7 shows the percentage of electricity generation cost saving by the VVCO/OECM compared to the VVCO. The results tell us that the proposed system not only flatten the demand and cost curves but also reduces the total production cost compared to

the conventional VVO system. We ran the simulation for each of the configuration (10, 15, 20, ..., 60 feeders) by placing compensation capacitors for 10, 20, ..., 50 communities. In every case, the total generation cost of the proposed VVCO/OECM system is lower than the conventional VVO system which compensates reactive power without flattening the demand curve. Also, the proposed system uses the renewable sources, EV in V2G mode and shifting the load which reduces the current flow through the distribution line; therefore, the amount of the reactive power is reduced. It is also found that the percentage of cost saving slightly increases with the increasing number of distribution lines (and the communities). The increase of saving is evident due to the more options available to the proposed system to shift the load from peak demand duration to off-peak demand duration and energy from off-peak to peak demand duration.

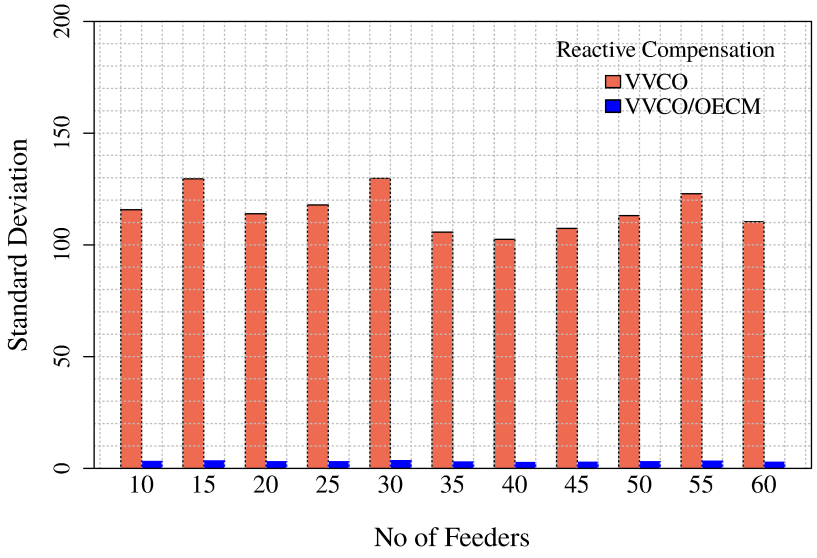

Figure 7.8: Reactive power compensation.

Fig. 7.8 shows the standard deviation of required capacity of the capacitor (or compensation device) throughout the day to minimize the reactive power loss of the distribution system. In the case of conventional VVO (here VVCO) system, the deviation between the required capacity of the capacitor varies over time which is

very significant than the variation necessary for the proposed method. The changes in the proposed method are minuscule which indicates that a fixed capacitor might be sufficient (with the small presence of the reactive power) for the distribution system or capacitor with an inexpensive switching system is required when the VVCO/OECM is used. On the other hand, in the case of conventional VVO system, a significant variation of the capacitance will need an expensive switching framework. Moreover, the deployment of the VVCO/OECM system will significantly increase the lifetime of the capacitor with the mechanical switch.

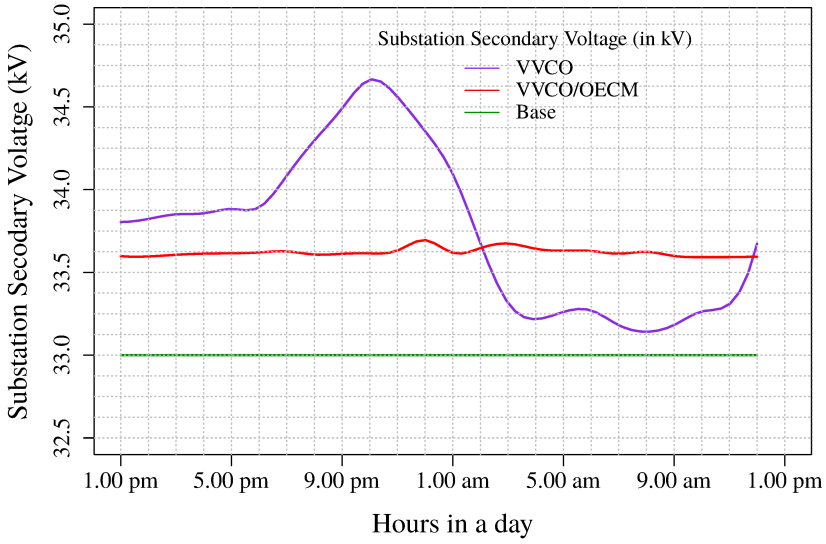

Figure 7.9: Substation Secondary Voltage.

In Fig. 7.9 the amount of secondary voltage needed for the distribution feeders after the compensation of the reactive loss, are shown for VVCO and proposed VVCO/OECM scheme. The base voltage of the distribution system is 33KV. The voltage drop varies in case of VVCO system: increases when the demand is high and decreases when demand is low. The voltage drop is mostly due to the resistance of the distribution feeders, and it will increase or decrease on the increase or decrease of the demand. The high voltage drop (VVCO at 7:00 pm - 11:00 pm) may cause extra energy loss due to the generation of heat, and may reduce the life of the distribution

line. Moreover, this significant variation of voltage in VVCO may increase the cost of the distribution system equipment such as OLTC transformer, breakers, the shunt capacitor, etc.

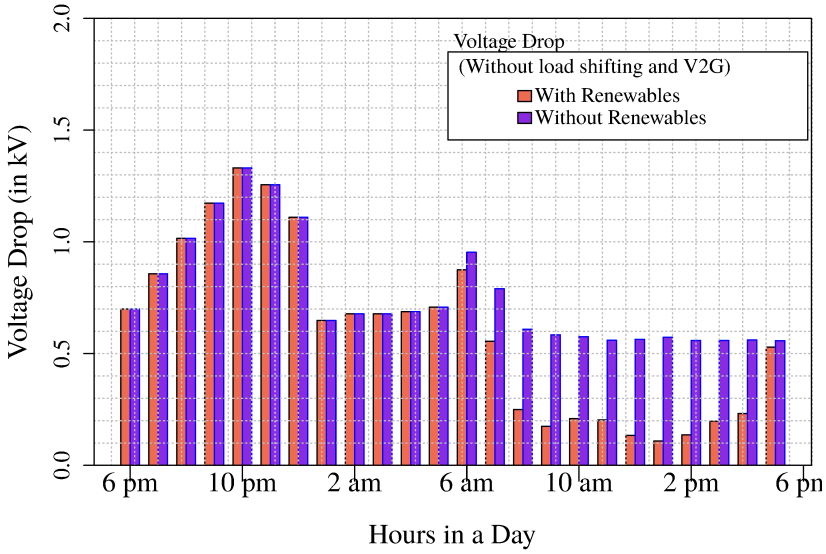

Figure 7.10: Use of renewable energy and its effect on the voltage drop.

Fig. 7.10 shows the significant impact of voltage drop in the distribution line when customers are using energy from the renewable sources. It is obvious that voltage drop decreases when the communities are using renewable energy. This is because the renewable energy reduces the cumulative load and therefore reduces the reactive and resistive loss of the system. Hence, the generator needs to generate less power. Moreover, the use of renewable energy and EV with V2G mode may add an extra benefit to reduce the voltage drop in the peak hours. This is because, in V2G mode, the EV can carry electricity from the generation period to peak consumption period when the production of renewable sources are small.

7.7 Conclusion

We developed a solution VVCO/OECM mixed strategy game based to solve Volt-VAR problem by exploiting EVs, RESs and customer shiftable loads and adjusting capacitor banks, OLTC TAP in a distributed fashion. We proved that the VVCO/OECM system solves the VVO problem by ensuring minimum electricity costs. We developed an Open MPI based simulation program to realize the distributed community environment and thus determine the terminal voltage locally and use it to help the substation to adjust the capacitor banks and OLTC transformer TAPS. The simulation result showed that the proposed VVCO/OECM system outperform the existing VVO system while ensuring the efficient operations of the home equipment.

Chapter 8

Discussion and Future work

8.1 Discussion

In this thesis, we addressed the several challenging issues for modernizing the existing power grid and presented intelligent solutions by using microgrid technologies and integrating and exploiting the electric vehicles, energy storage systems, home appliances, and renewable energy systems. Throughout this thesis, a couple of energy management schemes were developed to help achieve the objectives the modern power grid or smart grid is expected to meet. In each of proposed methods, we perform numerical analysis to show the validity of the model. We developed various simulation programs, and manifest the results in several graphs and tables to evaluate the performance of the proposed schemes. Starting from the micro-level which is energy management at home to the substation, and transmission and distribution system, we investigated various critical issues of the grid and proposed schemes to modernize it with the help of microgrid and smart grid technology. Electricity pricing models, minimization of electricity price, quality of service of power delivery, planning and balancing between energy production or purchase and real-time consumption, and reduction of the T&D losses were the primary goals of this thesis. Our proposed

systems successfully demonstrated the integration of renewable energy sources, energy storage systems, electric vehicles and shiftable loads to the power system and developed management systems which we believe will contribute to addressing the challenges of the microgrid or smart grid.

First, we proposed joint optimal scheduling schemes for home appliances and EVs in a grid-connected microgrid powered by renewable energy sources. The scheduling scheme is also known as centralized optimal consumption schedule (COPCS). The microgrid uses EVs for electricity storage to improve the efficiency and reliability of the system. We have observed that the optimal scheduling schemes clearly outperform the naive scheduling scheme by better managing the electricity consumption and shifting soft loads from high demand (and low power generation) periods to low demand (and high power generation) duration. For instance, our simulation results show that the performance improvement of optimally scheduling EVs with or without discharge capability is almost 175% for 400 EVs and 85% for 590 EVs, respectively, compared to naive scheduling. Also, the optimal algorithm with EV discharge outperforms the decentralized EV charging control method using a non-cooperative game. The running time of the proposed joint scheduling algorithm is small for a residential community. For 500 homes (3500 home appliances) with 1000 EVs, it took less than a second to 138 seconds for each iteration on a computer with Intel Core i5 processor and 4GB memory. In a real-time implementation, upon receiving the requests from the hard load appliances, the microgrid allocates energy with no delay. In the case of soft loads (types B and C), the microgrid determines the schedule of electricity allocation and allocates power according to the schedule. For a very large community, we observed that the algorithm may have some scalability issues in real-time implementations. The proposed algorithm has two very significant properties: (i) load

regulation and (ii) energy or power regulation. The proposed joint charging schedule optimally regulates power and load, which yields a minimum electricity import needed by the microgrid. This will save energy production costs of the electricity grid and ensure optimal use of locally generated renewable energy of the microgrid. The proposed joint, centralized scheduling schemes do not depend on several interactions between end systems and the central controller, which is essential for decentralized EV charging control methods to determine the optimal schedule. The interactions may not produce an optimal EV charging schedule due to inconsistencies in the flow of information. The proposed joint scheduling policies are capable of accommodating any energy source model. The optimal joint scheduling is sensitive to the variation of load, load characteristics and stochastic nature of renewable power generation. We have shown that our proposed model always produces optimal results for a microgrid with renewable, non-renewable, or both energy sources.

The centralized scheme, COPCS, does not scale well for a microgrid with a wide range of residential home. The execution time increases exponentially with the size of the microgrid which contains more than 800 residential users. Moreover, COPCS is an offline algorithm which processes and allocates energy based on predicted consumption of the equipment and EVs. Hence, the amount of energy generated from renewable energy sources, EVs arrival and departure time and target energy, consumption of home appliances vary at the time of consumption from the day ahead prediction. Also, COPCS needs device detail information for the projected time span such as consumption start and end time, the rate of consumption or charging, discharging rate of EV, the amount of renewable energy generation in different time slots, etc. Therefore, the consumer will have to send all this information to the EMS of microgrid which may cause an issue of privacy and security. To address these problems, we proposed a distributed real-time allocation (DRTA) scheme of electricity to

the homes in a grid-connected microgrid power by a mix of renewable and non-RES. The scheme is an online scheme schedule and allocates power as it is requested from the user. The microgrid uses EVs as the electricity storage to improve the energy efficiency and stability of the system. Each home in the microgrid independently schedules its home appliances and EVs to increase the overall social benefit of the microgrid. DRTA is a distributed real-time scheme which does not depend on the number of households in the smart grid or microgrid because, in DRTA scheme, each home independently optimizes its energy cost and increase the overall social benefit. In each time slot, DRTA modifies or adjusts the energy allocation plan according to the observed and predicted amount of load and energy, and allocates energy to all homes for the current time slot. We have also seen that, in all the cases, DRTA demonstrated a solution close to the COPCS scheme. Similar to the COPCS, DRTA has two very significant properties: (i) load regulation which shifts flexible load from high to the low demand duration, and (ii) energy regulation which stores excess energy to EVs batteries (G2V) from off-peak hours, and later use the stored energy (V2G) to meet the peak hours demand. The DRTA scheme converges to a stable state in few iterations (Fig. 4.6) and has the flexibility to terminate anytime, therefore, the proposed scheme is suitable and practical for a smart grid or microgrid operator of any size. The DRTA scheme with a centralized coordinator gives more control to the microgrid operator for real-time electricity pricing function; therefore, it is indeed a more practical approach. Conversely, the coordinator functions can easily be adapted to the customer point. In that case, each customer will send load information to all other customers, and the total current load and prices will be calculated locally. Each customer still needs to communicate with the operator to get the current information about the amount of electricity produced. In the practical implementation, the information of energy usage pattern of every home is exposed which may raise some

privacy issues.

DRTA is an online scheduling and allocating system which schedule and deliver electricity according to the immediate demand; it does not however help much the energy retailer or microgrid operator for a day ahead or hour before generation and purchase of energy. We addressed this problem and developed a real-time distributed energy management RDCDSM system to mitigate the intermittent nature of the RESs and fulfill the demand of a residential microgrid. The proposed RDCDSM processes the raw predicted load to produce a predicted load curve, balanced throughout time, for the microgrid and allocates electricity in real time in an intelligent way which reduces the gap between the predicted and distributed amount of power. Hence, the proposed system forces customers to produce a flat load profile collectively and stick to that profile at the time of actual consumption using a penalty. RDCDSM eases the integration of RESs with the grid by exploiting ESSs and EVs. We also developed a centralized allocation method to allocate electricity according to the day ahead simple prediction method to evaluate the performance of RDCDSM. The RDCDSM system took less time (less than a minute) to produce the results whereas the centralized scheme needs days (and sometimes weeks) to provide a solution for a large microgrid. The proposed system requires more sensible equipment (HEMS) whereas the centralized system required a less intelligent system in the user premises. The centralized system, however, needs detailed information on consumption from users which may violate their privacy.

Next, we proposed an optimal pricing scheme, MEPM, for minimizing the electricity price in a microgrid network. Originally, the power cost optimization problems are non-linear and non-convex. Hence, the problems are intractable, and no known polynomial solution exist to solve them. We have analyzed the minimum cost (MEPM) and decomposed the problem to solve it optimally, and compared with a first

come first server pricing scheme. For various configurations of the MGN, the MEPM method showed outstanding performance. The MEPM scheme takes less time to evaluate the electricity price of an enormous size MGN. Therefore, MEPM is a good choice for determining real-time electricity pricing of MGN. Moreover, the MEPM can identify and predict near accurate (optimal) electricity price for the variation of load and renewable energy generation of the MGN system. Also, the proposed model considers various energy sources including renewable energy and dynamic behavior of the smart microgrid in the electricity system as a seller or a buyer. Although we have presented the model for non-decreasing marginal cost function, the proposed algorithm produces optimal results for both general convex and monotonic marginal costs but not for the nonlinear marginal costs with peaks and valleys.

Finally, we proposed a new model (VVCO/OECM) for VVO, which acknowledges the current technological advancement of the power grid, evolution of the smart grid, and EVs. We found that the proposed model and its game-theoretic solution could solve the VVO problem optimally. The existing VVO method only solves the problem with the coarse-demand received from the customers. In our solution, we developed an interactive method which enables the utility to communicate with the customer to flatten the load and ultimately, reduces the reactive loss and flatten the generation. Thus, VVCO/OECM can reduce the overall production cost of the electricity. The VVCO/OECM system is scalable and can be implemented for any size power system infrastructure. The system can be deployed without the intervention of the substation by calculating the cost at the CEMS premises and adjust the compensation devices by the local demand.

To evaluate the models we developed simulation programs using C++, MPI, and IBM CPLEX. The centralized model is developed using C++ and CPLEX and performed the experiment as a single process with several instances of a microgrid or

microgrids. For the game based model including the mechanism design, we developed C++ MPI, IBM CPLEX based parallel program where each of the processes represents a player or agent of the game. Most of the experiments were executed on Calcul Quebec (Compute Canada) advanced research computing (ARC) system to emulate the parallel essence of the real system [99].

8.2 Future Work

The work presented in the thesis provided considerable effort to solve the challenges of the transition from a traditional power grid to a modern smart grid by integrating renewable energy sources, electric vehicles, shiftable loads, and energy storage systems. The objective was to minimize losses, optimal power management, and quality of electricity delivery to the customer with reducing electricity price. However, there remains several future research directions which may add extra benefits to meet the challenges of the future power grid.

In our energy management models for the residential microgrid (COPCS, DRTA, RDCDSM), we assumed that microgrid is connected to the traditional grid which is a reality. We assume that the shortage of electricity of the residential microgrid will be purchased from the power grid. In the islanded mode, when microgrid is disconnected from the power grid due to a natural disaster or cyber-physical attract, the microgrid needs a contingency and emergency energy management plan. Each residential home energy management system needs to identify the emergency or essential loads to be serviced such that all the households in the microgrid have the fair share of available power. The proper management of storage systems such as EVs and ESSs may always preserve a sufficient amount of energy to meet the demand of an emergency situation.

In the MGN and VVO/OECM system, we have considered active and reactive power in the power line due to the resistance and inductance of the power line.

We do not regard the capacitance of the transmission and distribution line, reactive power injected by loads (for MGN), renewable energy sources, heat loss, transformer losses, frequency variation, etc. These parameters may complicate the model, but it is essential for a perfect design of an energy management system. In general, the problem is a well known optimal power flow (OPF) problem. Much research has been done for several decades to solve the optimal power flow problem in the traditional electrical network which has centralized generation. The modern power system is more complicated due to the dynamic load, storage, bidirectional flow of energy and distributed generator; thereby the optimal power flow problem becomes more difficult. This needs intense investigation, modeling, and solution to address the power flow problem for the modern power network.

We have used PMU in VVCO/OECM which has potential synchronization and phase offset problems due to the unaligned clocks of PMU and PDC or central controller. Some control applications may not tolerate clocks drift greater than $1\mu s$. Therefore, clock synchronization between PMU and PDC or central controller (or EMS) may result in better management and control system for the power grid.

Alteration or tampering, denial of service, delay due to network congestion or cyber attract on control, demand, and various other messages may create an immediate problem in power delivery and increase the cost of operation and electricity. This may not jeopardize to achieve the objectives of the microgrid. Therefore, study and active research may improve the resiliency, reliability, and availability of power grid.

Microgrid and smart grid are nowadays an active research topic. A significant investment will be made over next decade to modernizing the century-old power grid. The experience and expertise obtained through microgrid research will provide market opportunities for participating enterprises as the demand for microgrid technologies raises around the world. To improve this position, and ensure continued success,

given the emphasis on research, the collaboration between national and international partners will be necessary. These efforts will help to educate all stakeholders and, also, will stimulate the improvement of next generation power grid, and energy economics.

Bibliography

[1] I. E. Agency. CO_2 emission for fuel combustion: highlights. Technical report, International Energy Agency, OECD/IEA, 9, rue de la Fdration, 75739 Paris Cedex 15, France, Oct 2011.

[2] I. E. Agency. Technology roadmap: Smart grids. Report, Internation Energy Agency, April 2011.

[3] I. E. Agency and S. Inage. Modelling load shifting using electric vehicles in a smart grid environment. *IEA working paper*, 2010.

[4] H. Ahmadi and J. Marti. Load decomposition at smart meters level using eigenloads approach. *IEEE Transactions on Power Systems*, PP(99):1–12, 2015.

[5] K. Anderson and A. Narayan. Simulating integrated volt/var control and distributed demand response using gridspice. In *Proc., IEEE First International Workshop on SGMS*, pages 84–89, Oct 2011.

[6] J. Bajada, M. Fox, and D. Long. Load modelling and simulation of household electricity consumption for the evaluation of demand-side management strategies. In *Proc., IEEE PES ISGT Europe 2013*, pages 1–5, Oct 2013.

[7] W. Bank. Electric power consumption (kwh per capita). `http://data.worldbank.org/indicator/EG.USE.ELEC.KH.PC`, 2016.

[8] S. Bifaretti, P. Zanchetta, A. Watson, L. Tarisciotti, and J. C. Clare. Advanced power electronic conversion and control system for universal and flexible power management. *IEEE Transactions on Smart Grid*, 2(2):231–243, June 2011.

[9] K. Binmore. *Game Theory: A Very Short Introduction*. Oxford University Press, 1st edition, Dec 2007.

[10] A. Bokhari, A. Alkan, R. Dogan, M. Diaz-Aguil, F. de Len, D. Czarkowski, Z. Zabar, L. Birenbaum, A. Noel, and R. E. Uosef. Experimental determination of the zip coefficients for modern residential, commercial, and industrial loads. *IEEE Transactions on Power Delivery*, 29(3):1372–1381, June 2014.

[11] S. Boyd and L. Vandenberghe. *Convex Optimization*. cambridge university press, 2004.

[12] S. A. Boyer. *Scada: Supervisory Control And Data Acquisition*. International Society of Automation, USA, 4th edition, 2009.

[13] T. H. Bradley and A. A. Frank. Design, demonstrations and sustainability impact assessments for plug-in hybrid electric vehicles. *Renewable and Sustainable Energy Reviews*, 13(1):115 – 128, 2009.

[14] K. Branker, M. Pathak, and J. Pearce. A review of solar photovoltaic levelized cost of electricity. *Renewable and Sustainable Energy Reviews*, 15(9):4470 – 4482, 2011.

[15] J.-N. Brub, J. Aubin, and W. McDermid. Transformer winding hot spot temperature determination. *Online Electric Energy*, March 2007.

[16] M. Campbell and et. al. The drivers of the levelized cost of electricity for utility-scale photovoltaics. Technical report, SUNPOWER Corporation, 2008.

[17] S. Caron and G. Kesidis. Incentive-based energy consumption scheduling algorithms for the smart grid. In *Proc., First IEEE International Conference on Smart Grid Communications (SmartGridComm)*, pages 391–396, Oct 2010.

[18] C. Chan. An overview of electric vehicle technology. *Proceedings of the IEEE*, 81(9):1202 –1213, Sep. 1993.

[19] C. Chen, S. Duan, T. Cai, B. Liu, and G. Hu. Smart energy management system for optimal microgrid economic operation. *Renewable Power Generation, IET*, 5(3):258–267, May 2011.

[20] S.-Y. Chen, C.-F. Lai, Y.-M. Huang, and Y.-L. Jeng. Intelligent home-appliance recognition over iot cloud network. In *Proc., 9th International Conference on IWCMC*, pages 639–643, July 2013.

[21] Z. Chen, L. Wu, and Y. Fu. Real-time price-based demand response management for residential appliances via stochastic optimization and robust optimization. *IEEE Transactions on Smart Grid*, 3(4):1822–1831, 2012.

[22] K. Clement-Nyns, E. Haesen, and J. Driesen. The impact of charging plug-in hybrid electric vehicles on a residential distribution grid. *IEEE Transactions on Power Systems*, 25(1):371–380, Feb. 2010.

[23] T. H. Cormen, C. Stein, R. L. Rivest, and C. E. Leiserson. *Introduction to Algorithms*. McGraw-Hill Higher Education, 2nd edition, 2001.

[24] C. L. DeMarco, C. A. Baone, Y. Han, and B. Lesieutre. Primary and secondary control for high penetration renewables. White paper, PSERC, University of Wisconsin-Madison, May 2012.

[25] Department of Transport. Transport statistics bulletin-natinal travel survey. Technical report, Department of Transport, UK, Apr 2008.

[26] A. P. T. Division. *Transformer Handbook*. ABB, Affolternstrasse 44, 8050 Zrich,SWITZERLAND, 2004.

[27] B.-H. E., C. Fachkha, M. Pourzandi, M. Debbabi, and C. Assi. Communication security for smart grid distribution networks. *IEEE Communications Magazine*, 51(1), 2013.

[28] W. El-Khattam, K. Bhattacharya, Y. Hegazy, and M. M. A. Salama. Optimal investment planning for distributed generation in a competitive electricity market. *IEEE Transactions on Power Systems*, 19(3):1674–1684, Aug 2004.

[29] G. Electric. *Distribution Data Book*. General Electric Schenectady, 1943.

[30] Electrification Coalition. Electrification roadmap: Revolutionizing transportation and achieving energy security. Technical report, Electrifi cation Coalition, 1111 19th street, NW suite 406 Washington, dC 20036, USA, Nov 2009.

[31] Environment Canada. Numerical weather prediction (nwp) model verification. `http://weather.gc.ca/verification/index_e.html`, 2013.

[32] U. E. P. A. (EPA). Inventory of u.s. greenhouse gas emissions and sinks: 1990-2014. Technical Report EPA 430-R-16-002, National Service Center for Environmental Publications, 1200 Pennsylvania Ave., N.W. Washington, DC 20460 U.S.A, April 2016.

[33] G. Ericsson. Cyber security and power system communication;essential parts of a smart grid infrastructure. *IEEE Transactions on Power Delivery*, 25(3):1501 –1507, july 2010.

[34] Z. Fadlullah, M. Fouda, N. Kato, A. Takeuchi, N. Iwasaki, and Y. Nozaki. Toward intelligent machine-to-machine communications in smart grid. *IEEE Communications Magazine*, 49(4):60 –65, april 2011.

[35] H. Farhangi. The path of the smart grid. *IEEE Power and Energy Magazine*, 8(1):18–28, January 2010.

[36] H. Farhangi. A road map to integration: Perspectives on smart grid development. *IEEE Power and Energy Magazine*, 12(3):52–66, May 2014.

[37] M. Farrokhifar. Optimal operation of energy storage devices with {RESs} to improve efficiency of distribution grids; technical and economical assessment. *International Journal of Electrical Power & Energy Systems*, 74:153 – 161, 2016.

[38] M. Fathi and H. Bevrani. Statistical cooperative power dispatching in interconnected microgrids. *IEEE Transactions on Sustainable Energy*, 4(3):586–593, July 2013.

[39] D. Fudenberg and J. Tirole. *Game Theory*. The MIT Press, 1st edition, Aug 1991.

[40] J. Gallardo-Lozano, E. Romero-Cadaval, V. Minambres-Marcos, D. Vinnikov, T. Jalakas, and H. Hoimoja. Grid reactive power compensation by using electric vehicles. In *Proc., Electric Power Quality and Supply Reliability Conference (PQ)*, pages 19–24, June 2014.

[41] L. Gan, U. Topcu, and S. Low. Optimal decentralized protocol for electric vehicle charging. In *Proc., 50th IEEE Conference on Decision and Control and European Control Conference (CDC-ECC)*, pages 5798–5804, Dec 2011.

[42] M. G. D. Giorgi, A. Ficarella, and M. Tarantino. Error analysis of short term wind power prediction models. *Applied Energy*, 88(4):1298 – 1311, 2011.

[43] T. Gönen. *Electric power distribution system engineering*. McGraw-Hill Series in Electrical Engineering. McGraw-Hill, 1986.

[44] D. Y. Goswami and F. Kreith, editors. *Energy Efficiency and Renewable Energy Handbook*. CRC Press,, Taylor & Francis Group, 6000 Broken Sound Parkway NW, Suit 300, Boca Raton, second edition, Nov 2014.

[45] M. Greer. *Electricity marginal cost pricing : applications in eliciting demand responses*. Amsterdam ; Boston : Butterworth-Heinemann/Elsevier, 2012.

[46] P. Gribik, W. Hogan, and S. Popeii. Market-clearing electricity prices and energy uplift. Technical report, Harvard University, Harvard University, USA, December 2007.

[47] C. Guille and G. Gross. A conceptual framework for the vehicle-to-grid (V2G) implementation. *Energy Policy*, 37(11):4379 – 4390, 2009.

[48] G. Hamoud and I. Bradley. Assessment of transmission congestion cost and locational marginal pricing in a competitive electricity market. *IEEE Transactions on Power Systems*, 19(2):769–775, May 2004.

[49] A. U. Haque, P. Mandal, M. E. Kaye, J. Meng, L. Chang, and T. Senjyu. A new strategy for predicting short-term wind speed using soft computing models. *Renewable and Sustainable Energy Reviews*, 16(7):4563–4573, Sep 2012.

[50] Y. He, B. Venkatesh, and L. Guan. Optimal scheduling for charging and discharging of electric vehicles. *IEEE Transactions on Smart Grid*, 3(3):1095–1105, Sept 2012.

[51] P. Hearps and D. McConnell. Renewable energy technology cost review. Technical paper series, Melbourne Energy Institute, University of Melbourne, Melbourne, Australia, March 2011.

[52] L. Hernandez, C. Baladron, J. M. Aguiar, B. Carro, A. J. Sanchez-Esguevillas, J. Lloret, and J. Massana. A survey on electric power demand forecasting:

Future trends in smart grids, microgrids and smart buildings. *IEEE Communications Surveys Tutorials*, 16(3):1460–1495, Third 2014.

[53] J. Hetzer, D. C. Yu, and K. Bhattarai. An economic dispatch model incorporating wind power. *IEEE Transactions on Energy Conversion*, 23(2):603–611, June 2008.

[54] W. W. Hogan. Competitive electricity market design: A wholesale primer. *John F. Kennedy School of Government, Harvard University*, December 1998.

[55] R. Huang, T. Huang, R. Gadh, and N. Li. Solar generation prediction using the arma model in a laboratory-level micro-grid. In *Proc., IEEE Third International Conference on Digital Object Identifier: Smart Grid Communications (SmartGridComm)*, pages 528–533. IEEE, Nov 2012.

[56] Y. Huang, S. Mao, and R. M. Nelms. Adaptive electricity scheduling in microgrids. *IEEE Transactions on Smart Grid*, 5(1):270–281, Jan 2014.

[57] K. Humphreys, A. Maithani, and J. Y. Yu. Crowdsourced electricity demand forecast. In *Proc. 11th Internation Conference on Autonomous Agents and Multiagent Systems*, May 2015.

[58] Hydro-Qubec. Hydro-Qubec annual report 2013. Technical Report 2013G250A, Hydro-Qubec, 2nd Quarter 2014.

[59] I. E. S. O. (IESO). Blackout 2003. `http://www.ieso.ca/imoweb/emergencyprep/blackout2003/default.asp`; Last accessed: 8/11/2012.

[60] E. V. Initiative. Global EV outlook: understanding the electric vehicle landscape to 2020. Technical report, IEA/Clean Energy Ministrial, April 2013.

[61] R. K. Jain, D.-M. W. Chiu, and W. R. Hawe. A quantitative measure of fairness and discrimination for resource allocation in shared computer systems. Technical report, Digital Equipment Corporation, Sep 1984.

[62] C.-F. Lai, R.-H. Hwang, H.-C. Chao, and Y.-H. Lai. A dynamic power features selection method for multi-appliance recognition on cloud-based smart grid. In *Proc., IEEE 17th International Conference on Computational Science and Engineering (CSE)*, pages 780–785, Dec 2014.

[63] C.-M. Lee and C.-N. Ko. Short-term load forecasting using lifting scheme and {ARIMA} models. *Expert Systems with Applications*, 38(5):5902 – 5911, 2011.

[64] D. Li and S. Jayaweera. Distributed smart-home decision-making in a hierarchical interactive smart grid architecture. *IEEE Transactions on Parallel and Distributed Systems*, PP(99):1–1, Feb 2014.

[65] D. Li and S. K. Jayaweera. Distributed smart-home decision-making in a hierarchical interactive smart grid architecture. *IEEE Transactions on Parallel and Distributed Systems*, 26(1):75–84, Jan 2015.

[66] W. Lin, Y. Tang, H. Sun, Q. Guo, H. Zhao, and B. Zeng. Blackout in brazil power grid on february 4, 2011 and inspirations for stable operation of power grid. *Automation of Electric Power Systems*, 9:002, 2011.

[67] T. Liu, X. Tan, B. Sun, Y. Wu, X. Guan, and D. H. K. Tsang. Energy management of cooperative microgrids with p2p energy sharing in distribution networks. In *Proc., IEEE International Conference on Smart Grid Communications (SmartGridComm)*, pages 410–415, Nov 2015.

[68] Y. Liu, C. Yuen, N. U. Hassan, S. Huang, R. Yu, and S. Xie. Electricity

cost minimization for a microgrid with distributed energy resource under different information availability. *IEEE Transactions on Industrial Electronics*, 62(4):2571–2583, April 2015.

[69] T. Logenthiran, D. Srinivasan, and T. Z. Shun. Demand side management in smart grid using heuristic optimization. *IEEE Transactions on Smart Grid*, 3(3):1244–1252, Sept 2012.

[70] Z. Ma, D. Callaway, and I. Hiskens. Decentralized charging control of large populations of plug-in electric vehicles. *IEEE Transactions on Control Systems Technology*, 21(1):67–78, Nov. 2013.

[71] N. Markushevich. The benefits and challenges of the integrated volt/var optimization in the smart grid environment. In *Proc., IEEE Power and Energy Society General Meeting*, pages 1–8, July 2011.

[72] G. Martinez, N. Gatsis, and G. Giannakis. Stochastic programming for energy planning in microgrids with renewables. In *Proc., IEEE 5th International Workshop on Computational Advances in Multi-Sensor Adaptive Processing (CAMSAP)*, pages 472–475, Dec 2013.

[73] M. K. C. Marwali, S. M. Shahidehpour, and M. Daneshdoost. Probabilistic production costing for photovoltaics-utility systems with battery storage. *IEEE Transactions on Energy Conversion*, 12(2):175–180, Aug. 2002.

[74] M. Masoum, M. Ladjevardi, A. Jafarian, and E. Fuchs. Optimal placement, replacement and sizing of capacitor banks in distorted distribution networks by genetic algorithms. *IEEE Transactions on Power Delivery*, 19(4):1794–1801, Oct 2004.

[75] W. A. McEachern. *Economics: A Contemporary Introduction*. South-Western College Pub, Mason, Ohio, 10 edition, December 2012.

[76] M. Meiqin, S. Shujuan, and L. Chang. Economic analysis of the microgrid with multi-energy and electric vehicles. In *Proc., 8th IEEE International Conference on Power Electronics and ECCE Asia (ICPE ECCE)*, pages 2067–2072, Jeju, Korea, May/June 2011.

[77] M. Meiqin, S. Shujuan, and L. Chang. Economic analysis of the microgrid with multi-energy and electric vehicles. In *Proc., 8th International Conference on Power Electronics - ECCE Asia*, pages 2067–2072, May 2011.

[78] A. P. S. Meliopoulos, G. J. Cokkinides, F. Galvan, B. Fardanesh, and P. Myrda. Delivering accurate and timely data to all. *IEEE Power and Energy Magazine*, 5(3):74–86, May 2007.

[79] W. Mert. Consumer acceptance of smart appliances. Technical Report D 5.5, IFZInter-University Research Centre for Technology, Dec 2008.

[80] A. H. Mohsenian-Rad, V. W. S. Wong, J. Jatskevich, R. Schober, and A. Leon-Garcia. Autonomous demand-side management based on game-theoretic energy consumption scheduling for the future smart grid. *IEEE Transactions on Smart Grid*, 1(3):320–331, Dec 2010.

[81] T. Motors. Model s: Performance and safety refined. `https://www.tesla.com/en_CA/models`, 2017.

[82] B. Narayanaswamy, V. Garg, and T. S. Jayram. Online optimization for the smart (micro) grid. In *Proc., Third International Conference on Future Energy Systems: Where Energy, Computing and Communication Meet (e-Energy)*, pages 1–10, May 2012.

[83] E. Ng and R. El-Shatshat. Multi-microgrid control systems (mmcs). In *Proc. IEEE Power and Energy Society General Meeting*, pages 1–6, Minneapolis, USA, July 2010.

[84] T. Niknam, M. Zare, and J. Aghaei. Scenario-based multiobjective volt/var control in distribution networks including renewable energy sources. *IEEE Transactions on Power Delivery*, 27(4):2004–2019, Oct 2012.

[85] D. Niyato, E. Hossain, and A. Fallahi. Sleep and wakeup strategies in solar-powered wireless sensor/mesh networks: Performance analysis and optimization. *IEEE Transactions on Mobile Computing*, 6(2):221–236, Feb. 2007.

[86] OECD. Smart sensor networks: Technologies and applications for green growth. Technical report, OECD, Dec 2009.

[87] OECD. Smart sensor networks: Technologies and applications for green growth. Technical report, OECD, Dec 2009.

[88] D. Olivares, C. Canizares, and M. Kazerani. A centralized optimal energy management system for microgrids. In *Proc., IEEE Power and Energy Society General Meeting*, pages 1–6, 2011.

[89] A. P. on Public Affairs (POPA). Integrating renewable electricity on the grid. Online, American Physical Society, 529 14th Street, NW, Suite 1050,Washington DC 20045, November 2010.

[90] P. Palensky and D. Dietrich. Demand side management: Demand response, intelligent energy systems, and smart loads. *IEEE Transactions on Industrial Informatics*, 7(3):381–388, Aug 2011.

[91] J. Parmar. How to calculate voltage regulation of distribution line. *Electric Engineering Portal*, June 2013.

[92] G. Pasaoglu, D. Fiorello, L. Zani, A. Martino, A. Zubaryeva, and C. Thiel. Projections for electric vehicle load profiles in europe based on travel survey data. Scientific and police report, Joint Research Centre(JRC), Institute for Institute for Energy and Transport, Joint Research Centre - IET, P.O. Box 2, 1755 ZG, Petten, the Netherlands, 2013.

[93] D. W. Pearce, editor. *The MIT Dictionary Of Modern Economics*. The MIT Press, fourth edition, Aug 1992.

[94] N. S. Pearre, W. Kempton, R. L. Guensler, and V. V. Elango. Electric vehicles: How much range is required for a days driving? *Transportation Research Part C: Emerging Technologies*, 19(6):1171 – 1184, 2011.

[95] S. B. Peterson, J. Whitacre, and J. Apt. The economics of using plug-in hybrid electric vehicle battery packs for grid storage. *Journal of Power Sources*, 195(8):2377 – 2384, 2010.

[96] P. Pikk and M. Viiding. The dangers of marginal cost based electricity pricing. *Baltic Journal of Economics*, 13(1):49–62, 2013.

[97] J. H. Pikul, H. G. Zhang, J. Cho, P. V. Braun, and W. P. King. High-power lithium ion microbatteries from interdigitated three-dimensional bicontinuous nanoporous electrodes. *Nature Communications*, 4:1–5, Apr 2013.

[98] P. Poggi, M. Muselli, G. Notton, C. Cristofari, and A. Louche. Forecasting and simulating wind speed in Corsica by using an autoregressive model. *Energy Conversion and Management*, 44(20):3177–3196, Dec 2003.

[99] C. Quebec. Calcul quebec, compute canada. `http://www.calculquebec.ca/en/`, 2017.

[100] S. Rahimi, S. Massucco, F. Silvestro, M. R. Hesamzadeh, and Y. Tohidi. Volt/var optimization function with load uncertainty for planning of mv distribution networks. In *Proc., IEEE Eindhoven PowerTech*, pages 1–6, June 2015.

[101] S. Rahimi, K. Zhu, S. Massucco, and F. Silvestro. Stochastic volt-var optimization function for planning of mv distribution networks. In *Proc., IEEE Power Energy Society General Meeting*, pages 1–5, July 2015.

[102] A. Ramos, M. Ventosa, and M. Rivier. Modeling competition in electric energy markets by equilibrium constraints. *Utilities Policy*, 7(4):233 – 242, 1999.

[103] P. Ranci and G. Cervigni. *The Economics of Electricity Markets*. The Loyola De Palacio Series on European Energy Policy. Edward Elgar Pub, 2013.

[104] L. Raykin, M. J. Roorda, and H. L. MacLean. Impacts of driving patterns on tank-to-wheel energy use of plug-in hybrid electric vehicles. *Transportation Research Part D: Transport and Environment*, 17(3):243 – 250, 2012.

[105] M. Rossi and D. Brunelli. Electricity demand forecasting of single residential units. In *Proc., IEEE Workshop on Environmental Energy and Structural Monitoring Systems (EESMS)*, pages 1–6, Sept 2013.

[106] A. Ruzzelli, C. Nicolas, A. Schoofs, and G. O'Hare. Real-time recognition and profiling of appliances through a single electricity sensor. In *Proc., 7th Annual IEEE Communications Society Conference on SECON*, pages 1–9, June 2010.

[107] W. Saad, Z. Han, and H. V. Poor. Coalitional game theory for cooperative micro-grid distribution networks. In *Proc., IEEE International Conference on Communications Workshops (ICC)*, pages 1–5, June 2011.

[108] P. Samadi, H. Mohsenian-Rad, R. Schober, and V. W. S. Wong. Advanced demand side management for the future smart grid using mechanism design. *IEEE Transactions on Smart Grid*, 3(3):1170–1180, Sept 2012.

[109] A. Santos, N. McGuckin, H. Nakamoto, D. Gray, and S. Liss. Summary of travel trends: 2009 national household travel survey. Trends in travel behavior FHWA-PL-ll-022, U.S. Department of Transportation, June 2011.

[110] I. G. Sardou, M. E. Khodayar, K. Khaledian, M. Soleimani-damaneh, and M. T. Ameli. Energy and reserve market clearing with microgrid aggregators. *IEEE Transactions on Smart Grid*, 2015.

[111] K. Schneider and T. Weaver. Volt-var optimization on american electric power feeders in northeast columbus. In *Proc., IEEE PES T&D Conference and Exposition*, pages 1–8, May 2012.

[112] R. A. Schwartz, M. G. Carew, and T. Maksimenko. *Micro Markets Workbook: A Market Structure Approach to Microeconomic Analysis*. John Wiley & Sons, Hoboken, New Jersey, April 2010.

[113] A. Shamshad, M. A. Bawadi, W. M. A. W. Hussin, T. A. Majid, and S. A. M. Sanusi. First and second order Markov chain models for synthetic generation of wind speed times series. *Energy*, 30(5):693–708, Apr. 2005.

[114] Y. Shoham and K. Leyton-Brown. *Multiagent Systems: Algorithmic, Game-Theoretic, and Logical Foundations*. Cambridge University Press, 2009.

[115] J. Solanki, N. Venkatesan, and S. Solanki. Coordination of demand response and volt/var control algorithm using multi agent system. In *Proc., IEEE PES T&D Conference and Exposition*, pages 1–4, May 2012.

[116] Z. Song, X. Geng, A. Kusiak, and C. Xu. Mining Markov chain transition matrix from wind speed time series data. *Expert Systems with Applications*, 38(8):10229–10239, Aug. 2011.

[117] S. Speidel and T. Brunl. Leaving the gridthe effect of combining home energy storage with renewable energy generation. *Renewable and Sustainable Energy Reviews*, 60:1213 – 1224, 2016.

[118] L. Toledo, M. Mota, and A. A. Mota. Load modeling at electric power distribution substations using dynamic load parameters estimation. *International Journal of Electrical Power & Energy Systems*, 26(10):805 – 811, 2004.

[119] Toronto Hydro. TIME-OF-USE (TOU) RATES. `http://www.torontohydro.com/sites/electricsystem/residential/yourbilloverview/Pages/TOURates.aspx`, 2013.

[120] M. Tushar, C. Assi, M. Maier, and M. Uddin. Smart microgrids: Optimal joint scheduling for electric vehicles and home appliances. *IEEE Transactions on Smart Grid*, 5(1):239–250, Jan 2014.

[121] M. H. K. Tushar, C. Assi, and M. Maier. Distributed real-time electricity allocation mechanism for large residential microgrid. *IEEE Transactions on Smart Grid*, 6(3):1353–1363, May 2015.

[122] B. Uluski. Volt/var control and optimization concepts and issues. `http://cialab.ee.washington.edu/nwess/2012/talks/uluski.pdf`, 2011.

[123] U.S. Energy Information Administration (EIA). Electric power annual 2012. Technical report, U.S. Department of Energy, Dec 2013.

[124] S. A. Vavasis. Quadratic programming is in NP. *Information Processing Letters*, 36(2):73 – 77, 1990.

[125] Q. Wang, G. Zhang, J. D. McCalley, T. Zheng, and E. Litvinov. Risk-based locational marginal pricing and congestion management. *IEEE Transactions on Power Systems*, 29(5):2518–2528, Sept 2014.

[126] Z. Wang, J. Wang, B. Chen, M. M. Begovic, and Y. He. Mpc-based voltage/var optimization for distribution circuits with distributed generators and exponential load models. *IEEE Transactions on Smart Grid*, 5(5):2412–2420, Sept 2014.

[127] C. Wei, Z. M. Fadlullah, N. Kato, and I. Stojmenovic. On optimally reducing power loss in micro-grids with power storage devices. *IEEE Journal on Selected Areas in Communications*, 32(7):1361–1370, July 2014.

[128] F. Wen, F. F. Wu, and Y. Ni. Generation capacity adequacy in the competitive electricity market environment. *International Journal of Electrical Power & Energy Systems*, 26(5):365 – 372, 2004.

[129] L. Wenpeng. Advanced metering infrastructure. *Southern Power System Technology*, 3(2):6–10, 2009.

[130] P. Werbos. Computational intelligence for the smart grid-history, challenges, and opportunities. *Computational Intelligence Magazine, IEEE*, 6(3):14–21, 2011.

[131] Q. Wu, A. H. Nielsen, J. Ostergaard, S. T. Cha, F. Marra, Y. Chen, and C. Trholt. Driving pattern analysis for electric vehicle (ev) grid integration study. In *Proc., IEEE PES Innovative Smart Grid Technologies Conference Europe (ISGT Europe)*, pages 1–6, Oct 2010.

[132] Y. Wu, X. Tan, L. Qian, D. H. K. Tsang, W. Z. Song, and L. Yu. Optimal

pricing and energy scheduling for hybrid energy trading market in future smart grid. *IEEE Transactions on Industrial Informatics*, 11(6):1585–1596, Dec 2015.

[133] L. Xiaoping, D. Ming, H. Jianghong, H. Pingping, and P. Yali. Dynamic economic dispatch for microgrids including battery energy storage. In *Proc., The 2nd International Symposium on Power Electronics for Distributed Generation Systems*, pages 914–917, June 2010.

[134] T. Yalcinoz and U. Eminoglu. Short term and medium term power distribution load forecasting by neural networks. *Energy Conversion and Management*, 46(910):1393 – 1405, 2005.

[135] E. Yao, P. Samadi, V. W. S. Wong, and R. Schober. Residential demand side management under high penetration of rooftop photovoltaic units. *IEEE Transactions on Smart Grid*, 7(3):1597–1608, May 2016.

[136] F. Ye, Y. Qian, and R. Q. Hu. A real-time information based demand-side management system in smart grid. *IEEE Transactions on Parallel and Distributed Systems*, 27(2):329–339, Feb 2016.

[137] Y. Yin, J. Guo, J. Zhao, and G. Bu. Preliminary analysis of large scale blackout in interconnected north america power grid on august 14 and lessons to be drawn. *Power system technology*, 10:001, 2003.

[138] J. You, R. Wu, K. Ye, Q. Bai, J. Rong, and C. Guo. Analysis of a blackout escalation caused by hidden failure lying in blocking logic between auto-switching protection and bus differential protection. *Dianli Xitong Zidonghua(Automation of Electric Power Systems)*, 35(7):102–107, 2011.

[139] M. Zhongjing, D. Callaway, and I. Hiskens. Decentralized charging control for large populations of plug-in electric vehicles: Application of the Nash certainty

equivalence principle. In *Proc., IEEE International Conference on Control Applications (CCA)*, pages 191–195, Yokohama, Japan, Sep. 2010.

[140] L. Zhu, F. Yu, B. Ning, and T. Tang. Stochastic charging management for plug-in electric vehicles in smart microgrids fueled by renewable energy sources. In *Proc., IEEE Online Conference on Green Communications (GreenCom)*, pages 7–12, Sep. 2011.

[141] L. Zhu, F. R. Yu, B. Ning, and T. Tang. Optimal charging control for electric vehicles in smart microgrids with renewable energy sources. In *Proc., IEEE 75th Vehicular Technology Conference (VTC Spring)*, pages 1–5, Yokohama, Japan, May 2012.